Department of Geology and Soil

Science Faculty of Sciences

Ghent University

2010 - 2011

CHRONOLOGY AND CORRELATION OF LATE WEICHSELIAN AND HOLOCENE SANDY DEPOSITIONAL ENVIRONMENTS IN BELGIUM AND THE NETHERLANDS BASED ON OPTICALLY STIMULATED LUMINESCENCE DATING

Thesis submitted as partial fulfilment of the requirements for the degree of Doctor (PhD) in Sciences: Geology

by

Cilia Derese

Promotor: Prof. Dr. P. Van den haute

Co-promotor: Dr. D.A.G. Vandenberghe

TABLE OF CONTENTS

LIST OF FIGURES

LIST OF TABLES

Chapter 1

Introduction

CHAPTER 1. INTRODUCTION

In his book 'Principles of Geology' (1830), Charles Lyell stated that 'the present is the key to the past'. Especially when it concerns the study of the Quaternary, the most recent geological period, the reverse however holds true as well. This period, extending from 2.58 Ma until the present (Gibbard et al., 2010), was characterised by an alternation of pronounced colder (glacial) and warmer (interglacial) periods, which in their turn were marked by numerous smaller climatic oscillations (stadials and interstadials). The reconstruction of the past climatic and associated environmental changes and their forcing factors may provide insights into the present and future climatic and environmental conditions, and hence into their (potential) impact on human life. An accurate reconstruction, however, requires a detailed and reliable chronological framework that allows deriving information concerning the timing and duration of the climatic and environmental events. This PhD thesis is intended to provide a contribution to the development of such a framework for some of the Late Weichselian to Holocene sandy sequences in N Belgium and The Netherlands, by means of optically stimulated luminescence dating.

1.1. WHY STUDYING THE LAST GLACIAL-INTERGLACIAL CYCLE?

The last glacial-interglacial cycle (or 'Weichselian-Holocene', spanning the last ~75 ka; Lowe and Walker, 1997) is probably the most extensively studied time interval of the Quaternary, attracting the interest of scientists from a range of disciplines, such as (Quaternary) geology, geography and geomorphology, ecology, palaeoclimatology and (geo)archaeology.

One reason is that a wealth of information is available for the palaeoclimatic and environmental reconstruction of this period in the high-resolution archives of the Greenland and Antarctic ice sheets (see e.g. Lorius et al., 1985; Dansgaard et al., 1993; Bender et al., 1994; Rasmussen et al., 2008), of the deep-ocean sedimentary sequences (see e.g. Van Campo et al., 1982; Porter and An, 1995; Heusser and Morley, 1997), and of the Chinese and Central European loess deposits (see e.g. Chen et al., 1997; Frechen et al., 2003; Bokhorst et al., 2009). A wide variety of techniques is at hand to study these high-resolution records. They allow investigating and correlating the different records while making use of the lithological evidence (e.g. grain-size and grain-shape analysis, geochemistry, palaeomagnetism), the

biological evidence (e.g. pollen analysis, diatom analysis, study of marine mollusca, study of fossil insect remains), and the geochronological evidence (e.g. radiocarbon dating, luminescence and electron spin resonance dating, tephrochronology, amino-acid racemisation, obsidian hydration dating). The study of glacial and periglacial landforms provides additional information to reconstruct the Quaternary environments (Lowe and Walker, 1997).
Moreover, the last glacial-interglacial cycle roughly coincides with the rise of modern man. A large amount of archaeological traces provides evidence for the cultural and technological developments, the organisation of human societies, and human migration and settlement. As such, the analysis and reconstruction of the palaeoenvironments during this period increasingly becomes the study of the environmental context of the social, cultural and economic evolution of man.

1.2. THE LAST GLACIAL-INTERGLACIAL CYCLE IN THE NW EUROPEAN LOWLANDS

Whilst during the last glacial the north of Europe was covered by the Fennoscandian ice sheet, extending westwards to the continental shelf and southwards into Denmark and Poland (Fig. 1.1), the NW European lowlands were reigned by periglacial conditions. Continuous permafrost occurred during the Weichselian Early Pleniglacial and Late Pleniglacial, whereas a generally less cold but wetter climate marked the intervening Middle Pleniglacial (Van Huissteden, 1990). This resulted in a barren steppe/tundra environment, which existed throughout much of the Weichselian with the exception of the warmer interstadials, during which it was replaced by shrub tundra. Tree growth was impeded by strong wind activity (Kolstrup and Wijmstra, 1977), resulting in transport and deposition of aeolian sediments in the periglacial zone (Figs. 1.1 and 1.2).
According to Huijzer and Vandenberghe (1998), aeolian sands were deposited throughout the major part of the Early Pleniglacial in The Netherlands. In the S Netherlands, N Belgium and W Germany, loess deposition took place from ca. 65-60 ka (Guiter et al., 2003). Sediments from the Early Pleniglacial are generally characterised by large frost wedges.
As the environmental conditions during the Middle Pleniglacial were less favourable to loess deposition, the loess profiles from this period show an abundance of interstratified organic levels (Guiter et al., 2003). Accumulation of sand sheets with intercalated silty layers occurred in the northern regions (e.g. Denmark; Huijzer and Vandenberghe, 1998). River valleys of the NW European lowlands and N Germany were dominated by fluvial to

niveofluvial sand deposition (Van der Hammen and Wijmstra, 1971; Van Huissteden, 1990). Organic matter, clay, silt, gyttja and peat layers are interbedded within the fluvial sandy deposits.

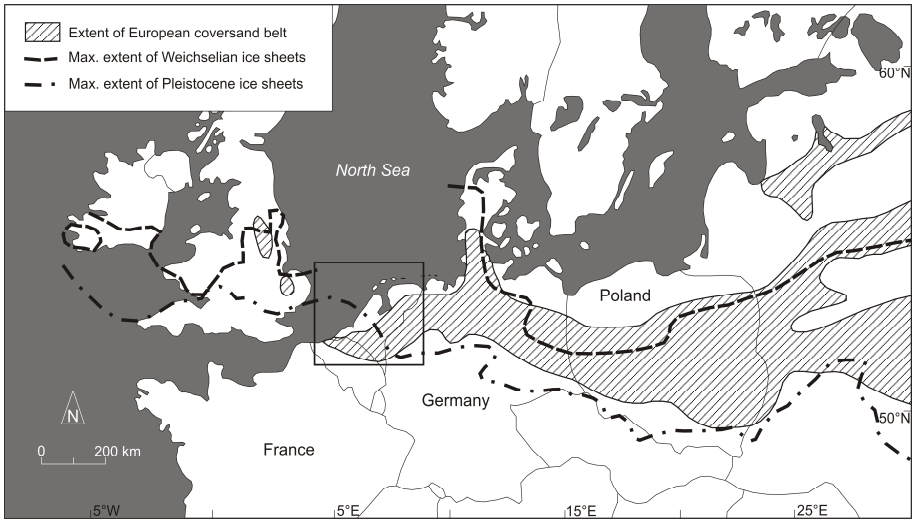

Fig. 1.1: Maximal extent of the Fennoscandian ice sheet during the Pleistocene and during the Weichselian. Extent of the European coversand belt in the periglacial zone. The study area of this thesis is indicated with an open square (adapted from Kasse, 1997; 2002).

The Late Pleniglacial sequences in the E and S Netherlands, N Germany and N Belgium typically consist of fluvial and fluvio-aeolian sands, characterised by periglacial features such as large ice-wedge casts and large-scale periglacial involutions. They are truncated by the Beuningen Gravel Bed (previously named 'Desert pavement 3' in Belgium; Paepe and Vanhoorne, 1967), consisting of a locally occurring coarse-grained fluvial deposit and a widespread gravelly desert pavement. The Beuningen Gravel Bed is considered as a lithostratigraphic marker for permafrost degradation, shallow channelling and large-scale aeolian deflation at the end of the Late Pleniglacial. The synchronism of this bed throughout Belgium and The Netherlands is not fully established. In the S Netherlands, central Belgium, N France and England, loess-derived silt loams developed during the Late Pleniglacial (Huijzer and Vandenberghe, 1998).

The close of the Weichselian glacial, the so-called Late Glacial, was characterised by abrupt and pronounced climatic shifts that left a signature in the sedimentary and environmental archives (see Chapters 2-6). Temperature differences between stadial and interstadial periods of up to 12-13°C have been recorded. The occurrence of cold episodes was inferred from the discovery of remnants of steppe/tundra plants, notably *Dryas octopetala*, in N European strata;

hence the time periods during which the cold climate was thought to have prevailed were named 'Dryas' (see e.g. De Klerk, 2004). Pollen investigations on gyttja deposits in Denmark further resulted in the definition of two warmer climatic episodes: Allerød and Bølling. The pollen zonation defined in N Europe was subsequently implemented in The Netherlands and N Belgium, and consisted of the following biozones: Earliest Dryas stadial (15.5 – 14.8 ka calBP), Bølling interstadial (14.8 – 14.1 ka calBP), Early Dryas stadial (14.1 – 14.0 ka calBP), Allerød interstadial (14.0 – 13.0 ka calBP) and Late Dryas stadial (13.0 – 11.7 ka calBP; see e.g. Fig. 5.1). The time periods quoted between brackets were determined later, mostly on the basis of radiocarbon dating (see e.g. Hoek, 1997; 2001). The palaeoenvironmental and –climatological changes that were derived from the interpretation of the plant assemblages characteristic for the biozones were later verified by investigating other proxies (e.g. micro- and macrofauna, oxygen isotopes). Because of the short duration of the Early Dryas stadial and its absence in many sedimentary sequences, some authors (see e.g. Lowe and Walker, 1997) consider the Bølling and Allerød interstadials as a single period of significantly warmer conditions, known as the Late Glacial interstadial.

The aforementioned biozonation and especially its relation to time periods have been questioned by several authors. De Klerk (2004) focused on the development of the stratigraphical and geochronological subdivision of the Late Glacial and more specifically on the flaws in this subdivision, which appear to be due to a combination of wrongly used stratigraphical concepts, incorrect interpretations and erroneous correlation between various sites and records. He concluded that almost all of the stratigraphic schemes and terms have lost their original value. Vanhoorne and Verbruggen (1975) showed that the interpretation of pollen assemblages in terms of chronology is not always straightforward. The pollen spectra for peat layers in sandy sequences situated at the westernmost extension of the Maldegem-Stekene coversand ridge (N Belgium; see Chapter 5) indicated an (almost) continuous occurrence of an open birch-dominated forest on the sand ridge from the Bølling up to the beginning of the Allerød. Based on the palynology, a distinction between these three time periods was not possible on the basis of the pollen data.

Throughout the Late Glacial, the NW European lowlands were again subjected to aeolian sedimentation, evolving from widespread sand sheet deposition during the Earliest Dryas to more localised low dune accumulation, among this also the formation of river dunes along the Scheldt River, during the Late Dryas. Loess sequences dating from this period are found in N France and SE Germany. The former periglacial zone was marked by vegetational revival dynamics, involving pioneer herbaceous vegetation with steppic plants such as *Artemisia*,

followed by the development of open *Betula* and *Pinus* forests during the interstadials. The slow response of the vegetation to the temperature increase during the interstadial periods has been explained by the poorly developed soils, frequently still characterised by relict permafrost during the Bølling, and the great distance from refuges (Hoek, 2001; Guiter et al., 2003).

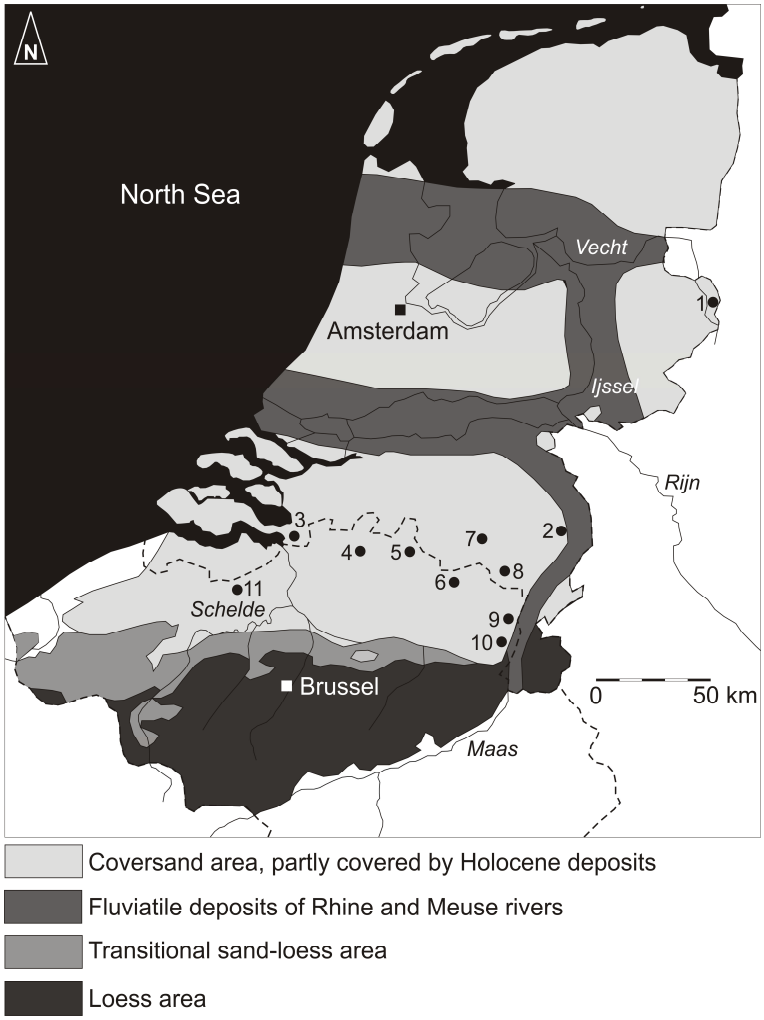

Fig. 1.2: Schematic map of the study area, showing the main sedimentation areas during the Weichselian and the location of some previously investigated sites by the Ghent Luminescence Laboratory and the sites investigated during the present study (adapted from Kasse, 1997). 1: Lutterzand; 2: Grubbenvorst; 3: Ossendrecht; 4: Pulle; 5: Arendonk; 6: Lommel; 7: Aalsterhut; 8: Weerterbergen; 9:Rotem; 10: Opgrimbie; 11: Heidebos.

The onset of the Holocene was marked by abrupt warming, followed by a number of climatic oscillations, which had a certain impact on vegetation development (alternating expansion of forests and grasslands). The overall climatic amelioration however resulted in the immigration of *Corylus* and other thermophilous trees from the Boreal onwards (Hoek, 1997). The expansion of the vegetation cover was associated with a decrease of the sedimentation rate

and eventually an interruption in the sand deposition. From ~1.3-1.1 ka up to the present, local resedimentation by wind of terrestrial deposits (usually Weichselian coversands) occurred on large scale. This so-called sand-drifting is thought to be linked to an increasing population pressure, resulting in large-scale deforestation, intensified heathland exploitation and rapid expansion of arable fields (Koster, 1982; Castel et al., 1989).

1.3. SOURCE AND SEDIMENTOLOGY OF THE COVER- AND DRIFT-SANDS

The coversands deposited in the NW European lowlands form part of the European coversand belt, which stretches from Great Britain, over the NW European lowlands, N Germany, Denmark and Poland to Russia (Fig. 1.1; see e.g. Kasse, 2002, and references therein). According to Schwan (1986), their main source area during the Weichselian Pleniglacial was situated in the present-day North Sea region, which was then characterised by a considerably lower sea level. As the subsequent Late Glacial was marked by recession of the ice sheet margin, reinundation of the North Sea basin, changes in the atmospheric pressure system and a denser vegetation cover, the depositional regime was modified. Environmental changes now only allowed transport from nearby sources, such as the pre-existing aeolian sediments and temporarily dry water courses, by mainly westerly winds.
The fluvio-aeolian and aeolian sediments are usually fine-grained sands with a modal grain size between 105 and 210 µm. Silty intercalations or locally coarser sands may be present within these sediments. Four sedimentary facies have been distinguished within the coversand sequences (see e.g. Schwan, 1986; 1988; Kasse, 2002): (1) massive and indistinct horizontally bedded sands, (2) alternation of sands and silty fine sands, (3) horizontally laminated to low-angle cross-bedded sands, and (4) large-scale cross-bedded sands.

The occurrence of Holocene drift-sands is more or less restricted to the coversand area of the NW European lowlands, as this region also acts as the main source of the sediments. In The Netherlands, for example, the drift-sands cover a total area of about 790 km². The sediments are generally fine, well sorted, unimodal sands. They are characterised by a yellow-greyish colour, a relatively loose grain-packing, the presence of layers rich in organic material and an absence of periglacial structures (Castel et al., 1989).

1.4. LITHOSTRATIGRAPHY AND CHRONOLOGY OF THE COVER- AND DRIFT-SANDS

The classic lithostratigraphic subdivision of the Weichselian Pleniglacial and Late Glacial deposits in The Netherlands comprises the following succession: Older Coversand I, Beuningen Gravel Bed, Older Coversand II, Younger Coversand I, Usselo Soil and Younger Coversand II (see e.g. Fig. 5.1 and Van der Hammen, 1951; Van der Hammen and Wijmstra, 1971). Later, this lithostratigraphy was revised by Van Huissteden (1990) and Van Huissteden et al. (2001). Most recently, Schokker et al. (2003; see also Schokker et al., 2007) tried to address the main problem associated with the classic stratigraphic scheme of Van der Hammen (1951) and Van der Hammen and Wijmstra (1971), in that it represents a mixture of lithological, stratigraphic and age elements. They therefore incorporated all fine-grained sediments into a newly-defined Boxtel Formation, with a holostratotype in the central part of the Roer Valley Graben.

In Belgium, several authors presented their own stratigraphical schemes, based on international and already existing climato-genic systems, before Paepe and Vanhoorne (1967) set the goal to define a generally accepted lithostratigraphic subdivision. These authors tried to step away from the assumption that litho-, bio- and chronostratigraphy evolved parallelly through time. The following units were distinguished within the Late Pleniglacial and Late Glacial deposits: Coversand 1, Desert pavement 3 and large frost wedge row, Coversand 2, Stabroek soil (peat and loam), Late Coversand 1, Humic layer with fine frost wedges and cryoturbations, and Late Coversand 2. This stratigraphic subdivision shows some parallels with the classic subdivision of Van der Hammen (1951) and Van der Hammen and Wijmstra (1971) in The Netherlands. The current subdivision by Gullentops et al. (2001) gathers all coversand units within the Gent Formation and all inland dune sands, e.g. river dunes, drift-sand dunes, within the Hechtel Formation.

Until about 20 years ago, the chronological information and correlation of the fluvio-aeolian and aeolian sandy deposits in the NW European lowlands was mostly based on pollen analyses and radiocarbon dating of intercalated organic matter (see e.g. Paepe and Vanhoorne, 1967; Paulissen and Munaut, 1969; Van der Hammen and Wijmstra, 1971; Kolstrup, 1980; Van Geel et al., 1989). It should be noted that pollen analysis on itself is not an accurate geochronometer, as local differences in ecology can hinder correlation. The vegetation histories during the Late Glacial in Belgium and The Netherlands do show similarities but

there are differences as well. While the onset of the Late Glacial in The Netherlands is defined by a rise of *Artemisia* pollen, the Late Glacial pollen spectra from N Belgium ('Sandy Flanders') show an increase of herb pollen prior to that of *Artemisia* pollen (Verbruggen, 1979). Moreover, westernmost part of the Maldegem-Stekene coversand ridge in Sandy Flanders appears to have been covered with an open *Betula* forest from the Bølling to the Early Allerød (Vanhoorne and Verbruggen, 1975), while the same period in The Netherlands was generally characterised by open birch copses within a predominantly open landscape, followed by an expansion of *Salix* and *Juniperus*, and subsequently again open birch forests (Hoek, 2001). Radiocarbon dating is generally an accurate geochronological tool (see also Chapter 7), but has the limitation that it can only be applied on organic material, such as plant remains and carbonate shells. As the coversands in N Belgium and The Netherlands on itself are poor in organic matter, mainly intercalated soil horizons and peats can be dated using this technique and only upper and lower time boundaries for the sediment units can be obtained. Luminescence dating techniques do allow direct age determination of the clastic component of the sandy sediments. The first studies in the NW European lowlands were employing a thermal stimulation of the luminescent signal and acknowledged some methodological problems (see e.g. Dijkmans and Wintle, 1991; Dijkmans et al., 1992; Frechen and Van den Berg, 2002). Later on, optically stimulated luminescence (OSL) dating was shown to yield more precise and accurate results (see e.g. Bateman and Van Huissteden, 1999; Koster, 2005; Schokker et al., 2005; Kasse et al., 2007; Wallinga et al., 2007; Vandenberghe et al., 2004; 2009; Buylaert et al., 2009). The optical dating method, often applied in combination with radiocarbon dating, is increasingly becoming the method of choice to obtain age information for Quaternary deposits, for instance at archaeological sites in the NW European lowlands. Wallinga et al. (2007) provided an review of the age results obtained with luminescence dating on sediments (e.g. Weichselian coversands, fimic soils, coastal dunes and inland drift sands, fluvial and colluvial deposits) from The Netherlands and compared them with independent age estimates. They found a good agreement between the OSL and independent age information in the range from a few years to ~125 ka. For the Belgian aeolian sediments, such an overview and comparison is not yet available, also because the application of luminescence dating on cover- and drift-sands in Belgium was until now limited to the studies of Frechen et al. (2001) and Vandenberghe et al. (2009). Buylaert et al. (2009) determined optical ages for 14 relict sand wedges and composite wedge-pseudomorphs within the coversands of N Belgium. This thesis aims at establishing a more comprehensive OSL dataset of especially the Belgian part of the NW European coversand belt.

1.5. OPTICALLY STIMULATED LUMINESCENCE DATING

This thesis is based on the application of optically stimulated luminescence (OSL) dating (see e.g. Aitken, 1998; Vandenberghe, 2004). Vandenberghe (2004) elaborately discussed the basis principles of optically stimulated luminescence dating, the different measurement protocols and their respective advantages and disadvantages, and the choice of the measurement parameters. Hence, the dating method is only briefly outlined in this thesis.

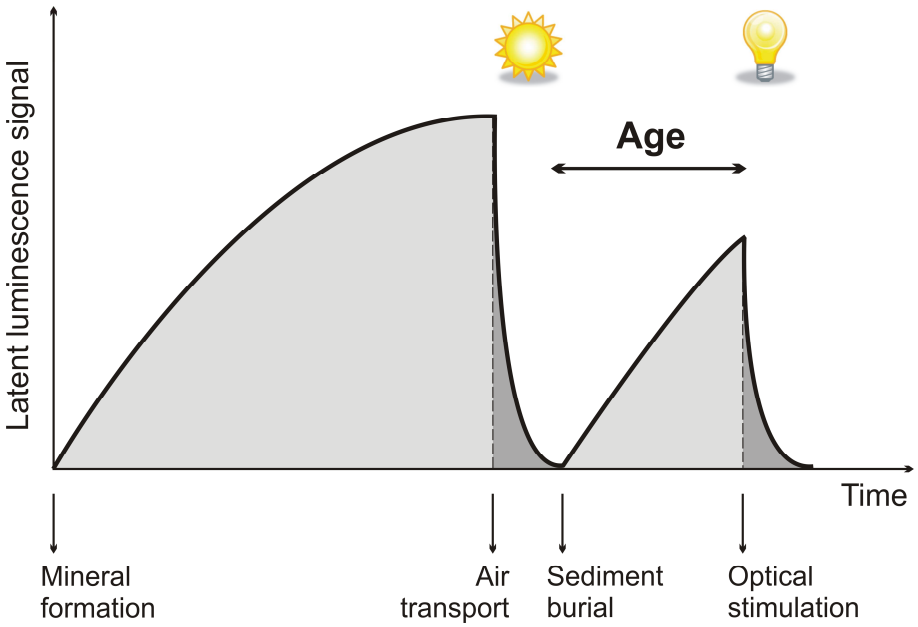

Fig. 1.3: Schematic representation of the principle of luminescence dating (modified from Vandenberghe, 2004; after Vancraeynest, 1998). Minerals are continuously exposed to low-level natural radioactivity, from which a part of the energy is trapped in the crystal structure as a latent luminescence signal. When the minerals are exposed to sunlight, as a result of erosion and transport (through air, in the case of aeolian sediments), the acquired luminescence signal is removed ('zeroing' or 'bleaching'). Once deposited and buried under other grains and therefore shielded from sunlight, the luminescence signal starts to build up again until the moment of measurement in the lab. As a consequence, the obtained luminescence age is equal to the time passed since the last zeroing event and the burial of the mineral grains.

Luminescence dating belongs to the group of the radiation damage dating methods, which also includes fission-track dating and electron spin resonance dating (Aitken, 1985; 1998). These dating methods are based on the time-dependent accumulation of radiation damage in minerals as a result of their exposure to low-level ionising radiation from the decay of natural radionuclides, mainly members of the ^{238}U and ^{232}Th decay series and ^{40}K, and to a lesser degree from ^{87}Rb and cosmic rays. Part of the energy from this radiation is stored within the

crystal structure of the minerals as a latent luminescence signal (Fig. 1.3). When the crystals are heated or exposed to light of a specific wavelength, the trapped energy is released as a small light signal ('luminescence'). The removal of the trapped charge is called 'zeroing'. In the case of sediment dating, the zeroing event is the exposure to daylight during erosion, transport and deposition of the mineral grains and hence it is referred to as 'bleaching'. As soon as the zeroing agent is not longer operative, for example when the sediment grains are deposited and buried under other grains and thus shielded from sunlight, the trapped charge population starts to build up again.

In luminescence dating, the zeroing process is realised in the laboratory using an artifical heat or light source, in the case of thermoluminescence (TL) or optically stimulated luminescence (OSL) dating, respectively. The emitted 'natural' luminescence signal is measured using a photomultiplier tube and subsequently compared with luminescence signals induced by known beta doses given in the laboratory, to determine an equivalent dose (D_e, in Gy[1]): this is the laboratory dose necessary to induce a luminescence signal of exactly the same magnitude as their natural signal. In this thesis, equivalent dose determination was carried out on coarse quartz grains, generally the most abundant minerals in the aeolian sands from the NW European lowlands using the single-aliquot regenerative-dose (SAR) protocol of Murray and Wintle (2000; 2003). This measurement protocol is widely accepted as the technique of choice for obtaining direct ages of sediments in a wide range of sedimentary environments, including the aeolian one (see e.g. Murray and Olley, 2002; Bateman, 2008; Madsen and Murray, 2009). It consists of several measurement cycles that are all carried out on a single aliquot, in this way allowing automatisation of the measurement process. One measurement cycle consists of the following sequence: irradiation (0 Gy in first cycle; increasing regenerative doses in following cycles) – fixed preheat for 10 s – OSL measurement – irradiation (fixed test dose) – fixed cutheat – OSL measurement – hot bleach. During the first cycle, the natural luminescence signal (L_n) that has built up in nature is measured. In the following measurement cycles, increasing laboratory doses (named 'regenerative doses') are administered, after which the response luminescence signal (L_x) is measured. Sensitivity changes can occur during the successive measurement cycles. The response to a fixed test dose (T_x) is thought to change in accordance with the response to the regenerative dose; hence, this signal can be used to correct for the sensitivity changes. This is done by determining the

[1] Gy or gray is the SI unit of absorbed radiation dose of ionising radiation. One gray corresponds to one joule of energy, in the form of ionising radiation, per kilogram of matter.

ratio of the response to the regenerative dose and that to the test dose (L_x/T_x) for each cycle. The ratios calculated for each measurement cycle are then shown as a function of the administered regenerative doses to obtain a 'growth curve'. The ratio of the natural luminescence signal and the response to the test dose administered during the first measurement cycle (L_n/T_n) can be plotted onto the growth curve to obtain the 'equivalent dose' (see Figs. 2.3, 3.3, 4.8, 5.6 and 6.5). The SAR protocol also includes some internal tests (see also Chapters 2-6), to evaluate whether the growth curve passes through the origin (by determining the response to a zero dose: 'recuperation value') and whether the sensitivity correction is working properly (by measuring the response to the first regenerative dose twice: 'recycling ratio'). Moreover, some specific tests to check the suitability of the applied SAR protocol can be carried out. These are more elaborately discussed in the following chapters (2-6).

Apart from the equivalent dose, a second parameter has to be measured as well: the dose rate (in Gy ka^{-1}). This parameter represents the rate of energy absorption within the crystal structure of the minerals and is determined by measuring the concentrations or activities of the naturally occurring radionuclides in the sediments. This measurement can be performed using a range of analytical techniques, such as instrumental neutron activation analysis (INAA), gamma-ray spectrometry and thick-source alpha counting. In this work, the radionuclide activities have been determined with high-resolution low-background gamma-ray spectrometry with a high-purity coaxial Ge-detector and converted to dose rates using conversion factors derived from the nuclear energy releases tabulated by Adamiec and Aitken (1998). Allowance is made for the effect of water within the sediment pores, as the pore water absorbs part of the energy that would otherwise be experienced by the mineral grains. As a general rule for judging the influence of the water content on the optical age, it is assumed that 1% increase in the water content causes the age to increase with 1%. Hence a good estimation of the time-averaged moisture content is a significant step in calculating the dose rate and thus optical age. In this stud, separate undisturbed samples have systematically been taken to assess the present-day (W_n) and the saturation moisture contents (W). The time-averaged moisture content was then determined following Aitken (1985). Field evidence, such as the proximity of open water and sedimentary structures, allowed estimating how the time-averaged moisture content relates to the present-day and saturation moisture contents; this time-averaged moisture content was expressed as a fraction (F value) of the saturation content, so that F*W equals the time-averaged moisture content. The contribution from cosmic rays, consisting of a 'soft' and a 'hard' component (i.e. electrons and photons, and muons,

respectively), has to be taken into account as well, as it can have a major influence on the dose rate in quartz-rich sediments (such as coversands), which have a very low internal radioactivity. This contribution is dependent on the geographical latitude and altitude of the site, and on the burial depth of the sampled sedimentary horizon (Prescott and Hutton, 1994). As a general rule, OSL samples are never taken within the uppermost 50 cm of a sedimentary sequence, in order to avoid a possible influence from the 'soft' component of cosmic radiation. More information concerning the determination of the equivalent dose and dose rate can be found in Aitken (1985; 1998) and Vandenberghe (2004).
Once the equivalent dose and the dose rate have been determined, the luminescence age can be calculated using the following equation:

$$Age\ (ka) = \frac{Equivalent\ dose\ (Gy)}{Dose\ rate\ (Gy\ ka^{-1})}$$

1.6. AIM AND OUTLINE OF THIS THESIS

The overall objective of this thesis was the application of the quartz SAR-OSL dating to establish a precise and accurate chronology for some Late Weichselian coversand and the Late Holocene drift-sand deposits in N Belgium and The Netherlands. A total of six sites were investigated into detail, in close collaboration with experts in the fields of archaeology, geography, geomorphology, palaeontology and soil science.

Chapter 2 describes the application of optically stimulated luminescence dating to Holocene drift-sands at Pulle (NE Belgium), in the frame of an archaeological study performed by the Flemish Heritage Institute (VIOE). The investigated site consisted of building structures and ceramics that were partly covered by a drift-sand dune, suggesting that the accumulation of the aeolian sediments might have resulted in the deterioration of the living conditions and eventually in the abandonment of the site. The aim of the study was twofold: (1) to investigate the applicability of the dating method for this type of sediment in the study area, and (2) to determine a terminus ante quem for the abandonment of the site.
In the third chapter (**Chapter 3**), OSL dating was applied to reinvestigate the type locality for Late Glacial aeolian sand deposition at Opgrimbie (NE Belgium). Previous research by Paulissen and Munaut (1969), using sedimentological and palynological analyses in

combination with radiocarbon dating, had indicated that both Bølling and Allerød organics and bleached horizons were present within the dune sand sequence, but no direct ages were obtained for the sediments. The chronology of the site was therefore reinvestigated using optical dating of the aeolian deposits and AMS radiocarbon dating of the intercalated organic matter, as one of the first steps towards the establishment of a reliable chronological framework for the Late Glacial in NE Belgium.

As Chapter 3 showed that the aeolian sands in NE Belgium have satisfactory luminescence characteristics, the SAR-OSL dating technique was further used to date Late Glacial sandy ridge sequences at the archaeological sites of Arendonk-*Korhaan* and Lommel-*Maatheide* (**Chapter 4**). Both sites contained evidence of both Final Palaeolithic *Federmesser* and Mesolithic occupation. Of particular importance was that the two human occupation phases were stratigraphically separated. As such, these sites offered a unique means to study the possible relation between human occupation patterns and the climatic and environmental changes during the Weichselian-Holocene transition in the Campine region (NE Belgium). The chronological framework for this reconstruction of the physical landscape was provided by OSL dating.

Chapter 5 deals with the application of OSL dating to a sedimentary core taken at the locality of Heidebos, situated on the top of the Maldegem-Stekene coversand ridge and to the north of a Late Glacial palaeolake, known as the Moervaart depression (N Belgium). The region around the Moervaart depression including the coversand ridge is considered as a key-site for human occupation during the Late Glacial and Early Holocene, and it is currently being investigated in the frame of a multidisciplinary research project entitled "*Prehistoric settlement and land use systems in Sandy Flanders (NW Belgium): a diachronic and geo-archaeological approach"*. Our optical dating study aims at contributing to the realisation of an absolute and robust chronological framework for the sedimentary environments in the area around the Moervaart depression.

Chapter 6 describes the reinvestigation of the Late Weichselian periglacial sediments and Holocene drift-sands at the classic type locality Lutterzand in the E Netherlands, using sedimentological analyses in combination with radiocarbon and optically stimulated luminescence dating. Although this site has been the focus of a wide range of palaeoclimatic, palaeoenvironmental and geochronological studies in the past, the number of absolute ages for the sediments remained rather limited. This part of the thesis aimed at addressing this matter and at deriving a detailed and accurate chronological framework for the deposits at Lutterzand, which then could be compared and correlated with the luminescence chronologies obtained at

other localities studied in this thesis and in previous investigations concerning the sandy sediments in the NW European lowlands.

The last chapter of this thesis (**Chapter 7**) discusses the results of quartz SAR-OSL dating in terms of precision and accuracy, and combines the chronological information obtained for fluvio-aeolian and aeolian sands in N Belgium and The Netherlands to reconstruct their depositional history. It illustrates the suitability of optical dating as a chronological tool for the investigated timeframe (Late Weichselian to Holocene) and shows where further advances can be made, both for the quartz SAR-OSL dating method and for the study of (fluvio-) aeolian sedimentary environments in the NW European lowlands.

Chapter 2

A medieval settlement caught in the sand: Optical dating of sand-drifting at Pulle (N Belgium)

Chapter published in full as:

Derese, C., Vandenberghe, D., Eggermont, N., Bastiaens, J., Annaert, R., Van den haute, P., 2010. A medieval settlement caught in the sand: Optical dating of sand-drifting at Pulle (N Belgium). Quaternary Geochronology 5, 336-341.

CHAPTER 2. A MEDIEVAL SETTLEMENT CAUGHT IN THE SAND: OPTICAL DATING OF SAND-DRIFTING AT PULLE (N BELGIUM)

2.1. ABSTRACT

Close to the village of Pulle (N Belgium), six trenches were opened for archaeological research. This resulted in the discovery of a dense spread of traces of human settlement. Only a relatively small number of artefacts was found, but these allowed attributing the traces to habitation during the Iron Age and Early Middle Ages. In one of the trenches, the level with the archaeological finds was covered by a drift-sand dune. The accumulation of these aeolian sediments presumably put an end to the human occupation. Hence, dating these sediments might provide essential information as to the chronology of the occupational history of the site.

Quartz-based optical dating was applied to constrain the timing of sand-drifting at Pulle. All samples showed satisfactory luminescence characteristics and yielded an internally consistent set of optical ages. Within analytical uncertainty, the age results show no increase with depth and do not allow differentiating between distinct phases of sand-drifting. An average age of 1.2 ± 0.1 ka was obtained, which is interpreted as an upper age limit for human occupation at the site. The results also illustrate (the limit on) the time resolution that can be achieved through conventional quartz single-aliquot optical dating techniques; considering these limitations, we conclude that the sand-drifting at Pulle occurred during a single, fairly short event in the Early Middle Ages.

2.2. INTRODUCTION

The subsurface of northern Belgium represents a rich archive of the cultural heritage. It documents human migration and occupation in the past 250 ka across the NW European lowlands. The archaeological finds are located within or on top of sequences of aeolian sands and intercalated soil horizons, which reflect the alternation of glacial and interglacial periods during the Quaternary. Many of the ancient human settlements are located on elevated areas, such as (the southern flanks of) coversand ridges, as they provide protection against the wind and groundwater and are characterised by a higher incidence of sunlight.

In northern Belgium, the Flemish Heritage Institute (VIOE) investigates sites where the potential archaeological patrimony is threatened by human activities (such as construction works and exploitation of natural resources). In 2007, exploratory archaeological trenching near the village of Pulle resulted in the discovery of a dense spread of building structures and ceramics indicating human occupation at this locality. The remains were partly covered by a drift-sand dune, suggesting that the accumulation of these aeolian sediments deteriorated the living conditions and resulted in the abandonment of the settlement. Therefore, the onset and rate (or periodicity) of the sand-drifting provide essential information as to the chronology of the occupational history of the site.

So far, the timing of sand-drifting has mainly been based on radiocarbon dating of associated organic material. In the NW European lowlands, only a few studies applied luminescence dating (e.g. Dijkmans and Wintle, 1991; Dijkmans et al., 1992; Bateman and Van Huissteden, 1999); in Belgium, no direct sedimentation ages are available for the drift-sand deposits.

In this paper, we report on the application of optically stimulated luminescence (OSL) dating to constrain the timing of sand-drifting at Pulle. The aim of the study is twofold: (1) to investigate the applicability of OSL dating for this type of sediment in the study area, and (2) to determine a terminus ante quem for the abandonment of the site.

2.3. GEOLOGICAL CONTEXT AND INDEPENDENT AGE INFORMATION

The investigated site is located near the village of Pulle in N Belgium (Fig. 2.1). It is situated on a coversand ridge within the NW European coversand belt (Baeyens, 1971). The ridge is ~10 m high; it has an E-W extension and is bordered by two river valleys, one with an E-W orientation to the south of the ridge and one with a NE-SW orientation to the west (areas in

light green on the digital elevation map in Fig. 2.1). The coversands were presumably deposited during the Weichselian. During the Holocene, they were locally remobilised and blown into so-called drift-sand dunes; this was also the case at Pulle. According to Koster (1982), the term 'drift-sand' is used to denote those aeolian sands that originate with relatively 'young', local resedimentation of terrestrial Pleistocene deposits and that usually display a chaotic dune relief. In the Belgian lithostratigraphic record, they are considered to be part of the Hechtel Formation (Gullentops et al., 2001), which correlates with the Kootwijk Formation in the Netherlands (Koster, 1982).

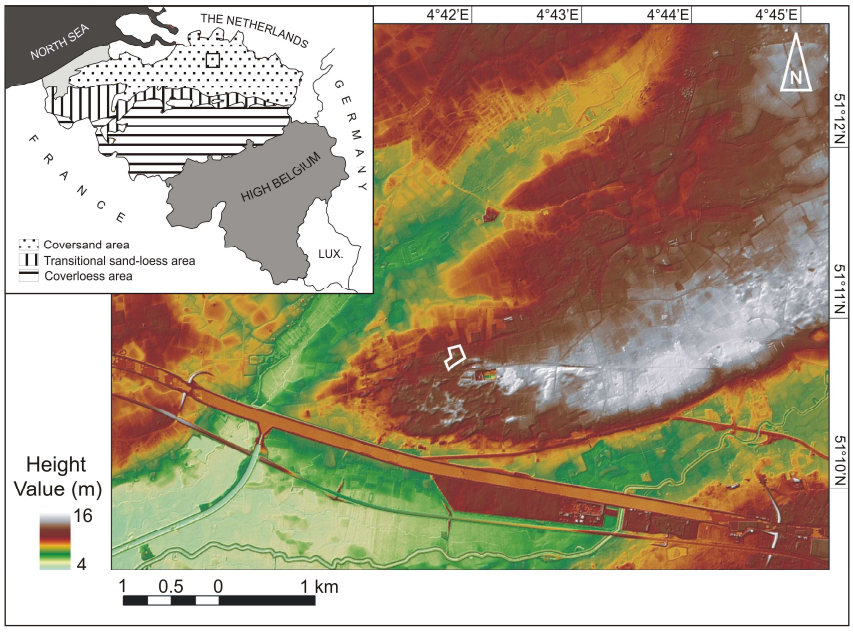

Fig. 2.1: Digital elevation map of the area, showing the location of the investigated site (bordered by a white line) on a coversand ridge (elevated areas in dark grey and white). The inset situates the archaeological site (open square) in its broader context.

Six trenches were opened for archaeological research, which led to the discovery of an ancient human settlement; a dense spread of ceramics was found, as well as remains of building structures and wells. The majority of the artefacts was typologically undatable; the few pottery sherds that did exhibit characteristic stylistic features indicate human occupation during the Iron Age and Early Middle Ages (roughly from the 6th to the 1st century BC and from the 6th to the 9th century AD, respectively). Radiocarbon dating of the wooden shuttering of two wells yielded ages of AD 430-600 (95.4% probability), AD 640-780 (95.4%) and AD

770-900 (86.0%)[2], which corresponds with the medieval occupation period. It should be noted, however, that radiocarbon dating not necessarily dates the event(s) of interest; it dates the fixation of atmospheric carbon, which does not necessarily coincide with the time that the wells were built. Dendrochronological research of fragments from the well shuttering and preliminary pollen investigations did not result in useful data (Eggermont et al., 2008).
In one of the trenches, a ~40 cm thick settlement level with archaeological traces was partly covered by drift-sands. The accumulation of these sediments presumably made the site unfit for further human habitation. Therefore, the results from typological analysis and radiocarbon dating yield a terminus post quem for the abandonment of the site. Optical dating of the drift-sands was performed to obtain a terminus ante quem and to improve our understanding of the cultural development at this locality.

2.4. SAMPLING AND SAMPLE PREPARATION

A ~3.5 m high profile, encompassing the drift-sand dune and the top of the coversand ridge, was sampled for optical dating (Fig. 2.2). The drift-sand succession is characterised by a subhorizontal stratification with black organic-rich laminae alternating with quartz-rich light-coloured sediments. Nine samples in total, seven above and two below the settlement level, were collected by hammering stainless steel cylinders into a freshly cleaned exposure. Three of the drift-sand samples were taken from the same stratigraphic level to allow evaluating the internal reproducibility of the applied dating procedure. About 1 kg of the surrounding sediment was sampled for dose rate determination. Two undisturbed samples were collected for evaluation of the present-day and saturation water content.
In the laboratory, coarse (180-212µm diameter) quartz grains were extracted from the inner cores of the sample cylinders using conventional sample preparation techniques (HCl, H_2O_2, sieving, HF, HCl). The purity of the quartz extracts was confirmed by the absence of a significant infrared stimulated luminescence (IRSL) response to a large regenerative β-dose.

[2] The uncalibrated radiocarbon ages are 1,535 ± 25 BP, 1,320 ± 40 BP and 1,180 ± 30 BP, respectively. The calibration of these ages was carried out using OxCal v3.10 and the IntCal04 calibration curve (Reimer et al., 2004; Eggermont et al., 2008).

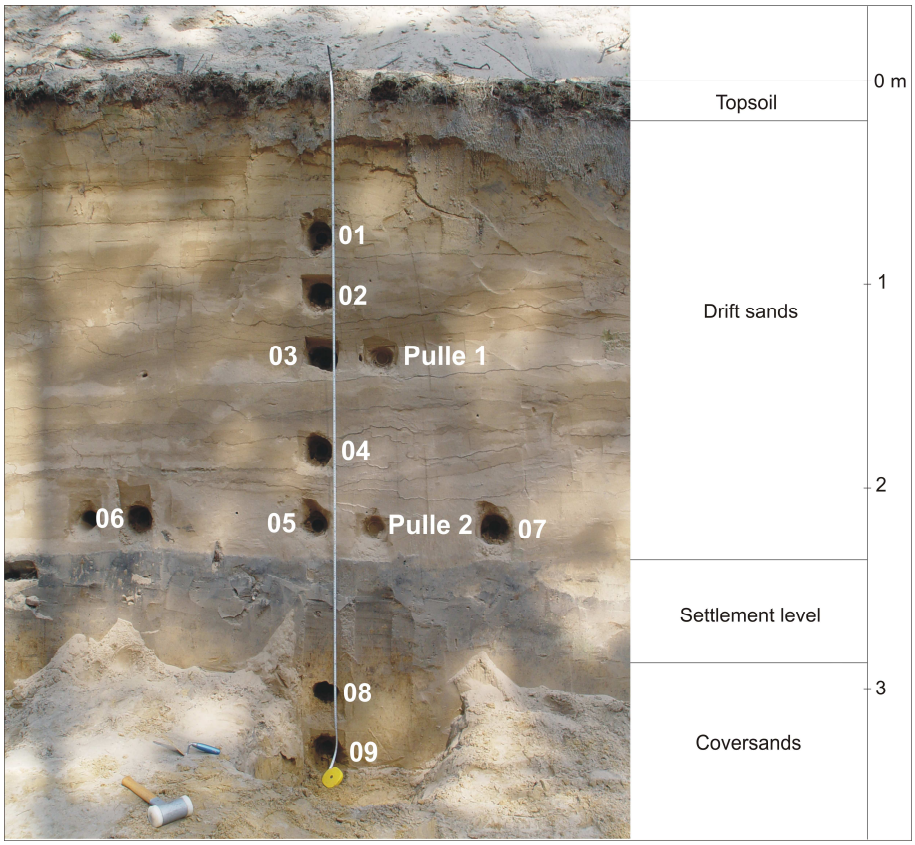

Fig. 2.2: Photograph of the investigated dune profile, showing the location of the samples collected for optical dating. Pulle 1 and 2 are samples taken for evaluation of the time-averaged moisture content.

2.5. LUMINESCENCE ANALYSIS

2.5.1. Analytical facilities

All OSL measurements were performed using an automated Risø TL/OSL-DA-15 reader, equipped with blue (470 ± 30 nm) LEDs and an IR diodes (875 nm); the quartz luminescence emissions were detected through 7.5 mm of Hoya U-340 UV filter. Details on the measurement apparatus can be found in Bøtter-Jensen et al. (2003).

2.5.2. Luminescence characteristics and equivalent dose determination

The luminescence characteristics were investigated by applying the single-aliquot regenerative-dose (SAR) protocol (Murray and Wintle, 2000) to large (7 mm diameter)

aliquots of quartz. Optical stimulation with the blue LEDs was for 40 s at 125°C. The initial 0.32 s of the decay curve was used in further calculations, less a background evaluated from the following 0.32 s of stimulation. After the measurement of each test dose signal, a high-temperature bleach was performed by stimulation with the blue diodes for 40 s at 280°C (Murray and Wintle, 2003). For each aliquot, a complete growth curve was constructed by measuring the response to five regenerative doses (up to 2.5 times the estimated equivalent dose). The SAR protocol also involved the measurement of the response to a zero dose to determine whether the growth curve passes through the origin (recuperation), and a repeat measurement of the response to the lowest regenerative dose to evaluate the performance of the sensitivity correction (recycling ratio). Additionally, a second measurement of the response to the highest regenerative dose was carried out. This time, however, the sensitivity to IR stimulation was checked before stimulation with blue diodes in order to identify aliquots with a significant feldspar contamination. The measured aliquots were accepted if the recuperation and IRSL/BLSL ratio (Vandenberghe, 2004) did not exceed a threshold set at 10% and if the IR depletion ratio (Duller, 2003) and the recycling ratio were within 10% of unity. None of the analysed aliquots had to be rejected on the basis of these criteria.

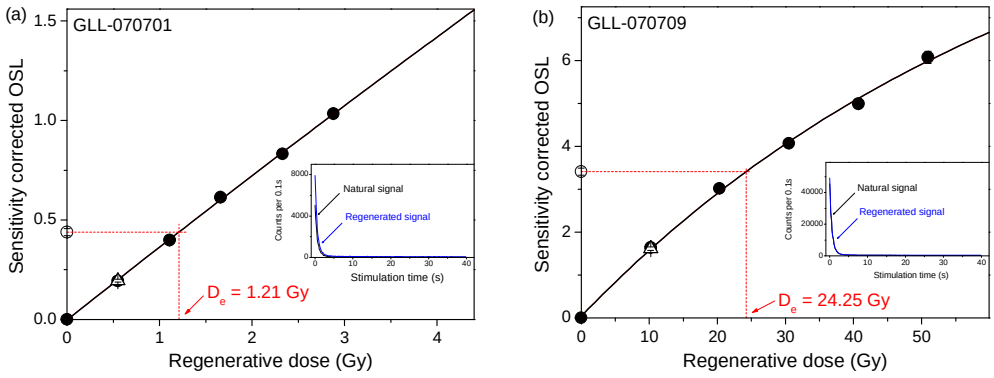

Fig. 2.3: SAR growth and OSL decay curves (inset) for (a) drift-sand sample GLL-070701, and (b) coversand sample GLL-070709. The solid line is the fit of the data to a linear (a) and a single saturated exponential function (b). The open triangle shows the recycling point. The equivalent dose (D_e) is obtained by interpolation of the sensitivity-corrected natural OSL signal (open circle) on the corrected growth curve.

Representative luminescence decay and SAR growth curves are shown in Fig. 2.3 for an aliquot of quartz extracted from one of the drift-sand (a) and one of the coversand (b) samples. The growth curves are well represented by linear or single saturating exponential functions. Fig. 2.3 also illustrates the generally good behaviour of the samples in the SAR protocol.

Especially for young samples, it is important to investigate the influence of preheating. This thermal pre-treatment may transfer charge from thermally shallow, light-insensitive traps to deeper light-sensitive traps, resulting in an overestimation of the equivalent dose (see e.g. Ballarini et al., 2003; Kiyak and Canel, 2006; Vandenberghe et al., 2007). We investigated the influence of the preheat temperature on the measured dose through both a preheat plateau (Murray and Wintle, 2000) and a dose recovery test (Murray and Wintle, 2003). In the preheat plateau test, three natural aliquots of sample GLL-070701 were measured at each of seven different preheat temperatures in the range of 160°C to 280°C. For the dose recovery test, new aliquots of this sample were bleached at room temperature using the blue diodes (2 times 250 s with a 10 ks pause in between) and given a dose close to the expected natural dose; the dependence on the preheat temperature was then measured. The results show that both the natural dose and the ratio of the measured to given dose are insensitive to preheats in the 160-240°C temperature interval (Figs. 2.4a and 2.4b, solid circles). The measured doses rapidly increase at higher temperatures, which is probably due to thermal transfer. This is confirmed by a thermal-transfer test, in which new aliquots of sample GLL-070701 were artificially bleached as in the dose recovery test, and the dependence of the residual dose on the preheat temperature measured (Fig. 2.4b, open circles). The rise in residual dose matches the trend observed in the plots of equivalent dose and dose recovery as a function of preheat temperature. Based on these results, we adopted a preheat of 10 s at 180°C for all further analyses of the drift-sand samples; the thermally transferred dose arising from this thermal pre-treatment was found to be 0.00 ± 0.01 Gy (see Fig. 2.4b). A preheat of 10 s at 240°C was adopted for the coversands, based on previous work in this region (Vandenberghe et al., 2009; Derese et al., 2009).

An important limiting factor in the dating of young samples is the low intensity of the luminescence signals. To this respect, it is advantageous if the intensity of the test-dose signal can be increased so that its relative contribution to the measurement precision is negligible (Murray and Wintle, 2000). Therefore, the dependence of the measured dose on the size of the test dose was explicitly investigated for all drift-sand samples. This was done through dose recovery tests; aliquots were bleached and given a dose as outlined before, and then measured using test doses of 0.54 Gy, 1.08 Gy and 2.82 Gy. The variation in the ratio of the measured to given dose with the size of the test dose is shown in Fig. 2.5. Within analytical uncertainty, there is no detectable dependency of the measured dose on the size of the test dose. A second thermal-transfer test (see higher) was then conducted for sample GLL-070701; this time, the dependence of the residual dose on the size of the test dose was measured. The results are

shown in Fig. 2.6. Considering the analytical uncertainty (1 standard error), it appears that the residual dose is insensitive to the size of the test dose. We conclude that there is no impediment in using test doses that are 2-3 times higher than the natural dose. A test dose of 2.82 Gy was used for all further analysis of the drift-sands; for the coversands, the test dose amounted to ~50% of the estimated natural dose.

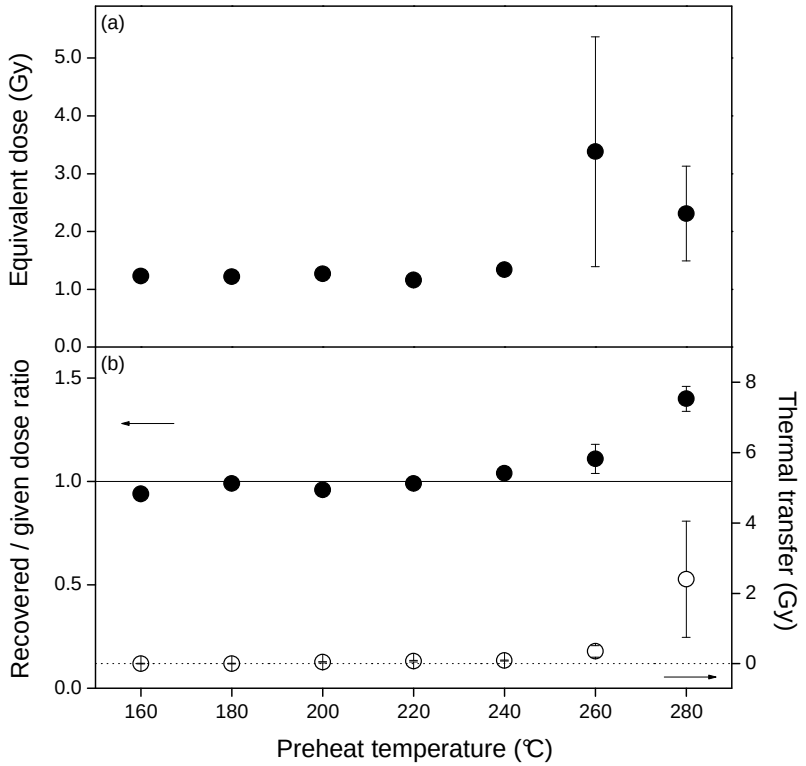

Fig. 2.4: Dependence of equivalent dose (a; filled circles), measured to given dose ratio (b; filled circles) and thermally transferred dose (b; open circles) on the preheat temperature. Each datapoint represents the average ± 1 standard error of three measurements. The solid line in (b) represents a recovered to given dose ratio equal to unity (eye guide); the dotted line (eye guide) represents a thermally transferred dose equal to zero.

A dose recovery test was carried out for the two coversand samples as well; it was conducted as outlined in the above and the results are included in Fig. 2.5. The entire set of dose recovery measurements demonstrates that the SAR protocol is able to measure laboratory doses with acceptable accuracy and precision. In general, individual measured to given dose ratios do not deviate more than 10% from unity. The overall average measured to given dose ratios (± 1 standard error) for the drift- and coversand samples are 0.95 ± 0.02 (n=21) and 1.06 ± 0.01 (n=6), respectively (open symbols in Fig. 2.5).

For each sample, 18 replicate measurements of the equivalent dose were made. The average values (± 1 standard error) are summarised in Table 1.1.

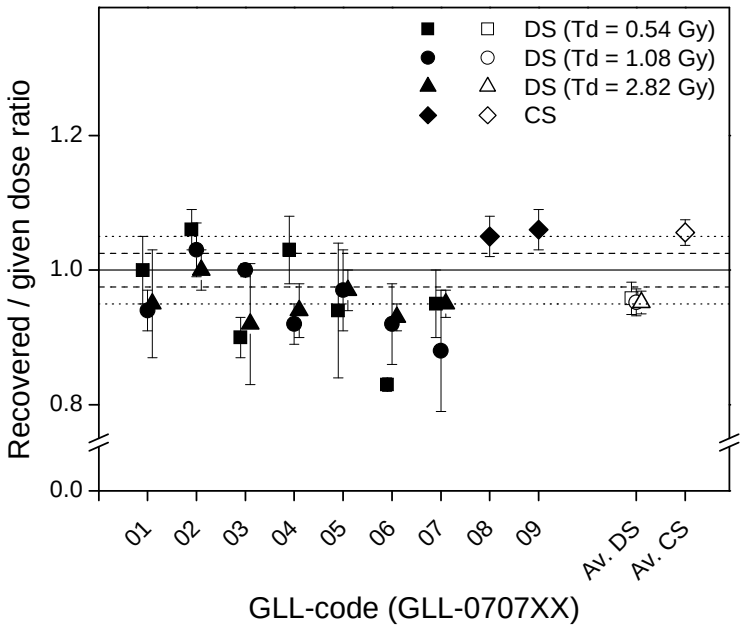

Fig. 2.5: Summary of the dose recovery data. Squares, circles and triangles show the measured to given dose ratios for the drift-sands (DS), obtained using the indicated test doses. Diamonds show the ratios obtained for the coversands (CS). Each datapoint (filled symbols) represents the average ± 1 standard error of three measurements; the open symbols show the overall averages ± 1 standard error. The solid line (eye guide) represents a recovered to given dose ratio equal to unity; the dashed and dotted lines (eye guides) bracket a 2.5% and a 5% deviation from unity, respectively.

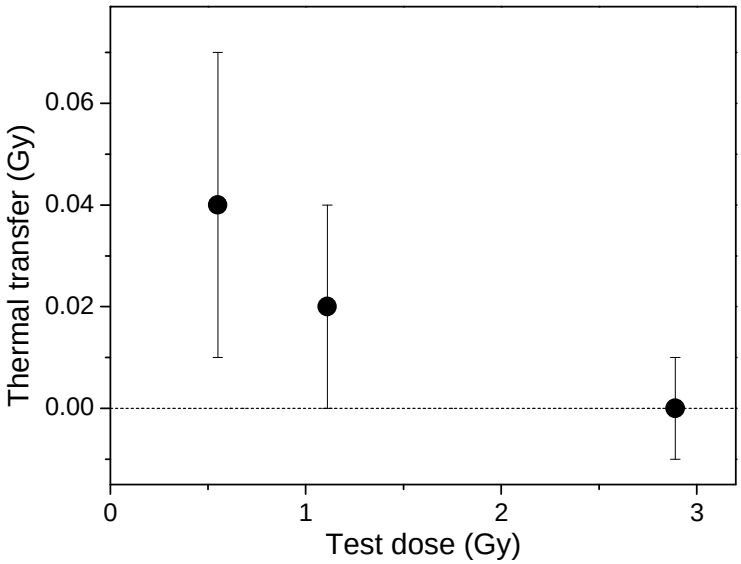

Fig. 2.6: Dependence of the thermally transferred dose on of the size of the test dose.

Sample GLL-code	Depth (cm)	^{234}Th (Bq kg^{-1})	^{226}Ra (Bq kg^{-1})	^{210}Pb (Bq kg^{-1})	^{232}Th (Bq kg^{-1})	^{40}K (Bq kg^{-1})	Water Content (%)	Total Dose rate (Gy ka^{-1})	D_e (Gy)	Age (ka)	σ_r (%)	σ_{sys} (%)	σ_{tot}	
													(%)	(ka)
070701	90	10 ± 1	12 ± 1	9 ± 1	9.1 ± 0.2	169 ± 2	10 ± 3	0.99 ± 0.01	1.22 ± 0.03	1.2	2.9	7.7	8.2	0.1
070702	120	9 ± 1	7 ± 1	11 ± 1	7.5 ± 0.1	161 ± 2	10 ± 3	0.95 ± 0.02	1.13 ± 0.03	1.2	3.2	7.7	8.3	0.1
070703	150	8 ± 1	6 ± 1	9 ± 1	5.5 ± 0.1	159 ± 2	10 ± 3	0.87 ± 0.01	1.06 ± 0.02	1.2	2.7	7.7	8.2	0.1
070704	190	9 ± 1	7 ± 1	10 ± 1	5.9 ± 0.1	169 ± 2	10 ± 3	0.92 ± 0.02	1.08 ± 0.02	1.2	2.7	7.7	8.2	0.1
070705	225	8 ± 1	6 ± 1	10 ± 2	5.3 ± 0.2	162 ± 2	10 ± 3	0.87 ± 0.02	1.11 ± 0.04	1.3	4.4	8.1	9.2	0.1
070706	225	8 ± 1	7 ± 1	10 ± 1	5.9 ± 0.2	161 ± 2	10 ± 3	0.88 ± 0.01	1.10 ± 0.02	1.3	2.5	8.1	8.5	0.1
070707	225	5 ± 1	6 ± 1	7 ± 1	4.5 ± 0.1	162 ± 2	10 ± 3	0.81 ± 0.01	1.03 ± 0.02	1.3	2.6	8.1	8.5	0.1
070708	300	14 ± 1	17 ± 1	18 ± 1	13.4 ± 0.2	264 ± 3	12 ± 3	1.39 ± 0.02	21.0 ± 0.6	15.1	3.2	8.5	9.0	1.4
070709	325	13 ± 1	17 ± 2	17 ± 1	13.7 ± 0.2	260 ± 3	12 ± 3	1.35 ± 0.02	24.0 ± 0.8	17.7	3.6	8.5	9.2	1.6

Table 2.1: Summary of the radionuclide activities, estimated time-averaged moisture contents, calculated dose rates, equivalent doses (De), optical ages, and random (σr), systematic (σsys) and total uncertainties (σtot). The uncertainties mentioned with the dosimetry and De data are random; all uncertainties represent 1σ. All sources of systematic uncertainty were assessed following Vandenberghe et al. (2004; see also Vandenberghe, 2004). The uncertainties were propagated following the error assessment system proposed by Aitken and Alldred (1972) and Aitken (1976).

2.6. DOSIMETRY

Radionuclide concentrations were derived from high-resolution gamma-ray spectrometry and the dose rates were calculated from the measured specific activities using conversion factors derived from the nuclear energy releases tabulated by Adamiec and Aitken (1998). A factor of 0.9 (± 5% relative uncertainty) was adopted to correct the external beta dose rates for the effects of attenuation and etching (Aitken, 1985). An internal dose rate in quartz grains of 0.010 ± 0.002 Gy/ka was assumed (Vandenberghe et al., 2008). Taking into account that the site is situated on an elevated and therefore drier location, we adopted a time-averaged moisture content of 10 ± 3% and 12 ± 3% for the drift- and coversands, respectively; increasing the water content with 1% increases the optical age by ~1%. The contribution from cosmic radiation was calculated following Prescott and Hutton (1994). The dosimetric information is summarised in Table 1.1.

2.7. LUMINESCENCE AGES AND DISCUSSION

The optical ages are synthesised in Table 1.1 and in Fig. 2.7. It can be seen that the systematic uncertainty is dominant in the overall uncertainty on the ages, which amounts to ~8-9% (1□). As the sources of systematic uncertainty are largely correlated from sample to sample, only the random uncertainties (~3-4%) are considered to evaluate the internal consistency of the optical ages. Within this uncertainty, the dataset contains no outliers and the age results are consistent with the stratigraphic position of the samples. Therefore, it is concluded that all sources of random uncertainty have been properly accounted for and that the observed variation in the age results is not larger than that expected from the individual uncertainties.

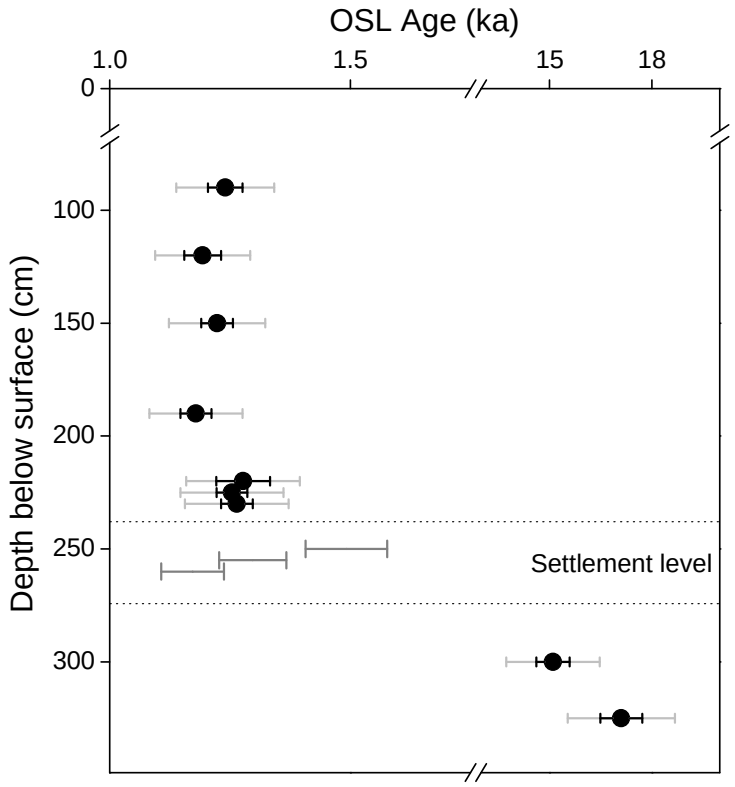

Fig. 2.7: Plot of the optical and radiocarbon ages against the depth below the surface. The optical ages are shown as filled circles, with the associated random and total uncertainties indicated by the black and grey error bars, respectively. The calibrated radiocarbon ages (expressed as ka before 2007) are shown as age ranges in dark grey. The dotted lines indicate the level of the settlement.

The optical ages for the drift-sands do not increase with depth. The average age of all seven samples is 1.2 ± 0.1 ka, which points to deposition during the Early Middle Ages. This date is in line with the radiocarbon ages obtained for the wooden fragments of the well shuttering and the typological age of the ceramics (Section 2.3). The lack of significant differences among the ages is interpreted as evidence for the rapid sedimentation of the drift-sands. An alternative explanation is post-depositional mixing of the entire deposit. However, this hypothesis is not considered to be very likely, because of the good conservation of sedimentation structures and the absence of macroscopic evidence for turbation processes.

The two coversand samples yield optical ages of 15.1 ± 1.4 ka and 17.7 ± 1.6 ka, which confirms that the settlement is situated on a sequence of coversands that was deposited during the Weichselian Late Pleniglacial.

2.8. CONCLUSIONS

Dating of the drift-sand deposits at Pulle yielded an internally consistent set of optical ages, which are in agreement with the independent age information for the underlying settlement level. We conclude that sand-drifting at Pulle occurred during a single, fairly short event in the Early Middle Ages. As no archaeological remains dating from the post-sand-drifting period were found, it is most likely that sand-drifting put an end to the human occupation at Pulle. After the sand-drifting event, man may have left the site until agricultural activities intensified, as is suggested by the presence of plaggen soils on the flanks of the drift-sand dune.

Although minor drift-sand sedimentation occurred before, major phases of sand-drifting in NW Europe are generally thought to have started in the 10^{th}-12^{th} century (Castel et al., 1989; Koster et al., 1993). These large-scale drifting events are believed to originate with an increasing population pressure, resulting in large-scale deforestation, intensified heathland exploitation and rapid expansion of arable fields. This study illustrates that human cultural activities could exceed the capacity of the local environment at earlier times as well. This contrasts with the commonly held assumption that, in our study area, the Early Middle Ages represent a phase of landscape stability during which the human impact on the landscape was not large enough to cause sand-drifting. As such, the present study illustrates how optical dating may contribute to an improved understanding of the interaction between human activity and geomorphological processes. The results also illustrate (the limit on) the time resolution by which phases of sand-drifting can be distinguished through conventional quartz single-aliquot OSL dating.


C16
C31
C32
C0
C34
C26
C11

Chapter 3

Revisiting a type locality for Late Glacial aeolian sand deposition in NW Europe: Optical dating of the dune complex at Opgrimbie (NE Belgium)

Chapter published in full as:
Derese, C., Vandenberghe, D., Paulissen, E., Van den haute, P., 2009. Revisiting a type locality for Late Glacial aeolian sand deposition in NW Europe: Optical dating of the dune complex at Opgrimbie (NE Belgium). Geomorphology 109, 27-35.

CHAPTER 3. REVISITING A TYPE LOCALITY FOR LATE GLACIAL AEOLIAN SAND DEPOSITION IN NW EUROPE: OPTICAL DATING OF THE DUNE COMPLEX AT OPGRIMBIE (NE BELGIUM)

3.1. ABSTRACT

The Late Glacial dune complex at Opgrimbie (NE Belgium) is thought to represent a complete record of the Late Pleniglacial to Holocene change in the southernmost part of the coversand area. In this work, the chronology of the site was reinvestigated using quartz-based single-aliquot optical dating. Nine samples in total were collected from sediments above and below a bleached horizon, the Opgrimbie layer, which laterally passes into a sandy peat layer; earlier radiometric radiocarbon dating and pollen analyses showed the latter to be of Bølling age (14.8-14.1 ka calBP). The sampled sequence is overlain by a second horizon, the Usselo horizon, for which an Allerød age (14.0-13.0 ka calBP) was deduced from one radiometric ^{14}C age and palynological evidence. This was confirmed by AMS data obtained as part of this study.

All nine quartz samples showed satisfactory luminescence characteristics, and yielded an internally consistent set of optical ages. The dataset contains no clear outliers and the observed variation is not much larger than that expected from uncertainties. The sediments over- and underlying the lowermost bleached horizon are dated at 12.9 ± 0.9 ka (n=6) and 13.0 ± 0.8 ka (n=3), respectively. These ages do not confirm the Bølling age that was previously established for this horizon; the optical ages are, however, consistent with the chronostratigraphical position of the sediments below the Usselo soil of Allerød age. As such, the OSL ages question if the Lateglacial aeolian succession is fully developed at Opgrimbie, and they challenge its significance as a type locality.

3.2. INTRODUCTION

The Late Glacial, which is the transition interval from the Weichselian Late Pleniglacial to the present interglacial (Holocene), is characterised by pronounced climatic oscillations that are recorded in high-resolution palaeoenvironmental archives, such as marine and limnic varves, ice-cores and terrestrial sediments (see e.g. Yu et al., 2008). In the NW European coversand belt, the climatic fluctuations resulted in varying intensities of aeolian activity and vegetation growth and thus in an alternation of phases of widespread sand deposition and periods marked by landscape stabilisation, reflected in soil formation and eventually peat growth. The ages of the Late Glacial pollen zone boundaries in NW Europe are reviewed by Hoek (2001) and have resulted in the following ^{14}C based time scale: Earliest Dryas (15.5-14.8 ka calBP), Bølling (14.8-14.1 ka calBP), Early Dryas (14.1-14.0 ka calBP), Allerød (14.0-13.0 ka calBP) and Late Dryas (13.0-11.7 ka calBP). This chronostratigraphical framework will be employed in this study. Nearly identical age boundaries have been obtained by Magny (2001) on the Swiss Plateau and in Eastern France, except for the Allerød which, according to this author, ranges between 13.9 and 12.7 ka calBP.

Only a few places exist within the NW European coversand belt where both Bølling and Allerød organics or soil horizons can be identified and thus where these stadial episodes can be differentiated. In most cases, organic matter and soil horizons formed during the Bølling period are lacking, and the sediments dating from the Late Pleniglacial and from the Early Dryas period form a single unit below the frequently occurring Allerød soil (Kasse, 2002; Kasse et al., 2007). The scarcity of Bølling soils and organics is generally explained by the continuation of aeolian deposition throughout the entire early Late Glacial until the Allerød period (Kasse, 1999; 2002; Kasse et al., 2007). Peat formation during the Bølling appears to have occurred only in local wet environments (seepage zones), for example at Opgrimbie (Paulissen and Munaut, 1969), Usselo (Van Geel et al., 1989) and Oud-Lutten (Kasse, 1999). At these specific sites, the organic deposits are very sandy or contain sandy laminae, pointing to a continued aeolian activity and/or erosion by runoff waters from the dune slopes during the organic accumulation.

Due to the presence of both Bølling and Allerød peat at Opgrimbie, individually grading into a bleached layer, the dune complex at Opgrimbie is generally considered as a key section for the stratigraphy of the Late Glacial sandy aeolian deposits in the southernmost part of the NW European coversand belt. The site has been previously investigated by Paulissen and Munaut

(1969). Their detailed study used radiometric radiocarbon dating of bulk organic samples, combined with sedimentological and palynological analyses to reconstruct the local palaeoenvironment and to constrain the age of the dune complex. Since then, however, considerable advances in dating technology have been made, such as the introduction of accelerator mass spectrometry (AMS) in radiocarbon dating, and new techniques, such as luminescence dating, have become available. Luminescence dating is a more appropriate method for determining the time of sediment deposition and accumulation; it uses the constituent mineral grains of the sediment itself and establishes when they were last exposed to sunlight. The technique is increasingly used in a wide variety of Quaternary studies and it has been successfully applied to comparable deposits in the West European lowlands (see e.g. Vandenberghe et al., 2004; Kasse et al., 2007; Vandenberghe et al., 2009).

In the present study, the chronology of the Late Glacial dune complex at Opgrimbie was reinvestigated using quartz-based optical dating of the aeolian deposits and AMS radiocarbon dating of intercalated organic matter. This optical dating study is one of the first steps towards the establishment of a reliable chronological framework for the Late Glacial in NE Belgium.

3.3. GEOLOGICAL SETTING AND SEDIMENTARY SUCCESSION

The village of Opgrimbie is situated in the northeastern part of Belgium, ~10 km north of the southernmost edge of the NW European coversand belt (Fig. 3.1). It is located in the Meuse valley, close to the eastern scarp delimiting the Campine plateau. In this area, the plateau is composed of fan-shaped fluvial gravel and sand deposits that rise about 25 m above the river valley to form one of the high terraces of the Meuse River. The Campine plateau is covered with windblown sands mainly of Weichselian age. According to the most recent lithostratigraphic subdivision of the Belgian Quaternary (Gullentops et al., 2001), these coversands belong to the Wildert Member of the Gent Formation. During the Late Glacial and Holocene, the sands were locally blown up into coversand ridges and land dunes, for instance at Opgrimbie.

Fig. 3.2a shows a schematic profile of the lee side of the dune complex at Opgrimbie (adapted from Paulissen and Munaut, 1969), of which the main part (including the dune crest) was quarried during the early 1960s. As our optical dating study was focused on a ~1 m wide vertical section in the dune flank only (Fig. 3.2b), the following description of the entire dune complex is based on the observations by Paulissen and Munaut (1969). The sedimentary

succession consists of a ca. 3.5 m high sequence of aeolian sands and two intercalated peat layers at the lee side of the dune, which laterally pass into bleached horizons near the dune crest. According to Paulissen and Munaut (1969), the dune sands were deposited on top of a slightly inclined gravel bed. This gravel deposit was identified as the alluvial fan of the Kikbeek River, one of the small rivers draining the eastern slope of the Campine plateau. During (part of) the Holocene, a humo-ferric podzol developed in the upper part of the dune sediments and this stabilised the dune. The grain size of the sandy deposits is very uniform, with a mean mode of 160 µm. Both the silt and clay fractions amount to less than 2% of the sediment, except in the two bleached horizons where the fine fraction constitutes more than 5% of the total. This high level of sorting is due to the renewed transportation and deposition of the coversands as dune sands. With regard to the intercalated peat horizons, the lowermost horizon consists of a sandy peat, slightly affected by cryoturbation. The lower part of the uppermost peat horizon is marked by a gradual transition from dune sand to pure peat, whereas its upper boundary is characterised by an alternation of sand and peat layers due to the recurrent interruption of the peat accumulation by aeolian deposition at the beginning of the Late Dryas period.

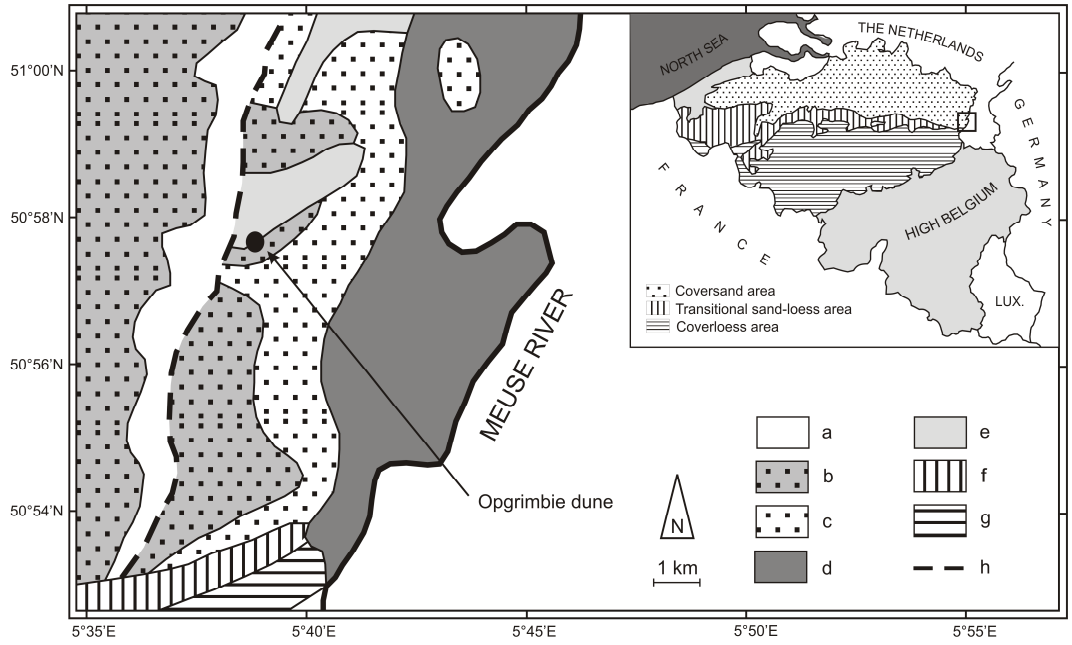

Fig. 3.1: Location map of the study site, showing the distribution of Quaternary deposits in the region (adapted from Maréchal, 1992). a: areas with a thin cover of or without Quaternary deposits, b: gravel beds, c: gravel beds covered by sands, d: alluvial deposits, e: sands (land dunes), f: sand-loess, g: loess, h: eastern scarp of the high terrace of the Meuse river (Campine plateau). The inset illustrates the location of the dune complex in a broader context.

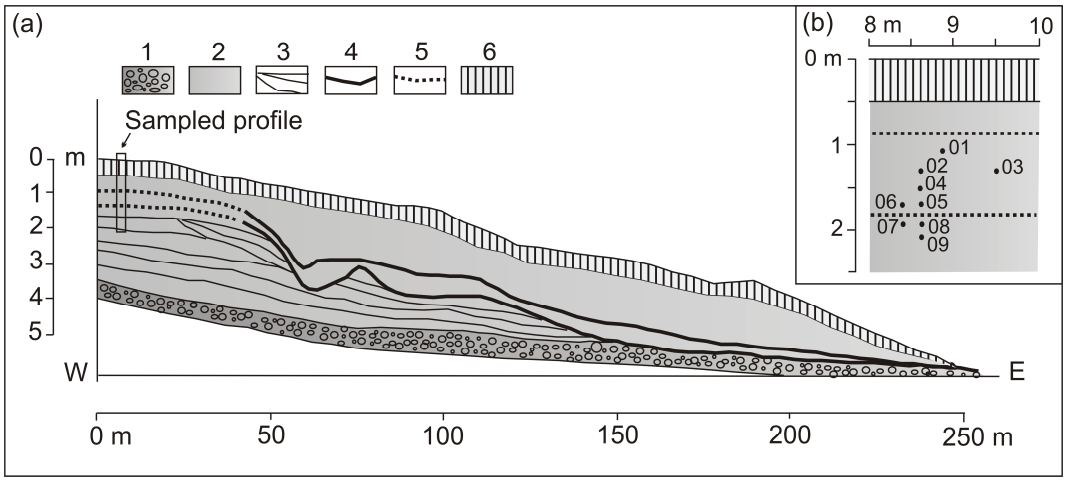

Fig. 3.2: (a) Schematic profile of the dune complex at Opgrimbie (adapted from Paulissen and Munaut, 1969). 1: gravel bed, 2: sand, 3: cross-bedded lamination, 4: peat layer, 5: bleached horizon, and 6: Holocene soil. The inset (b) is a simplified representation of the sampled section, showing the location of the samples for luminescence dating.

3.4. INDIRECT AGE DETERMINATION OF THE AEOLIAN ACTIVITY

Paulissen and Munaut (1969) derived the timing of the aeolian activity from radiometric radiocarbon dating of bulk material from each of the intercalated organic layers and from palynological analyses. Their main findings can be summarised as follows. Phases of aeolian activity are mainly characterised by a herbaceous vegetation, whereas the periods of dune stabilisation and soil formation are marked by an expansion of birch and a birch/pine succession, for the lower and upper peat layer, respectively. Based on the palynological data, the lowermost humic layer was attributed to the Bølling Interstadial period and the uppermost organic horizon to the Allerød period. Radiocarbon dating of both peat layers confirmed the interpretation of their pollen assemblages (Lv-456 and Lv-457 in Table 3.1). Table 3.1 summarises the conventional and calibrated radiocarbon ages. The conventional ^{14}C ages were calibrated using the OxCal program (version 4.0; Bronk Ramsey, 1995; 2001) and the IntCal04 calibration curve (Reimer et al., 2004). To facilitate comparison with the results from optical dating, the calibrated radiocarbon ages are expressed as the 68.2% probability age range in ka calBP, with AD 2000 defined as the present (obtained by adding 50 years to the CalBP years). The lowermost sandy peat layer was dated at 15.2-14.5 ka calBP (sample Lv-456), while the uppermost humic horizon was dated at 14.0-13.6 ka calBP (sample Lv-457). Based on these findings, Paulissen and Munaut (1969) distinguished three successive phases of dune formation and concluded that these occurred during the Earliest Dryas (15.5-

14.8 ka calBP), the Early Dryas (14.1-14.0 ka calBP) and the Late Dryas (13.0-11.7 ka calBP; absolute ages according to Hoek, 2001). Following this, Paulissen and Munaut (1969) proposed names for the two bleached horizons, laterally grading into the ^{14}C-dated peat layers. The uppermost horizon was considered as the lateral equivalent of the widespread Usselo soil of Allerød age and was therefore named after this marker horizon. The lowermost horizon of Bølling age was defined as the Opgrimbie soil.

Sample lab code	**Method**	**Material**	**δ^{13C} (‰PDB)**	**^{14}C age**	**Calibrated age (ka before AD 2000)**
Lv-457	Radiometric	Uncharred remains from uppermost peat horizon (bulk)	No data	11 910 ± 170 BP (measured)	14.0-13.6 (68.2%)
Beta-233428	AMS	Charcoal from uppermost bleached horizon	-25.3	11 870 ± 60 BP (conventional)	13.9-13.7 (68.2%)
Beta-233429	AMS	Charcoal from uppermost bleached horizon	-26.1	11 160 ± 50 BP (conventional)	13.2-13.0 (68.2%)
Lv-456	Radiometric	Uncharred remains from lowermost sandy peat horizon (bulk)	No data	12 640 ± 190 BP (measured)	15.2-14.5 (68.2%)

Table 3.1: Summary of the new and existing ^{14}C ages and δ^{13}C values (where available). Calibration of the ^{14}C ages was performed using OxCal (Bronk Ramsey, 1995; 2001); probabilities are given between parentheses. To facilititate comparison with the OSL ages, 50 yr was added to the calibrated BP (1950 AD) ages. Samples Lv-457 and Lv-456 were collected from the peat layers at the lee side of the dune and were dated by Paulissen and Munaut (1969). Samples Beta-233428 and Beta-233429 were dated using AMS in this study and were collected from the uppermost bleached horizon in the dune crest. Unlike the AMS data, the ^{14}C ages of the peat were not determined using the conventions introduced by Stuiver and Polach (1977). To make this distinction, the terms "measured" and "conventional" are used to denote the previously and newly obtained radiocarbon ages, respectively.

Within the context of this work, two new AMS radiocarbon dates were obtained for macroscopic charcoal fragments from the uppermost bleached horizon, the Usselo layer. No (charred) material suitable for ^{14}C dating could be retrieved from the lowermost bleached horizon, the Opgrimbie layer. A calibrated age of 13.9-13.7 ka calBP was obtained for sample Beta-233428, while sample Beta-233429 was dated at 13.2-13.0 ka calBP (Table 3.1).

Overall, the AMS radiocarbon dataset is in good agreement with the previous interpretation that the uppermost bleached horizon represents the Usselo layer of Allerød age (normally attributed to 14.0 to 13.0 ka calBP). However, the ages of the two charcoal fragments are

significantly different, with one charcoal sample situated at the beginning and the other near the end of the Allerød. One interpretation of the overall presence of charcoal fragments in the Usselo layer is that, near the end of the Allerød period, the extensive and dense pine forests became prone to forest fires and burnt down over large areas; numerous charcoal fragments were left behind, which were incorporated in the soil by bioturbation (Paulissen and Munaut, 1969; Hoek and Bohncke, 2002). The AMS radiocarbon age of 13.2-13.0 ka calBP is consistent with this interpretation. The radiocarbon age of 13.9-13.7 ka calBP dates from the beginning of the Allerød; however, this single age estimate does not allow evaluating the scale and significance of the event to which it relates.

3.5. OPTICALLY STIMULATED LUMINESCENCE (OSL) DATING

3.5.1. Sampling

For this optical dating study, a ~210 cm high profile at the lee side of the dune, near the dune crest, was investigated (Fig. 3.2). A high-resolution sampling strategy was applied with the sediments being sampled at intervals of ~20 cm and multiple samples being taken from the same stratigraphic level, to give nine samples in total (Fig. 3.2b). Six OSL samples were collected from the ca. 0.80 m thick sediment unit intercalated between the two bleached horizons and three samples from the top of the ca 2.30 m thick sandy deposit underlying the Opgrimbie layer. Three undisturbed samples were taken for evaluation of the time-averaged wetness of the sediments; they were collected from the same stratigraphic level as samples GLL-060702, -04 and -07, respectively (two above and one below the Opgrimbie layer). No samples could be collected from the 1 m thick sand layer above the uppermost bleached horizon, because there were too many perturbations with roots and burrows related to the podzolisation processes. All samples were collected by gently hammering stainless steel cylinders into the freshly cleaned sediment wall. About 1 kg of the surrounding sediment was taken for dose rate determination.

3.5.2. Sample preparation and analytical facilities

Coarse (180-212 µm diameter) quartz grains were extracted using conventional sample preparation techniques (HCl, H_2O_2, sieving, heavy liquids, HF). The purity of the quartz extracts was confirmed by the absence of a significant infrared stimulated luminescence (IRSL) response at 60°C to a large (~50 Gy) regenerative β-dose. The sensitivity to infrared stimulation was defined as significant if the resulting signal amounted to more than 10% of the corresponding OSL signal (Vandenberghe, 2004) or if the IR depletion ratio deviated more than 10% from unity (Duller, 2003).

All OSL measurements were performed using an automated Risø TL/OSL-DA-12 reader, equipped with blue (470 ± 30 nm) LEDs and an IR laser diode (830 nm); the quartz luminescence emissions were detected through 7.5 mm of Hoya U-340 UV filter. Details on the measurement apparatus can be found in Bøtter-Jensen et al. (2003).

3.5.3. Equivalent dose determination

The equivalent dose (D_e) was determined using the single-aliquot regenerative-dose (SAR) procedure (Murray and Wintle, 2000). Our protocol used stimulation with blue LEDs for 40 s at a temperature of 125°C, and the initial 0.32 s of the decay curve was used in further calculations, less a background evaluated from the last 4 s of stimulation. The same background as calculated for the natural and regenerated signals was used for the corresponding test dose signals. A preheat of 10 s at 240°C and a test-dose cutheat to 160°C were adopted; the size of the test dose amounted to ~50% of the estimated natural dose. After the measurement of each test dose signal, a high-temperature bleach was performed by stimulation with the blue diodes for 40 s at 280°C (Murray and Wintle, 2003). For each aliquot that was measured, a complete growth curve was constructed based on the measurement of the response to five regenerative doses (up to 2.5 times the estimated equivalent dose). The SAR protocol also involved the measurement of the response to a zero dose to determine whether the growth curve passes through the origin (to assess recuperation), and a repeat measurement of the response to the lowest regenerative dose to evaluate the performance of the sensitivity correction (known as the recycling ratio). At the end of the measurement sequence, a second measurement of the response to the highest regenerative dose was performed. This time, however, the sensitivity to IR stimulation was checked before

stimulation with blue diodes in order to identify aliquots with a significant feldspar contamination. The measured aliquots were accepted if the recuperation and IRSL/OSL ratio did not exceed a threshold set at 10% and if both the recycling ratio and the IR depletion ratio were within 10% of unity. None of the analysed aliquots had to be rejected on the basis of these criteria.

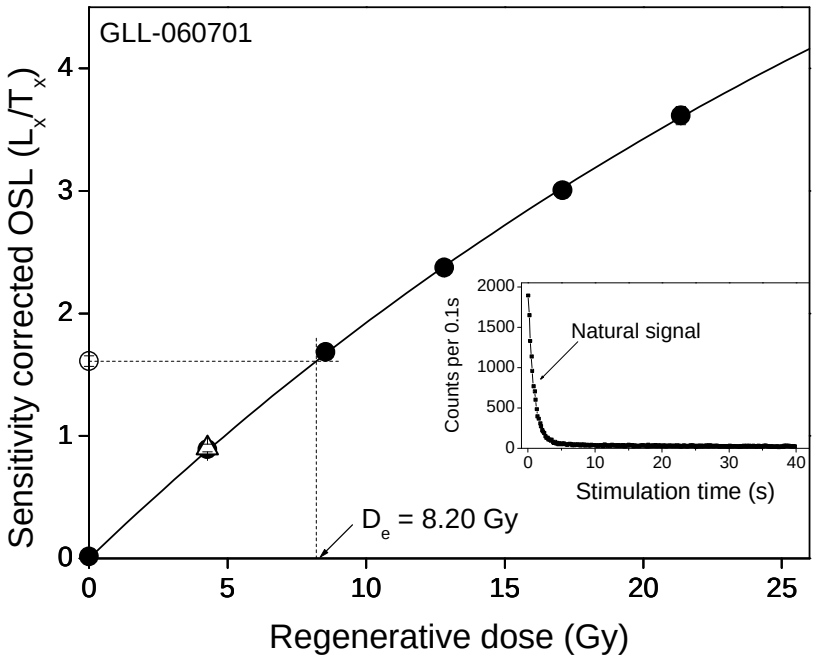

Fig. 3.3: Illustrative SAR growth curve and natural luminescence decay curve (inset) for an aliquot of 180-212 µm quartz extracted from sample GLL-060701. The solid line is the fit of the data to a single saturating exponential function. The open triangle represents a recycling point. The equivalent dose is obtained by interpolation of the sensitivity-corrected natural OSL signal (open circle) on the corrected growth curve.

A representative SAR growth curve for an aliquot of sample GLL-060701 is shown in Fig. 3.3; it illustrates the generally good behaviour of the samples in the SAR protocol, with recycling ratios close to unity and recuperation less than a few % of the corrected natural signal.For each sample, 18 measurements of the D_e were made on large (7 mm diameter) aliquots; the unweighted mean D_e values and corresponding standard errors are summarised in Table 3.2.

3.5.4. Dose recovery tests

Dose recovery tests (Murray and Wintle, 2003) were performed to evaluate the performance of the applied SAR procedure. Natural aliquots were bleached twice for 250 s using the blue diodes at room temperature; the two bleaching treatments were separated by a 10 ks pause. The aliquots were then given a known laboratory dose equal to their estimated equivalent dose and measured using the SAR protocol. For three samples, dose recovery tests were performed using eight different preheat temperatures ranging from 160°C to 300°C. The results for sample GLL-060701 are summarised in Fig. 3.4; the dose recovery tests for the two other samples yielded similar results. The measured doses are insensitive to preheat temperatures up to 280°C and match the given doses acceptably well. For the remaining six samples, dose recovery tests were carried out using a preheat of 10 s at 240°C only. The results for all nine samples at this preheat are shown in Fig. 3.5. Averaged over all samples, a measured to given dose ratio (± 1 standard error) of 0.974 ± 0.013 (n=9) was derived. The overall average recycling ratio is 0.972 ± 0.009, while the overall average recuperation is 2.3 ± 0.3%. The results from the dose recovery tests indicate that the SAR protocol is suitable to measure a laboratory dose given prior to any heat treatment.

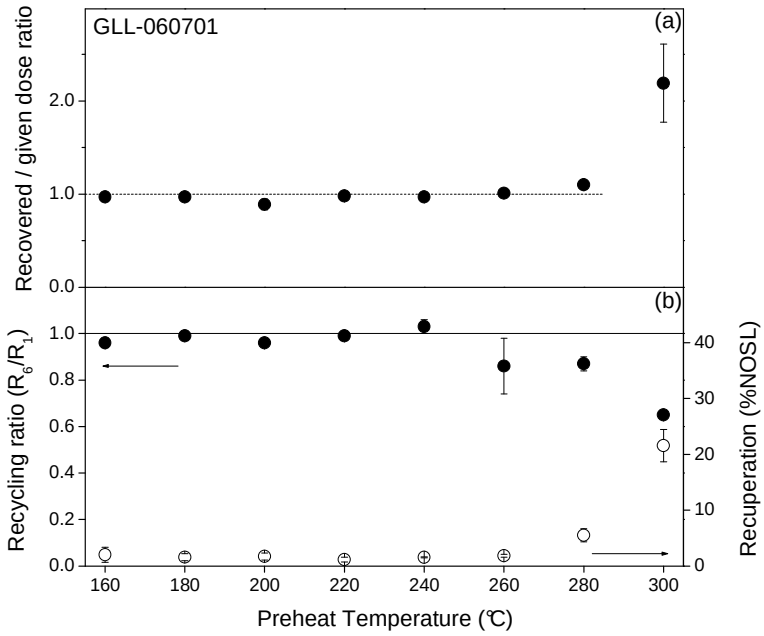

Fig. 3.4: (a) Recovered to given dose ratios as a function of preheat temperature for sample GLL-060701. Each datapoint represents the average ± 1 standard error of three measurements. The dotted line (eye guide) represents a measured to given dose ratio equal to unity. (b) Recycling ratios (filled circles) and recuperation values (open circles) observed for the same aliquots. The solid line (eye guide) represents a recycling ratio equal to unity.

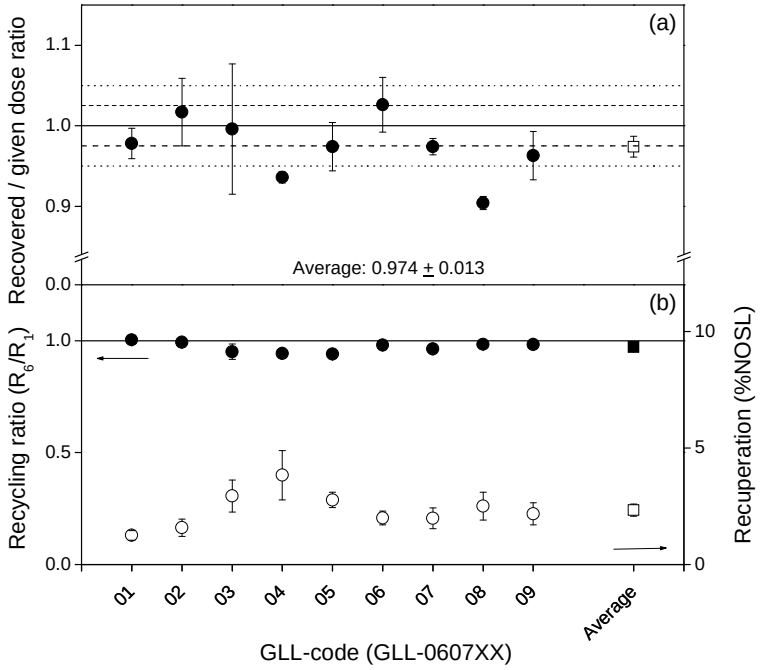

Fig. 3.5: (a) Synthesis of the dose recovery data. Each datapoint (filled circle) represents the average ± 1 standard error of six measurements; the open square represents the overall average measured to given dose ratio ± 1 standard error. The solid line (eye guide) represents a recovered to given dose ratio equal to unity. The dashed and dotted lines (eye guides) bracket a 2.5% and a 5% deviation of the ratio from unity, respectively. (b) Corresponding recycling ratios (filled circles) and recuperation values (open circles).

3.5.5. Dose distribution

For sample GLL-060708, the distribution of equivalent doses was investigated using small aliquots (2 mm diameter, with each aliquot containing a few tens of grains). This sample was chosen because of its position below the Opgrimbie layer presumed to be of Bølling age (see Section 3.4). 119 small aliquots were analysed using the SAR protocol as outlined above. No aliquots were rejected based on the criteria outlined in the previous section. The D_e results from 119 small aliquots are presented both as a radial plot in Fig. 3.6a and as a histogram in Fig. 3.6b. A plot of D_e versus uncertainty is shown above the histogram.

The radial plot displays the individual D_e values and the related measurement precision, and allows evaluating whether 95% of these values indeed fall within ± 2σ of the central value. In this case, 91% of the D_e values fall within ±2σ of the weighted mean value of 8.02 Gy . The histogram (Fig. 3.6b) illustrates that the distribution is broad and slightly asymmetric, with a relative standard deviation of ~27%.

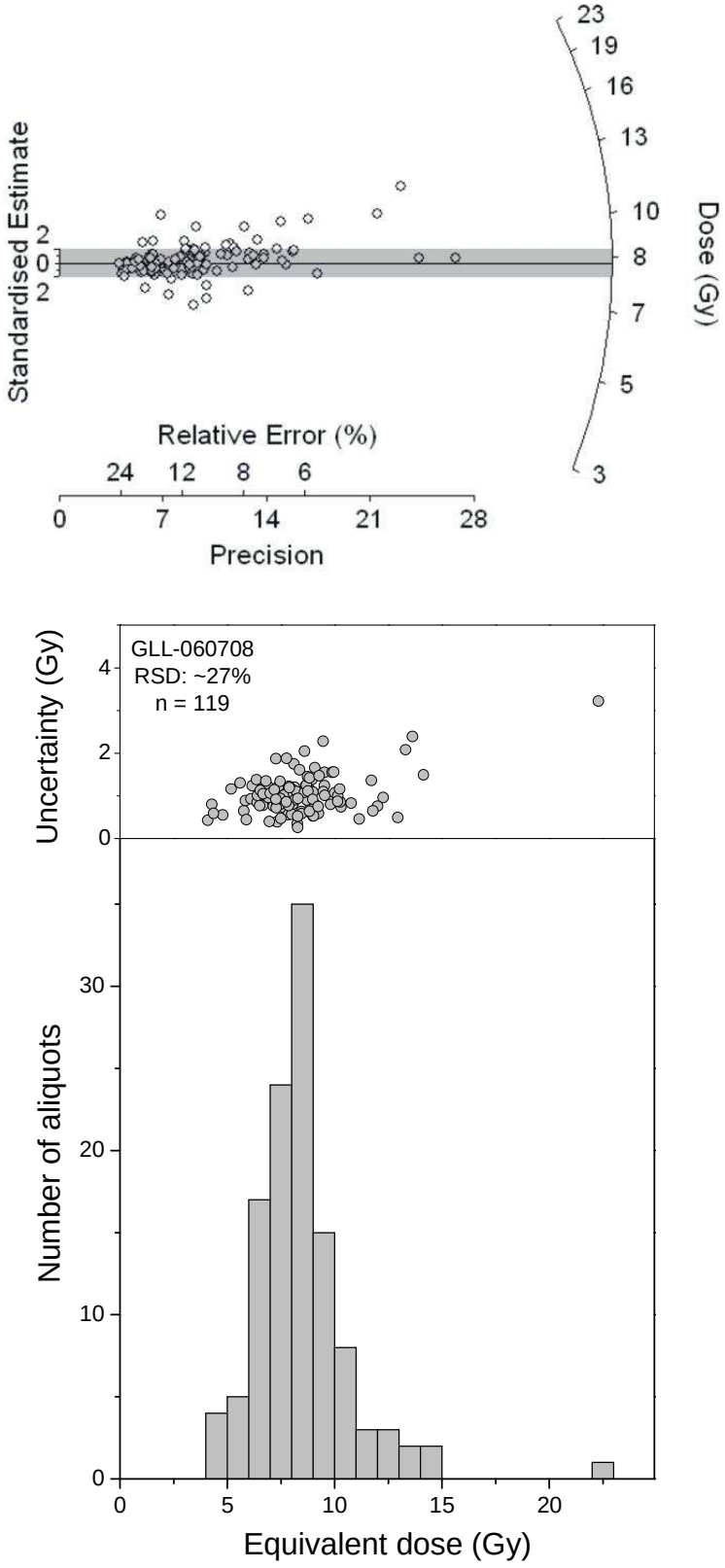

Fig. 3.6: Radial plot (above) and histogram (below) of the D_e values obtained for 119 small aliquots of sample GLL-060708. An instrumental uncertainty of 1% per OSL measurement has been incorporated in the uncertainty on the individual D_e values. A plot of the uncertainty versus D_e is shown above the histogram; the median from this uncertainty distribution was used for binning the data, resulting in a bin width of 1 Gy.

Typically, an uncertainty of about 1 Gy (or ~12% of the D_e) is associated with the individual D_e values. Both the radial plot and the D_e-uncertainty plot illustrate that counting statistics and instrument uncertainty (estimated at 1%) do not fully account for the observed spread in the data. Given the windblown nature of the investigated sediments and the absence of visible (bio)turbation structures in the sediment profile, partial bleaching and post-depositional mixing are not considered as plausible explanations for the observed distribution. Broad and slightly asymmetric distributions, with a spread in doses that is larger than expected from measurement and instrumental uncertainties, have previously been reported for well-bleached, undisturbed sediments (see e.g. Vandenberghe, 2004; Vandenberghe et al., 2003; 2009). Therefore, the dose distribution is interpreted as that for a well-bleached sample that is not affected by post-depositional mixing. Small-scale variations in dose rate are another potential source of variability and were found to the most likely explanation for the scatter in dose distributions of aeolian samples (coversands) in the southern Netherlands (Vandenberghe et al., 2003). This possibility was not explicitly investigated in the present study. However, if microdosimetric variations account for the spread in our small-aliquot data, they are not expected to have major implications towards the accuracy of the age determinations, provided that the scale of analysis (for sampling, and D_e and annual dose determination) is large enough to average out its effects. Hence, this was the approach followed throughout this work; equivalent dose determination used large (7 mm diameter) aliquots, while that of the annual dose used large (~130 g) subsamples taken from ~1 kg of homogenised sediment.

3.5.6. Dosimetry

Radionuclide activity concentrations were derived from high-resolution gamma-ray spectrometry and the dose rates were calculated from the measured present-day radionuclide activities using conversion factors derived from the nuclear energy releases tabulated by Adamiec and Aitken (1998). A factor of 0.9 (± 5% relative uncertainty) was adopted to correct the external beta dose rates for the effects of attenuation and etching (Mejdahl, 1979). An internal dose rate in quartz grains of 0.010 ± 0.002 $Gy.ka^{-1}$ was assumed (Vandenberghe et al., 2008). The evaluation of the time-averaged moisture content, and the corresponding correction for it of the dose rates, was performed following the procedure outlined in Aitken (1985). The water content in fully saturated sediment was measured in the laboratory using the samples that were specifically collected for this purpose (see Section 3.5.1). Values in the

range of 17-19% were obtained (see Table 3.2; W-values). The time-averaged water content was estimated to be equal to 90 ± 10% of the saturation content. The contribution from cosmic radiation was calculated following Prescott and Hutton (1994). The dosimetric information is summarised in Table 3.2.

3.5.7. Optical ages

Table 3.2 summarises the resulting optical ages and their associated uncertainties. The systematic uncertainty is dominant in the overall uncertainty on the ages, which varies in between ~7-9% (1σ). The overall contribution from random sources of uncertainty is in the range of ~2 to ~5%; it can be seen that, within this uncertainty, the dataset contains no clear outliers and shows no increase with depth (Table 3.2 and Fig. 3.7). Samples that were collected from exactly the same stratigraphic level (samples GLL-060702 and -03, GLL-060705 and -06, and GLL-060707 and -08) yield consistent age results as well. Therefore, it is concluded that all sources of random uncertainty have been properly accounted for, and that the observed variation in the age results is not (much) larger than that expected from the individual uncertainties.

An average optical age of 12.9 ± 0.9 ka (n=6) was obtained for the sediment unit between the two bleached horizons, while the sediments underlying the lowermost bleached horizon yield an age of 13.0 ± 0.8 ka (n=3). These results illustrate the time-resolution that can be achieved using the techniques employed in this work.

3.6. DISCUSSION

Within uncertainty, the average age of 12.9 ± 0.9 ka (n=6) for the sediment unit between the two bleached horizons agrees with the newly obtained AMS ^{14}C ages of 13.9-13.7 ka and 13.2-13.0 ka calBP for the uppermost bleached horizon and with the previously obtained bulk ^{14}C age (14.0-13.6 ka calBP) for the corresponding peat layer at the lee side of the dune (Table 3.1 and Fig. 3.7). The average optical age of 13.0 ± 0.8 ka (n=3) for the lowermost sediment unit, on the other hand, is significantly younger than the radiocarbon age of 15.2-14.5 ka calBP for the sandy peat layer.

In a recent investigation of two laminated Lateglacial aeolian sediment sequences in western Jutland (Denmark), Kolstrup et al. (2007) reported an apparent OSL age underestimation of ~10% compared to the corresponding ^{14}C data. Kolstrup et al. (2007) attributed this age difference to effects on the dose rate: (i) underestimation of the true saturated water content of the sediment layers and (ii) underestimation of the gamma dose rate because of the effects of the water-saturated organic layers. However, their investigated profiles consisted of an alternation of organic and inorganic layers, while our dune sequence is built up of aeolian sands and two intercalated bleached horizons. We have already made the assumption that the dune sediments were at saturation for 90% of their burial period. An increase in water content of 1% corresponds to an increase in the optical age of about 1%; when saturation for the whole time interval is presumed, the dose rate decreases and the ages increase by about 1.5% or 0.2 ka. However, it is highly unlikely that our samples were completely saturated throughout their entire burial period.

Another factor of uncertainty in the calculation of the dose rate is the internal radioactivity of the quartz grains. We assumed a value of 0.010 ± 0.002 $Gy.ka^{-1}$ as an upper limit to the internal dose rate, based on recent investigations by Vandenberghe et al. (2008). When the internal radioactivity is neglected, the ages increase by about 1.8% or 0.2 ka.

The assumption of both a zero internal radioactivity and complete saturation throughout the entire burial period increases the OSL results by ~3% (0.4 ka). However, a reduction of the dose rate by about 15% would be necessary to make the OSL results for the lowermost sediment unit consistent with the ^{14}C age of the overlying horizon. None of the effects outlined above can account for such a reduction. Therefore we conclude that we cannot identify any aspects of the dosimetry that are a sufficiently large source of error to account for the discrepancy between the OSL and the bulk ^{14}C date.

Post-depositional mixing (i.e. by dung beetles during the Allerød), resulting in erroneous equivalent doses, might lead to optical ages which do not accurately reflect the true time of sedimentation (see e.g. Vandenberghe et al., 2009). This hypothesis, however, cannot be supported by field observations (the sediments were stratified, no animal burrows have been found) or small aliquot analyses (Fig. 3.6).

Sample GLL-code	Depth (cm)	^{234}Th (Bq kg^{-1})	^{226}Ra (Bq kg^{-1})	^{210}Pb (Bq kg^{-1})	^{232}Th (Bq kg^{-1})	^{40}K (Bq kg^{-1})	W	Total Dose rate (Gy ka^{-1})	D_e (Gy)	Age (ka)	σ_r (%)	σ_{sys} (%)	σ_{tot}	
													(%)	(ka)
060701	107.5	4.1 ± 0.7	6.2 ± 0.9	5.2 ± 0.8	4.0 ± 0.2	129 ± 2	0.175	0.676 ± 0.012	8.9 ± 0.3	13.1	3.8	7.0	8.0	1.0
060702	130.5	3.4 ± 0.5	3.1 ± 0.7	3.5 ± 0.8	3.1 ± 0.1	80 ± 1	0.175	0.501 ± 0.010	7.0 ± 0.3	13.9	5.2	7.6	9.2	1.2
060703	130.5	4.6 ± 0.6	5.6 ± 0.9	5.2 ± 0.7	3.4 ± 0.2	80 ± 1	0.175	0.536 ± 0.010	7.0 ± 0.3	13	4.0	7.4	8.4	1.0
060704	154.5	3.8 ± 0.8	4.8 ± 0.9	3.4 ± 0.5	3.1 ± 0.1	109 ± 1	0.182	0.574 ± 0.008	7.1 ± 0.2	12.3	3.3	7.3	8.0	0.9
060705	169.5	3.9 ± 0.7	4.1 ± 0.9	3.4 ± 0.7	3.5 ± 0.1	151 ± 2	0.182	0.684 ± 0.010	8.8 ± 0.3	12.9	3.3	7.0	7.8	1.0
060706	169.5	3.1 ± 0.7	5.8 ± 0.8	4.4 ± 0.7	3.8 ± 0.1	164 ± 2	0.182	0.734 ± 0.010	9.0 ± 0.3	12.3	3.2	7.0	7.6	0.9
060707	191.0	5.6 ± 0.9	7.5 ± 0.9	5.0 ± 0.6	4.9 ± 0.1	163 ± 2	0.195	0.750 ± 0.010	9.1 ± 0.2	12.2	2.2	7.0	7.3	0.9
060708	191.0	5.6 ± 0.7	6.9 ± 0.7	5.5 ± 0.7	4.9 ± 0.1	152 ± 2	0.195	0.722 ± 0.011	9.4 ± 0.2	13	2.8	7.0	7.6	0.9
060709	206.0	4.4 ± 0.8	3.9 ± 1.0	2.9 ± 0.6	3.5 ± 0.2	139 ± 2	0.195	0.631 ± 0.009	8.7 ± 0.2	13.7	2.5	7.2	7.6	1.0

Table 3.2: Summary of the radionuclide activities, W values, calculated dose rates, equivalent doses (D_e), optical ages, and random (σ_r), systematic (σ_s) and total uncertainties (σ_{tot}). The uncertainties mentioned with the dosimetry and D_e data are random; all uncertainties represent 1σ.

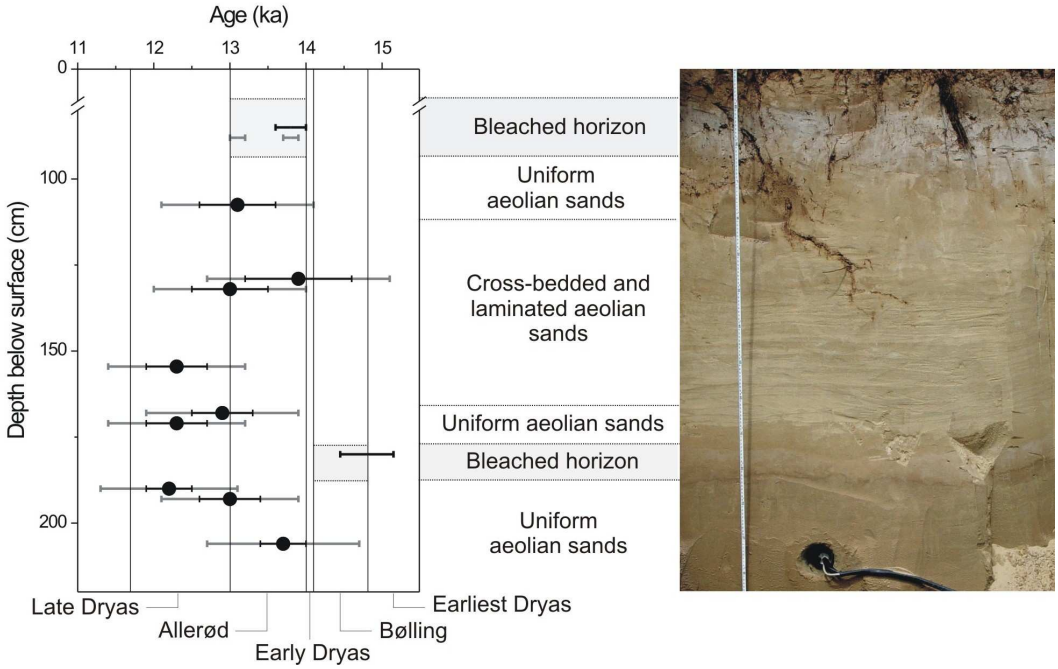

Fig. 3.7: Plot of the optical and radiocarbon ages against the depth below the surface. The optical ages are represented by black dots, while the associated random and total uncertainties are shown by black and dark grey error bars, respectively. The calibrated radiocarbon ages are represented as age ranges, the radiometric ages on the bulk samples in black and the AMS data on charcoal in dark grey. The vertical lines on the plot illustrate the ^{14}C based age boundaries of the biostratigraphic units of the Late Glacial, as reviewed by Hoek (2001). The shaded areas show where the two bleached horizons are situated in the dune profile, as is also illustrated on the photograph.

In conclusion, we find no evidence for effects that may cause the ages to be significantly and systematically in error. It is pointed out that such effects (such as an erroneous assessment of the true water content) are expected to affect all ages (almost) equally so that such a dataset could still show an increase with depth or reveal hiatuses in a sediment sequence. To this respect, the optical ages quoted in Table 3.2 rather point at a single event, at least within the time-resolution that could be achieved using the techniques employed in this work. In general, there is no evidence for quartz SAR-OSL ages to be affected by significant systematic errors (Murray and Olley, 2002). Previous studies of aeolian sequences in the southern Netherlands (Vandenberghe et al., 2004) and north-eastern Belgium (Vandenberghe et al., 2009) also reported a good agreement between optical dating and independent (^{14}C) age information. In the present study, the good agreement between the OSL dataset and the AMS ages for the

uppermost bleached horizon provides the local evidence for the reliability of the optical ages. It is therefore concluded that all the evidence points to the optical age results to represent an accurate sedimentation chronology for the dune sands at Opgrimbie.

Another possible explanation for the discrepancy between OSL and the bulk radiocarbon age for the sandy peat is an inaccurate ^{14}C date for sample Lv-456. It is well known that radiocarbon bulk dates of peat can be problematic (Olsson, 1986; Törnqvist et al., 1992; Shore et al., 1995; Lowe and Walker, 1997; 2000); they can be either too young or too old, for a number of reasons. However, as it is impossible to investigate the material that was dated more then 40 years ago, it is difficult to evaluate the intrinsic accuracy of the ^{14}C date for sample Lv-456.

Thus we conclude that the causes for the discrepancy are not yet understood, but, from the above, we have no reason to doubt the accuracy of the luminescence dataset. On the basis of the optical age results, it appears that the two bleached horizons belong to one soil complex that formed during the Allerød Interstadial, implying that the lowermost soil horizon, characterised by the presence of birch pollen (Paulissen and Munaut, 1969), would represent the *Betula* phase of this period. Interestingly, a similar soil complex consisting of two superimposed bleached horizons has previously been observed in Noord-Brabant (S Netherlands) by Wouters (1957). There, the layers, which contained charcoal and artefacts, were found to represent an inter-fingered Usselo soil of Allerød age. If the same situation is indeed reflected at Opgrimbie, this would mean that a significant part of the dune sequence accumulated subsequent to the Bølling period. In this case, the dune complex at Opgrimbie can no longer be retained as a type locality for the Late Glacial in the southernmost part of the NW European coversand belt. At the very least, the OSL and AMS results provide evidence for significant aeolian activity and fairly rapid sand deposition during the pre-Allerød period of the Late Glacial.

Further research is necessary to identify the cause for the discrepancy between the newly established OSL chronology and the previous chronostratigraphic interpretation of the dune complex. A detailed chronological investigation using both OSL and AMS ^{14}C methods of the succession at the lee side of the dune will help to resolve this matter.

3.7. CONCLUSIONS

The chronology of the Late Glacial dune complex at Opgrimbie (NE Belgium) was reinvestigated using quartz-based SAR-OSL dating. Laboratory tests indicate that the SAR protocol is suitable for our samples, and that the sediments are well bleached and unaffected by post-depositional mixing. Two sediment units underlying a bleached horizon, previously correlated with the Usselo soil of Allerød age, were dated at 12.9 ± 0.9 and 13.0 ± 0.8 ka. The ages for the uppermost aeolian deposit are consistent with the newly obtained AMS results of charcoal from this bleached horizon, and confirm its Allerød age. From the good agreement between the OSL and the AMS ^{14}C ages, we conclude that the SAR-based quartz OSL ages are accurate, which confirms previous findings concerning the accuracy and robustness of this approach (Murray and Olley, 2002; Vandenberghe et al., 2004; 2009). However, the optical ages do not support the previous interpretation of a second bleached horizon that is intercalated between the two sediment units, in that it represents a soil formed during the Bølling Interstadial. As such, the results from this chronological study conflict with the previous interpretation in that the Lateglacial aeolian succession is fully developed at Opgrimbie, and they question its significance as a type locality. At present, the causes for this discrepancy are not understood and further research is necessary to resolve this matter. Nevertheless, the optical ages do document that sand deposition and dune formation at this locality occurred fairly rapidly during the pre-Allerød period. In general, the results also illustrate (the limit on) the time resolution by which Late Glacial phases of aeolian deposition and/or land surface stability can be distinguished through optical dating.

Chapter 4

Final Palaeolithic settlements of the Campine region (NE Belgium) in their environmental context: Optical age constraints

Chapter (to be) published in full as:

Derese, C., Vandenberghe, D.A.G., Van Gils, M., Mees, F., Paulissen, E., Van den haute, P., in press. Final Palaeolithic settlements of the Campine region (NE Belgium) in their environmental context: optical age constraints. Quaternary International, doi: 10.1016/j.quaint.2011.03.023.

Chapter based on:

Derese, C., Vandenberghe, D.A.G., Van Gils, M., Vanmontfort, B., Meirsman, E., Mees, F., Van den haute, P., 2011. Establishing a chronology for landscape evolution around a Final Palaeolithic site at Arendonk-Korhaan (NE Belgium): First results from optically stimulated luminescence dating. Mediterranean Archaeology and Archaeometry 10, 43-51.

CHAPTER 4. FINAL PALAEOLITHIC SETTLEMENTS OF THE CAMPINE REGION (NE BELGIUM) IN THEIR ENVIRONMENTAL CONTEXT: OPTICAL AGE CONSTRAINTS

4.1. ABSTRACT

The sand sequences exposed at the archaeological sites of Arendonk-*Korhaan* and Lommel-*Maatheide* offer a unique means to study the possible relation between human occupation patterns and climatic and environmental changes during the Weichselian-Holocene transition in the Campine region (NE Belgium). Of particular importance is that, at these localities, the Final Palaeolithic and Early Mesolithic settlement phases are stratigraphically separated. We report on the application of optically stimulated luminescence (OSL) dating to establish a chronology for the evolution of the physical landscape around these sites; such a framework is essential when trying to understand settlement dynamics in response to environmental forcing. Thirty samples in total were dated using quartz SAR-OSL. The luminescence ages range from 16.2 ± 1.4 ka to 10.6 ± 0.7 ka. They indicate that sand deposition at Arendonk-*Korhaan* and Lommel-*Maatheide* was already going on during the final phase of the Late Pleniglacial and/or the onset of the Late Glacial. At Arendonk-*Korhaan*, sediments and soils from the early Late Glacial until the Allerød are missing, whereas a single interruption in the aeolian activity during the Allerød interstadial is reported for Lommel-*Maatheide*. Landscape stabilisation during the Allerød is also suggested by stratigraphical evidence, i.e. the presence of a bleached horizon both at elevated and low-lying flat areas, and extensive peat growth in wet depressions. The Bølling interstadial, on the other hand, has not been recognised in the lithostratigraphic record; this corroborates earlier suggestions that the climatic amelioration during the Bølling was not accompanied by a general stabilisation of the land surface in the NW European lowlands.

The continuation of sand transport and deposition across the Late Pleniglacial/Late Glacial boundary may explain why human societies did not occupy the Campine region until the Allerød. During this interstadial, environmental conditions improved sufficiently to attract Final Palaeolithic *Federmessergruppen* to settle on higher grounds in the area. The climate deteriorated at the onset of the Late Dryas and, as a consequence, aeolian activity intensified again at Arendonk-*Korhaan* and Lommel-*Maatheide*, with at least 0.5 – 1 m of sand being

deposited in a period of ~1 ka; this may have caused the *Federmesser* to leave the area. At both localities, no occupation has been attested for the Late Dryas period until the Early Holocene, when Early Mesolithic societies settled in the area. Our study illustrates how luminescence dating can contribute to an improved understanding of the environmental context around archaeological sites in the Campine region.

4.2. INTRODUCTION

Of all the glacial-interglacial cycles occurring during the Pleistocene epoch, the Weichselian, and more specifically the Weichselian-Holocene transition period (the so-called Late Glacial), is probably the most intensively studied in NW Europe. One reason is that a multitude of high-resolution palaeoclimatic and –environmental records are available for this period, such as marine and limnic varves, ice-cores and terrestrial sediments (see e.g. Yu et al., 2008). Another reason is that the Late Glacial terrestrial sequences contain a detailed archive of human settlement, and thus allow investigating the interaction between past human societies and their natural environment (see e.g. Bos and Janssen, 1996; De Bie and Vermeersch, 1998; Street, 1998; Vermeersch, 2008; in press).

The Weichselian-Holocene transition period was characterised by rapid and abrupt climatic changes, and by an overall amelioration of the climate. In the NW European coversand belt, these oscillations resulted in varying intensities of aeolian activity and vegetation growth. It is generally thought that widespread aeolian sand deposition prevailed during the drier and colder stadial (Dryas) periods, while the warmer and wetter atmospheric conditions during the interstadials (Bølling and Allerød) led to a decrease in aeolian activity and thus to landscape stabilisation and eventually soil development (see e.g. Van der Hammen and Wijmstra, 1971), and to modifications in the fluvial systems (see e.g. Vandenberghe et al., 1987; 1994; Antoine et al., 2003). This, on its turn, encouraged migration of Palaeolithic societies towards the NW European lowlands (N Belgium and The Netherlands). De Bie and Vermeersch (1998) and Vermeersch (2008; in press) reviewed the chronological and environmental information available for the human occupation during the Weichselian-Holocene transition and addressed some of the difficulties associated with the accurate dating of the settlement phases in the NW European lowlands. Problems are, for instance, the significant regional divergence of the palynological records, the questionable association between the industries and the radiocarbon dated samples, and the uncertainties related to thermoluminescence (TL) dating of sediments. The lack of reliable age information complicates the correlation between various proxy records and thus the more detailed investigation into the relationship between the settlement dynamics and changes in the physical environment (De Bie and Vermeersch, 1998; Vanmontfort et al., 2010b).

Optically stimulated luminescence (OSL) dating circumvents the difficulties associated with the above-mentioned dating methods. In contrast to radiocarbon dating, the OSL technique

does not require calibration or a sufficient amount of suitable organic matter. The technique makes use of the mineral components (e.g. quartz, feldspar) of the sediments at the archaeological sites and determines the timing of their deposition. Unlike TL dating, OSL dating of aeolian sediments is usually not complicated by partial bleaching. A number of studies have shown that luminescence dating is a powerful and reliable chronological tool, particularly when the OSL signals from quartz are used in combination with the single-aliquot regenerative-dose (SAR) protocol (Murray and Olley, 2002; Vandenberghe et al., 2004; Wintle and Murray, 2006; Madsen and Murray, 2009; Derese et al., 2010(a)). Until now, only a few studies have applied the method to infer the timing of aeolian activity in the Belgian part of the NW European coversand belt (Buylaert et al., 2009; Derese et al., 2009; Vandenberghe et al., 2009). In an archaeological context, the SAR-OSL dating technique has seen two applications, on Holocene drift-sands at Pulle (NE Belgium; Derese et al., 2010(a)) and on Late Weichselian coversands at Heidebos (N Belgium; Derese et al., 2010(b)).

This paper reports on the application of OSL dating and micromorphological analysis of sediment sequences at the archaeological sites of Arendonk-*Korhaan* and Lommel-*Maatheide*, two of the most extensive Final-Palaeolithic and Mesolithic site-complexes in the Campine region (NE Belgium). Preliminary OSL results of one profile at Arendonk-*Korhaan*, obtained with tentative estimates of the environmental parameters (e.g. time-averaged water content, cosmic radiation), have been reported by Derese et al. (2011). The present study presents the final and complete OSL dataset at both localities in the Campine region and compares it with the age information obtained at other sites in the NW European lowlands with a comparable stratigraphy. As such, it aims at establishing a solid chronological framework for the landscape reconstruction around archaeological sites dating from the Weichselian-Holocene transition. The OSL dataset is complemented with conventional and AMS radiocarbon data obtained during previous studies and in the course of the present study. All radiocarbon ages have been calibrated using Oxcal v4.1.5 (Bronk Ramsey, 2009) and the IntCal09 calibration curve (Reimer et al., 2009), and they are expressed as the 68.2% probability range (unless stated differently) in ka calBP, with AD2000 defined as the present.

4.3. HUMAN OCCUPATION IN THE CAMPINE REGION

Since 2001, the Flemish Heritage Institute (VIOE) systematically prospects and evaluates traces of human occupation during the Final Palaeolithic and Mesolithic periods in the

Campine region (Fig. 4.1) with the intention to properly manage the archaeological heritage in the area. The region contains a rich archive of human settlements that is now continuously threatened by human activities such as construction and agriculture (Van Gils and De Bie, 2006; De Bie and Van Gils, 2009).

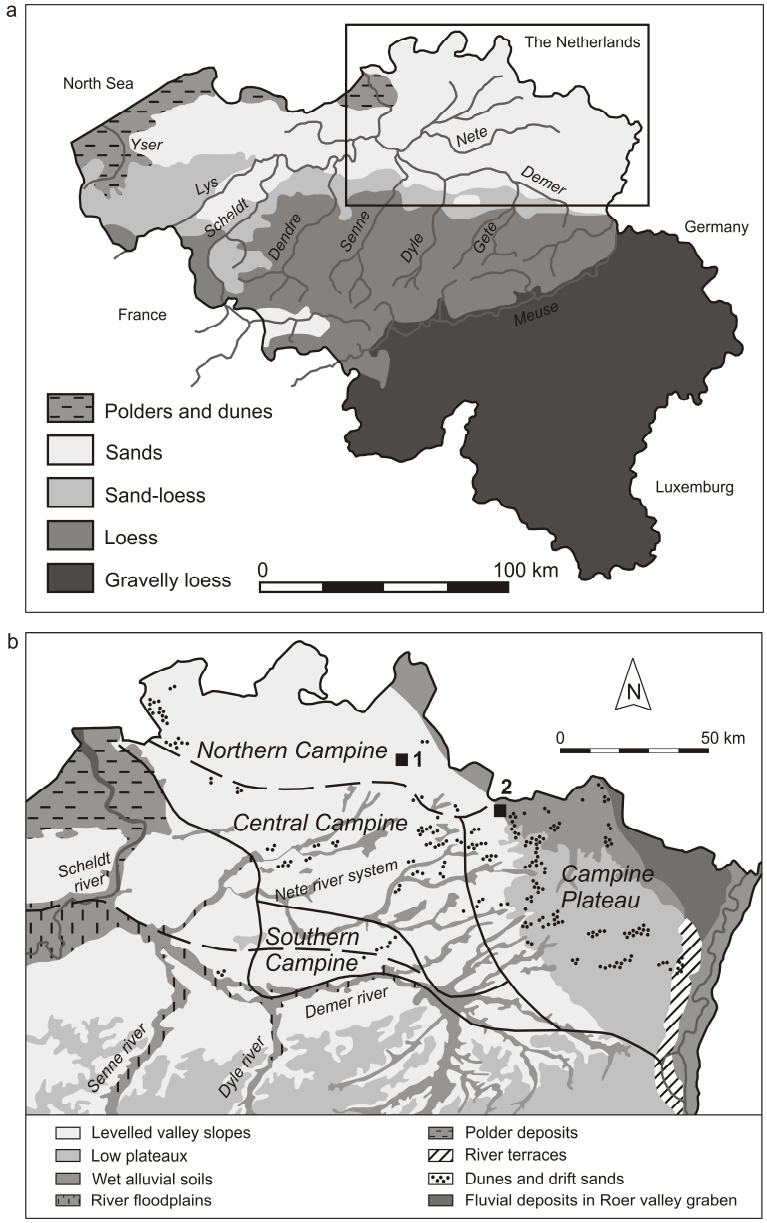

Fig. 4.1: (a) Schematic map of Belgium, showing the main Quaternary sedimentation areas and the hydrological system of Flanders. The rectangle shows the location of the investigated area in NE Belgium. (b) Schematic map of the investigated region, illustrating the main morphological units and the subdivision of the Campine area (adapted from Wouters and Vandenberghe, 1994). The filled squares indicate the location of the archaeological sites Arendonk-*Korhaan* (1) and Lommel-*Maatheide* (2).

A chronology of human occupation during the Pleistocene-Holocene transition is provided by De Bie and Vermeersch (1998) and Vermeersch (2008; in press). After the Last Glacial Maximum (LGM), the Campine region presumably remained uninhabited until the Allerød interstadial (14.0 – 13.0 ka calBP; time boundaries established by Hoek, 2001), when the improved climatic and environmental conditions may have favoured the northward spread of Final Palaeolithic hunter-gatherer-fisherman societies originating from N France and S Germany. These so-called *Federmessergruppen*, named after the curved backed 'penknife' (*'Federmesser'* in German) shape of their arrow points (Schwabedissen, 1954), were mobile and mainly frequented open-air sites, which were in the Campine region typically located on sand ridges in the vicinity of open water (De Bie and Vermeersch, 1998; Van Gils and De Bie, 2006; De Bie and Van Gils, 2009). Baales (2006) suggested that their nomadic mode of existence was related to their diet, which consisted of less gregarious and thus more mobile animals (e.g. red deer, elk, large bovid and beaver, and more rarely roe deer and horse; Street, 1998). The mobility of the *Federmessergruppen* allowed them to maintain long-distance social relationships between settlements. Based on the heterogeneity of their lithic raw materials (e.g. quartzite, flint, lydite, chalcedony, both of local and exogenous origin; De Bie and Vermeersch, 1998; Baales, 2001; 2006), their activity radius was estimated to range between 100 and 200 km. This long-range travelling of the groups did not only allow collecting raw materials, but also exchanging knowledge and skills. As such, the *Federmesser* industries were characterised by a large degree of uniformity. According to De Bie and Vermeersch (1998) and Vermeersch (in press), the *Federmesser* occupation in the NW European lowlands was connected to the Allerød interstadial. This age is mainly based on the stratigraphic position of the artefacts within the Usselo horizon of Allerød age and radiocarbon dating of associated charcoal fragments. At present, only a single unambiguous radiocarbon date is available for a *Federmesser* assemblage in the Campine region; this date of 11,350 ± 150 ^{14}C BP (OxA-942; De Bie and Vermeersch, 1998), calibrated 13.4 – 13.1 ka calBP (68.2% probability) or 13.6 – 12.9 ka calBP (94.4%), was obtained on resin on a curved backed point at Rekem (NE Belgium). At the same locality, thermoluminescence (TL) dating on fired quartzite pebbles from scattered hearths resulted in ages between 11.1 ± 1.2 ka and 13.0 ± 1.5 ka (De Bie, 1997; De Bie and Caspar, 2000). Folz et al. (2001) tested the potential of OSL dating on fluvial quartz-rich sediments at the Federmesser site of Le Closeau (France), but found that their luminescence ages systematically overestimated the existing ^{14}C chronology by about 40% (equivalent to ~6 ka). The possibility of incomplete bleaching was ruled out by dose distribution and OSL decay curve analysis (Folz et al., 2001; Jain et al.,

2004), and no clear problems with the luminescence dating procedure were observed that could cast doubt on the validity of the measurements. A third suggestion by Folz et al. (2001) to explain the discrepancy, i.e. the recent migration of very fine particles rich in isotopes (perhaps due to the artificial drop of the water table), could not further be investigated. Although the combined age information available for the Federmesser in the NW European lowlands cannot exclude Federmesser occupation during the Late Dryas, the *Federmesser* groups seem to have disappeared fairly rapidly from the area after the Allerød interstadial. The reason for this sudden disappearance is as yet unclear, but might be sought in the abrupt climatic cooling, in combination with extensive forest fires, at the Allerød-Late Dryas transition (De Bie and Vermeersch, 1998; Vermeersch, in press).

In contrast to the widespread *Federmesser* occupation, post-*Federmesser* (e.g. Ahrensburgian, Early Mesolithic) industries tended to be more strictly concentrated in regional niches (De Bie and Vermeersch, 1998). In the Belgian Campine region, the presence of Ahrensburgian was unequivocally established at only one open-air site (Zonhoven). The radiocarbon date of 10,760 ± 70 ^{14}C BP (UtC-3720; De Bie and Vermeersch, 1998; Vermeersch, 2008; in press), calibrated 12.8 – 12.6 ka calBP (68.2%) or 12.9 – 12.6 ka calBP (95.4%), obtained at this locality suggested that the Ahrensburgian culture may have appeared soon after the onset of the Late Dryas and after the presumed southern migration of the *Federmessergruppen*. The transition from Late Dryas industries to Early Holocene (Mesolithic) societies is not well understood. Some of the Early Mesolithic assemblages show close resemblance to the Ahrensburgian, whereas others show, on a technological basis, more affinity with *Federmesser* knapping techniques. However, it is noteworthy that many Early Mesolithic sites in the Campine region are located closely to former *Federmesser* settlements. In most cases, the remains of both periods are preserved together, without any stratigraphical separation, within a podzol that has developed in the top of the Late Glacial aeolian sediments. The age of the sediments in which the podzol has formed is unknown; an Early Holocene age cannot be excluded a priori. These circumstances make the homogeneity of the assemblages hard to establish, which complicates the archaeological interpretation. Only at specific localities, where aeolian sediments covered the Usselo horizon and the associated *Federmesser* artefacts before the start of the Holocene and the Mesolithic settlement phase, both assemblages are stratigraphically separated. At the time of this study, only two archaeological sites in the Campine region, Arendonk-*Korhaan* and Lommel-*Maatheide*, were shown to present such a stratigraphical context. These sites have therefore been considered as type-localities for *Federmesser* (and Early Mesolithic) occupation in the region (De Bie and

Van Gils, 2004); no evidence for Ahrensburgian occupation has currently been identified at the sites. Recent investigations have identified another site exposing a similar stratigraphical separation between *Federmesser* and Early Mesolithic occupation levels in the Campine region, at Lommel-*Molse Nete* (Vanmontfort et al., 2010a).

4.4. GEOLOGICAL SETTING

The archaeological sites Arendonk-*Korhaan* and Lommel-*Maatheide* are both situated in the northernmost part of the Campine region (NE Belgium; Figs. 4.1a and 4.1b), at a distance of about 20 km from each other. Morphologically, the Campine region can be subdivided into four distinct areas: the northern, central and southern Campine, and the Campine plateau (Fig. 4.1b). The differences in morphology are mainly related to the geological structure. In the southern and Central Campine, Tertiary marine sediments are typically exposed; in the northern Campine, Quaternary estuarine, fluvial and aeolian sediments are present at the surface. The Campine plateau resulted from differential erosion of the Meuse terraces (Wouters and Vandenberghe, 1994).

During the Pliocene-Pleistocene transition, the northern Campine was situated at the shores of the North Sea, close to the Meuse-Moselle estuary. In this environment, the pure white estuarine sands of the Mol Formation (which are now being exploited at, for example, Lommel-*Maatheide*) were deposited. When the sea retreated, the fine-grained sandy-clayey sediments of the Kempen Group accumulated as a result of the alternating estuarine and fluvial conditions during the Tiglian (Wouters and Vandenberghe, 1994; Gullentops et al., 2001; Bogemans, 2005). From the Eburonian onwards, the landscape development was mainly determined by sediment deposition by meandering and braided river systems, which were supplied by the Meuse during the Menapian. In contrast, the tectonic activity during the Cromerian resulted in an uplift of the study area; accumulation of fluvial sediments was thereby delimited to the Rhine and Meuse basins, whereas the other areas were characterised by river incision. In the Early and Middle Weichselian, the resulting valleys were filled with fluvial sediments originating from braided rivers (Bogemans, 2005). The sedimentary environment of the Late Weichselian, however, was mainly characterised by aeolian activity; the sediments are collected in the Gent Formation (Gullentops et al., 2001). Lithostratigraphically, this sedimentary unit can be subdivided into the Sint-Lenaerts Member, consisting of niveo-aeolian sands with intercalated silt and peat layers, and the Wildert

Member, consisting of slightly silty aeolian sands. During the Late Weichselian, the sands of the Wildert Member were locally remobilised by wind and deposited as inland dunes; this unit is known as the Hechtel Formation. Locally, deforestation and intensification of agriculture resulted in sand-drifting from the Early Middle Ages onwards (Gullentops et al., 2001; Derese et al., 2010(a)).

Arendonk-*Korhaan* is located on a sand ridge adjacent to a wet depression: this is the typical setting for Final-Palaeolithic and Mesolithic occupation complexes in the Campine region (see e.g. De Bie et al., 2009; Vanmontfort et al., 2010b). The NE-SW running sand ridge (locally known as "*Korhaan*"; Fig. 4.2) is clearly visible in the landscape as the southernmost part of a dune field situated in the so-called "*Landschap De Liereman*" area. A swampy depression is present to the south of the ridge complex. The differences in elevation and moisture between the ridge and the depression are emphasised by the distinct vegetation: the ridge is marked by a cover of conifers and heathland, whereas the depression is characterised by meadows and fields (Van Gils et al., 2009).

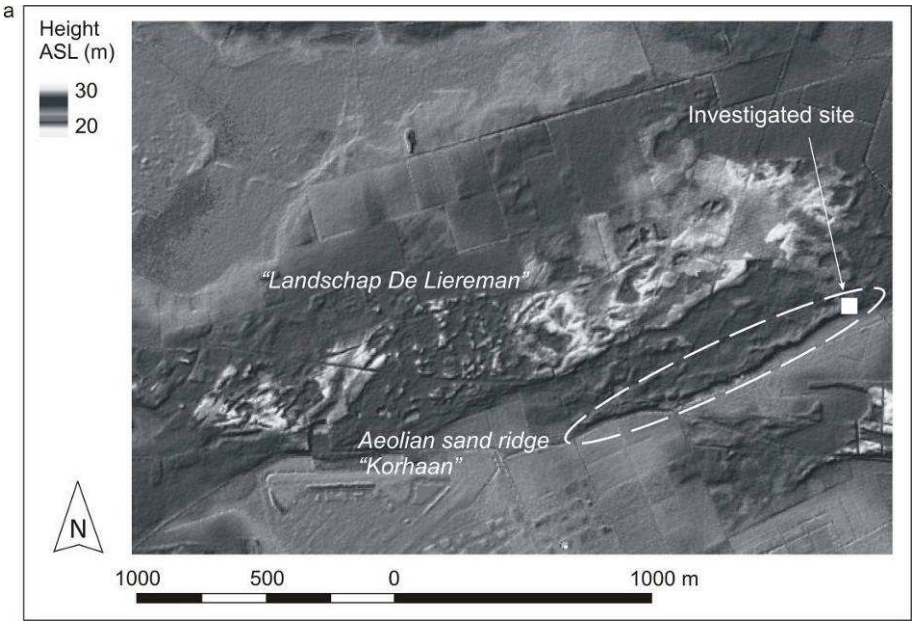

Fig. 4.2: Digital elevation model of the ridge complex Landschap De Liereman at Arendonk, showing the location of the investigated site on the sand ridge 'Korhaan'.

The studied section at Lommel-*Maatheide* is situated in the head of a small shallow valley draining towards the west, and more precisely on a nearly flat area adjacent to the southern valley border. The original topography is poorly preserved: heavy industry during the 20th century resulted in the death of the plant cover, so that the dominant southwesterly winds could easily erode and level the affected areas. Close to the studied section at Lommel-

Maatheide, Federmesser assemblages have been discovered (Van Gils and De Bie, 2004; De Bie et al., 2009).

4.5. PROFILE DESCRIPTION

For Arendonk-*Korhaan*, the geomorphology, litho- and chronostratigraphy are described in detail by Meirsman et al. (2008) and Vanmontfort et al. (2010). In this study two profiles have been investigated, which were both exposed in pits of ~2 x 2 m. A first profile is situated near the base of the ridge and has a height of ~1.5 m (Fig. 4.3a; in pit B of Vanmontfort et al., 2010). The lowermost unit encompasses a massive peat layer of ~25 – 30 cm thick. The peat is covered by a sandy unit of ~80 cm thickness; in the following, this sand unit will be referred to as 'Unit 3'. Unit 3 is composed of nearly pure medium to coarse quartz sand and shows a dense pattern of irregular dark brown veins in the northern part of the profile, and an alternation of sandy and organic layers in the southern part. The uppermost part of the profile consists of a ~40 cm thick, almost white podzolic horizon that is disturbed by clear ploughing marks. Below this disturbed part of Unit 3, many small cracks – interpreted as frost cracks – occur (Fig. 4.3a). A second profile (Fig. 4.3b; in pit A of Vanmontfort et al., 2010b), situated near the sand ridge crest, also shows a ~1.5 m thick sedimentary sequence. The lowermost unit, Unit 1 with an average thickness of ~60 cm, is made up of an alternation of coarse- and fine-grained quartz-rich sand layers with an cross-bedded stratification (~50 cm thick), capped by horizontally layered sands with a thickness of 5 – 10 cm. The cross-bedded layers were deposited in a SE direction by NW winds and are thought to represent the prograding slip face of the sand ridge; at the end of the ridge building process, the horizontally stratified sand were deposited (Meirsman et al., 2008; Vanmontfort et al., 2010b). Unit 1 is separated from the sands of Unit 3 by a 10 – 20 cm thick bleached horizon containing no visible charcoal (Unit 2). This horizon can be subdivided into two subunits: (1) a white, sandy layer at the base, and (2) a light grey siltier unit at the top, in which most Final Palaeolithic artefacts were found. Based on the results of systematic hand augering, the bleached horizon is considered as the lateral equivalent of the peat layer near the base of the ridge (Fig. 4.4; Vanmontfort et al., 2010b). Based on its stratigraphic position and lithological characteristics, this bleached horizon is thought to be equivalent to the Usselo horizon, which was first described by Hijszeler (1947; 1957; see section 4.6; for details, see Vanmontfort et al., 2010b). The bleached layer is covered by 60-70 cm of yellow-coloured aeolian sands with a more

massive bedding (Unit 3). A ~30 cm thick podzol developed in the top of this sandy unit; this podzol was partly disturbed by ploughing marks.

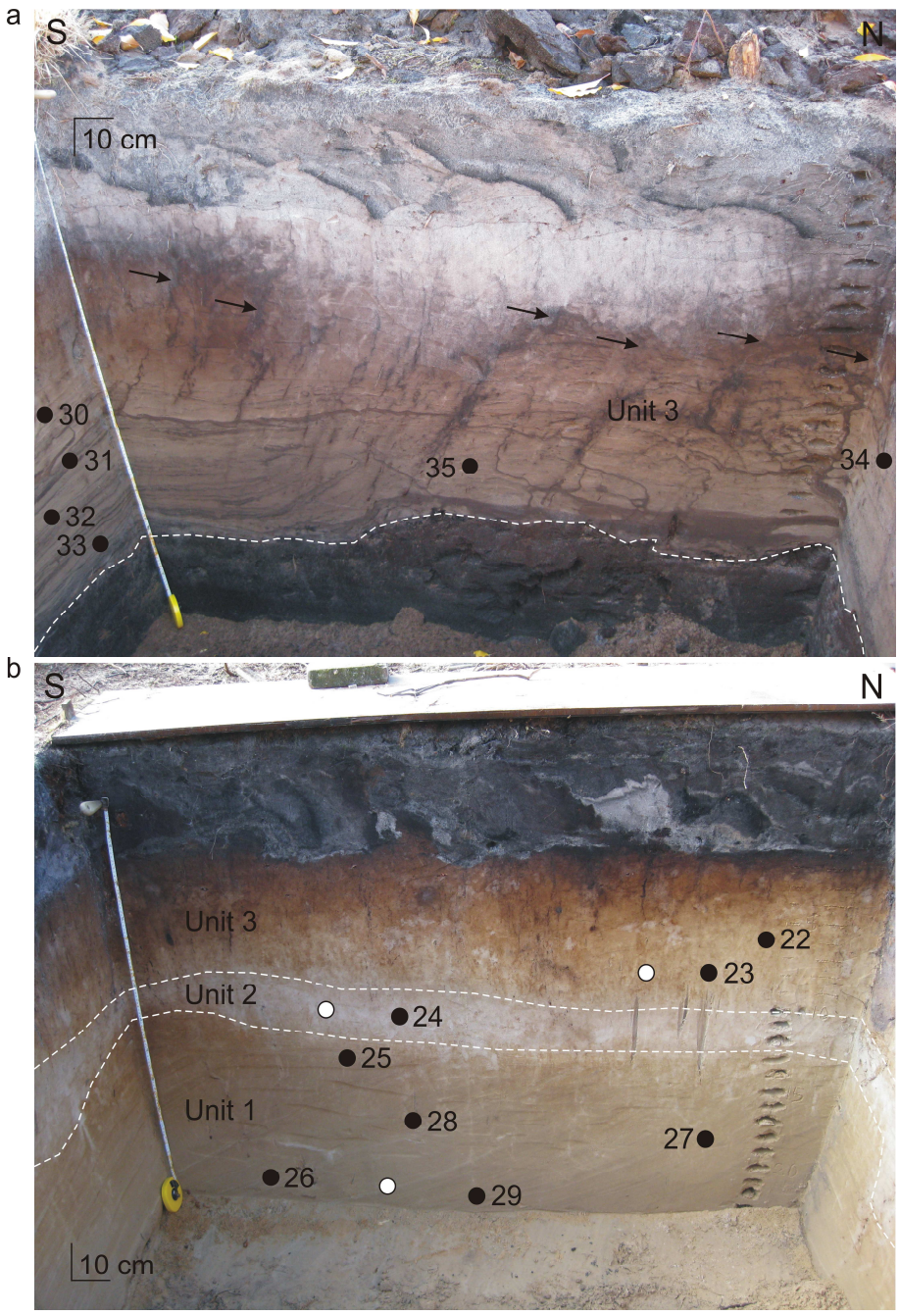

Fig. 4.3: (a) Photograph of pit B at the base of the sand ridge at Arendonk-Korhaan. Note the difference in sedimentary structure between the northern and the southern side of the profile, which was investigated through micromorphological analysis. The small cracks that are interpreted as frost cracks are indicated by black arrows. (b) Photograph of pit A at the sand ridge crest at the same site. The stratigraphy and sedimentology of both aeolian sand sequences is described into detail in section 4.5. Filled circles indicate the location of the OSL samples in both profiles, with the associated number being part of the sample code (GLL-0807XX), and the white circles show where the moisture samples have been collected; in profile 1 (Fig. 4.3a), one additional moisture sample was taken 'to the left' of sample GLL-080732 (outside the picture).

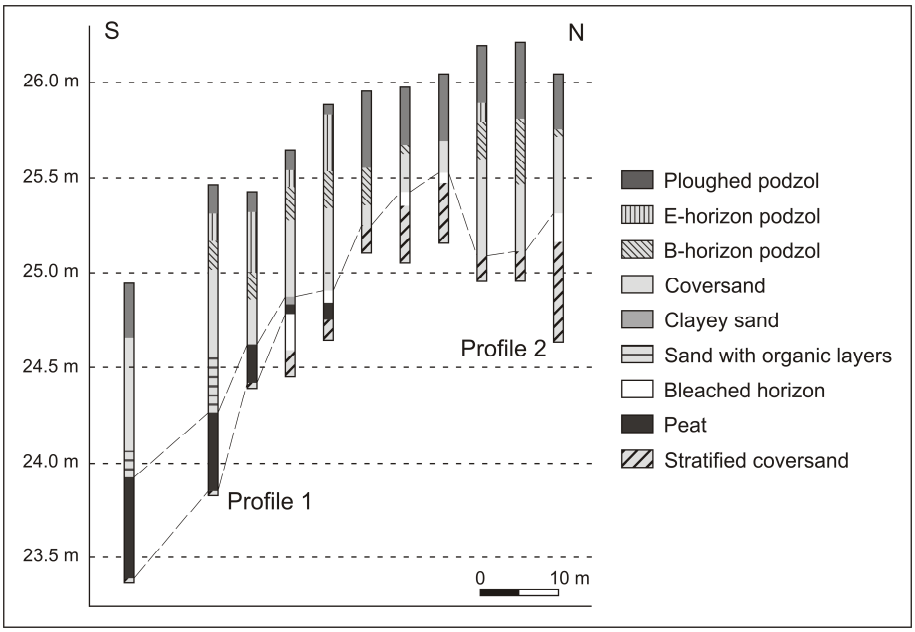

Fig. 4.4: Results of the augering transect across the sand ridge 'Korhaan', illustrating the changes in the stratigraphy and the toposequence peat (base of ridge) to bleached horizon (ridge crest; adapted from Vanmontfort et al., 2010b).

The stratigraphy at Lommel-*Maatheide* is comparable to that at Arendonk-*Korhaan*, although the podzol at the top of the sequences has not been preserved as a result of recent wind erosion. As the research was carried out in a ~20 m long trench (Fig. 4.5), the lateral transition from peat layer to bleached horizon – both nearly at the same level – was clearly visible. Three profiles, reflecting this change, were selected for a detailed study (Fig. 4.6). In profile 1, closest to the depression, a ~17 cm thick peat unit is present, composed of a ~5 cm thick sandy peat underlying a ~12 cm massive peat; the peat unit separates a ~1.5 m thick horizontally layered sand unit underneath (Unit 1) and a more homogeneous sand unit above the organic layer (Unit 3), respectively. In profile 2, the peat is only ~7 cm thick and it covers a ~5 cm thick bleached horizon (Unit 2), which, based on field observations, has been referred to by Van Gils and De Bie (2004) as Usselo horizon. In profile 3, the peat is completely absent; the 15 – 20 cm thick bleached horizon is capped by a 1-2 cm thick layer of organics. The underlying (~50 cm thick) sands (Unit 1) have a grey colour; at the base of the profile, the colour changes locally to yellow-orange, probably as the result of the higher iron content of these sands. The sands covering the bleached horizon (Unit 3) contain some lenses of fine gravels and granules. They originate from local fluvial deposits from the rivers Rhine and Meuse, and have a composition that is largely dominated by quartz and additionally by flint and quartzites. A widely spaced polygonal pattern of frost cracks is present within Unit 3, starting in its upper part and extending down to the peat.

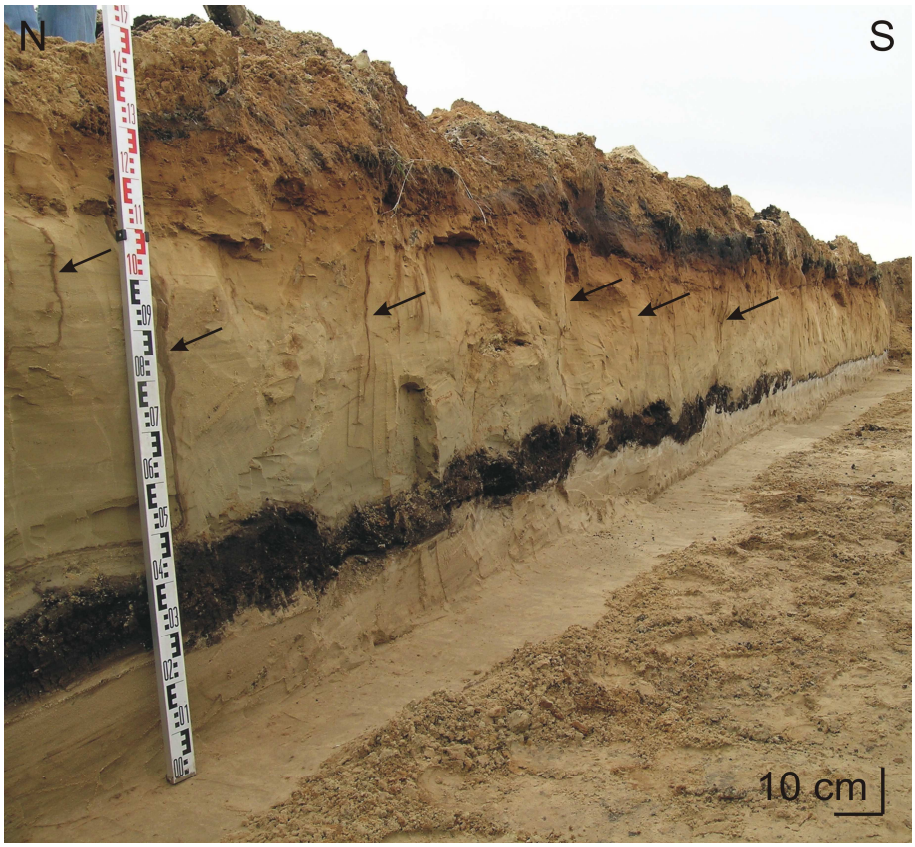

Fig. 4.5: Photograph of the trench profile at Lommel-Maatheide, showing the transition between peat and bleached horizon. The frost cracks in Unit 3 are indicated with black arrows.

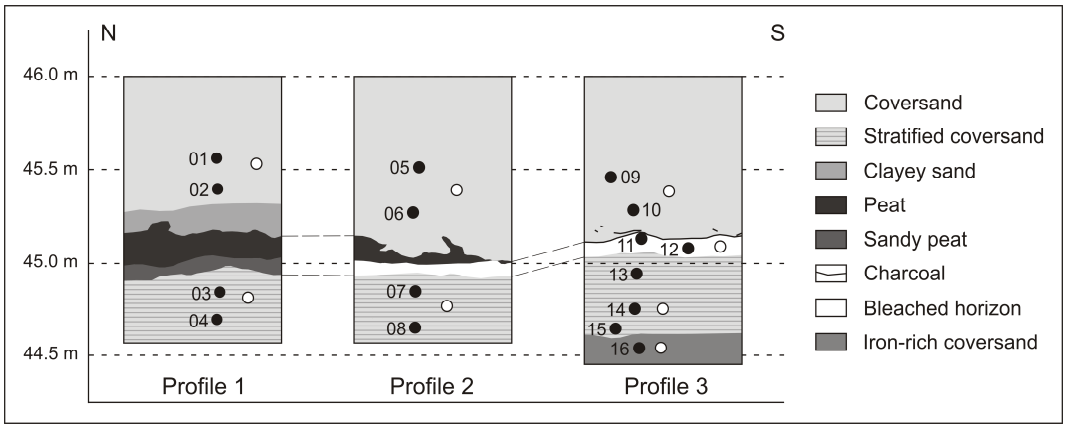

Fig. 4.6: Scheme of the investigated profiles in the trench at Lommel-Maatheide, showing the aeolian sand stratigraphy and the presence of a toposequence, equivalent to that at Arendonk-Korhaan. The filled circles indicate the location of the OSL samples, the associated number is part of the sample code (GLL-0807XX). The white circles indicate the location of the additional undisturbed sediment samples, taken for the estimation of the time-averaged moisture content.

4.6. PREVIOUS AGE INFORMATION

Radiocarbon dates and previous OSL dates are available for the Arendonk-*Korhaan* site, while archaeological evidence is present at Arendonk-*Korhaan* and Lommel-*Maatheide*. At both sites, artefacts have been preserved in two stratigraphic positions, in the bleached horizon and in the podzol. The typology of the assemblages in the bleached horizon allowed attributing them to the Final Palaeolithic, in Arendonk-*Korhaan* (pit A) probably and in Lommel-*Maatheide* (loci to the north and west of the studied section) certainly to the *Federmessergruppen*. The assemblages in the podzol, where separated from the bleached horizon, could be attributed to the Mesolithic (De Bie et al., 2009; Vanmontfort et al., 2010b).
At Arendonk-*Korhaan*, sampling for AMS radiocarbon dating took place in two profiles, one situated on the ridge crest some 20 m west of pit A (further denoted as pit C – not represented here, but see Vanmontfort et al., 2010) and one near the base of the sand ridge (pit B). Pit C reveals a similar lithostratigraphic sequence as pit A, with intercalated between aeolian sands a bleached horizon containing dispersed charcoal fragments (Unit 2), with all characteristics of the Usselo horizon as defined by Hijszeler (1947; 1957). The bleached clastic layer is split very locally (over 2 m) into 2 horizons, both with charcoal and separated by 10 cm yellow-gray medium aeolian sediment. Charcoal fragments from both horizons were sampled for radiocarbon dating. In pit B, samples from both the base and the top of the peat layer were taken.
The ^{14}C results, discussed in Vanmontfort et al. (2010b), are summarised in Table 4.1. The ~40 cm thick peat in pit B was dated at 11,960 ± 60 ^{14}C BP (Poz-28519), equivalent to 13.9 – 13.8 ka calBP, at the very base and 11,000 ± 60 ^{14}C BP (Poz-28168), equivalent to 13.0 – 12.8 ka calBP, at the very top; the radiocarbon ages point to peat accumulation throughout the entire Allerød interstadial. Radiocarbon dating of charcoal in the lowermost bleached layer in pit C yielded ages of 11,010 ± 50 ^{14}C BP (Poz-28517; calibrated 13.0 – 12.8 ka calBP; 64.7%) and 11,240 ± 120 ^{14}C BP (Poz-28518; 13.3 – 13.1 ka calBP; 58.5%); the upper horizon was dated at 10,480 ± 60 ^{14}C BP (Poz-28515; calibrated 12.6 – 12.4 ka calBP; 59.8%) and 10,880 ± 60 ^{14}C BP (Poz-28516; 12.9 – 12.7 ka calBP). These dates generally fall within the timeframe established for the Allerød interstadial. Based on the radiocarbon ages and the presence of *Federmesser* artefacts, Vanmontfort et al. (2010b) concluded that the bleached horizon can indeed be correlated with the Usselo horizon of Allerød age, as had been put forward by the field observations.

Sample number	Locus	Context	Material	Remarks	Conventional age	Calibrated age in a before AD2000	
						1 sigma	2 sigma
Poz-28515	Korhaan pit C	upper bleached layer	one single charcoal piece		10,480 ± 60 ^{14}C BP	12,608 (59,8%) 12,430 12,313 (8,4%) 12,273	12,631 (88.9%) 12,254 12,247 (6.5%) 12,190
Poz-28516	Korhaan pit C	upper bleached layer	one single charcoal piece	0.8 mg C	10,880 ± 60 ^{14}C BP	12,885 (68,2%) 12,705	12,970 (95.4%) 12,660
Poz-28517	Korhaan pit C	lower bleached layer	one single charcoal piece		11,010 ± 50 ^{14}C BP	13,099 (3,5%) 13,083 13,017 (64,7%) 12,802	13,135 (95.4%) 12,749
Poz-28518	Korhaan pit C	lower bleached layer	one single charcoal piece	0.4 mg C	11,240 ± 120 ^{14}C BP	13,326 (58,5%) 13,108 13,073 (9,7%) 13,020	13,408 (95.4%) 12,847
Poz-28168	Korhaan pit B	top peat layer	uncharred seeds		11,000 ± 60 ^{14}C BP	13,015 (68,2%) 12,785	13,134 (95.4%) 12,738
Poz-28519	Korhaan pit B	base peat layer	uncharred seeds		11,960 ± 60 ^{14}C BP	13,942 (68.2%) 13,795	14,040 (95.4%) 13,706

Table 4.1: Overview of the radiocarbon data, available for Arendonk-Korhaan (Vanmontfort et al., 2010b). All ages were obtained through AMS radiocarbon dating, and have been calibrated using Oxcal v4.1.5 (Bronk Ramsey, 2009) and the IntCal09 calibration curve (Reimer et al., 2009).

Moreover, they suggested that the distinct ages of 12.9 – 12.7 ka calBP (Poz-28516), 13.0 – 12.8 ka calBP (Poz-28517) and 13.3 – 13.1 ka calBP (Poz-28518) might represent different fire events, the origins of which are unknown. However, this hypothesis could not be held on the 95% confidence level. Statistical tests however did show that the age of 12.6 – 12.4 ka calBP (Poz-28515) was significantly different from the other aforementioned ages with 99% probability; according to Vanmontfort et al. (2010b), this may indicate that fire events also occurred at the beginning of the Late Dryas or, at the very least, that the Usselo horizon was exposed at the surface at that time.

The sands underlying the bleached horizon in pit C were also sampled for OSL dating in 2004. One sample was taken from an apparently homogeneous unit, the second sample from the underlying eastward dipping stratified sand unit. The original OSL ages were recalculated on the basis of the present estimates of the time-averaged water contents; as such, ages of 15.8 ± 1.2 ka and 16.8 ± 1.3 ka were obtained for the uppermost and lowermost sample, respectively (Table 4.2; Vandenberghe, 2005). These ages are consistent with the assumption that the overlying bleached horizon represents the Usselo horizon of Allerød age. In pit A, no macroscopic charcoal fragments suitable for AMS dating were found. Hand augering indicated that the Usselo horizon in pit C and the bleached layer in pit A are lateral equivalents and, hence, that they both can be correlated with the peat layer in pit B. The bleached horizon in pit A is therefore interpreted as the lateral equivalent of the Usselo horizon in pit C (see also section 4.5).

4.7. MICROMORPHOLOGICAL ANALYSES

At Arendonk-*Korhaan*, the two profiles were sampled into detail for micromorphological analyses; samples were collected within each unit and at the boundary between two units. In total, 15 undisturbed, oriented sediment samples were collected using metal Kubiena boxes. Subsequently, thin sections were prepared after impregnation of the undisturbed samples with a polyester resin. They were described using the concepts and terminology of Stoops (2003).

Sample GLL-code	Depth (cm)	^{234}Th (Bq kg^{-1})	^{226}Ra (Bq kg^{-1})	^{210}Pb (Bq kg^{-1})	^{232}Th (Bq kg^{-1})	^{40}K (Bq kg^{-1})	F*W (%)	Total Dose rate (Gy ka^{-1})	D_e (Gy)	Age (ka)	σ_r (%)	σ_{sys} (%)	σ_{tot} (%)	σ_{tot} (ka)
040404	124	4.1 ± 0.8	4.3 ± 0.3	3.8 ± 1.1	3.6 ± 0.1	73 ± 1	14 ± 3	0.51 ± 0.01	8.1 ± 0.1	15.8	3.2	7.2	7.9	1.2
040403	160	3.7 ± 0.5	3.8 ± 0.2	1.8 ± 0.9	3.3 ± 0.1	69 ± 1	15 ± 3	0.46 ± 0.01	7.7 ± 0.1	16.8	3.2	7.4	8.0	1.3

Table 4.2: Overview of the previously obtained OSL data at Arendonk-Korhaan (Vandenberghe, 2005). The table summarises the radionuclide activities, time-averaged moisture content, dose rate, equivalent dose and OSL age.

4.7.1. Pit B (at base of sand ridge)

The stratigraphy of this profile is visualised in Fig. 4.3a and described into detail in section 4.5. The massive peat bed below Unit 3 is an accumulation of plant remains, including large intact fragments and smaller tissue remains (Fig. 4.7a). All organic remains are fragments of larger structures and do not show indications of preserved original growth positions, whereby the latter does not necessarily imply a strong degree of disturbance or long-distance transport. The deposit also includes a significant admixture of siliciclastic silt to sand grains, as fine-grained material that was wind-deposited or washed-in during peat accumulation. For the overlying layered interval in the southern part of the profile (Unit 3), thin section observations confirm that the dark layers recognised in the field are peat-like intercalations, alternating with sand layers. The nature of the layers with organic material ranges from pure accumulations of plant remains to sand with an admixture of organic residues, whereby gradual transitions between both types of occurrences are common (Fig. 4.7b). One sample includes a lens with an angular outline and one large round aggregate (Fig. 4.7c). All pure accumulations of plant remains clearly have an admixture of silt to sand, as in the massive peat bed; the remains show horizontal to random orientations, without any structures recording in situ development. The organic material in the layered deposits is almost certainly derived from the lateral equivalent of the underlying peat bed, as available source of identical material. The variable degree of medium to coarse sand admixture, with the same grain size as the intervening sand layers, shows that the plant remains have been transported, accumulating with or without associated detrital sand deposition and without major changes in sedimentation type. Angular and rounded clusters that are present appear to be reworked as a whole, which would require short-distance transport without dispersion of the constituent plant remains.

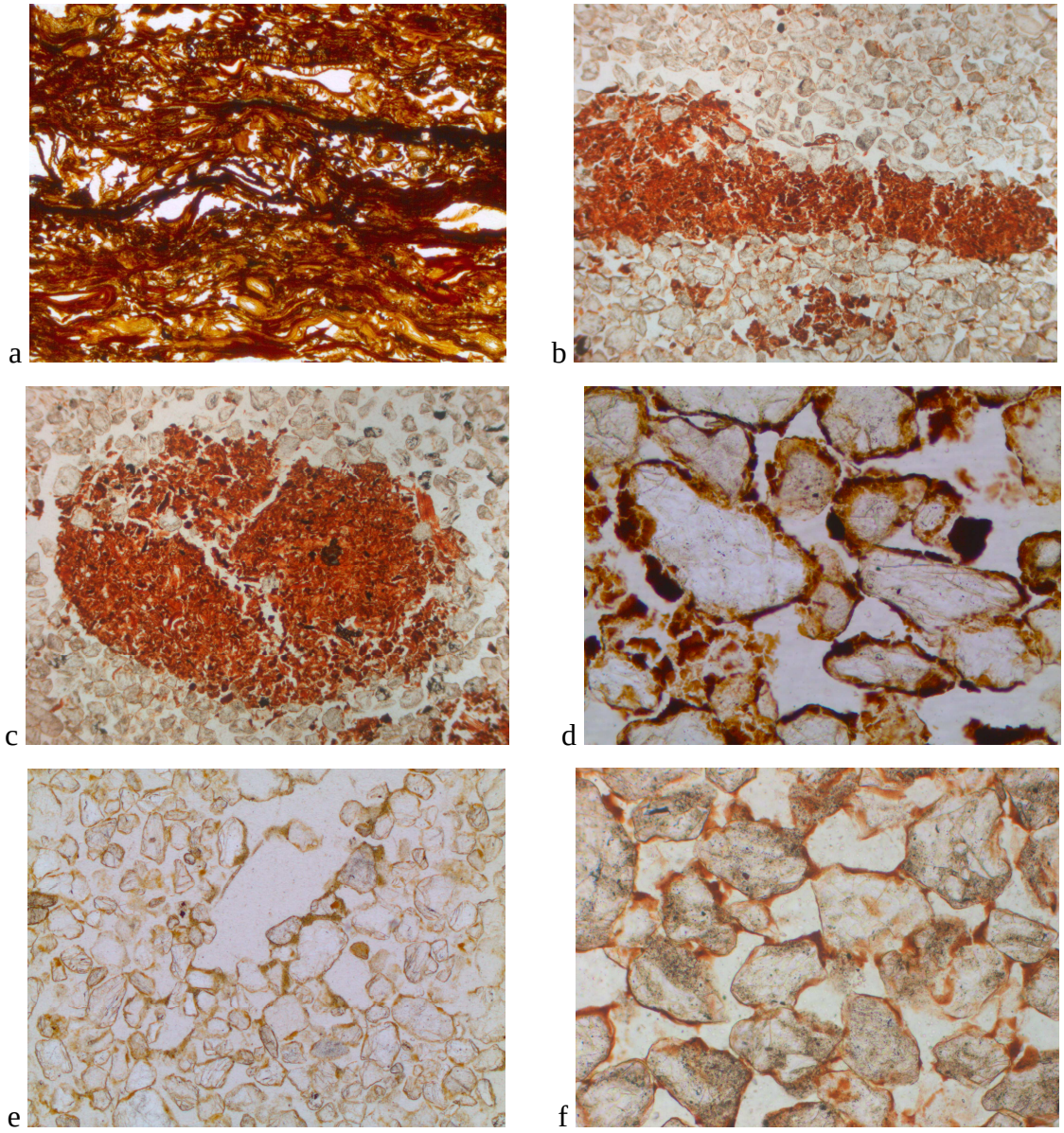

Fig. 4.7: (a) Accumulation of plant remains (peat layer; frame width 2.6 mm); (b) Layer composed of pure accumulation of small orange brown plant remains, sand admixture in upper part (layered deposits; frame width 3.8 mm); (c) Round aggregate (layered deposits; frame width 3.8 mm); (d) Dark organic fine material, with common cracking (layered deposits; frame width 650 µm); (e) Fine material associated with a pore (frame width 2.6 mm); (f) Fine illuvial clay, as coatings that continue along neighbouring sand grains (layered deposits; frame width 950 µm). Figs. 7a to 7d show detailed photographs of samples taken for micromorphology in Pit B, whereas Figs. 7e and 7f represent samples taken in Pit A.

In the upper part of Unit 3, as well as in one sample considered to include clay bands in the field (in the northern part of the profile), the deposits include accumulations of dark brown fine material, occurring around and between the sand grains (Fig. 4.7d). This material is optically isotropic and commonly affected by cracking, compatible with an organic nature,

rather than with an occurrence of illuvial fine clay. In one sample, this fine organic material mainly occurs near vertical root remains.
This association suggests that these, as well as other, occurrences represent a local redistribution of organic material derived from plant remains by decay, rather than being related to illuviation of organic material during spodic horizon development.

4.7.2. Pit A (near ridge crest)

The deposits throughout the profile consist predominantly of medium to coarse sand and contain only a small amount of fine material (micromass). In the upper part of the bleached horizon, as well as in the overlying material, this relatively coarse-grained micromass locally occurs along the sides of channels (Fig. 4.7e), as discontinuous textural coatings that only rarely show a parallel alignment of clay particles. Minor occurrences of illuvial material are common in eluvial horizons (Kühn et al., 2010), but the observed type of relatively coarse-grained void-associated material can be translocated at any stage within a profile, without requiring conditions favouring chemical dispersion that would result in Bt horizon development. Illuvial textural features, composed of coarse or fine clay, are absent below the Usselo interval in the studied profile. Two samples, taken at the same level from the layered deposits directly underlying the Usselo horizon, do include horizontal bands with brown limpid illuvial clay (Fig. 4.7f), recording the occurrence of clay illuviation in the area at some stage. Overall, micromorphological analyses for the studied site cannot give a decisive answer regarding the nature of the bleached horizon, mainly due to the strongly sand-dominated texture of the deposits, providing a poor record of pedogenic processes in thin section.

4.8. LUMINESCENCE ANALYSES

4.8.1. Sampling, sample preparation and analytical facilities

At both localities, a high-resolution sampling strategy for OSL dating was adopted, with multiple samples being taken from each lithostratigraphic unit, including the bleached horizon. This resulted in 14 samples being taken at Arendonk-*Korhaan* (Fig. 4.3a-b) and 16 samples

being collected at Lommel-*Maatheide* (Fig. 4.6). All OSL samples were taken by gently hammering opaque PVC cylinders into freshly cleaned exposures. About 1 kg of the surrounding sediment was collected for dose rate determination in the laboratory. From each sediment unit (per profile), an undisturbed sediment sample was taken for evaluation of the time-averaged water content; these samples were double wrapped in plastic bags and tightly sealed with duct tape to prevent them from drying out.

Coarse (180-212 µm) quartz grains were extracted from the inner part of the sample tubes using conventional sample preparation techniques, involving treatment with HCl and H_2O_2 (to remove carbonates and organic matter, respectively), sieving (to obtain the desired grain-size fraction) and etching with 40% HF. The purity of the quartz extracts was confirmed by the absence of a significant infrared stimulated luminescence (IRSL) response at 60°C to a large (~50 Gy) regenerative beta dose. The sensitivity to infrared was defined as significant if the resulting signal amounted to more than 10% of the corresponding OSL signal (Vandenberghe, 2004), or if the IR depletion ratio deviated more than 10% from unity (Duller, 2003).

For measurement, the quartz grains were fixed on the inner 8 mm of 9.7 mm diameter stainless steel discs using silicon spray. All OSL measurements were performed using an automated Risø TL/OSL-DA-12 reader, equipped with blue (470 ± 30 nm) LEDs and an IR laser diode (830 nm). The quartz luminescence emissions were detected through 7.5 mm of Hoya U-340 UV filter. Details on the measurement apparatus can be found in Bøtter-Jensen et al. (2003).

The determination of the dose rate was based on high-resolution low-background gamma-ray spectrometry. The sediment was dried at 110°C (until constant weight), and pulverised and homogenised. A subsample of ~140 g was subsequently cast in wax (see e.g. De Corte et al., 2006) and stored for one month before being measured on top of the detector.

4.8.2. Luminescence characteristics

Previous luminescence studies on sandy aeolian deposits in the region (e.g. Derese et al., 2009; 2010(a); 2010(b); in press; Vandenberghe et al., 2009) have demonstrated the suitability of the single-aliquot regenerative-dose (SAR) protocol (Murray and Wintle, 2000) for equivalent dose determination; hence, this protocol was adopted in this study. Optical stimulation with blue LEDs was for 40 s at 125°C and the initial 0.32 s of the OSL decay curve was used in all calculations, minus a background evaluated from the 1.44 – 2.08 s interval. Natural and

regenerative doses were measured after a preheat of 10 s at 240°C; the responses to a test dose (~2.2 Gy in all experiments) after a cutheat to 160°C. To minimise possible recuperation effects, a high-temperature bleach was performed after each measurement of the test dose signal by stimulating with the blue LEDs for 40°C at 280°C (Murray and Wintle, 2003). The SAR protocol involved the measurement of the natural luminescence signal, followed by the measurement of the responses to three regenerative doses (equivalent to 50%, 100% and 200% of the estimated natural dose) and to a zero dose, and a repeat measurement of the response to the first regenerative dose. The response to the largest regenerative dose was measured twice; the second time, the sensitivity to infrared stimulated luminescence was checked before stimulating with the blue LEDs in order to identify aliquots with a significant feldspar contamination. The response to the zero dose was measured to determine if the growth curve passes through the origin (recuperation). The repeat measurement of the response to the lowest regenerative dose was carried out to evaluate the performance of the sensitivity correction (recycling ratio). The measured aliquots were accepted when the recuperation and the IRSL/OSL ratio did not exceed a threshold set at 10% and when the recycling ratio and the IR depletion ratio were within 10% of unity. Out of 630 aliquots measured in total, only one aliquot (of sample GLL-080706) had to be rejected due to a deviating recycling ratio of 0.78 ± 0.03.

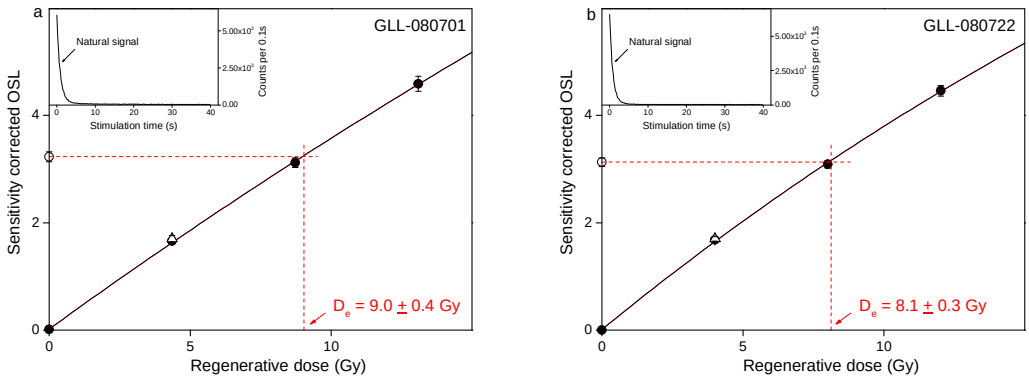

Fig. 4.8: Illustrative growth and luminescence decay curves of a sample taken at (a) Lommel-Maatheide (GLL-080701) and (b) Arendonk-Korhaan (GLL-080722). The filled circles show the responses to several regenerative doses, including a zero dose; the growth curve is obtained by fitting a single saturating exponential function to these measurement points. The open triangle is obtained by a repeat measurement of the first regenerative dose. The open circle is the natural luminescence signal; the equivalent dose D_e is determined by plotting the natural signal onto the growth curve.

Fig. 4.8 shows representative luminescence decay and growth curves for a sample from Lommel-*Maatheide* (GLL-080701; Fig. 4.8a) and a sample from Arendonk-*Korhaan* (GLL-080722; Fig. 4.8b). The luminescence signal decays rapidly with stimulation time (Fig. 4.8a-b, inset); this is characteristic for quartz dominated by the fast component. The dose-response curves could be well approximated by a single saturating exponential growth. The recycling points (open triangles in Fig. 4.8a-b) match the results of the first measurements and the growth curves pass through the origin; this indicates the generally good behaviour of the samples in the SAR protocol. Dose recovery tests were carried out to further check the reliability of the applied measurement procedure (Murray and Wintle, 2003). Three natural aliquots of each sample were bleached twice for 250 s using the blue LEDs at room temperature; the bleaching treatments were separated by a 10 ks pause. Subsequently, the aliquots were given a laboratory dose close to the expected natural dose before any heat treatment was applied; this dose was measured using the SAR protocol as outlined in the above. Fig. 4.9 summarises the results of the dose recovery tests. Some spread can be observed in the dose recovery data, and there is a clear difference in precision between the datasets of Arendonk-*Korhaan* and Lommel-*Maatheide*. For Arendonk-*Korhaan*, the true uncertainty on the measurement results is generally smaller than the expected uncertainty. For Lommel-*Maatheide*, however, seven samples (GLL-080702, -03, -04, -06, -08, -10 and -12) are characterised by larger uncertainty than expected on the basis of the individual uncertainties; the reason for this is unclear, but it may be related to the lower initial intensity of the signal measured in these samples. An overall average recovered to given dose ratio of 1.02 ± 0.01 (n=48) was obtained for the sediments at Lommel-*Maatheide*; the corresponding overall average recycling ratio and recuperation value are 1.00 ± 0.01 and 0.24 ± 0.03% of the sensitivity-corrected natural OSL signal. The sediments at Arendonk-*Korhaan* are characterised by an overall average dose recovery ratio of 1.05 ± 0.01 (n=42); the associated overall average recycling ratio is 0.98 ± 0.01, while the recuperated signal amounts to 0.21 ± 0.02% of the sensitivity-corrected natural signal. A small but systematic overestimation of the given dose can be observed for the Arendonk-*Korhaan* samples; it is desirable to further investigate the causes of this overestimation. Nevertheless, the deviation of the dose recovery ratios from unity falls within the uncertainty of the dating results and, as such, the influence of the overestimation on the luminescence dataset is expected to be negligible.

On the whole, the results from the dose recovery tests demonstrate that the SAR protocol is able to measure laboratory doses given to bleached samples prior to any heat treatment with

acceptable accuracy. For each sample, 18 replicate measurements of the equivalent doses are made. The average values (± 1 standard error) are summarised in Tables 4.3 and 4.4.

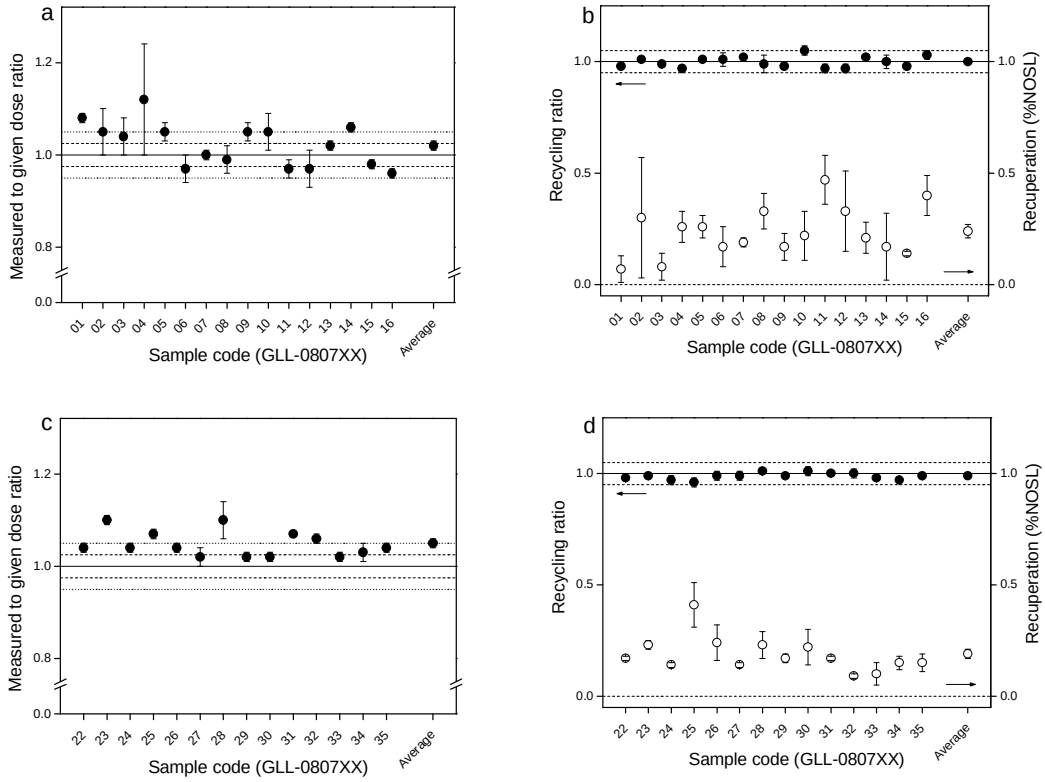

Fig. 4.9: Summary of the dose recovery test results for (a-b) Lommel-Maatheide and (c-d) Arendonk-Korhaan. (a) and (c) summarise the average dose recovery ratios (n=3) obtained for each sample and the averall average dose recovery ratios (n=48 for Lommel-Maatheide and n=42 for Arendonk-Korhaan). The solid line (eye guide) represents a measured to given dose ratio equal to unity; the dashed and dotted lines (eye guides) bracket a 2.5% and a 5% deviation of the ratio from unity, respectively. (b) and (d) show the associated average recycling ratios (filled circles) and recuperation values (given as a percentage of the natural luminescence signal; open circles). The solid line (eye guide) represents a recycling ratio equal to unity.

4.8.3. Dose rate determination

The dosimetric information is synthesised in Tables 4.3 and 4.4. The radionuclide activity concentrations were obtained by high-resolution gamma-ray spectrometry and converted to dose rates using factors derived from the nuclear energy releases tabulated by Adamiec and Aitken (1998). A factor of 0.9 (± 5% relative uncertainty) was adopted to correct the external beta dose rates for the effects of attenuation and etching (Mejdahl, 1979). An internal dose rate in quartz grains of 0.010 ± 0.002 Gy/ka was assumed (Vandenberghe et al., 2008).

Sample GLL-code	Unit	Depth (cm	^{234}Th (Bq kg^{-1})	^{226}Ra (Bq kg^{-1})	^{210}Pb (Bq kg^{-1})	^{232}Th (Bq kg^{-1})	^{40}K (Bq kg^{-1})	F*W (%	Total Dose rate (Gy ka^{-1})	D_e (Gy	Age (ka)	σ_r (%)	σ_{sys} (%)	σ_{tot}	
														(%)	(ka)
080701	3	50	3.8 ± 0.9	6.5 ± 0.3	9.1 ± 0.9	5.0 ± 0.2	128 ± 2	18 ± 2	0.75 ± 0.01	9.0 ± 0.2	12.0	3.3	6.3	7.1	0.9
080702	3	65	8.7 ± 0.9	8.3 ± 0.3	8.8 ± 0.8	6.2 ± 0.1	125 ± 2	18 ± 2	0.77 ± 0.01	8.9 ± 0.1	11.6	2.1	6.2	6.6	0.8
080703	1	118	5.3 ± 0.7	6.0 ± 0.4	4.6 ± 0.7	4.3 ± 0.1	90 ± 2	17 ± 2	0.56 ± 0.01	7.5 ± 0.2	13.3	3.2	6.5	7.3	1.0
080704	1	135	5.0 ± 0.6	6.8 ± 0.2	7.1 ± 0.8	5.0 ± 0.1	113 ± 2	17 ± 2	0.66 ± 0.01	10.1 ± 0.3	15.3	3.7	6.2	7.2	1.1
080705	3	52	3.7 ± 0.9	5.7 ± 0.2	6.3 ± 0.6	4.3 ± 0.1	155 ± 2	17 ± 2	0.77 ± 0.01	9.1 ± 0.2	11.7	2.8	6.3	6.8	0.8
080706	3	72	5.3 ± 0.8	6.9 ± 0.3	6.9 ± 0.7	5.2 ± 0.1	139 ± 2	17 ± 2	0.75 ± 0.01	9.1 ± 0.5	12.3	1.8	6.2	6.5	0.8
080707	1	110	5.9 ± 0.7	7.3 ± 0.2	7.3 ± 0.7	5.8 ± 0.1	101 ± 2	17 ± 2	0.65 ± 0.01	8.1 ± 0.2	12.4	3.0	6.3	7.0	0.9
080708	1	127	4.1 ± 1.0	5.2 ± 0.3	6.3 ± 0.9	4.1 ± 0.1	101 ± 2	17 ± 2	0.60 ± 0.01	8.4 ± 0.2	14.0	2.9	6.4	7.0	1.0
080709	3	52	6.2 ± 0.9	7.0 ± 0.3	7.7 ± 0.8	5.3 ± 0.1	141 ± 2	17 ± 2	0.78 ± 0.01	8.6 ± 0.1	11.0	2.3	6.2	6.7	0.7
080710	3	67	6.5 ± 1.2	7.9 ± 0.3	8.9 ± 0.9	6.2 ± 0.1	130 ± 2	17 ± 2	0.78 ± 0.01	8.9 ± 0.2	11.5	2.9	6.2	6.8	0.8
080711	2	83	7.7 ± 0.7	8.0 ± 0.3	8.8 ± 0.9	7.1 ± 0.1	130 ± 3	20 ± 2	0.77 ± 0.01	8.2 ± 0.2	10.6	3.1	6.2	7.0	0.7
080712	2	85	6.8 ± 0.9	7.0 ± 0.2	8.2 ± 0.9	6.0 ± 0.1	116 ± 2	20 ± 2	0.71 ± 0.01	8.8 ± 0.2	12.4	2.8	6.3	6.9	0.9
080713	1	98	4.7 ± 0.7	6.2 ± 0.2	6.0 ± 0.7	4.4 ± 0.1	87 ± 1	18 ± 2	0.57 ± 0.01	7.9 ± 0.2	13.7	3.0	6.6	7.3	1.0
080714	1	118	6.1 ± 0.8	6.7 ± 0.3	6.0 ± 0.7	5.1 ± 0.1	133 ± 2	18 ± 2	0.70 ± 0.01	10.2 ± 0.4	14.5	4.1	6.2	7.4	1.1
080715	1	130	4.6 ± 0.7	6.1 ± 0.3	6.8 ± 0.5	4.7 ± 0.2	106 ± 2	19 ± 2	0.62 ± 0.01	7.9 ± 0.2	12.7	2.8	6.4	6.9	0.9
080716	1	145	2.8 ± 0.6	4.2 ± 0.2	4.3 ± 0.5	3.4 ± 0.1	86 ± 2	19 ± 2	0.51 ± 0.01	6.8 ± 0.1	13.3	2.4	6.7	7.1	0.9

Table 4.3: Summary of the radionuclide activities, estimated time-averaged moisture contents, calculated dose rates, equivalent doses (D_e), optical ages, and random (σ_r), systematic (σ_{sys}) and total (σ_{tot}) uncertainties, obtained for the samples taken at Lommel-Maatheide. The uncertainties mentioned with the dosimetry and D_e data are random; all uncertainties represent 1σ.

The evaluation of the time-averaged moisture content, and the corresponding correction for it of the dose rates, was performed following the procedure outlined in Aitken (1985). The water content in fully saturated sediment was measured in the laboratory using the samples that were specifically collected for this purpose (see Section 4.8.1). Values in the range of 17-22% were obtained. For the profile closest to the top of the sand ridge at Arendonk-*Korhaan*, the sediments were assumed to be in saturation for 80% (± 20% relative uncertainty) of the burial period. For the profile at the base of the ridge at Arendonk-*Korhaan* and for the profiles at Lommel-*Maatheide*, the time-averaged moisture content was estimated to amount to 90% (± 10% relative uncertainty) of the water content at saturation level. An increase in the pore water content of 1% results in an equal increase in the optical age. The contribution from cosmic radiation was calculated following Prescott and Hutton (1994) and a relative systematic uncertainty of 15% was associated with this value.
The dose rates show little variation with depth, and range from ~0.42 to 0.65 Gy ka^{-1} at Arendonk-*Korhaan* and from ~0.52 to 0.79 Gy ka^{-1} at Lommel-*Maatheide*. These values are typical for quartz-rich aeolian sands in the region.

4.8.4. OSL ages

The OSL ages and their associated uncertainties are summarised in Tables 4.3 and 4.4, and in Fig. 4.10. Uncertainties on the optical ages were calculated following the error assessment system proposed by Aitken and Alldred (1972) and Aitken (1976). The systematic uncertainty is dominant in the overall uncertainty on the ages and varies between ~6 and 8% (1 σ). As the sources of systematic uncertainty are largely shared between all samples, only the random uncertainty (~2 – 4%; visualised by the black error bars in Fig. 4.9) is taken into account to evaluate the internal consistency of the ages.
At Arendonk-*Korhaan*, OSL dating of Unit 1 results in ages from 13.0 ± 0.4 to 16.2 ± 0.6 ka. Unit 2 is dated at 15.2 ± 0.5 ka, and the ages of Unit 3 range between 11.1 ± 0.3 ka and 13.0 ± 0.4 ka. The datasets obtained for each sedimentary unit do not show a clear increase with depth. In pit A, the age of 13.0 ± 0.4 ka for sample GLL-080727 appears to be significantly

younger than the other ages obtained for Unit 1 (~15 – 16 ka). Derese et al. (2011) applied the Q test (Dean and Dixon, 1951) to evaluate whether this date represents an outlier; the result of this test indicated that the age of 13.0 ± 0.4 ka is not significantly different from the other values at the 95% confidence level.

At Lommel-*Maatheide*, the ages for Unit 1 vary between 12.4 ± 0.4 and 15.3 ± 0.6 ka. The bleached horizon (Unit 2) is dated at 10.6 ± 0.3 ka to 12.4 ± 0.3 ka, and the sands of Unit 3 yield ages between 11.0 ± 0.3 ka and 12.3 ± 0.2 ka. In each profile, an increase of the ages with depth can be observed; however, the dataset for the individual sedimentary units (2 dates, except for unit 3 in profile 3) is too small to establish unambiguously whether this increase is genuine. Some spread in optical ages can be observed; in profile 3, the ages of samples GLL-080715 and -16 (12.7 ± 0.4 ka and 13.3 ± 0.3 ka, respectively) are younger than the age of the overlying sample (14.5 ± 0.6 ka). However, they are not significantly different within two sigma.

On the whole, the ages obtained at both Arendonk-*Korhaan* and Lommel-*Maatheide* are, within the random (1 σ) uncertainty, in agreement with the stratigraphic position of the samples and they form an internally consisted dataset. The observed variability in the OSL datasets illustrates the importance of determining multiple age estimates per stratigraphical unit.

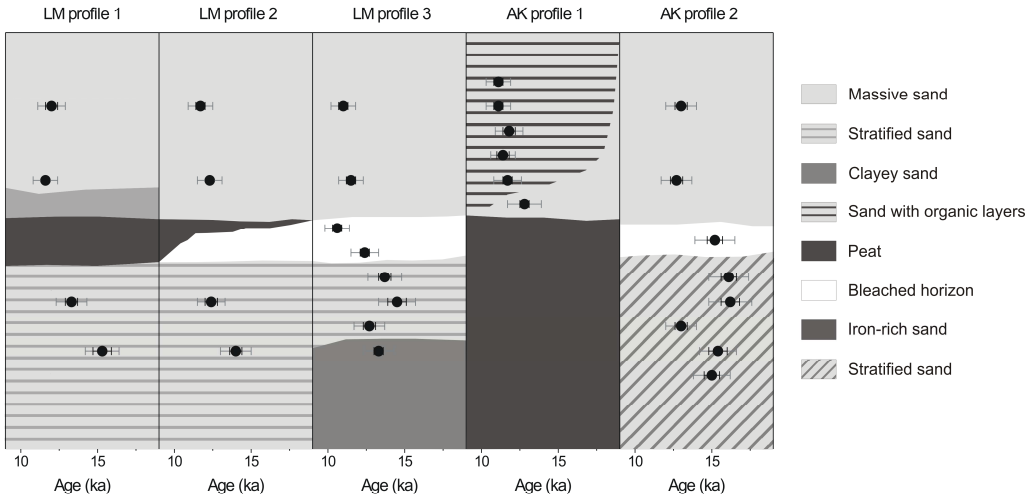

Fig. 4.10: Synthesis of the optical ages obtained at Lommel-*Maatheide* (LM) and Arendonk-*Korhaan* (AK). The black error bars represent the random uncertainty and can be used to evaluate the internal consistency of the OSL dataset, as the sources of systematic uncertainty are generally shared. The grey error bars represent the total uncertainty on the ages. To facilitate the evaluation of the OSL ages in view of the depositional history and landscape evolution, the stratigraphy of each profile is schematically indicated on the figure.

4.9. DISCUSSION

In the following, the OSL ages are mentioned with their total (1 σ) uncertainties, as they are compared with independent age information, mainly derived from radiocarbon dating, and with optical ages obtained on the same and other sites in the NW European lowlands. Firstly, the three sedimentary units will be discussed separately and a chronological timeframe for aeolian deposition at Lommel-*Maatheide* and Arendonk-*Korhaan* will be established. Secondly, the implications for the human occupation patterns observed at the sites will be addressed.

4.9.1. Unit 1

At Lommel-*Maatheide,* ages for the lowermost unit (Unit 1) between 15.3 ± 1.1 ka and 12.4 ± 0.9 ka were obtained. The stratigraphically equivalent unit at Arendonk-*Korhaan* yields ages between 16.2 ± 1.4 ka and 13.0 ± 1.0 ka. The latter results match the previously obtained OSL ages of 15.8 ± 1.2 ka and 16.8 ± 1.3 ka for the same unit in pit C at Arendonk-*Korhaan* (Table 4.2; Vandenberghe, 2005) and are anterior to the radiocarbon ages of the charcoal in the overlying Usselo horizon (Table 4.1). At none of both localities, a clear break in sedimentation can be observed in Unit 1, neither in the field nor in the OSL dataset.

The combined OSL dataset for Unit 1 at Arendonk-*Korhaan*, with an average of 15.1 ± 1.1 ka (n=5), suggests that sand deposition already occurred at the end of the Late Pleniglacial (20 – 15 ka calBP; time boundaries based on Renssen et al., 2007), and continued across the Late Pleniglacial/Late Glacial boundary. This is in agreement with the conclusion of Vanmontfort et al. (2010b) that the morphology of the sand ridge at Arendonk-*Korhaan* is mainly an inherited pre-Allerød morphology, determined by unidirectional cross-laminated sands deposited by northwesterly winds and prograding towards the southeast. Sediments and soils witnessing environmental and climatic changes during the pre-Allerød Late Glacial appear to be missing from the record. At Lommel-*Maatheide*, there are no clear indications for sedimentation during the Late Pleniglacial in the OSL dataset; within uncertainty and taking into account the average age of 13.6 ± 0.9 ka (n=8) for Unit 1, it cannot be excluded that the sand deposition was confined to the pre-Allerød Late Glacial.

Sample GLL-code	Unit	Depth (cm)	^{234}Th (Bq kg^{-1})	^{226}Ra (Bq kg^{-1})	^{210}Pb (Bq kg^{-1})	^{232}Th (Bq kg^{-1})	^{40}K (Bq kg^{-1})	F*W (%)	Total Dose rate (Gy ka^{-1})	D_e (Gy)	Age (ka)	σ_r (%)	σ_{sys} (%)	σ_{tot} (%)	σ_{tot} (ka)
080722	3	57	5.1 ± 0.8	6.0 ± 0.3	5.5 ± 0.8	5.0 ± 0.1	89 ± 2	18 ± 4	0.61 ± 0.01	7.9 ± 0.2	13.0	3.1	7.5	8.1	1.0
080723	3	67	5.1 ± 1.2	6.6 ± 0.3	6.8 ± 0.9	5.2 ± 0.2	99 ± 2	18 ± 4	0.65 ± 0.01	8.2 ± 0.2	12.7	2.8	7.3	7.8	1.0
080724	2	80	2.7 ± 0.8	3.2 ± 0.2	3.4 ± 0.7	2.6 ± 0.1	54 ± 1	17 ± 3	0.44 ± 0.01	6.7 ± 0.2	15.2	3.2	8.2	8.8	1.3
080725	1	97	4.3 ± 1.0	5.2 ± 0.5	4.7 ± 0.8	3.6 ± 0.1	65 ± 2	14 ± 3	0.50 ± 0.01	8.1 ± 0.1	16.1	2.9	7.3	7.9	1.3
080726	1	129	3.4 ± 0.8	3.7 ± 0.2	3.3 ± 0.6	3.0 ± 0.2	48 ± 1	14 ± 3	0.42 ± 0.01	6.8 ± 0.2	16.2	3.6	7.8	8.5	1.4
080727	1	118	4.8 ± 0.9	5.3 ± 0.3	4.7 ± 0.6	4.0 ± 0.1	79 ± 2	14 ± 3	0.54 ± 0.01	7.1 ± 0.1	13.0	2.7	7.1	7.6	1.0
080728	1	116	4.5 ± 0.9	5.6 ± 0.4	4.6 ± 0.7	4.0 ± 0.1	71 ± 2	14 ± 3	0.52 ± 0.01	8.0 ± 0.3	15.4	3.8	7.1	8.1	1.2
080729	1	135	4.6 ± 0.8	4.9 ± 0.2	4.7 ± 0.9	3.9 ± 0.1	72 ± 1	14 ± 3	0.52 ± 0.01	7.8 ± 0.2	15.0	3.4	7.1	7.9	1.2
080730	3	80	3.1 ± 0.6	3.9 ± 0.2	4.9 ± 0.7	3.2 ± 0.2	72 ± 2	18 ± 2	0.50 ± 0.01	5.6 ± 0.1	11.1	2.8	7.1	7.6	0.8
080731	3	98	3.5 ± 0.9	3.7 ± 0.2	4.8 ± 0.8	3.4 ± 0.1	96 ± 2	18 ± 2	0.56 ± 0.01	6.3 ± 0.1	11.1	2.4	6.7	7.1	0.8
080732	3	107	4.4 ± 1.0	4.2 ± 0.3	4.8 ± 0.7	4.1 ± 0.1	89 ± 2	18 ± 2	0.56 ± 0.01	6.6 ± 0.2	11.8	3.4	6.7	7.5	0.9
080733	3	120	3.7 ± 1.0	4.4 ± 0.2	5.1 ± 0.6	4.1 ± 0.2	97 ± 2	18 ± 2	0.57 ± 0.01	6.5 ± 0.1	11.4	2.1	6.6	6.9	0.8
080734	3	75	1.1 ± 0.5	3.3 ± 0.3	3.1 ± 0.6	2.4 ± 0.1	55 ± 1	18 ± 2	0.42 ± 0.01	5.4 ± 0.1	12.8	2.7	7.9	8.3	1.1
080735	3	95	2.4 ± 0.6	3.4 ± 0.3	4.3 ± 0.8	3.1 ± 0.1	83 ± 2	18 ± 2	0.52 ± 0.01	6.1 ± 0.1	11.7	2.6	6.9	7.4	0.9

Table 4.4: Summary of the radionuclide activities, estimated time-averaged moisture contents, calculated dose rates, equivalent doses (D_e), optical ages, and random (σ_r), systematic (σ_{sys}) and total (σ_{tot}) uncertainties, obtained for the samples taken at Arendonk-Korhaan. The uncertainties mentioned with the dosimetry and D_e data are random; all uncertainties represent 1σ.

On the whole, there is no evidence in the lithostratigraphic and chronological record of the Arendonk-*Korhaan* and Lommel-*Maatheide* sections that aeolian activity was interrupted prior to the Allerød interstadial (14.0 – 13.0 ka calBP; Hoek, 2001). The continuation of aeolian activity throughout the entire pre-Allerød Late Glacial has been reported before at other localities in the NW European lowlands. Based on the age of Unit 1, it is equivalent to the Older Coversand 2 and/or Younger Coversand 1 in the classic stratigraphic record in The Netherlands. In its type locality in the southern Netherlands (Grubbenvorst), this unit yielded ages of 16.3 ± 1.1 ka to 12.7 ± 0.9 ka (Kasse et al.,2007); at Ossendrecht (S Netherlands), ages of 15.3 ± 0.9 ka to 14.6 ± 0.9 ka were obtained (Vandenberghe et al., 2004). Furthermore, the Older Coversand 2 and/or Younger Coversand 1 was dated between 17.6 ± 2.6 ka and 13.9 ± 1.3 ka at the type locality Lutterzand in the eastern Netherlands (Bateman and Van Huissteden, 1999). As such, the OSL results obtained at various sites in the NW European lowlands suggest that the rapid climatic improvement during the Bølling interstadial (at ~14.7 ka calBP), although clearly recorded in the oxygen isotope curves from the Greenland ice-cores (see e.g. Hoek, 2001) and in the geomorphological and lithological records of some of the major NW European river systems (see e.g. Vandenberghe et al., 1987; 1994; Antoine et al., 2003), is not necessarily reflected in the terrestrial record of the NW European coversand belt. The persistence of the aeolian activity and sand deposition after the sudden temperature increase around 14.7 ka calBP appears to be related to the delayed response of the vegetation, as a result of the relatively slow and discontinuous migration of the plants to the periglacial zone, the lack of available nutrients and soils, and the occurrence of deep seasonal frost and strong winds at the onset of the Late Glacial (Hoek, 2001; Kasse et al., 2007). Kasse (2002) and Kasse et al. (2007) suggested that a decrease of the aeolian activity, resulting in loam deposition or peat formation, could only occur in local wet environments (e.g. seepage zones, wet depressions).

4.9.2. Unit 2

Unit 2 has been identified as Usselo horizon based on the stratigraphic and archaeological evidence and on the radiocarbon ages. OSL dating of this unit resulted in ages of 15.2 ± 1.3 ka at Arendonk-*Korhaan* and of 10.6 ± 0.7 ka and 12.4 ± 0.9 ka at Lommel-*Maatheide*, respectively. Within uncertainty, the ages of 15.2 ± 1.3 ka and 12.4 ± 0.9 ka are in agreement with the generally accepted age for the Allerød interstadial (14.0 – 13.0 ka calBP; Hoek, 2001). This is consistent with the lithostratigraphic and archaeological evidence, and with the radiocarbon dates of the peat in pit B at Arendonk-*Korhaan* (13.9 – 13.8 ka calBP at the base and 13.0 – 12.8 ka calBP at the top; Table 4.1). On the other hand, the age of 15.2 ± 1.3 ka, obtained on the bleached horizon in pit A at Arendonk-*Korhaan*, is not in agreement with the radiocarbon ages determined for its lithostratigraphic equivalent in pit C (13.0 – 12.8 ka calBP and 13.3 – 13.1 ka calBP for lowermost horizon, and 12.6 – 12.4 ka calBP and 12.9 – 12.7 ka calBP for uppermost horizon; Table 4.1). Moreover, the OSL ages at the sites of Lommel-*Maatheide* and Arendonk-*Korhaan* are considerably different.

At Arendonk-*Korhaan*, the OSL age of 15.2 ± 1.3 ka for Unit 2 matches the average age of 15.1 ± 1.1 ka (n=5) that was determined for the underlying cross-laminated sands of Unit 1; it is therefore thought to reflect the depositional age of the sediments in which the whitish horizon developed without significantly disturbing the sediment. It is suggested that the bleached layer observed in the field perhaps only represents the lowermost part of the original Usselo horizon. This could explain the general absence of charcoal at the top of the Usselo horizon in pit A in contrast to the abundant presence in nearby situated pit C, the presence of sand between the two bleached horizons in pit C, and the admixture of sand within the peat layer in pit B, which suggest (at least local) sedimentary processes during the Allerød. However, no sharp boundary between Units 2 and 3 could be recognised in the field or microscopically in thin sections. Some traces of biological (burrowing) activity have been recorded in the Usselo interval, but it is not clear from micromorphological analysis whether they were formed synchronously with the development of this interval. Moreover, the nature of the Usselo horizon is not apparent on the basis of micromorphology; the finer material present within the horizon forms part of the groundmass, which implies that it cannot be identified as a product of soil formation processes. This contrasts with the work of Kaiser et al. (2009), which identified the Usselo horizon as an albic arenosol on the basis of its sedimentological and pedological features. At Lommel-*Maatheide*, the ages of 10.6 ± 0.7 ka

and 12.4 ± 0.9 ka are in accordance with the average age of the overlying unit (11.7 ± 0.8 ka; n=6). This may be explained by post-depositional mixing of buried sediment grains with light-exposed grains from the surface, as a result of bioturbation, and suggests that soil development may have persisted across the Allerød-Late Dryas boundary.

Kaiser et al. (2009) reported similar experiences with the luminescence dating of the sedimentary component of soils, including the Usselo horizon; their ages were found to represent those of the parent material, or to be younger as a result of synsedimentary soil development and bioturbation. In their study, they considered the ages obtained on the aeolian sands covering the palaeosol as the most reliable ages; they provided a minimum age for the end of the soil formation. At Arendonk-*Korhaan*, the average ages of the sediments under- and overlying the bleached horizon are 15.1 ± 1.1 ka (n=5) and 12.8 ± 1.0 ka (n=2), respectively, while the time boundaries for Unit 2 at Lommel-*Maatheide* are 13.5 ± 0.9 ka (n=4) and 11.3 ± 0.8 ka (n=2). In the southern Netherlands, the Usselo horizon at Grubbenvorst developed between 13.8 ± 1.0 ka and 12.7 ± 0.9 ka (Kasse et al., 2007), and at Ossendrecht between 14.7 ± 0.6 ka and 12.3 ± 0.8 ka (Vandenberghe et al., 2004). As such, our optical ages confirm that the bleached horizon of Unit 2 can indeed be correlated with the Usselo horizon. Due to the relatively large uncertainties associated with the OSL ages, it cannot be unequivocally concluded whether the Usselo horizon developed synchronously at the aforementioned localities or whether local conditions (e.g. geomorphological setting, density of vegetation cover, groundwater level) played a part in the accumulation and preservation of sediments, as had been suggested by Kolstrup (2007).

4.9.3. Unit 3

At Lommel-*Maatheide*, the ages for the uppermost sand unit range between 11.0 ± 0.7 ka and 12.3 ± 0.8 ka, with an average age of 11.7 ± 0.7 ka (n=6). At Arendonk-*Korhaan*, an average age of 12.8 ± 1.0 ka (n=2) was obtained for Unit 3 at the top of the sand ridge (pit A), whereas the more massive sands in the N profile and the layered deposits in the S profile of pit B yielded ages of 12.8 ± 1.1 ka (n=1) and 11.4 ± 0.8 ka (n=5), respectively. It should be noted that the upper ~50 cm of Unit 3 at neither of the two localities was sampled for OSL dating, to avoid having to take into account the 'soft' component of cosmic radiation in the OSL age calculations and to avoid any influences of the podzolisation process on the dose rates and equivalent doses; as such, the ages of the uppermost samples (GLL-080701, -05, -09, -22, -30,

-34 and -35; see Tables 4.3 and 4.4) should be regarded as minimum ages for the end of the sediment deposition.

In general, the OSL ages indicate that the deposition of Unit 3 started during the Late Dryas. The sedimentation of this unit did not alter the pre-Allerød morphology of the sand ridge at Arendonk-*Korhaan* but only increased its height (Vanmontfort et al., 2010b). The small difference in age between the sediments deposited closer to the top (pit A and the northern part of pit B; ~11 ka) and those closer to the base of the sand ridge at Arendonk-*Korhaan* (southern part of pit B; ~13 ka), as well as the presence of layered sediments in the southern part of pit B, suggests that the sediments at the base underwent local erosion and sedimentation during the Late Dryas. This is consistent with the micromorphological features of these sediments, which indicate that they underwent short-distance transport, perhaps under the influence of the water in the depression. The layered sediments were dated at 11.4 ± 0.8 ka (n=5); as the possibility of incomplete bleaching was not investigated in these sediments, their age should as yet be considered as a maximum age for the local erosion and sedimentation event. On the whole, this observation illustrates the dynamic character of the sand ridge environment at Arendonk-*Korhaan*.

Unit 3 is, based on its lithostratigraphic position above the Usselo horizon and its OSL ages, considered as the equivalent of the Younger Coversand 2 unit in the Dutch stratigraphy. In the southern Netherlands, this unit is characterised by OSL ages of 13.8 ± 1.0 ka (n=1; Grubbenvorst; Kasse et al., 2007) and 12.3 ± 0.8 ka (n=3; Ossendrecht; Vandenberghe et al., 2004). At the type locality Lutterzand in the eastern Netherlands, the Younger Coversand 2 yielded an age of 13.3 ± 0.9 ka (n=1; Bateman and Van Huissteden, 1999). The combined OSL information shows the widespread occurrence of Late Dryas aeolian sands; at some localities (e.g. Heidebos; Derese et al., 2010(b)), the sands reach thicknesses of tens to hundreds cm. This indicates that, in the NW European lowlands, the Late Dryas was marked by renewed landscape instability and (extensive and rapid) aeolian activity as a result of climatic cooling, increased aridity and the opening of the vegetation cover (Kasse, 2002; Kasse et al., 2007). It is not clear from the OSL datasets for Unit 3 at Arendonk-*Korhaan* and Lommel-*Maatheide* whether the aeolian activity was constrained to the Late Dryas or persisted over the Late Dryas-Holocene boundary. The latter cannot be excluded on the basis of the average optical age of 11.7 ± 0.7 ka (n=6), obtained for Unit 3 at Lommel-*Maatheide*. The frost cracks, extending downwards from the upper part of Unit 3 at both Arendonk-*Korhaan* and Lommel-*Maatheide* and pointing to the occurrence of deep seasonal frost, however suggest that sand accumulation was mainly confined to the Late Dryas.

4.9.4. Implications for the human occupation patterns in the region

As the OSL results illustrate, Arendonk-*Korhaan* was marked by aeolian activity resulting in sand ridge development during the Late Pleniglacial and the Late Glacial; soils and sediments dating from the pre-Allerød Late Glacial appear to be missing from the record. Further research is needed to establish whether they are missing as a result of non-deposition or erosion. At Lommel-*Maatheide*, the OSL ages suggest deposition throughout the Late Glacial. There are no indications in the lithostratigraphic or chronological records that aeolian activity was interrupted prior to the Allerød; these records do not reflect the climatic amelioration during the earlier Bølling interstadial. Perhaps the extensive aeolian activity, in combination with or as a result of the slow and intermittent migration of shrubs and trees towards the NW European lowlands, inhibited landscape stabilisation during this period. As such, these localities appear to have been inhospitable at that time, with little or no protection (e.g. from trees) against the harsh climatic and environmental conditions. In contrast, the climatic amelioration during the Allerød interstadial, although less pronounced than during the Bølling, did result in the decrease of the aeolian activity and in the expansion of the vegetation cover, and hence in the further stabilisation of the landscape. This is attested by the presence of bleached horizons and peats at Lommel-*Maatheide* and Arendonk-*Korhaan*. According to Hoek (2001), the development of the vegetation took place in two steps: (1) at the beginning of the Allerød, the environment was marked by the development of juniper shrubs, preceding that of the characteristic open birch forest; (2) subsequently, pine trees arrived in the area from the southeast and most likely colonised the (drier) uplands and valley slopes. From the Allerød interstadial onwards, the investigated localities, as well as other sites in the Campine region (e.g. Lommel-*Molse Nete*, Meer-*Meirberg*, Weelde-*Eindegoorheide*, Zundert-*De Matjes*; Vanmontfort et al., 2010b, and references therein), were colonised by nomadic *Federmesser* societies. Typically, extensive *Federmesser* site complexes are found on well-drained ridges bordering wet depressions or palaeolakes, probably because the latter offered an access to both potable water and a variety of plants and animals as food resources (De Bie and Van Gils, 2009).

At the Allerod/Late Dryas transition and possibly even during the Late Dryas (Vanmontfort et al., 2010b), one or more phases with forest fires took place at the investigated localities, as is shown by the presence of macroscopic charcoal particles at the top of the Usselo horizon (Van der Hammen and Van Geel, 2008). According to Hoek and Bohncke (2002), the forest fires

mainly affected the many pine trees that were not longer in equilibrium with the wetter atmospheric conditions and for a large part died back at the end of the Allerød. The death of the vegetation cover, in combination with the cooling down of the climate and the associated intensification of the winds, resulted in the resumption of the aeolian activity in the Late Dryas; this inhospitable environmental context probably led the nomadic *Federmessergruppen* to make tracks and never return. A present, there is no archaeological indication that Ahrensburgian societies settled at Arendonk-*Korhaan* and Lommel-*Maatheide*. Their presence is established, however, at the sites of Zonhoven-*Molenheide* and Zonhoven-*Kapelberg*, and at other localities in the Campine region (Vermeersch, 2008; in press). In Belgium, The Netherlands and N France, however, there appears to have been a clear decline of settlement during the Late Dryas, compared to the Allerød (Fagnart and Coudret, 2000; Vermeersch, in press); this is perhaps related to changes in climate and environment.

At Lommel-*Maatheide* and Arendonk-*Korhaan*, the archaeological evidence does point to renewed human settlement from the Holocene onwards. Interestingly, the Early Mesolithic groups often occupied the same grounds as the Final Palaeolithic societies. This observation led Vanmontfort et al. (2010b) to classify the site of Arendonk-*Korhaan* as a microregional variant of a 'persistent place', characterised by intermittent occupation over thousands of years. Repeated visits of hunter-gatherer societies to the area were probably encouraged by the fact that its general morphology, characterised by higher and/or drier grounds, did not alter significantly by the Late Dryas sedimentation. As the Early Mesolithic groups had a similar economy and way of organising their societies as the *Federmessergruppen*, they probably had the same preferences concerning the localities of their settlements.

4.10. SUMMARY AND CONCLUSIONS

High-resolution quartz-based SAR-OSL dating contributes to the establishment of a reliable chronological framework for the landscape evolution at two type sites for the human occupation during the Weichselian-Holocene transition in the Belgian Campine region. Both sites, Lommel-*Maatheide* and Arendonk-*Korhaan*, present a similar stratigraphy: pure sands intercalated by a bleached horizon that laterally grades into a peat layer.

The optical ages of 15.3 ± 1.1 ka to 10.6 ± 0.7 ka at Lommel-*Maatheide* and of 16.2 ± 1.4 ka to 11.1 ± 0.8 ka at Arendonk-*Korhaan*, respectively, suggest that sand deposition in the Campine region was already going on during the last part of the Late Pleniglacial. Whereas

the optical ages suggest that soils and sediments dating from the first part of the Late Glacial are missing at Arendonk-*Korhaan*, the deposition at Lommel-*Maatheide* appears to have continued until the Allerød interstadial. At none of the investigated localities, the lithostratigraphic and chronological records indicate a clear interruption of the aeolian activity prior to the Allerød; this is in accordance with observations made at similar localities in the NW European lowlands.

Apparently the climatic amelioration during the earlier Bølling interstadial did not result in a general stabilisation of the landscape. However, the combined lithostratigraphic and chronological evidence illustrates that the aeolian activity decreased during the Allerød interstadial; this promoted the development of a bleached horizon and peat. Micromorphological analysis of the peat show some admixture of clastic grains; at the very least, local sedimentation processes still occurred on the sand ridges. Radiocarbon and OSL dates confirm earlier suggestions that the bleached clastic horizon is equivalent to the Usselo horizon; it is not clear from micromorphological analysis whether the presence of this horizon is due to soil formation processes. At Arendonk-*Korhaan*, the time boundaries of the Usselo horizon are dated at 15.1 ± 1.1 ka and 12.8 ± 1.0 ka, at Lommel-*Maatheide* between 13.5 ± 0.9 ka and 11.3 ± 0.8 ka. Subsequent aeolian sand deposition during the Late Dryas did not notably alter the morphology of the sand ridge at Arendonk-*Korhaan*, merely its height, but did result in drier grounds at Lommel-*Maatheide*. From the Holocene onwards, the sand areas were stabilised, mainly as a result of the expansion of the vegetation cover.

Human settlement was presumably constrained to phases of landscape stability; in this respect, a clear interaction was found between the human occupation patterns and the changes in environmental context at the sites. As both localities were characterised by repeated phases of human occupation throughout thousands of years, they can be defined as ‘persistent places’. The favourable location of elevated and/or dry areas for settlement and the close occurrence of open water and rich biotopes in the adjacent depressions probably encouraged human societies to visit the sites. When the aeolian activity resumed, these societies disappeared from the region.

As such, this paper illustrates how quartz-based SAR-OSL dating can contribute to an improved understanding of the landscape dynamics during the Weichselian-Holocene transition in the Belgian Campine region in general, and of the environmental variables that may have influenced settlement patterns in particular.

Chapter 5

The timing of aeolian events near archaeological settlements around Heidebos (Moervaart area, N Belgium)

Chapter published in full as:

Derese, C., Vandenberghe, D.A.G., Zwertvaegher, A., Court-Picon, M., Crombé, Ph., Verniers, J., Van den haute, P., 2010(b). The timing of aeolian events near archaeological settlements around Heidebos (Moervaart area, N Belgium). Netherlands Journal of Geosciences 89, 173-186.

CHAPTER 5. THE TIMING OF AEOLIAN EVENTS NEAR ARCHAEOLOGICAL SETTLEMENTS AROUND HEIDEBOS (MOERVAART AREA, N BELGIUM)

5.1. ABSTRACT

At the locality of Heidebos (Moervaart area, N Flanders, Belgium), a sedimentary core was taken in the Maldegem-Stekene coversand ridge and dated using optically stimulated luminescence (OSL). The study aimed at contributing to an improved understanding of the evolution of the physical landscape around archaeological settlements in this area. The core comprised a 7 m thick series of laminated and massive aeolian sands, in which several organic layers were intercalated. From this sequence, 11 samples were collected for quartz-based SAR-OSL dating; an internally consistent dataset was obtained. The ages of the lowermost 1 m of the sedimentary sequence (15.5 ± 1.1 ka and 17.3 ± 1.3 ka) imply that these sediments may represent the time-equivalent deposit of a deflation phase that occurred during the Late Pleniglacial and led to the formation of a widespread desert pavement, regionally known as the Beuningen Gravel Bed. However, a significant part of the sediments (at least 4 m) was deposited later, i.e. during the Allerød and/or the Late Dryas. As such, the results allow establishing the genesis of the coversand ridge at the Heidebos locality on the basis of direct age information. The relatively high sedimentation rate and the absence of extensive soil formation in the record reflect periods of pronounced aeolian activity and landscape instability during the Late Glacial, which provides part of the environmental framework for human occupation in the area.

5.2. INTRODUCTION

In NW Europe, the Weichselian-Holocene transition period has been the focus of a multitude of studies investigating the interaction between past human societies and their natural environment (e.g. Bos and Janssen, 1996; De Bie and Vermeersch, 1998; Street, 1998). This period, the so-called Late Glacial, was marked by pronounced climatic and environmental changes, which had a major influence on the human migration patterns and the regional distribution of human settlements. The time boundaries of the Late Glacial, as well as of all other chronostratigraphical and archaeological periods mentioned below, are summarised in Fig. 5.1. An overview of the human occupation in the NW European lowlands was provided by De Bie and Vermeersch (1998) and Deeben and Rensink (2005). According to these authors, the area remained uninhabited until after the Last Glacial Maximum (~21 ka calBP). Palaeolithic hunter-gatherer societies presumably reached the NW European lowlands (Belgium and The Netherlands) around 13 ka ^{14}C BP (~15.5 ka calBP), and settled in the Belgian loess belt and Meuse basin (from the Bølling onwards) and in the coversand area of the N Netherlands (during the Bølling interstadial and Early Dryas). The southernmost part of the NW European coversand belt (N Belgium and S Netherlands) remained unpopulated until the Allerød interstadial, when so-called *Federmessergruppen*, presumably originating from N France and S Germany, spread all over the NW European lowlands. The widespread occurrence of *Federmesser* settlements, which may have been a result of their highly mobile lifestyle, contrasts sharply with that of the post-*Federmesser* industries (Ahrensburgian), which tended to concentrate more strictly in regional niches, perhaps because of the rapid climatic cooling at the start of the Late Dryas stadial (Deeben and Rensink, 2005). Only from the Early Holocene (Early Mesolithic) onwards, the population density in the NW European lowlands increased again (De Bie and Vermeersch, 1998; Crombé and Cauwe, 2001). Although the broad framework for human occupation in the NW European lowlands appears to have been established, the possible causal relationships between Late Palaeolithic to Mesolithic settlement dynamics and changes in the physical environment are poorly understood. The problems are typically related to the general lack of reliable absolute age information, which makes correlation between various proxy records difficult (De Bie and Vermeersch, 1998). Optically stimulated luminescence (OSL) dating allows determining the time of sediment deposition directly.

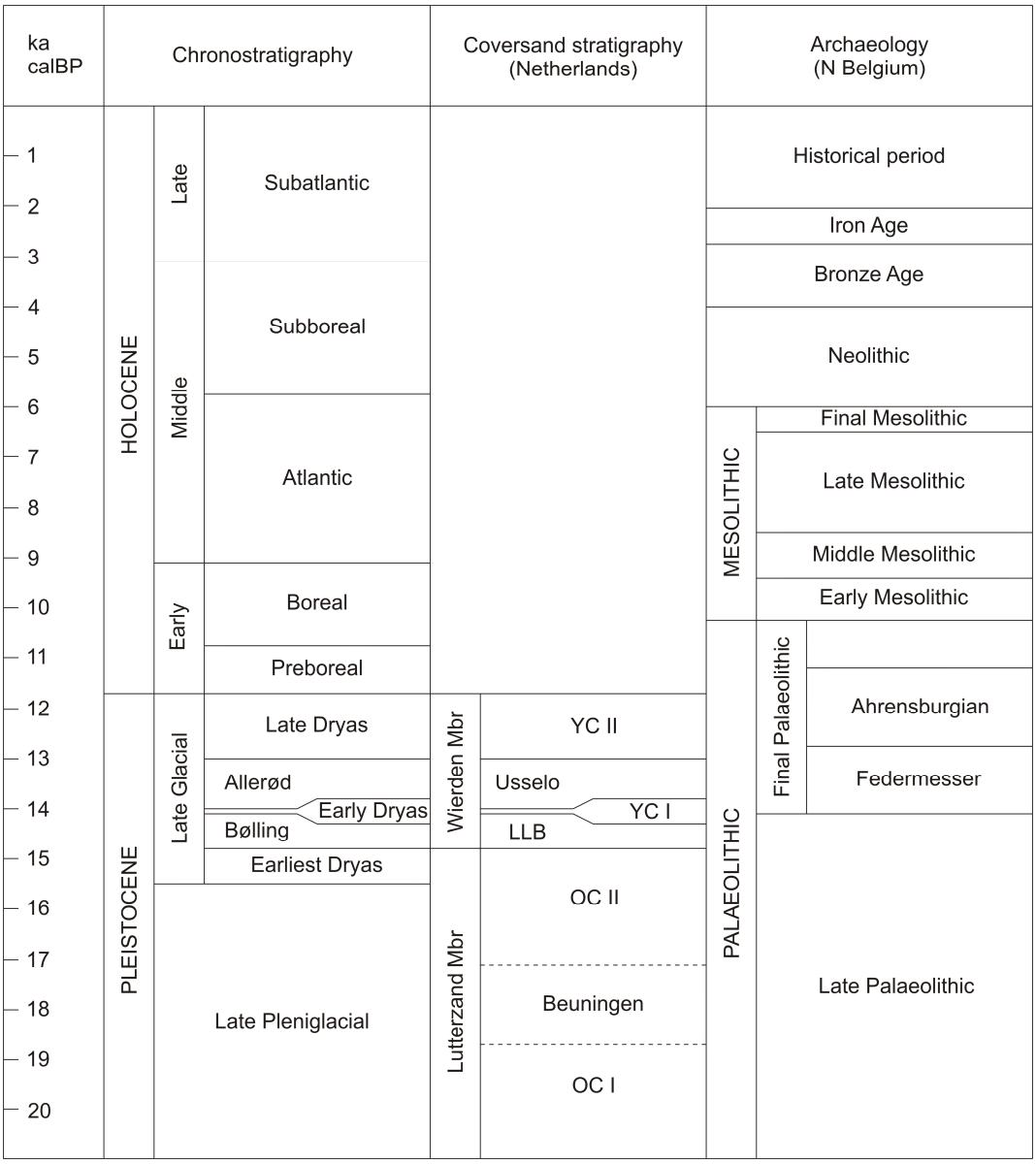

Fig. 5.1: Table summarising the subdivision of the last ~20 ka in terms of chronostratigraphy, coversand stratigraphy and archaeology. The chronostratigraphical subdivision of the Late Pleistocene is based on the ^{14}C dated time boundaries of the pollen zones (revised by Hoek, 2001), that of the Holocene is based on Terberger et al. (2009). Calibration of the radiocarbon ages was carried out using OxCal v4.1.5 (Bronk Ramsey, 2009) and the IntCal09 calibration curve (Reimer et al., 2009), and they are expressed as the 68.2% probability interval (unless stated differently) before AD 2000 ("BP") to allow comparison with the OSL ages. The stratigraphical subdivision is based on the classic subdivision of the coversands by Van der Hammen (1951) and Van der Hammen and Wijmstra (1971), and the revised subdivision by Van Huissteden (1990) and Van Huissteden et al. (2001). Used abbreviations: OC = Older Coversands, YC = Younger Coversands, LLB = Lower Loamy Bed.

The method uses the constituents of material that is readily available in the sedimentary context of archaeological sites, i.e. the mineral grains of the sediment itself. Several studies have demonstrated that luminescence dating is a powerful and reliable chronological tool,

particularly when OSL signals from quartz are used in combination with the single-aliquot regenerative-dose (SAR) protocol (Murray and Olley, 2002; Vandenberghe et al., 2004; Koster, 2005; Wintle and Murray, 2006; Wallinga et al., 2007, and references therein; Madsen and Murray, 2009; Derese et al., 2010(a)). So far, however, only few studies have applied the method to infer the timing of aeolian activity in Flanders (Vandenberghe et al., 2009; Buylaert et al., 2009; Derese et al., 2009; 2010(a)). As such, the chronology of the sedimentary record in the Flemish subsurface is still poorly understood; this seriously hampers its interpretation in terms of palaeoenvironmental and -climatic changes, and makes it difficult to assess the impact of these changes on the settlement patterns in the region.

This paper reports on the application of quartz-based SAR-OSL dating to a 7 m long sediment core that was collected from a coversand ridge bordering a vast but shallow Late Glacial palaeolake, known as the Moervaart depression, in N Belgium (Fig. 5.2a-c). The region around the Moervaart depression including the coversand ridge (further denoted as the "Moervaart area") is considered as a key-site for human occupation during the Late Glacial and Early Holocene, given the high amount of sites and site-complexes along the borders of the lake and on the coversand ridge (Crombé and Verbruggen, 2002; Sergant et al., 2009; Bats et al., 2009). Intriguingly, settlement locations seem to have changed through time and, from the Middle Holocene onwards, the area appears to have been abandoned (Bats et al., 2009). In order to understand these shifts in human occupation, it is necessary to gain insight into the evolution of the former landscape and the processes that shaped it. This forms the main subject of an interdisciplinary research project in the Moervaart area, entitled "*Prehistoric settlement and land use systems in Sandy Flanders (NW Belgium): a diachronic and geo-archaeological approach*". The work presented here fits in with this project and specifically aims at contributing to the realisation of an absolute and robust chronological framework for the sedimentary environments in the Moervaart area.

5.3. GEOLOGICAL CONTEXT AND INDEPENDENT AGE INFORMATION

The Moervaart depression is situated in the coversand area of N Belgium, in a long-stretched, largely filled palaeovalley known as the Flemish Valley (Fig. 5.2), which extends from the coastal plain and polder areas in the north to the hills of S Flanders in the south, and from the hills of W Flanders in the west to the cuestas of Boom and Waasland in the east (Tavernier, 1946; De Moor, 1963; Tavernier and De Moor, 1974).

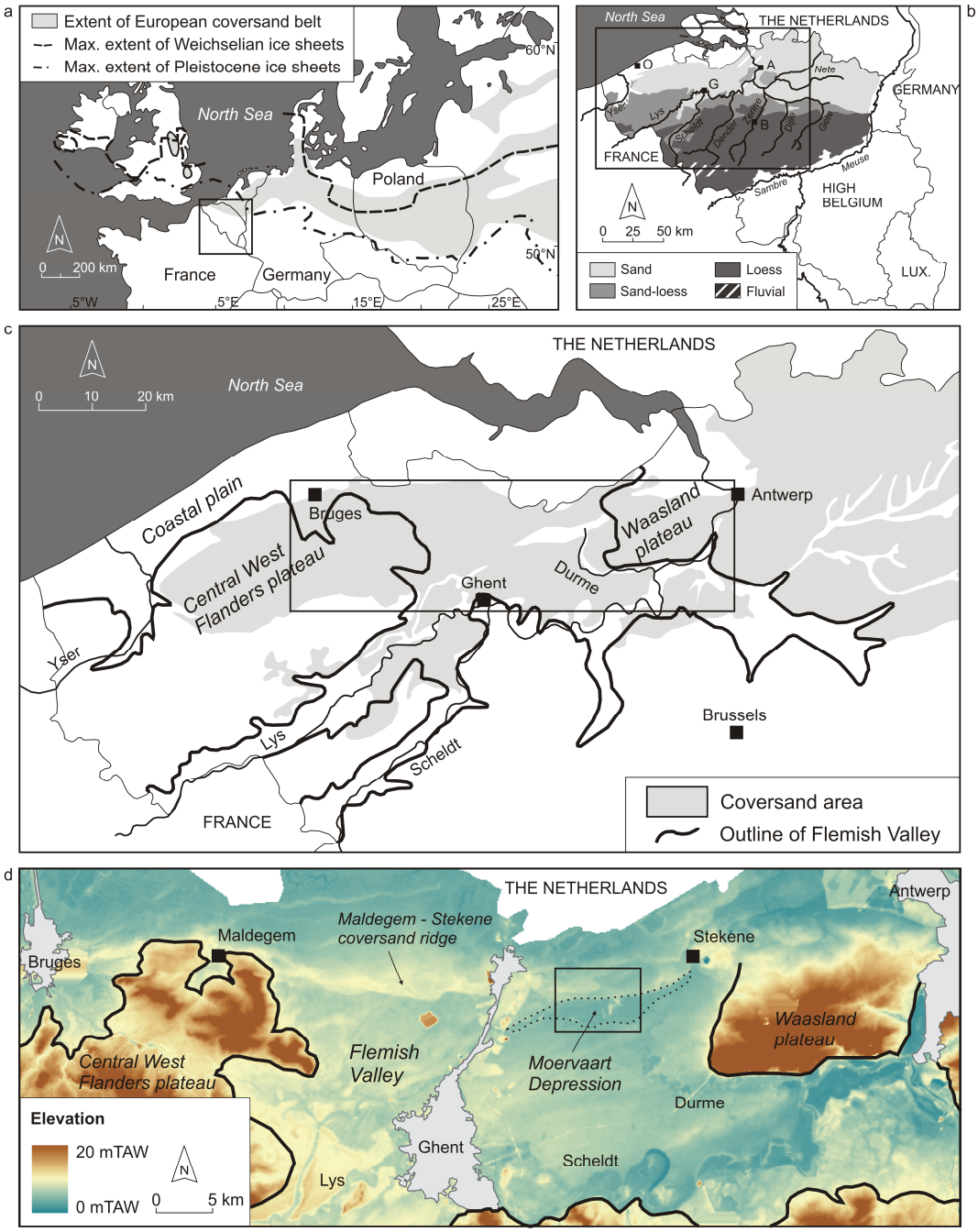

Fig. 5.2: (a) Extent of the European coversand belt (adapted from Kasse, 1997; 2000). The location of Belgium is indicated with an open square. (b) Schematic map of Belgium, showing some of the major rivers and the Pleistocene sedimentation areas in N Belgium (adapted from Paepe and Vanhoorne, 1967). The open square indicates the investigated area of the Flemish Valley. (c) Extent of the coversand area and major geomorphological units in NW Belgium (adapted from Buylaert et al., 2009). The boundary of the Flemish Valley is based on Tavernier and De Moor (1974) and the coversand area on Maréchal (1992). The study area within the Flemish Valley is indicated with an open square. (d) Digital elevation model of the study area, showing the main geomorphological units and the extent of the Flemish Valley (black line). The area indicated by the open square is enlarged in Fig. 3.

According to De Moor and Heyse (1978), this palaeovalley is a prominent geomorphological feature that developed during several phases of fluvial incision and infilling, as a result of the climatic fluctuations and corresponding sea level changes during the Pleistocene. The most important phase of infilling took place during the Weichselian, with the deposition of up to ~25 m fluvial and aeolian sediments in the central part of the valley. Extensive aeolian activity culminated in the accumulation of a series of west-east running coversand ridges, of which the Maldegem-Stekene coversand ridge (length: ~80 km, width: 1.5 to 3 km, height: ~5 m TAW on average; Heyse, 1979) is the most significant. This ridge is characterised by a microrelief of small ridges and irregularly shaped elongated depressions, indicating a complex depositional history.

The genesis of the Maldegem-Stekene coversand ridge, more specifically its westernmost extension near Maldegem, has been discussed in detail by Heyse (1979). The formation of the coversand ridge is thought to have started in the Late Pleniglacial, due to the climatic shift towards drier conditions and the subsequent decreasing fluvial and increasing aeolian activity in the Flemish Valley. The deflation of the Middle Pleniglacial fluvio-periglacial sands of the "Eeklo deposit" resulted in the development of a desert pavement, locally known as the "Middelburg Gravel". This gravel pavement may be equivalent to the Beuningen Gravel Bed (BGB); the BGB is an important marker in the European Late Weichselian coversand stratigraphy (Fig. 5.1). Kolstrup (1981) constrained its formation between approximately 15,500 ^{14}C BP (~18.7 ka calBP) and 14,000 ^{14}C BP (~17.1 ka calBP). On the basis of SAR-OSL dating, the BGB was bracketed between 17.2 ± 1.2 ka and 15.3 ± 1.0 ka at Grubbenvorst (S Netherlands; Kasse et al., 2007) and between 18.2 ± 1.3 ka and 15.9 ± 1.1 ka at Rotem (NE Belgium; Vandenberghe et al., 2009). According to Heyse (1979), the deflated sands were resedimented as low asymmetric coversand ridges under the influence of the dominating northern winds; these aeolian sands from the lowermost part of the "Maldegem deposit" can hence be interpreted as the time-equivalent deposit of the desert pavement.

Heyse (1979) recorded the occurrence of several peat layers within the "Maldegem deposit" around Maldegem, which were characterised mainly by *Betula* (birch) pollen and to a lesser degree by *Pinus* (pine), *Salix* (willow) and *Juniperus* (juniper). The pollenanalytic data were not interpreted in terms of age. However, radiocarbon dating of peat and wood fragments within the "Maldegem deposit" resulted in ages between 8,825 ± 50 ^{14}C BP (GrN-6072; 10.0 – 9.8 ka calBP; 53.1% probability) and 12,010 ± 65 ^{14}C BP (GrN-6073; 14.0 – 13.8 ka calBP), i.e. Late Glacial. Consistent ages were obtained by Kolstrup and Heyse (1980) in their pollenanalytic and radiocarbon dating study on a sedimentary sequence at Langelede, situated

some 5 km to the northwest of the Heidebos locality. On lithostratigraphic grounds, the profile at Langelede was interpreted as a Late Glacial sequence. This was confirmed by radiocarbon dates between 11,190 ± 120 ^{14}C BP (GrN-8445; 13.3 – 13.0 calBP) and 11,730 ± 120 ^{14}C BP (GrN-8286; 13.8 – 13.5 calBP), i.e. Allerød, for two intercalated sandy peat horizons and one moss layer. The Allerød interstadial was also recognised in the pollen stratigraphy, although it is represented at Langelede by a rather atypical pollen spectrum dominated by birch and willow. It was not possible to distinguish the Early Dryas from the Bølling, however, as the pollen diagram was found to be discontinuous and characterised by higher percentages of herbs and lower percentages of birch than the pollen spectra at other sites in the area.

Kolstrup and Heyse (1980) attributed the atypical character of the record to the instability of the surface layers due to aeolian activity in the area. Although the pollen assemblage was difficult to interpret, the combined evidence did suggest that the profile at Langelede represented a more or less complete record of the Late Glacial. As such, the results of both Heyse (1979) and Kolstrup and Heyse (1980) illustrate that the development of the coversand ridges did not stop at the end of the Late Pleniglacial, but continued during the Late Glacial.

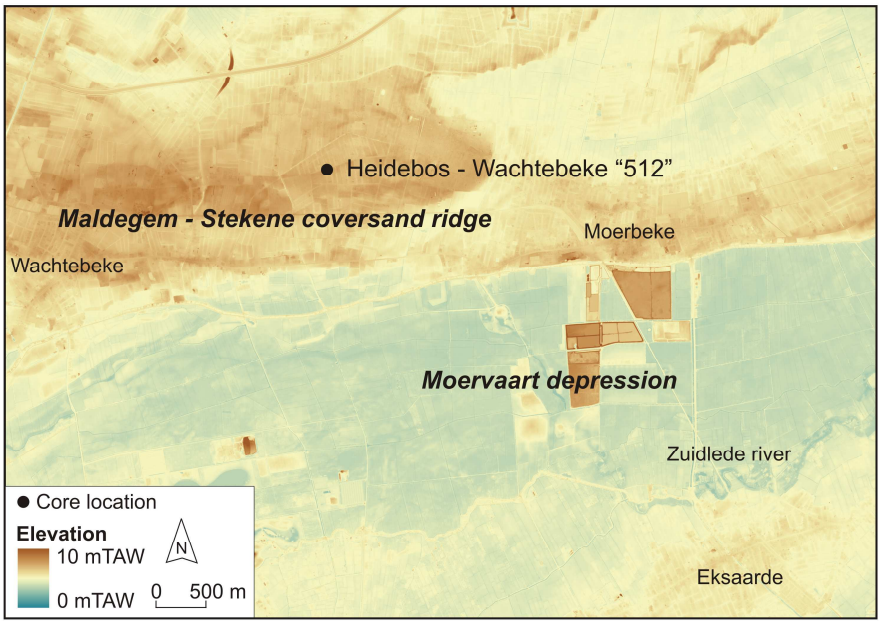

Fig. 5.3: Digital elevation model of the area around the Heidebos-Wachtebeke core "512", located near the top of the Maldegem-Stekene coversand ridge, to the north of the Moervaart depression.

The accumulation of aeolian sand deposits blocked the drainage of the Flemish Valley to the north, which led to the development of marshy areas and peat bogs to the south of the ridge,

including the Moervaart depression (De Moor and Heyse, 1978; Heyse, 1979; Spiers, 1986). This depression was filled with an alternation of aeolian sands, gyttjas or lake marls, and peat. In the past, two sequences from the deepest part of the Late Glacial lake have been studied using palynology and radiocarbon dating (Verbruggen, 1971; Van Strydonck, 2005). The ^{14}C results between 12,570 ± 55 ^{14}C BP (KIA-18750; 15.1 – 14.7 ka calBP) and 11,420 ± 50 ^{14}C BP (KIA-18757; 13.4 – 13.3 ka calBP) showed that the bulk of these sequences was deposited from the Earliest Dryas to the Allerød (Van Strydonck, 2005). The top of the sequence was placed in the Subatlantic period. This chronology has been largely confirmed by renewed multiproxy research (using e.g. pollen, spores, diatoms, chironomids, tephra, insects, mollusc) on the lake sequence (Bats et al., 2010). During the Holocene, the remaining low-lying areas, such as river valleys and depressions, were covered with flood plain sediments, while the elevated areas were locally subjected to sand-drifting (Baeté et al., 2004; Bats et al., 2009).

5.4. STRATIGRAPHY AND SEDIMENTOLOGY OF THE HEIDEBOS CORE

The present OSL study was carried out on a continuous (~7 m long) sedimentary sequence that was cored into the Maldegem-Stekene coversand ridge at the locality of Heidebos (X: 117031.77, Y: 207850.91 in Lambert 72 coordinates, Z: 7.293 mTAW; Fig. 5.3). The core locality was chosen on the ridge crest on the basis of previous exploratory studies, which reported the presence of several organic horizons within the sandy sequence. The core ("Heidebos-Wachtebeke 512") was drilled using opaque PVC tubes of 12.5 cm diameter and 1 m long. The tubes were split in half in the laboratory under subdued light conditions. One half was brought into daylight to allow a detailed description of the stratigraphy and the sediment characteristics; the other half was kept in the dark to take samples for OSL dating.
Fig. 5.4 gives a schematic log of the sedimentary sequence. High-resolution photographs of the sequence are shown in Fig. 5.5. The top of the sequence consists of a podzol (0 - 0.5 m depth) that probably developed during the Holocene and was subsequently disturbed by intensive ploughing (to a depth of 0.4 m). The underlying unit (0.5 - 0.9 m) is made up of unstratified sediments that contain various amounts of organic matter and bear traces of tree rooting. In between 1.0 and 2.0 m, the sediments are composed of a ~0.3 m thick massive sand unit, followed by horizontally stratified (1.48 – 1.77 m) and cross-laminated (1.77 – 1.97 m) sands. At a depth of 2.23 m, an organic horizon of ~0.03 m thickness occurs; the immediately over- and underlying sediments show deformation structures, which are thought

to originate with pressure during the drilling process. A natural origin for these deformation structures (cryoturbation) cannot be excluded, but is considered to be highly unlikely. This sequence is followed by horizontally laminated (2.71 – 2.80 m) and cross-bedded (2.80 – 2.94 m) sands. At a depth of 3.10 – 3.43 m, the core consists of a massive sand unit, overlying a slightly disturbed alternation of sandy and organic-rich layers. An organic horizon (3.50 – 3.57 m) separates this unit from a sequence of disturbed, mottled sands with a fairly high organic content. At a depth of 4.20 – 4.95 m, the sediments appear to be completely disturbed by the coring process, which is indicated by water-escape and deformation structures. The decalcification boundary is situated at around a depth of 5.75 m; the sediments underlying this boundary contain oxidised iron. From ~6 to 7 m, the sequence consists of massive-bedded sands with a very distinct yellow-orange colour.

Granulometric analyses on the sediments are still in progress, but qualitative observation revealed that they mainly consist of fine sands (typically 125-180 µm, or φ between +2.47 and +3). This is in agreement with the average grain sizes in the range of φ +3.47 to +1.77 (fine to very fine sands) obtained by Heyse (1979) on the sediments of the "Maldegem deposit" in the westernmost part of the Maldegem-Stekene coversand ridge. The grain-size distribution showed that the sands are well-sorted, pointing to a transport mechanism characterised by a relatively constant energy level and transport rate. This, in combination with the sedimentary structures, led Heyse (1979) to conclude that the sands were transported and deposited by wind. The aeolian sediments are intercalated by three organic layers. So far, the nature of these organic layers is not unambiguously established. In core "Heidebos-Wachtebeke 511" (X: 117033.25, Y: 207851.15 in Lambert 72 coordinates, Z: 7.315 mTAW), located in the vicinity of core "512", the organic layers are for the most part composed of silty sand and for 2-10% of organic matter. Therefore, none of the organic layers is thought to represent peat. In total, 100 samples were collected for pollen analysis of the sediments and intercalated organic horizons in core "511". The analyses are still ongoing but so far, it appears that the sand samples do not or hardly contain pollen; as for the organic layers, the preliminary pollen spectra could match any period from the Late Glacial. On the whole, the sequence seems to be deposited from the Late Pleniglacial to the Holocene (Bats et al., 2010).

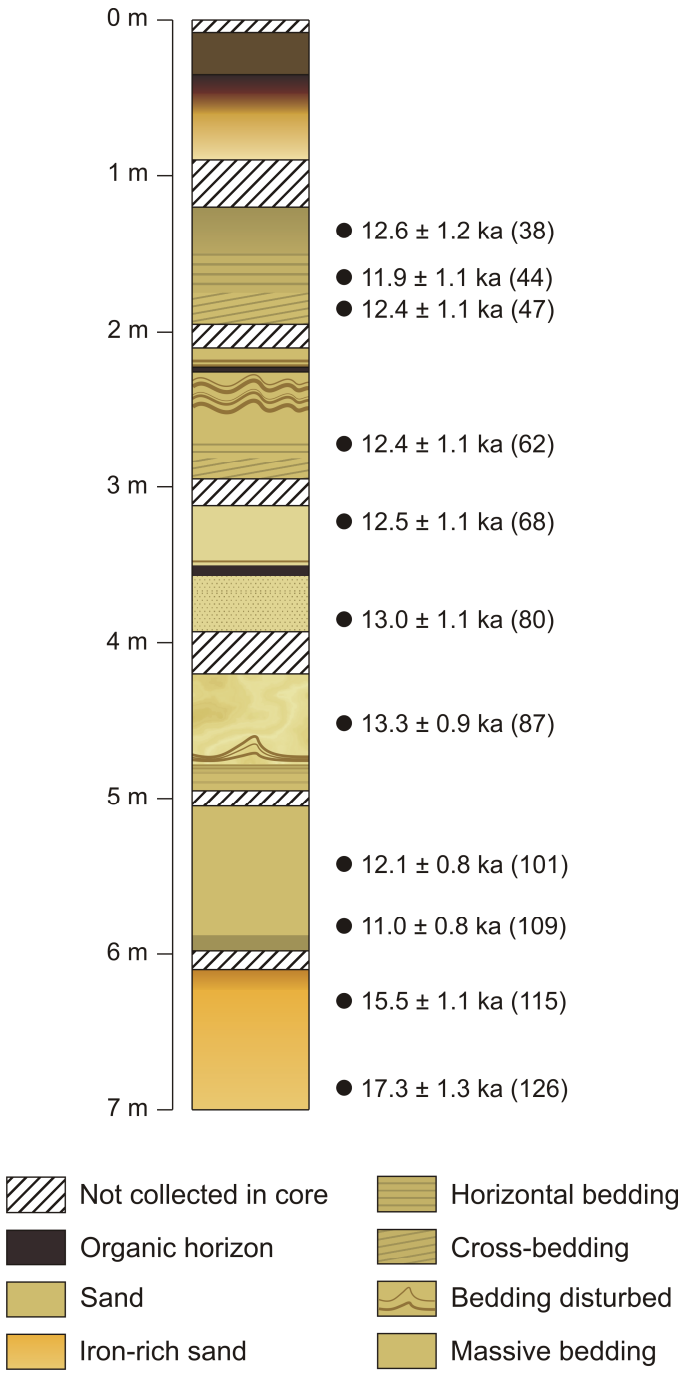

Fig. 5.4: Schematic log of the investigated sequence of coversands and intercalated soil horizons, showing the observed sedimentary structures and the location of the OSL samples. For each sample, the OSL age (± total uncertainty) and sample code (GLL-0907XX; XX given between brackets) are indicated on the figure.

The range of sedimentary structures observed in the core (e.g. massive bedding, horizontal bedding, cross-lamination) illustrates the dynamic character of the sedimentary environment. The occurrence of cross-lamination may reflect the progradation of the coversand ridge. According to Heyse (1979), the Maldegem-Stekene coversand ridge advanced mainly in southern direction; our observations in the unoriented core profile do not allow confirming

this. As the dune progressed, the windblown sands were increasingly transported over the windward flank of the dune, which was eroded; the erosional surface was subsequently covered with horizontally stratified sands. In the units marked by massive bedding, no macroscopically visible stratification has been observed; at present, these units are thought to be affected by syn- or post-depositional mixing processes.

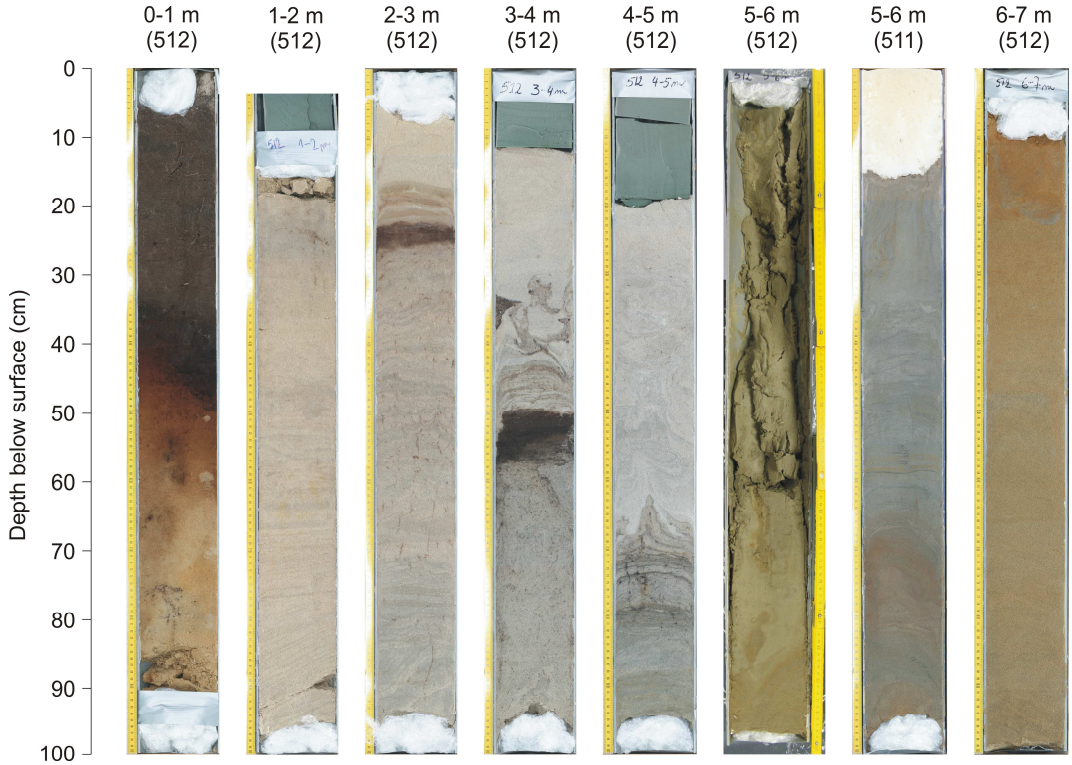

Fig. 5.5: High-resolution photographs of the Heidebos-Wachtebeke core "512". The photograph of the sequence taken at a depth of 5-6 m is not a high-resolution photograph, as this half of the core was completely disturbed during the coring process and the other half was kept in the dark for OSL sampling. The equivalent part of Heidebos-Wachtebeke core "511" (taken in the vicinity of core "512") is shown to the right of the disturbed sequence.

5.5. SAMPLING, SAMPLE PREPARATION AND ANALYTICAL FACILITIES

Alternating OSL and bulk samples were collected every ~5 cm from the inner part of the sediment core (the outer 1 cm was not sampled). This resulted in 44 OSL samples and 57 bulk samples, taken for the determination of the equivalent dose and the dose rate, respectively. From these, eleven OSL samples were selected for this luminescence dating study; the selection was based on the location of these samples at the base and top of units with a

distinct lithology (Fig. 5.4). However, the uppermost 1 m was not dated using OSL, as it might have been disturbed by post-depositional mixing (tree roots).

In the laboratory, coarse (125-180 µm) quartz grains were extracted from the OSL samples using conventional sample preparation techniques (treatment with HCl and H_2O_2, sieving, etching with 40% HF). The purity of the quartz extracts was confirmed by the absence of a significant infrared stimulated luminescence (IRSL) response at 60°C to a large (~50 Gy) regenerative beta dose. The sensitivity to IR stimulation was defined as significant if the resulting signal amounted to more than 10% of the corresponding OSL signal (Vandenberghe, 2004) or if the IR depletion ratio deviated more than 10% from unity (Duller, 2003).

For measurement, the quartz grains were fixed on the inner 8 mm of 9.7 mm diameter stainless steel discs using silicon spray. All OSL measurements were performed using an automated Risø TL/OSL-DA-12 reader, equipped with blue (470 ± 30 nm) LEDs and an IR laser diode (830 nm); the quartz luminescence emissions were detected through 7.5 mm of Hoya U-340 UV filter. Details on the measurement apparatus can be found in Bøtter-Jensen et al. (2003).

Determination of the dose rate was based on high-resolution gamma-ray spectrometry. The sediment samples that were collected above and below each OSL sample were dried (at 110°C until constant weight), pulverised and homogenised. A subsample of ~140-150 g was then cast in wax (see e.g. De Corte et al., 2006) and stored for one month before being measured on top of the detector.

5.6. LUMINESCENCE CHARACTERISTICS

The luminescence characteristics of the quartz extracts were investigated using the SAR protocol (Murray and Wintle, 2000). Optical stimulation with the blue LEDs was for 40 s at 125°C and the initial 0.32 s of the OSL decay curve was used in all calculations, minus a background evaluated from the 1.44 – 2.08 s interval. Natural and regenerated signals were measured after a preheat of 10 s at 240°C, the responses to a test dose (~3.5 Gy) after a cutheat to 180°C. To minimise possible recuperation effects, a high-temperature bleach was performed after each measurement of the test dose signal by stimulating with the blue LEDs for 40 s at 280°C (Murray and Wintle, 2003). The SAR procedure involved the measurement of the natural luminescence signal, followed by the measurement of the responses to three regenerative doses (equivalent to 50%, 100% and 200% of the estimated natural dose), a zero

dose and a repeat measurement of the response to the first regenerative dose. The response to the largest regenerative dose was measured twice. The second time, the sensitivity to IRSL was checked before stimulation with the blue LEDs, in order to identify aliquots with a significant feldspar contamination. The response to the zero dose was determined to evaluate whether the growth curve passes through the origin (recuperation). The measurement of the response to the lowest regenerative dose was repeated to investigate whether or not the sensitivity correction worked properly (recycling ratio). The measured aliquots were accepted if the recuperation and the IRSL/OSL ratio did not exceed a threshold set at 10% and if the recycling ratio and the IR depletion ratio did not differ more than 10% from unity. None of the aliquots had to be rejected based on these criteria.

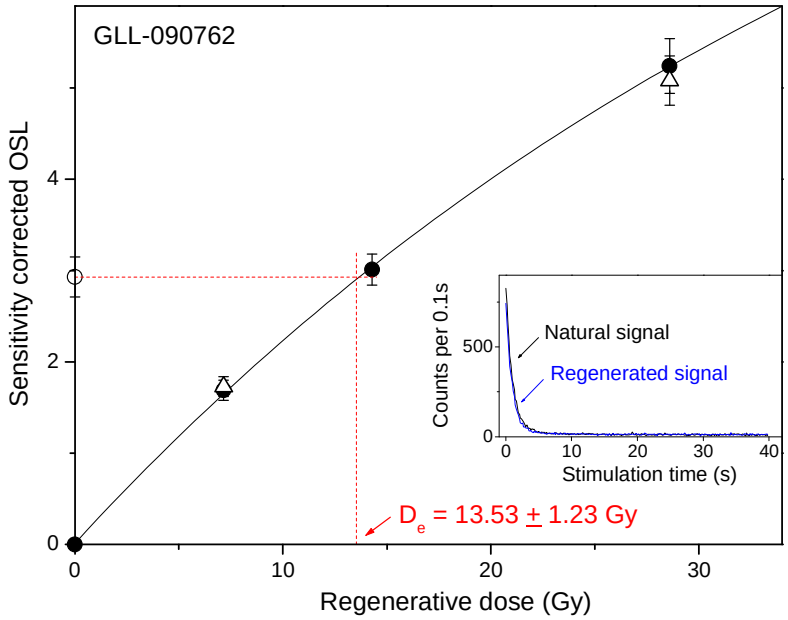

Fig. 5.6: Illustrative dose-response curve, and natural and regenerative OSL decay curve (inset) for an aliquot of 125-180 µm quartz grains extracted from sample GLL-090762. The solid line is the fit of the data to a single saturating exponential function. The open triangle represents a repeat measurement of the response to the first regenerative dose (recycling point). The equivalent dose (D_e) is obtained by interpolation of the sensitivity-corrected natural OSL signal (open circle) on the corrected growth curve.

Representative luminescence decay and growth curves are shown in Fig. 5.6 for one aliquot of sample GLL-090762. The OSL signal decays rapidly with stimulation time (Fig. 5.6, inset), which is characteristic for quartz dominated by the fast component. The dose-response curve is well approximated by a single saturating exponential function. The recycling point (open triangle on Fig. 5.6) matches the result of the first measurement, and the growth curve passes

through the origin; this demonstrates the generally good behaviour of the samples in the SAR protocol. A dose recovery test was performed to assess the reliability of the laboratory measurement procedure (Murray and Wintle, 2003). This test was performed on three natural aliquots of each sample. The aliquots were first bleached twice for 250 s using the blue LEDs at room temperature; the two bleaching steps were separated by a 10 ks pause. Subsequently, a laboratory dose close to the expected natural dose was administered to the aliquots before any heat treatment was applied. This laboratory dose was then measured using the SAR protocol as outlined in the above. Fig. 5.7a summarises the dose recovery data. The recovered to given dose ratios do not differ by more than 5% from unity and, within analytical uncertainty, the given dose can be recovered to within 2.5% for all but one sample. The overall average measured to given dose ratio is 1.00 ± 0.01 (n=33); the corresponding overall average recycling ratio and recuperation values are 0.99 ± 0.01 and 0.14 ± 0.03%, respectively (Fig. 5.7b).

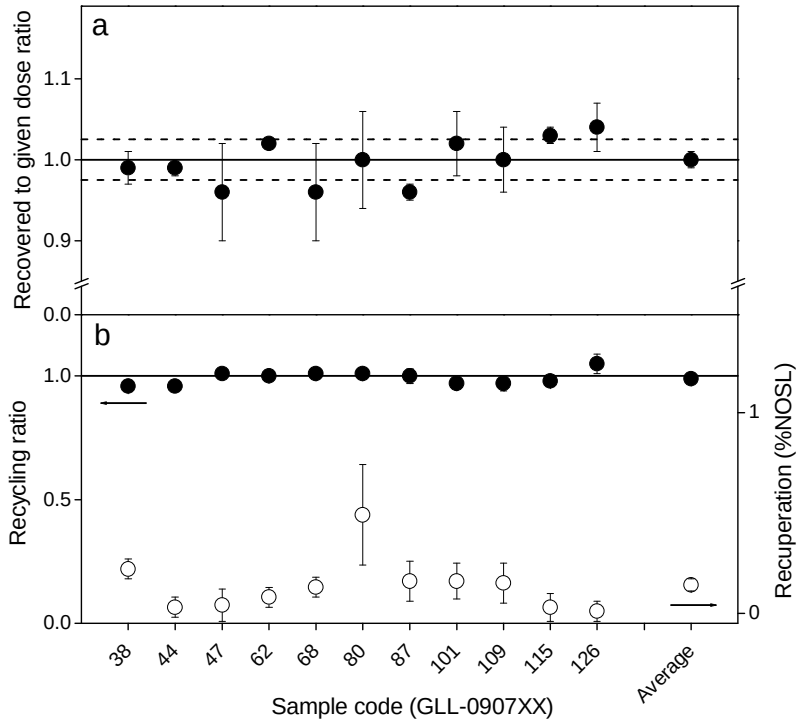

Fig. 5.7: Summary of the dose recovery data. (a) Recovered to given dose ratios. Each datapoint represents the average (± 1 standard error) of three measurements. The 'average' value represents the overall average measured to given dose ratio (± 1 standard error), obtained by averaging over 33 aliquots. The solid line (eye guide) represents a recovered to given dose ratio equal to unity; the dashed lines (eye guides) bracket a 5% deviation of the ratio from unity. (b) Corresponding recycling ratios (filled circles) and recuperation values (open circles). The solid line (eye guide) represents a recycling ratio equal to unity.

The results from the dose recovery tests indicate that the SAR protocol can accurately measure laboratory doses given prior to any heat treatment. For each sample, 18 replicate measurements of the equivalent dose (D_e) were made. The average values (± 1 standard error) are summarised in Fig. 5.8a and in Table 5.1.

5.7. DOSIMETRY

The dosimetric information is summarised in Tables 5.1 and 5.2 and in Fig. 5.8b. The radionuclide activity concentrations obtained through high-resolution gamma-ray spectrometry were converted to dose rates using conversion factors derived from the nuclear energy releases tabulated by Adamiec and Aitken (1998). A factor of 0.9 (± 5% relative uncertainty) was adopted to correct the external beta dose rates for the effects of attenuation and etching (Mejdahl, 1979). An internal dose rate in quartz grains of 0.010 ± 0.002 Gy ka^{-1} was assumed (Vandenberghe et al., 2008). The evaluation of the time-averaged moisture content, and the corresponding correction of the dose rates, was performed following the procedure outlined in Aitken (1985). As it was not possible to take separate undisturbed samples for determination of the saturated water content, this value had to be estimated. Based on the similar lithological characteristics of the sediments and those under investigation at other coversand sites in N Belgium (Derese et al., in press), the water content in fully saturated sediment (W value) was assumed to be in the range of 22% (expressed by weight); this value was used in all further calculations. Additionally, a gradient in F value (the fraction of saturation, averaged over the entire burial period) between 0.7 ± 0.2 (at the top of the sediment sequence) and 0.9 ± 0.1 (at the base) was adopted; the uncertainties on the F values were chosen to account for possible fluctuations in the groundwater level, which is presently situated at ~1.30 m depth. In this way, time-averaged water contents in the range of 15% – 20% were obtained (see Table 5.1). An increase in the water content of 1% increases the optical age by about 1% (or 10 years per ka). The contribution from cosmic radiation was calculated following Prescott and Hutton (1994) and a relative systematic uncertainty of 15% was associated with this value.

Sample GLL-code	Depth (cm)	Cosmic radiation (Gy ka^{-1})	Dose rate sediment (Gy ka^{-1})	Water content (%)	Total dose rate (Gy ka^{-1})	D_e (Gy)	Age (ka)	σ_r (%)	σ_{sys} (%)	σ_{tot}	
										(%)	(ka)
090738	133-138	0.18 ± 0.03	1.08 ± 0.07	15 ± 4	1.27 ± 0.02	16.0 ± 0.8	12.6	5.1	7.8	9.3	1.2
090744	163-168	0.17 ± 0.03	1.03 ± 0.05	15 ± 4	1.21 ± 0.02	14.4 ± 0.5	11.9	3.8	8.0	8.9	1.1
090747	183-188	0.17 ± 0.03	0.92 ± 0.04	15 ± 4	1.10 ± 0.02	13.5 ± 0.4	12.4	3.2	8.0	8.6	1.1
090762	270-275	0.15 ± 0.02	0.95 ± 0.05	17 ± 4	1.11 ± 0.03	13.8 ± 0.4	12.4	3.9	8.0	8.9	1.1
090768	320-325	0.14 ± 0.02	1.01 ± 0.01	17 ± 4	1.17 ± 0.02	14.6 ± 0.2	12.5	2.3	8.1	8.4	1.1
090780	383-388	0.13 ± 0.02	0.94 ± 0.02	17 ± 4	1.08 ± 0.02	14.1 ± 0.3	13.0	3.2	8.0	8.6	1.1
090787	450-455	0.12 ± 0.02	1.009 ± 0.003	20 ± 2	1.14 ± 0.02	15.2 ± 0.5	13.3	3.5	6.2	7.1	0.9
0907101	540-545	0.11 ± 0.02	1.519 ± 0.002	20 ± 2	1.64 ± 0.02	19.9 ± 0.5	12.1	2.8	6.3	6.8	0.8
0907109	580-585	0.11 ± 0.02	1.6 ± 0.1	20 ± 2	1.75 ± 0.04	19.3 ± 0.5	11.0	3.3	6.2	7.1	0.8
0907115	627-632	0.10 ± 0.02	0.99 ± 0.08	20 ± 2	1.10 ± 0.02	17.0 ± 0.4	15.5	3.1	6.2	6.9	1.1
0907126	684-689	0.10 ± 0.01	0.84 ± 0.01	20 ± 2	0.95 ± 0.02	16.4 ± 0.7	17.3	4.5	6.2	7.7	1.3

Table 5.1: Summary of the estimated cosmic radiation, effective external dose rates provided by surrounding sediment, estimated time-averaged moisture contents, total effective dose rates (including the estimated contribution from internal radioactivity; 0.010 ± 0.002 Gy ka-1), equivalent doses (D_e), optical ages, and random (σ_r), systematic (σ_{sys}) and total (σ_{tot}) uncertainties. For each sample, the effective external dose rate was calculated as the average of the dose rate provided by the immediately over- and underlying sediment. The uncertainties mentioned with the dosimetry and De data are random; all uncertainties represent 1σ.

Sample GLL-code	**Depth (cm)**	**^{40}K (Bq kg^{-1})**	**^{234}Th (Bq kg^{-1})**	**^{226}Ra (Bq kg^{-1})**	**^{210}Pb (Bq kg^{-1})**	**^{232}Th (Bq kg^{-1})**	**Dose rate (Gy ka^{-1})**
090736	125-128	309 ± 3	12.1 ± 1.2	11.9 ± 0.3	12.5 ± 0.9	10.9 ± 0.3	1.20 ± 0.01
090737	128-133	298 ± 3	7.9 ± 0.9	10.2 ± 0.3	9.6 ± 0.7	9.0 ± 0.1	1.10 ± 0.01
090739	138-143	273 ± 2	5.8 ± 0.8	7.2 ± 0.2	7.7 ± 0.7	6.8 ± 0.1	0.95 ± 0.01
090743	158-163	297 ± 4	6.1 ± 1.0	9.4 ± 0.3	9.7 ± 1.1	8.7 ± 0.2	1.08 ± 0.01
090745	168-173	279 ± 3	4.2 ± 0.8	7.7 ± 0.2	7.9 ± 0.8	7.8 ± 0.2	0.98 ± 0.01
090746	178-183	264 ± 3	3.7 ± 0.9	6.6 ± 0.3	5.2 ± 0.7	6.3 ± 0.2	0.88 ± 0.01
090748	188-193	280 ± 3	6.7 ± 1.1	6.8 ± 0.3	6.2 ± 0.9	6.5 ± 0.2	0.95 ± 0.01
090761	265-270	257 ± 2	6.4 ± 1.2	6.4 ± 0.3	6.0 ± 1.1	5.6 ± 0.1	0.86 ± 0.01
090763	275-279	300 ± 3	8.0 ± 0.9	8.8 ± 0.2	8.5 ± 0.9	8.3 ± 0.3	1.04 ± 0.01
090764	281-286	277 ± 3	7.1 ± 0.8	7.3 ± 0.2	8.1 ± 1.0	6.6 ± 0.1	0.95 ± 0.01
090767	315-320	290 ± 3	6.3 ± 0.8	7.9 ± 0.6	8.2 ± 0.8	7.6 ± 0.1	1.00 ± 0.01
090769	325-330	305 ± 3	6.4 ± 0.9	8.7 ± 0.3	7.3 ± 0.8	7.7 ± 0.2	1.03 ± 0.01
090779	378-383	263 ± 2	5.7 ± 0.8	8.1 ± 0.5	10.6 ± 1.0	7.3 ± 0.1	0.95 ± 0.01
090781	388-393	256 ± 3	5.5 ± 1.1	7.9 ± 0.3	10.1 ± 1.2	7.0 ± 0.2	0.92 ± 0.02
090786	445-450	280 ± 3	9.5 ± 0.6	9.3 ± 0.3	10.3 ± 0.8	8.7 ± 0.1	1.01 ± 0.01
090788	455-460	285 ± 3	9.2 ± 0.7	10.0 ± 0.6	9.5 ± 1.0	9.1 ± 0.2	1.01 ± 0.01
0907100	535-540	369 ± 4	17.2 ± 1.6	20.0 ± 0.7	19.8 ± 1.1	18.3 ± 0.2	1.52 ± 0.02
0907102	545-550	372 ± 3	19.5 ± 1.3	19.6 ± 0.3	18.5 ± 0.8	18.1 ± 0.3	1.52 ± 0.01
0907108	575-580	387 ± 4	25.1 ± 1.8	20.6 ± 0.5	31.2 ± 2.3	20.6 ± 0.2	1.77 ± 0.03
0907110	585-590	362 ± 3	15.3 ± 1.5	19.9 ± 0.8	20.2 ± 1.4	18.3 ± 0.2	1.50 ± 0.02
0907114	622-627	256 ± 3	13.7 ± 1.2	15.4 ± 0.4	13.2 ± 1.2	13.3 ± 0.2	1.06 ± 0.02
0907116	632-637	261 ± 3	7.0 ± 1.0	7.9 ± 0.2	8.5 ± 0.7	7.6 ± 0.2	0.91 ± 0.01
0907125	679-684	247 ± 3	5.4 ± 1.2	7.1 ± 0.2	7.8 ± 0.7	7.4 ± 0.1	0.86 ± 0.01
0907127	689-694	249 ± 3	7.0 ± 1.0	6.7 ± 0.3	5.8 ± 0.8	6.6 ± 0.2	0.83 ± 0.01

Table 5.2: Summary of the radionuclide activities and resulting effective dose rates (corrected for the effects of moisture and attenuation; excluding the internal radioactivity and cosmic radiation) determined for the sediment samples immediately over- and underlying the OSL samples mentioned in Table 1.

As outlined above (section 5.5), radionuclide activity concentrations and dose rates were obtained for the sediments over- and underlying each OSL sample. There is little variation in

dose rate with depth and most values range from ~1.0 to ~1.2 Gy ka^{-1} (Fig. 5.8b); these values are typical for quartz-rich coversands in the NW European lowlands (see e.g. Kasse et al., 2007; Vandenberghe et al., 2009). The dose rate for samples GLL-0907101 and GLL-0907109 is somewhat higher, with values in the range of ~1.6 to 1.8 Gy ka^{-1}. The observed equilibrium in the ^{238}U series shows that precipitation of radionuclides at a later time probably does not account for the higher dose rate, as this would have resulted in a preferential enrichment of certain radioelements (e.g. radium). Moreover, the peak in dose rates was followed by a peak in equivalent dose (Figs. 5.8a and 5.8b).

Although all samples were collected from sand layers that appeared homogeneous over a vertical distance of at least ~15 cm, and the gamma-ray spectrometric analysis was performed on ~150 g subsamples of a few 100 g of homogenised sediment, the dose rate provided by the under- and overlying sediment is not always consistent within analytical uncertainty (Table 5.2; Fig. 5.8b); the results obtained for sample GLL-0907109 illustrate this most clearly. Vandenberghe et al. (2009) previously reported that the dose rate may vary significantly in apparently homogeneous coversands. As the cause for such variations is not yet understood, the dose rate appropriate to each OSL sample was simply obtained as the mean value of the dose rate in the immediately under- and overlying sediment. The latter are given in Table 5.2, while the mean values are summarised in Table 5.1.

5.8. LUMINESCENCE AGES

Table 5.1 synthesises all the information relevant to the age and uncertainty calculation. Uncertainties on the optical ages were calculated following the error assessment system formalised by Aitken and Alldred (1972) and Aitken (1976). It can be seen that the systematic uncertainty is dominant in the overall uncertainty on the ages and that it ranges from ~6 to 8% (Table 5.1).

In Fig. 5.8c, the resulting OSL ages, and their associated random and total uncertainties are plotted as a function of the depth of the samples. As the sources of systematic uncertainty (arising from e.g. beta source calibration, conversion of radionuclide activities to dose rates, estimation of the contribution from cosmic radiation and internal radioactivity) are largely shared between the samples, only the random uncertainty (~2 – 5%) is taken into account to evaluate the internal consistency of the OSL dataset. The optical ages vary between 11.0 ± 0.4 ka and 17.3 ± 0.8 ka. The dataset can be looked at in two different ways. When considering

the whole dataset, the ages obtained for the upper 6 m of sediment (samples GLL-090738 to GLL-0907109) appear to show little increase with depth and to be spread around an average value of 12.3 ± 0.1 ka (weighted mean ± 1 expected random uncertainty); all ages are consistent with this value within 1 random uncertainty, with the exception of sample GLL-0907109 at 5.8 m depth, which is only consistent at the two sigma level. The two lowermost samples between 6 and 7 m (GLL-0907115 and -126) yield ages of 15.5 ± 0.5 ka and 17.3 ± 0.8 ka; within two random uncertainties, the results cannot be considered as significantly different and their weighted mean (± 1 expected random uncertainty) is 16.3 ± 0.4 ka. However, it could be argued that samples GLL-0907101 and GLL-0907109, which show unexpectedly high dose rates and, in the case of sample GLL-0907109, diverging dose rates in the over- and underlying sediment (see above), should be excluded from this dataset. If done so, an increase of the age with depth may be observed within the dataset, from 12.6 ± 0.6 ka at the top of the sequence to 17.3 ± 0.8 ka at the base.

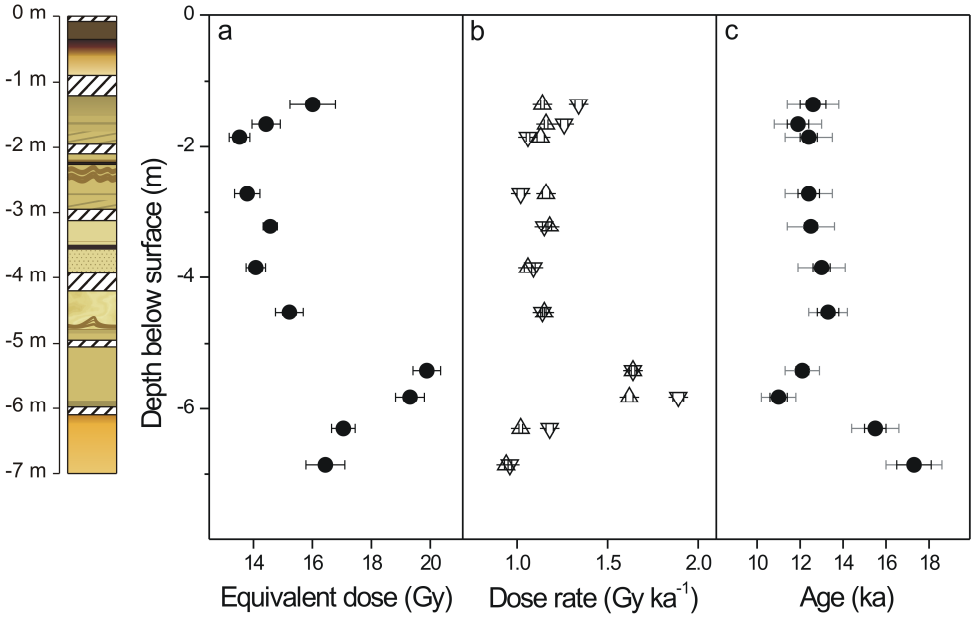

Fig. 5.8: Plot of the (a) equivalent doses, (b) dose rates, and (c) resulting optical ages as a function of the depth of the samples. The sedimentary log is the same as shown in Fig. 5.4. The open triangles and inverted open triangles circles represent the dose rates provided by the sediment immediately over- and underlying the OSL samples, respectively; for each sample, the average was used for calculating the OSL age. Both the random (black error bars) and total (grey error bars) uncertainties associated with the optical ages are indicated on the figure.

It is concluded that the OSL ages are generally in agreement with the stratigraphic position of the samples and form an internally consistent dataset. Although some uncertainty exists as to the uniformity of the dose rate (see above), the observed variation is not much larger than expected from individual uncertainties; this suggests that all sources of random uncertainty have been properly identified and accounted for.

5.9. INTERPRETATION AND DISCUSSION

To allow interpreting the optical ages in terms of the depositional history of the sediments and to allow a more straightforward comparison with other age information, the ages are mentioned with their total uncertainties in the following discussion. As stated in the above, the OSL dataset can be interpreted in two different ways. If all data are considered, at least two distinct phases of coversand deposition can be differentiated in the Heidebos core, one during the Late Pleniglacial (16.3 ± 1.1 ka (n=2) between 6-7 m depth) and one during the Late Dryas period (12.3 ± 0.9 ka (n=9) between 1-6 m depth). The ages thus point to a marked hiatus within the coversand sequence, which appears to encompass the early Late Glacial up to the Late Dryas. However, if the ages of 12.1 ± 0.8 ka and 11.0 ± 0.8 (samples GLL-0907101 and -109, respectively) are considered as unreliable and hence excluded from the dataset, the hiatus in the OSL dataset around ~6 m is much less clear and a semi-continuous coversand deposition from the final phase of the Late Pleniglacial until the Late Dryas or perhaps the Holocene (as the upper 1 m was not sampled for OSL dating) cannot be excluded. In the following, we explore the arguments pro and contra the occurrence of a marked hiatus or semi-continuous sedimentation throughout the Late Glacial.

Several sedimentary ‘processes’ could be held responsible for the occurrence of a gap in an OSL dataset, in this case most likely (1) non-deposition, and/or (2) erosion. A prolonged phase of land surface stability, due to the decrease or stagnation of aeolian activity, would have affected the sediment in between samples GLL-0907109 and GLL-0907115 by soil formation processes. We observed no such soil horizon, although it cannot be ruled out that it was present in the ~10-15 cm interval that is missing from the core; its presence may be indicated by the decalcification boundary around 5.75 m depth and by the difference in iron oxidation between the 6 m thick stack of gray-coloured sands and the lowermost 1 m thick unit of sediments with a yellow-orange colour (see Fig. 5.4). However, it is well documented that the Late Glacial was a period with marked climatic and environmental changes and

previous investigations on equivalent coversand sequences have demonstrated that, in the NW European lowlands, aeolian coversand deposition persisted across the Late Pleniglacial to Late Glacial boundary (Vandenberghe et al., 2004; Kasse et al., 2007). At the type locality for coversand lithostratigraphy in the S Netherlands, Kasse et al. (2007) reported SAR-OSL ages between 15.3 ± 1.0 ka and 12.7 ± 0.9 ka for the Older Coversands II and Younger Coversands I, which represent regionally the most extensive sedimentary unit in northwest and central Europe.

As mentioned in section 5.3, many Late Weichselian coversand profiles in the NW European lowlands show evidence of a large-scale deflation event at the end of the Late Pleniglacial through a lithostratigraphic horizon known as the Beuningen Gravel Bed (BGB). In the "Heidebos-Wachtebeke 512" core, no gravel layer has been reported in the interval corresponding to the time-gap; again, it may not have been observed because this interval was incompletely sampled. In terms of time, however, it seems hard to reconcile the period of deflation that resulted in the BGB with the hiatus that may be observed in the core. Indeed, quartz-based SAR-OSL dating allowed bracketing the age of the BGB between 17.2 ± 1.2 ka and 15.3 ± 1.0 ka in the S Netherlands (Kasse et al., 2007) and between 18.2 ± 1.3 ka and 15.9 ± 1.1 ka in NE Belgium (Vandenberghe et al., 2009). It should be noted that it remains to be established whether the BGB is truly an isochronous marker. However, while it seems logical that the formation of the BGB may have started earlier at some wind-exposed localities (Kasse, 1997), it is more difficult to envisage that the conditions required to form such a widespread desert pavement (cold, dry, no or little vegetation) prevailed during the Late Glacial (warmer, wetter, increased land surface stability). The available age information thus constrains the age of the BGB to the (Late) Pleniglacial, while it would be a substantial part of the Late Glacial that is missing from the core. The hiatus could only be interpreted as a signature of local erosion, possibly caused by increased aeolian activity, at some stage between 15.5 ± 1.1 ka and 13.3 ± 0.9 ka.

In conclusion, it cannot be unequivocally established on the basis of the present OSL dataset whether the coversand ridge at the Heidebos locality developed during two distinct phases of aeolian deposition or whether it developed as a result of semi-continuous accumulation of aeolian sands, which was only interrupted during fairly short intervals reflected in the coversand sequence by the occurrence of disconformities (erosional surfaces between cross-laminated and horizontally laminated units). On the one hand, there is no convincing argument to exclude samples GLL-0907101 and -109 from the OSL dataset. On the other hand, the hypothesis of semi-continuous deposition is corroborated by the presence of sandy

layers within the lake marl and peat sequences in the Moervaart depression (see section 5.3). As these sequences have been dated to the Late Glacial, this implies that sediment must have been available, transported and deposited during this period.

The average age of 16.3 ± 1.1 ka (n=2) for the lowermost 1 m of sediment matches the above-mentioned age bracket for the BGB. This could suggest that the deposition of this part of the core was coeval with the formation of this desert pavement. However, the OSL ages for the overlying 6 m of sediment also demonstrate that a significant part of the ridge at Heidebos was shaped much later. The widespread occurrence of the BGB suggests large-scale sand removal and it has been a quandary as to explain where all the deflated sand was transported to. It has been suggested that the BGB may not have (entirely) formed by deflation of the previously deposited Older Coversands I, but through accumulation of coarser material by creep or surficial runoff from higher areas, and/or that it may not be an isochronous marker (Kasse et al., 2007; see higher). An alternative explanation emerging from this and other recent optical dating studies is that the preservation potential of the original deposits of deflated sand may have been low. Indeed, optical dates for cover- and dune sands at various localities in The Netherlands and Belgium such as Ossendrecht (Vandenberghe et al., 2004), Opgrimbie (Derese et al., 2009), Arendonk and Lommel (Derese et al., in press) document periods of pronounced aeolian activity throughout the Late Glacial, despite periods of rapid climate warming, wetting and land surface stability. Obviously, explaining the genesis of these deposits also requires that their source of sediment is identified.

Although the OSL dataset at present does not allow unequivocally establishing whether the coversands were deposited during two clearly separated phases of coversand deposition or not, our results allow in any case refining the ideas put forward by Heyse (1979) and Kolstrup and Heyse (1980) as to the genesis of the Maldegem-Stekene coversand ridge (see section 5.3). The luminescence chronology demonstrates that the ridge formation started during the Late Pleniglacial; moreover, it suggests that the area may have been characterised by extensive aeolian activity during the Allerød and/or Late Dryas. The OSL dataset also illustrates that the sedimentation rate increased significantly from the Late Pleniglacial (~0.5 m per ka on average) up to the Late Dryas (at least ~2 m per ka on average). It can be noted that the OSL ages do not exclude that one or more of the organic horizons in the Heidebos core are of Allerød age; this implies significant aeolian deposition during a phase that is generally considered as being marked by landscape stabilisation and soil formation. Interestingly, this idea does not conflict with the results obtained by Derese et al. (2009) for the dune complex at Opgrimbie (NE Belgium), where two sediment units underlying the Usselo soil of Allerød age

were dated at 12.9 ± 0.9 ka and 13.0 ± 0.8 ka. To our view, the apparent discrepancy illustrates that the time resolution of luminescence dating techniques may be too limited to allow unambiguously correlating an aeolian unit to a particular period of the Late Glacial; on the other hand, one may wonder to what extent aeolian activity should be strictly restricted to stadials, especially as only relatively few direct sedimentation ages are available.

The OSL ages provide essential information for the landscape reconstruction in relation to the human occupation patterns during the Late Glacial – Early Holocene transition in this region. Although the optical ages and sedimentary structures do not clearly seem to point to landscape stabilisation during the Allerød, the presence of the palaeolake of the Moervaart, which by then had reached its maximal extension (Bats et al., 2010), may have favoured human settlement in the area. As a matter of fact, the first human presence did not appear earlier than the Allerød (Crombé and Verbruggen, 2002; Sergant et al., 2009; Bats et al., 2009), suggesting that the prehistoric man belonging to the *Federmesser* culture waited for favourable conditions to colonise the area. Occupation clustered mainly on the northern bank of the palaeolake and on small sandy outcrops within the lake. The extremely high density of *Federmesser* sites probably indicates a higher frequency of site re-occupation, occupation by larger groups and/or occupation for longer periods within the annual cycles compared to elsewhere in N Flanders. Clearly the massive coversand dune combined with the adjacent lake formed one of the principal “central foci” or “persistent places” in the Late Glacial hunter-gatherer landscape of N Flanders (Sergant et al., 2009). At some stage during the Allerød and/or Late Dryas, aeolian activity intensified dramatically, resulting in the deposition of perhaps several meters of coversands; simultaneously the palaeolake started to dry out (Bats et al., 2010). These important environmental events most likely had a considerable impact on human life. It is not unlikely that, during the Late Dryas, the environment was too inhospitable for human occupation, explaining why Final Palaeolithic societies seemingly disappeared from the area. Recolonisation took place only at the start of the Early Holocene, not before 11 ka calBP.

5.10. CONCLUSIONS

High-resolution quartz-based SAR-OSL dating was applied to a sequence of coversands bordering the Moervaart depression at Heidebos (N Belgium). An internally consistent set of optical ages ranging from 17.3 ± 0.8 ka to 12.6 ± 0.6 ka was obtained, indicating sediment

deposition during the Late Pleniglacial and during the Allerød and/or Late Dryas. The lowest 1 m of the sequence may be considered as the time-equivalent deposit of a desert pavement, known in the classic coversand lithostratigraphic record as the Beuningen Gravel Bed (BGB). However, the bulk of the coversand ridge at Heidebos was probably deposited during the Allerød interstadial and/or the Late Dryas stadial. It remains to be investigated to what extent the intercalated organic layers reflect phases of landscape stability; considering that uppermost 6 m of sediment may have been deposited in less than 2 ka, it is unlikely that they represent important phases of soil formation and land surface stability.

The study documents pronounced phases of aeolian activity during the Late Glacial, and contributes to an improved understanding of the environmental variables that may have influenced settlement patterns along the Moervaart area. Further investigations of the lake infill, including optical dating of clastic layers, are ongoing. It is expected that these will allow gaining further insight in the spatial and temporal relationship between the evolution of the lake and the coversand ridge, the geomorphic and climatic processes that shaped them, and how these affected the colonisation of the area.

Chapter 6

Late Weichselian (fluvio-)aeolian sediments and Holocene drift-sands of the classic type locality in Twente (E Netherlands): A high-resolution dating study using optically stimulated luminescence

Chapter to be published as:

Derese, C., Vandenberghe, D.A.G., Kasse, C., Van den haute, P., in prep. Late Weichselian (fluvio-) aeolian sediments and Holocene drift-sands of the classic type locality in Twente (E Netherlands): A high-resolution dating study using optically stimulated luminescence.

CHAPTER 6. LATE WEICHSELIAN (FLUVIO-)AEOLIAN SEDIMENTS AND HOLOCENE DRIFT-SANDS OF THE CLASSIC TYPE LOCALITY IN TWENTE (E NETHERLANDS): A HIGH-RESOLUTION DATING STUDY USING OPTICALLY STIMULATED LUMINESCENCE

6.1. ABSTRACT

The Late Weichselian and Holocene (fluvio-)aeolian sands of the type locality Lutterzand in the E Netherlands have been the focus of many palaeoclimatic, palaeoenvironmental and geochronological studies. In the present study, the sedimentological characteristics of the fluvio-aeolian and aeolian sequences have been reinvestigated, and a detailed chronological framework has been established using radiocarbon and optically stimulated luminescence dating.

Three main phases of sedimentation have been differentiated in the Lutterzand sections, consistent with the final phase of the Late Pleniglacial, the Late Glacial and the Late Holocene. From at least 25.2 ± 1.9 ka up to 19.9 ± 1.6 ka, the area was marked by a transition from fluvial to fluvio-aeolian deposition. The sediments have been affected by periglacial phenomena providing evidence for permafrost conditions and were truncated by the Beuningen Gravel Bed. The Beuningen Gravel Bed is considered as the lithostratigraphic marker for permafrost degradation, shallow channelling and aeolian deflation associated with the formation of a desert pavement. Localised fluvial sedimentation in shallow channels took place between approximately 23.4 ± 1.9 ka and 16.1 ± 1.3 ka; the OSL ages should be regarded as maximum ages, as it cannot be unequivocally said that the sediments were fully bleached. The desert pavement at the top of the Beuningen Gravel Bed was most narrowly bracketed between 16.1 ± 1.3 ka and 13.8 ± 1.1 ka. The aeolian sediments overlying this polar desert pavement were deposited as sand sheets and low dunes and yielded ages between 15.8 ± 1.4 ka and 12.2 ± 0.9 ka. The OSL ages point to fairly continuous coversand sedimentation. The lithostratigraphic evidence, i.e. the presence of organic and silty horizons within the aeolian sediments, however illustrates that phases characterised by a decrease or break in aeolian activity did occur during the Late Glacial. This shows the limit on the time resolution that can be achieved using quartz SAR-OSL dating. During the major part of the Holocene,

the landscape stabilised due to increased vegetation and a podzol developed in the top of the aeolian sediments. Probably due to human activities, sand-drifting events locally resulted in the removal of the upper part of the Late Glacial sequences and in deposition elsewhere. The drift-sands were dated between 0.40 ± 0.04 ka and 0.20 ± 0.02 ka.

6.2. INTRODUCTION

The classical lithostratigraphic subdivision of the Late Weichselian fluvio-aeolian and aeolian sediments in the NW European lowlands (Belgium and The Netherlands) was first described in the Lutterzand area (Twente, E Netherlands; Van der Hammen, 1951; Van der Hammen and Wijmstra, 1971) and comprises the following succession: Older Coversand I, Beuningen Gravel Bed, Older Coversand II, Lower Loamy Bed, Younger Coversand I, Usselo Soil and Younger Coversand II. The alternation of coversand units, a deflation bed and soil horizons was thought to reflect the rapid climatic and environmental changes during the Late Weichselian and the Weichselian-Holocene transition. Since then, the lithostratigraphic units have been recognised and correlated in large parts of NW and Central Europe (Kasse et al., 2007, and references therein), mainly on the basis of their stratigraphic position, sedimentological features, pollen analysis and radiocarbon dating of organic horizons intercalated between the coversands. Establishing a chronological framework for the fluvio-aeolian and aeolian deposits in the NW European lowlands was long hampered by some of the limitations inherent to the radiocarbon dating technique. Radiocarbon dating can only be applied to organic material, while the sediments in Belgium and The Netherlands are usually sterile, i.e. they do not contain a sufficient amount of organic material for radiocarbon dating. Direct age information can only be obtained for interbedded soils and peats, while the timing of sand deposition cannot be determined in a direct way. It follows that, using radiocarbon dating, information about sedimentation rates or the occurrence of sedimentary hiatuses cannot be obtained. Luminescence dating, on the other hand, does allow directly dating the mineral component of the sediments. At the type locality Lutterzand, attempts to date the sections using thermoluminescence dating (Dijkmans et al., 1988; Dijkmans and Wintle, 1991) failed due to methodological problems. Optically stimulated luminescence dating (Stokes, 1991; Bateman and Van Huissteden, 1999) yielded more accurate results. The dataset, however, was rather limited and it was obtained using a dating technology that is now obsolete. These observations led us to reinvestigate the sequences at Lutterzand using a high-resolution sampling strategy and a modern luminescence dating method (i.e. the single-aliquot regenerative-dose protocol; Murray and Wintle, 2000). Quartz SAR-OSL dating is considered as a reliable chronological tool in a range of geomorphological settings (see e.g. Murray and Olley, 2002; Madsen and Murray, 2009) and it has already been successfully applied at several Late Weichselian fluvio-aeolian and aeolian sand sequences deposited during oxygen

isotope stages (OIS) 1 and 2 in the NW European lowlands (e.g. Vandenberghe et al., 2004; 2009; Kasse et al., 2007; Buylaert et al., 2009; Derese et al., 2009; 2010(a); 2010(b); in press; 2011; van Mourik et al., 2010; Bogemans and Vandenberghe, submitted). The main aims of the present study are to establish a detailed and accurate chronological framework for the fluvio-aeolian and aeolian sediments at the type locality Lutterzand in the E Netherlands, and to reconstruct the depositional history and changes in the sedimentary environment during the Late Weichselian and Holocene. The age information was provided by quartz SAR-OSL dating of 57 samples taken in four natural exposures along the Dinkel river at Lutterzand, complemented with radiocarbon dating. Additionally, all sedimentary units were sampled for grain size analysis.

6.3. GEOLOGICAL SETTING

Fluvio-aeolian and aeolian sands dating from the Weichselian occur in an area extending from Great Britain, over the NW European lowlands, N Germany, Denmark and Poland to Russia (see Kasse, 2002, and references therein); often, this area is referred to as 'the European coversand belt' (Fig. 6.1a). The sediments of Weichselian Pleniglacial age are considered to originate mainly from the present North Sea region, of which large parts were exposed during the Last Glacial Maximum as a result of lower sea levels (Koster, 1982; Schwan, 1986; Bateman, 1995). To a lesser degree, the large delta plains of the Rhine and Meuse rivers and the (pro)glacial areas along the Pleistocene glacial limits also contributed (Kasse, 2002). The different conditions during the Weichselian Late Glacial, resulting from recession of the ice sheet margin, reinundation of the North Sea basin, changes in the atmospheric pressure system and increasing density of the vegetation cover, rather promoted transport from nearer sources. The aeolian deposits from this period are thought to be derived from pre-existing aeolian formations and from temporarily dry water courses (Schwan, 1986).

The Weichselian fluvio-aeolian and aeolian sediments form a substantial part of the surficial deposits in The Netherlands (Koster, 1982). However, sedimentary sequences thought to give an overall picture of the changes in the sedimentary environments from the Weichselian Pleniglacial up to the Holocene are relatively rare. One of the relatively complete Late Weichselian sequences of The Netherlands is situated in the Lutterzand area (Twente, E Netherlands) according to Van der Hammen and Wijmstra (1971), where natural exposures can be found over a distance of ~2 km along the Dinkel river (Figs. 6.1b and 6.1c).

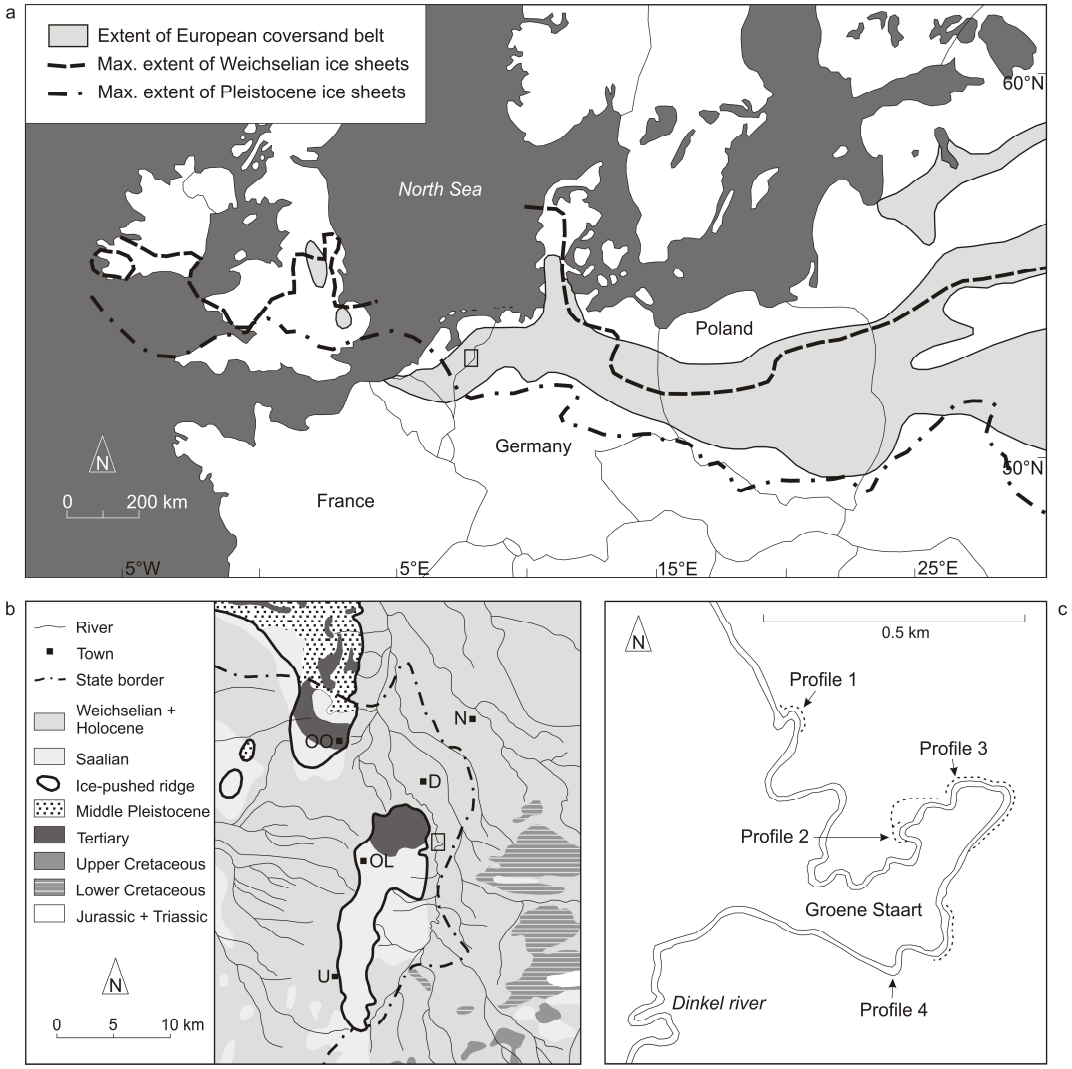

Fig. 6.1: (a) Extent of the European coversand region. The location of the investigated area is indicated with an open rectangle. (b) Geological map of the Dinkel valley. The hydrological system and the most striking geomorphological features (ice-pushed ridges) are indicated on the map. The Lutterzand area is indicated with an open square. (c) Schematic map of the Lutterzand area, on which the course of the Dinkel river and the natural exposures of the Late Weichselian and Holocene sediments are shown. The investigated profiles are indicated with arrows.

Its completeness is probably related to the geomorphological evolution of the region, which has been discussed by Van der Hammen and Wijmstra (1971), Van Huissteden (1990) and Van Huissteden et al. (2001). The presence of glaciers, extending from the N European continental ice sheet during the Saalian, resulted in the development of north-south oriented ice-pushed ridges and intermediate glacial basins. During the Weichselian, the Saalian topographically elevated landforms in E Netherlands were affected by periglacial erosion, while sedimentation processes occurred in the adjacent depressions, resulting in valley and

basin fills of more than 25 m thickness. During the Late Glacial, the present-day floodplain of the Dinkel river was shaped by a fluvial incision phase (Van Huissteden, 1990). At present, the Dinkel valley is bordered to the east by outcrops of Early Cretaceous shales and sandstones, and to the west by the ice-pushed ridges of Oldenzaal and Ootmarsum, dating from the Saalian. The northern part of the valley consists of a glacial basin, the so-called Nordhorn Basin (W Germany), in which Eemian and Weichselian fluvial and aeolian sediments reach thicknesses of more than 25 m (Van Huissteden et al., 2001; Fig. 6.1b).

6.4. SEDIMENTARY SUCCESSION AND SEDIMENTOLOGICAL CHARACTERISTICS

The stratigraphy of the Late Quaternary sediments in the Lutterzand area was studied in detail by Van der Hammen and Wijmstra (1971), mainly in natural exposures along the Dinkel river and in excavations for the Dinkel regulation canal. The subdivision of the sedimentary succession was primarily based on the presence of intercalated soil horizons and periglacial phenomena, on the pollen content and to a certain extent on the sedimentological characteristics. In the present study, four of the profiles described by Van der Hammen and Wijmstra (1971) were selected for OSL dating (Fig. 6.1c). Our profile 1 was equivalent to profile 13 of Van der Hammen and Wijmstra (1971), and thus also to section A of Dijkmans and Wintle (1991) and to the northern section of Bateman and Van Huissteden (1999). Profile 2 matched profile 5 of Van der Hammen and Wijmstra (1971) and section B of Dijkmans and Wintle (1991). Profile 3 was at the same location of profile 4 of Van der Hammen and Wijmstra (1971) and section C of Dijkmans and Wintle (1991), while profile 4 matched profile 1 of Van der Hammen and Wijmstra (1971) and the southern section of Bateman and Van Huissteden (1999).

The four profiles along the Dinkel river were sampled for grain-size analyses to further characterise and correlate the fluvio-aeolian and aeolian sands and intercalated clastic or peaty soil horizons The samples were collected at the same level as the OSL samples (see Fig. 6.2 and section 6.6.1). In the laboratory, representative subsamples of ~5 – 10 g were taken from the 52 homogenised field samples and chemically dispersed with sodium pyrophosphate. The grain size distributions were subsequently measured using a Helos KR laser particle sizer; the results of these analyses are shown in Fig. 6.3. The grain-size distributions show a transition from fluvial to fluvio-aeolian sediments at the base of the Lutterzand sequences to aeolian coversands and drift-sands at the top.

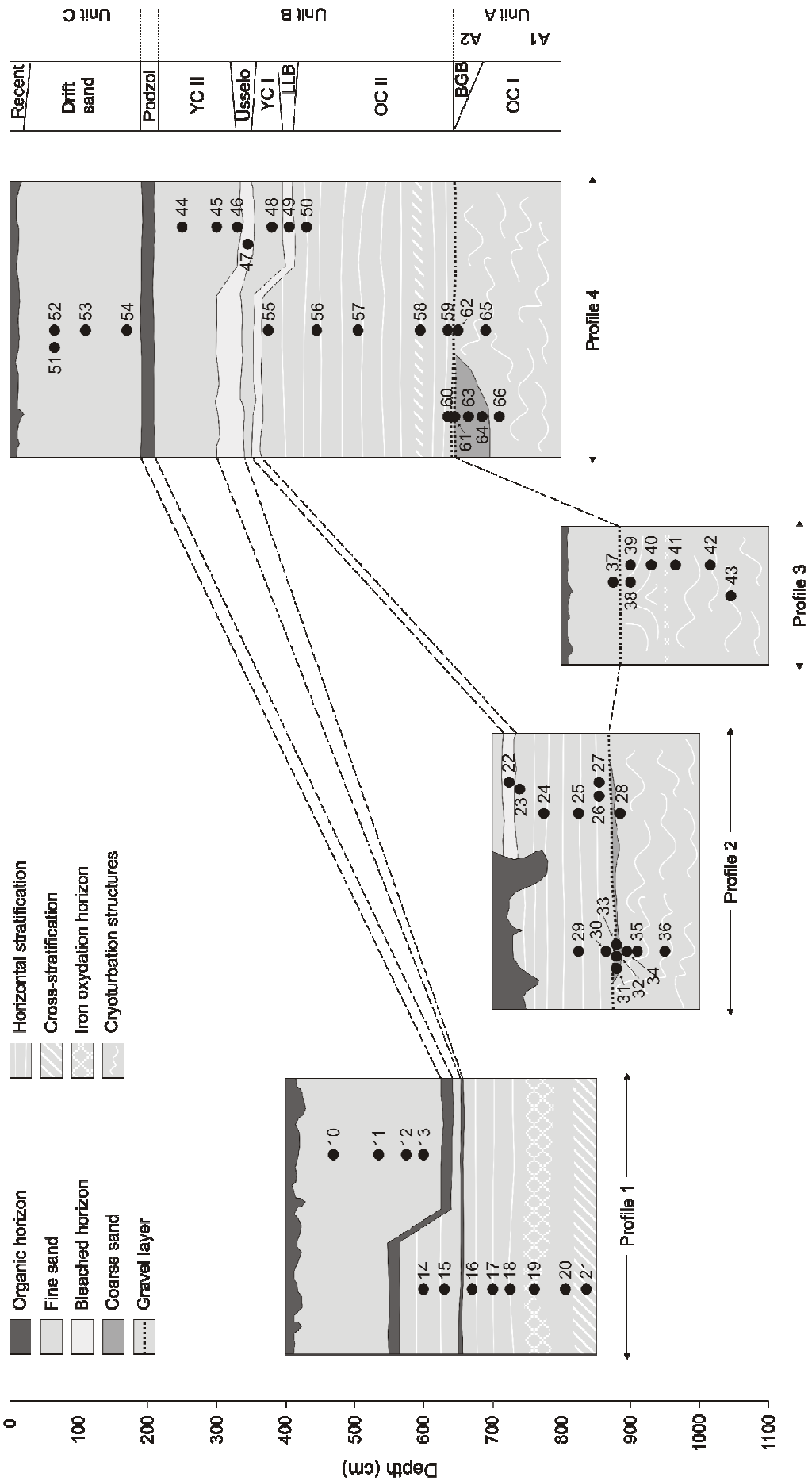
Unit C
Unit B
Unit A
A2
A1
Recent
Drift sand
Podzol
YC II
Usselo
YC I
LLB
OC II
BGB
OC I
Profile 4
Profile 3
Profile 2
Profile 1
Horizontal stratification
Cross-stratification
Iron oxydation horizon
Cryoturbation structures
Organic horizon
Fine sand
Bleached horizon
Coarse sand
Gravel layer
Depth (cm)
0
100
200
300
400
500
600
700
800
900
1000
1100

Fig. 6.2: Schematic overview and lithostratigraphy of the investigated profiles. The lithostratigraphic units are correlated with dashed lines and the location of the OSL samples is indicated with filled circles. Samples for grain-size analyses were taken at the exact same stratigraphic level as the samples for luminescence dating.

Three main sedimentary units could be distinguished based on their stratigraphic position and sedimentological differences; their specific features are discussed in detail in the following paragraphs.

6.4.1. Unit A

Unit A represents the lowermost unit in the Lutterzand sequences and was observed in profiles 2, 3 and 4. The major part of this unit (further denoted as unit A1) consists of silty fine-grained sands with mean grain size of ~170 µm, characterised by a weakly developed alternation of coarser- and finer-grained laminae. Alternating bedding of fine sand and silty fine sand is generally attributed to deposition and adhesion of sediment on an alternating dry and wet depositional sand sheet surface and/or seasonal variations in wind velocity (Kasse, 2002, and references therein). In the Lutterzand area, the original horizontal bedding is strongly disturbed by syn- and post-depositional periglacial deformation, such as drop- or tongue-shaped loading structures, small- and large-scale involutions, and frost cracks. The base of unit A1, especially in profile 3, is characterised by decimetre-scale fining-upward sequences (Fig. 6.3), pointing to an evolution from a fluvial to a fluvio-aeolian depositional environment, in which aeolian activity contributed to the supply of sediment to the braided river system (Van Huissteden et al., 2000; 2001). The admixture of some clay (less than 5%) might point to the discontinuous occurrence of small pools on the floodplain, in which the clays could settle from suspension. Unit A1 is overlain and truncated by unit A2. This unit contains medium, locally coarse-grained, gravelly fluvial sand (Fig. 6.3) and its thickness varies from a single gravel string in profile 3 to circa 60 cm in profile 4 (Fig. 6.2). The localised character of the fluvial sediments reflects their deposition in small and shallow channels. In contrast to unit A1, unit A2 is not strongly affected by periglacial deformation.In profile 4 (samples GLL-060764, -63 and -61), the lower part of unit A2 is still slightly deformed, while the upper part is undisturbed by cryogenic processes. The top of unit A2 shows a continuous string of fine gravel that represents a desert pavement formed by deflation.

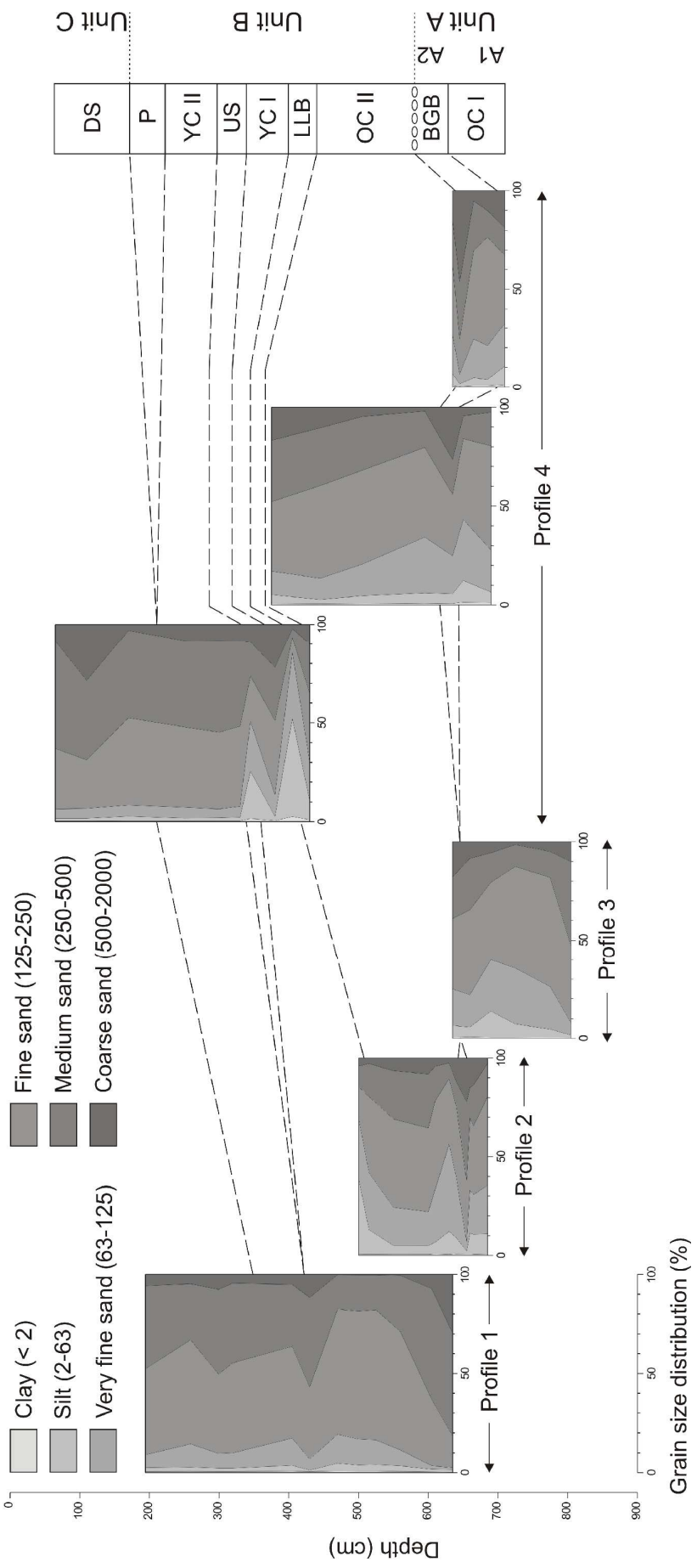
Unit C
Unit B
Unit A
A2
A1
DS
P
YC II
US
YC I
LLB
OC II
BGB
OC I
Clay (< 2)
Silt (2-63)
Very fine sand (63-125)
Fine sand (125-250)
Medium sand (250-500)
Coarse sand (500-2000)
Profile 1
Profile 2
Profile 3
Profile 4
Depth (cm)
Grain size distribution (%)

Fig. 6.3: Grain-size distributions obtained at the 4 investigated profiles in Lutterzand. Profile 4 was split up in three separate profiles, to allow visualisation of parallel samples taken within this profile.

According to the subdivision of Van der Hammen and Wijmstra (1971), our unit A1 comprises the Older Coversand I. In the formal Dutch lithostratigraphy, it has been described as the Beverborg Member of the Twente Formation (Van Huissteden, 1990; Van Huissteden et al., 2001) and as part of the Boxtel Formation (Schokker et al., 2003). It is separated from the overlying sands by a slightly gravely sand unit (A2), which truncates all underlying cryoturbated and homogenised deposits. Van der Hammen et al. (1967) observed this pebble bed for the first time at Lutterzand and described it as a desert pavement laterally passing into a coarse niveofluviatile deposit that consists of coarse sands, pebble bands or accumulations of small pebbles and is characterised by a typical undulating bedding and large frost polygons. This gravely unit, the so-called Beuningen Gravel Bed, is a widespread marker horizon within the NW European aeolian sand sequences (see e.g. Van der Hammen et al., 1967; Van der Hammen and Wijmstra, 1971; Kolstrup, 1980; Van Huissteden, 1990). According to Kolstrup (1980, and references therein), the development of the Beuningen Gravel Bed occurred in two phases: (1) the first phase was dominated by fluvial activity, while wind action was of secondary importance, and (2) the second phase was characterised by strong wind activity, due to the increased drought (Kolstrup, 1980), and some surficial run-off (Van Huissteden et al., 2000; 2001). This resulted in widespread deflation, in the erosion of the previously deposited sedimentary units and in the development of a pebbly horizon (desert pavement). In most cases, evidence from the fluvial phase is missing within the NW European coversands, illustrating the local character of the fluvial deposit, and the Beuningen Gravel Bed is represented by the desert pavement only. This led Kasse et al. (2007) to question the two-phase development of the Beuningen Gravel Bed and to suggest an alternative origin for the deposit. According to these authors, the deflation gravel and the fluvial unit may have formed simultaneously in a desert environment. Although aeolian activity and deflation would have been the dominating processes in such a context, ephemeral fluvial activity may have occurred during (rare) storm or snow-melt events. Changes over place and time in sheet flow and aeolian activity could thus have resulted in a sedimentary succession consisting of sheet flow deposits overlain by a desert pavement.

6.4.2. Unit B

Unit B consists of mostly aeolian sands, separated from the under- and overlying deposits by the Beuningen Gravel Bed and by a podzol, respectively. This unit is (partly) present in all investigated profiles and it is often intercalated by one or two bleached horizons or peat layers (Fig. 6.2). The sands of unit B have relatively uniform sedimentological characteristics: they are moderately well to moderately sorted, with a dominant grain size in the range of 150-250 µm (Fig. 6.3). The sands at the base of the unit, immediately overlying the gravel bed, are typically slightly siltier (profile 2 and 4b); the results of the grain size analyses (Fig. 6.3) correlate well with the observation of silty laminae in the natural exposures. In profile 4b, at the base of unit B, a cross-bedded set dipping to the northeast has been found, presumably as a result of the formation of low dunes or wind ripples by southwesterly winds. In profile 1, the basal one meter of unit B is characterised by medium to fine-grained, cross-bedded and cross-laminated sand in a fining-upward sequence indicating deposition in a fluvial channel environment changing upwards into aeolian deposition. However, the largest part of the sand unit is characterised by horizontal lamination that can sometimes be followed across considerable distances (Van der Hammen and Wijmstra, 1971; Kasse, 2002). This reflects its deposition in extensive sand sheets that blanketed the landscape and levelled the pre-existing relief (Van der Hammen and Wijmstra, 1971). As for unit A1, the horizontal lamination of unit B resulting from the alternation of coarser and finer-grained laminae points to seasonal variations in surface wetness and wind intensity. Towards the top, the stratification is less obvious due to soil formation, which complicates the interpretation of the depositional context. The aeolian sands of unit B do not show large-scale periglacial features and cryoturbations, indicating their deposition in a relatively warmer climate without permafrost.

In profiles 2 and 4, bleached clastic beds with sedimentological features that are clearly different from those of the over- and underlying sands are present within unit B: they are finer-grained, containing 20 – 50% silt grains. They were probably deposited during phases with lower wind velocities and a northward shift of the aeolian sedimentation areas (loess and sand belt), possibly related to climatic warming. Due to their silty character and their stratigraphic location within the sands overlying the Beuningen Gravel Bed, the bleached horizon in the top of profile 2 and the lowermost bleached layer in profile 4 are thought to represent the Lower Loamy Bed of Bølling age (Van der Hammen and Wijmstra, 1971). The topmost bleached horizon in profile 4 is slightly organic and bears traces of burrowing

activity by dung beetles, indicating that the landscape was stabilised to a certain extent during and/or after the development of this layer. On stratigraphical grounds, in combination with the presence of dung-beetle burrows, the uppermost bleached horizon is considered as the equivalent of the Usselo Soil of Allerød age, as defined by Hijszeler (1947; 1957) and Van der Hammen and Wijmstra (1971). According to the latter authors, the Usselo Soil is a bleached layer, locally marked by gley phenomena, on the coversand ridges due to its development under pine forest, whereas its lateral equivalents in the low-lying areas are hydromorphic soils and peats. Kaiser et al. (2009) investigated the nature of the Usselo Soil in northern central Europe and concluded that it can be classified as an albic arenosol. Derese et al. (in press) applied micromorphological analyses on the Usselo Soil at Arendonk-*Korhaan*, but concluded that this type of analyses could not give a decisive answer regarding its nature at the studied site, mainly due to the strongly sand-dominated texture of the deposits, providing a poor record of pedogenic processes in thin section. In profile 1, the sands of unit B are intercalated by a 1-2 cm thick peat layer. Based on its stratigraphical position in the upper part of Unit B and below the podzol, this peat layer is thought to represent the organic equivalent of the Usselo Soil. A similar lateral transition between the bleached Usselo Soil and a peat layer has also been reported in the Campine region (NE Belgium; Derese et al., 2009; in press).

Unit B thus contains the following subunits described by Van der Hammen and Wijmstra (1971): Older Coversand II, Lower Loamy Bed, Younger Coversand I, Usselo Soil and Younger Coversand II. According to the lithostratigraphic subdivision of Van Huissteden (1990) and Van Huissteden et al. (2001), our unit B agrees with the Lutterzand and Wierden Members of the Twente Formation. In the most recently published lithostratigraphy of The Netherlands (Schokker et al., 2003), this unit is consistent with the upper part of the Boxtel Formation. A ~0.5 m thick humic or ferro-humic podzol has developed in the top of unit B; the soil development may have been polycyclic, as attested by the presence of several eluviation and illuviation horizons in the top of profile 4.

6.4.3. Unit C

The sands of unit C represent the uppermost part of the investigated sequences and are present in profiles 1 and 4. They are generally well-sorted, with a mean grain size in the range of 200 – 300 µm and a negligible admixture of clay and silt grains. Based on their similarity with the

sediments in the upper part of unit B, it is thought that the sands of unit C originate from local erosion and resedimentation of these sediments. In profiles 2 and 3, the upper part of unit B and the Holocene podzol have been eroded. The local occurrence of coarser-grained lenses within unit C (Fig. 6.3, profile 4) probably reflects short intervals of deflation and granule ripple formation.

Typically, the sands of unit C are described as drift-sands and they are collected in the Kootwijk Formation (Koster, 1982) or in the Kootwijk Layer of the Boxtel Formation (Schokker et al., 2003). The top of unit C is affected by recent soil formation and associated bioturbation.

6.5. INDEPENDENT AGE INFORMATION

6.5.1. Pollen analysis and vegetation development

Van der Hammen and Wijmstra (1971) reported on the pollen analysis carried out on the Lutterzand sections. In the profiles along the Dinkel river, samples appear to have been collected from soil horizons and peats, but not from the sandy sediments. As such, it cannot be deduced whether the sediments themselves are sterile or whether they do contain evidence of the vegetation development at Lutterzand. In general, pollen analyses allowed correlating organics to the Allerød and to several periods during the Holocene (Boreal, Atlantic, Subboreal and Subatlantic). No organics of Bølling age could be identified, probably because the silty horizon identified as the Lower Loamy Bed was not sampled for pollen analyses or because it did not contain organic material. A thin peat bed, situated ~150 m southeast of our profile 1 and most likely equivalent to the lowermost peat bed observed in our profile 1 (in the upper part of unit B) was analysed. The *Betula* maximum at the base, followed by a *Pinus* maximum have been interpreted as the Allerød biozone (see Fig. 25c of Van der Hammen and Wijmstra, 1971). A peat layer separating the Younger Coversand II from the drift-sand (our units B and C), ~140 m southeast of our profile 1 and assumed to be equivalent to the podzol in our profile 1, was characterised by *Betula*, *Pinus* and *Corylus* in the lower part and *Alnus*, *Quercus*, *Tilia* and increasing *Ericaceae* values in the upper part (see their Figs. 25d and 25e). This succession was interpreted as reflecting the Boreal to Atlantic/Subboreal periods, respectively; this was confirmed by radiocarbon dating (see section 6.5.2). (The top of)

another peat layer, equivalent to the podzolic soil in our profile 4, revealed the presence of *Cerealia*, *Centaurea cyanus* and *Fagopyrum*, indicating a Late Subatlantic age younger than 1000 AD (see their Fig. 24b).

On the basis of the pollen data obtained for the Lutterzand sections and at other localities in the Dinkel valley, Van der Hammen and Wijmstra (1971) reconstructed the vegetational history of the area. The Late Pleniglacial was thought to be characterised by an "arctic" lichen steppe, based on the abundance of fungal spores of the lichen-type in some Pleniglacial sediments. These steppes might have been seasonally wet during thawing periods (spring), but dry throughout the rest of the year. This is consistent with the generally accepted idea that the Late Pleniglacial was cold and dry. The extreme cold (with mean annual air temperatures (MAAT) lower than -8°C, according to Kasse et al. (2007) and references therein) resulted in an almost barren surface or a polar desert towards the end of this period. This surface was subsequently covered with an extensive low lichen vegetation at the onset of the Late Glacial. During the Bølling interstadial, the vegetation gradually spread over the surface and a park landscape with some birch developed. However, a sudden drop in temperature, denoted by Van der Hammen and Wijmstra (1971) as the Earlier Dryas stadial, caused the birches to die off and the low vegetation cover to thin out. During the following Allerød interstadial, the whole area became covered with birch forest and later with pine forest, presumably with an undergrowth of shrubs such as crowberry (*Empetrum*). In the low-lying regions (e.g. recent and former brook valleys), however, birch was the most commonly growing tree, and relatively low percentages of pine pollen are found within the pollen diagrams of those areas. *Cyperaceae* (sedges) and *Artemisia* were present in the wetter marshy areas and the dry habitats, respectively. The rapid climatic cooling at the onset of the Late Dryas resulted in the dying-off of the pine forests, which became prone to forest fires. From the Preboreal onwards, birch forests and later pine forests discontinuously invaded the Dinkel valley again. At the beginning of the Boreal, thermophilous trees such as alder, hazel, oak, elm and ash migrated into the area. Around 5000 BP, Neolithic farmers arrived in the Dinkel valley; their agricultural activities, including cattle breeding, resulted in a fast degradation of the original soils and forests, increasing podzolisation and heathland development.

6.5.2. Radiocarbon dating

The following paragraph gives an overview of the radiocarbon dates available for the sediments and soils/peats in the Dinkel valley. All radiocarbon ages are calibrated using OxCal v4.1.5 (Bronk Ramsey, 2009) and the IntCal09 calibration curve (Reimer et al., 2009), and they are expressed as the 68.2% probability interval (unless stated differently) before AD2000 ('BP').

Of the 24 radiocarbon dates discussed by Van der Hammen and Wijmstra (1971), the majority corresponds to organic layers in the Dinkel canal section and in the sequence at Klokkenberg (Denekamp), some 5 km to the north of the Lutterzand sections. Ages for peat beds in the Younger Coversand (our unit B) of 11,630 ± 65 ^{14}C BP (GrN-4899; 13.6 – 13.4 ka calBP), 11,630 ± 90 ^{14}C BP (GrN-4900; 13.6 – 13.4 ka calBP) and 11,240 ± 65 ^{14}C BP (GrN-4901; 13.2 – 13.1 ka calBP) were obtained at Denekamp. As such, the peat accumulation appears to be associated with the Allerød interstadial, which is generally dated to 14.0 – 13.0 ka calBP (Hoek, 1997; 2001). In the Lutterzand sections, one sample of a peat layer overlying the Younger Coversand II (our unit B), laterally correlative with the podzolic soil in our profile 1, was dated to 7,535 ± 50 ^{14}C BP (GrN-5180; 8.4 – 8.3 ka calBP), which is in agreement with the Boreal to Atlantic age of this peat layer as derived from pollen analysis (see section 6.5.1).

The above-mentioned ages were determined using conventional bulk radiocarbon dating. Advances in radiocarbon dating technology, such as the introduction of accelerator mass spectrometry (AMS), and in calibration, such as the construction of the IntCal09 calibration curve (Reimer et al., 2009), allow obtaining more accurate radiocarbon results. Using this state-of-the-art radiocarbon dating technique, three ages were determined for soil and peat horizons in our profiles 1 and 4 (Table 6.1). In profile 1, macroscopic charcoal fragments collected from the peat layer (lateral equivalent of the Usselo Soil) in unit B yielded an AMS radiocarbon age of 10,480 ± 70 ^{14}C BP (UtC-14913; 12.6 – 12.4 ka calBP; 54.4%). In profile 4, both the peaty top of the podzol and the uppermost slightly humic soil horizon (Usselo Soil) in unit B were sampled for radiocarbon dating. Small plant remains from the clastic soil horizon, interpreted as the Usselo Soil (see section 6.4.2), were dated at 11,180 ± 80 ^{14}C BP (UtC-14912; 13.2 – 12.9 ka calBP). Charcoal from the peaty top part of the podzol yielded a radiocarbon age of 1,550 ± 43 ^{14}C BP (UtC-14914; 1.52 – 1.46 ka calBP (38.2%), 1.45 – 1.39 ka calBP (30.0%)). Although the peat layer from profile 1 is thought to be the lateral equivalent of the Usselo Soil from profile 4, the radiocarbon ages obtained for both horizons

are significantly different: the one obtained for the bleached Usselo Soil points to the end of the Allerød (14.0 – 13.0 ka calBP; Hoek, 2001), while the date of the peat layer is consistent with the time boundaries for the Late Dryas (13.0 – 11.7 ka calBP; Hoek, 2001).

Sample code	Depth (cm)	Stratigraphic level	Material	$\delta^{13}C$	^{14}C age (a)	Calibrated age (a calBP)
UtC-14913	450	Unit B: Usselo peat	charcoal	-28.1	10,480 ± 70	12,558 – 12,378 (54.4%) 12,342 – 12,322 (3.5%) 12,272 – 12,222 (10.3%)
UtC-14912	300	Unit B: Usselo soil	plant remains	-27.2	11,180 ± 80	13,173 – 12,946 (68.2%)
UtC-14914	200	podzol	charcoal	-27.5	1,550 ± 43	1,517 – 1,456 (38.2%) 1,445 – 1,393 (30.0%)

Table 6.1: Overview of the newly obtained radiocarbon data. All ages were obtained through AMS radiocarbon dating, and have been calibrated using Oxcal v4.1.5 (Bronk Ramsey, 2009) and the IntCal09 calibration curve (Reimer et al., 2009).

It should be noted that an influence of recent bioturbation (mainly tree rooting) in the peat layer cannot be fully excluded; despite careful selection of the charcoal fragments, recent microscopic root-hairs may have been present. Apart from that, however, there is no genuine reason to assume that any of the two radiocarbon dates is incorrect: ages of 12.6 – 12.4 ka calBP and 13.2 – 12.9 ka calBP have been reported before for charcoal fragments collected from the Usselo Soil (see e.g. Vandenberghe et al., 2004; Derese et al., 2009; in press). In general, it appears that the radiocarbon dates obtained at Lutterzand and at other localities in the NW European lowlands (e.g. Ossendrecht, Opgrimbie, Arendonk-*Korhaan*, Lommel-*Maatheide*) point to the occurrence of multiple phases with natural fires, both during the Allerød and the Late Dryas. The age for the peaty top of the podzol in profile 4 is consistent with the Subatlantic age (~3 ka calBP to present, according to Terberger et al., 2009) inferred from the pollen analyses, but is not in agreement with the conclusion of Van der Hammen and Wijmstra (1971) that the podzol developed less than 1 ka ago.

6.5.3. Luminescence dating

The first attempts to date Late Weichselian aeolian sequences in The Netherlands using luminescence dating techniques were carried out on the Lutterzand sections. Dijkmans et al. (1988) and Dijkmans and Wintle (1991) reported on the application of thermoluminescence (TL) dating to feldspar grains obtained from three sedimentary successions along the Dinkel river (see section 6.4 for the relation between their profiles and the ones investigated in this paper). Their TL ages increased with depth and differed distinctly between drift-sands and coversands, thus giving an indication of the relative ages of the aeolian sediments. Dijkmans and Wintle (1991) did, however, observe a systematic underestimation of the age by about 20 – 50%, which they attributed to methodological problems. A comparable underestimation had been encountered at other localities (e.g. coversands in Denmark) as well, but its causes were not fully understood. The uncertainties related to TL dating, in combination with the advantages offered by OSL dating (especially the rapid bleaching of the OSL signal by daylight), led Stokes (1991) to apply quartz-based optical dating to the aeolian sand sequences at Lutterzand. Ages for the Younger Coversand I of 13.2 ± 2.4 ka and for the Younger Coversand II of 11.4 ± 1.4 ka were obtained. In contrast to the TL results obtained by Dijkmans and Wintle (1991), these OSL ages did show a good agreement with the stratigraphic position of the coversands below and above the Usselo Soil with a ^{14}C age of 11.63 ± 0.09 ka. A more comprehensive optical dating study was carried out by Bateman and Van Huissteden (1999). This study was the first to apply not only multiple-aliquot but also single-aliquot techniques on the Lutterzand sediments. The results from both methods were found to be generally in close agreement. Nevertheless, the single-aliquot data were employed in the final age calculation, as the single-aliquot approach used only the signal from the most light-sensitive traps and had the highest reproducibility. This resulted in average ages of 21.9 ± 1.9 ka for the Older Coversand I, 15.8 ± 1.8 ka for the Older Coversand II, 12.5 ± 1.1 ka for the Younger Coversand I and II, and 0.6 ± 0.1 ka for the drift-sands. The Beuningen Gravel Bed was assigned to the period 22 – 17 ka.

6.6. OPTICALLY STIMULATED LUMINESCENCE (OSL) DATING

6.6.1. Sampling, sample preparation and analytical facilities

Four sections along the Dinkel river were sampled according to a high-resolution sampling strategy (Fig. 6.1c and Fig. 6.2). The samples were taken at closely-spaced (~30 cm) vertical intervals and, above and below important lithostratigraphic marker horizons (Beuningen Gravel Bed), multiple samples were taken at the exact same stratigraphic level. In total, 57 samples for luminescence dating were collected; their location is shown on Fig. 6.2. All samples were taken by gently hammering stainless steel cylinders into freshly cleaned sediment exposures. About 1 kg of the surrounding sediment was collected for dose rate determination. In each sediment unit, at least one undisturbed sample was collected for evaluating the time-averaged moisture content; these samples were tightly sealed with duct tape and double-wrapped in plastic bags to prevent them from drying out.

Equivalent dose determination was carried out using the single-aliquot regenerative-dose (SAR) protocol (Murray and Wintle, 2000), following earlier successful applications of this measurement procedure to sedimentary sequences in the NW European coversand belt (see e.g. Vandenberghe et al., 2004; 2009; Kasse et al., 2007; Derese et al., 2009; in press). For this, quartz grains from the 125-180 µm or 180-212 µm grain-size fractions were extracted from the inner part of the sampling tubes using conventional sample preparation techniques (HCl, H_2O_2, sieving, heavy liquids, HF) in the laboratory. The quartz grains were subsequently mounted on stainless steel discs using silicon oil and measured with either an automated Risø TL/OSL-DA-12 or a TL/OSL-DA-15 reader. Both readers were equipped with blue (470 ± 30 nm) LEDs. Stimulation with infrared light was through an IR laser diode (830 nm; DA-12) or through IR diodes (875 nm; DA-15). All luminescence emissions were detected through a 7.5 mm thick Hoya U-340 UV filter. Details on the measurement apparatus can be found in Bøtter-Jensen et al. (2003).

Dose rate determination was based on high-resolution low-background gamma-ray spectrometry in the laboratory. The bulk sediment samples collected around the OSL samples were dried (at 110°C until constant weight) and subsequently pulverised and homogenised. A subsample of ~150 g was packed in a cylindrical plastic container and stored for at least one month before being measured on top of the detector. The samples were counted for 2-3 days.

Details on instrumentation, spectrum evaluation and radionuclide concentration calculation can be found in Vandenberghe (2004).

6.6.2. The single-aliquot regenerative-dose (SAR) procedure

For equivalent dose determination, a conventional SAR protocol (Murray and Wintle, 2000) was carried out on large (8 mm) aliquots of quartz. Optical stimulation was for 40 s at a temperature of 125°C with the blue LEDs. After the measurement of each test dose signal, a high-temperature cleanout was performed by stimulation with the blue diodes for 40 s at 280°C; this additional step is expected to reduce possible recuperation effects (Murray and Wintle, 2003). For each aliquot, a complete growth curve was constructed by measuring the response to five regenerative doses (up to 2.5 times the estimated equivalent dose). A measurement of the response to a zero dose was carried out to determine whether the growth curve passes through the origin (recuperation), and a repeat measurement of the response to the lowest regenerative dose was achieved to evaluate the performance of the sensitivity correction (recycling ratio). Additionally, the response to the highest regenerative dose was measured twice. The second time, the sensitivity to IR stimulation was checked before stimulation with the blue LEDs with the purpose to identify aliquots with a significant feldspar contamination (see also section 6.6.3). The measured aliquots were accepted if the recuperation and IRSL/BLSL ratio (Vandenberghe, 2004) did not exceed a threshold set at 10% and if the recycling ratio and IR depletion ratio (Duller, 2003) did not deviate more than 10% from unity. None of the analysed aliquots had to be rejected based on these criteria.
For all samples, except those taken from the drift-sands (GLL-060710 to -13 and GLL-060751 to -54), a preheat of 10 s at 240°C and a test dose cutheat to 220°C were adopted. The size of the test dose amounted to ~25 to 50% of the estimated equivalent dose (depending on the size of this equivalent dose). For the drift-sand samples, the measurement parameters were chosen based on the experimental results of Derese et al. (2010(a)). A preheat temperature of 180°C was applied to reduce possible effects of thermal transfer, and the measurement of the test dose signal was preceded by a cutheat to 160°C. A fixed test dose of ~2 Gy (equal to ~5 times the estimated equivalent dose) was administered; as such, the relative contribution of the test dose signal intensity to the measurement precision was thought to be negligible (Murray and Wintle, 2000; Derese et al., 2010(a)).

For all samples, the performance of the applied measurement procedure was evaluated through dose recovery tests (Murray and Wintle, 2003). Natural aliquots (3 per OSL sample) were bleached using the blue LEDs at room temperature (2 times 250 s with a 10 ks pause in between) and given a dose close to the estimated equivalent dose. Subsequently they were measured using the SAR protocol outlined in the above.

6.6.3. Purity of the quartz extracts

As described in section 6.6.1, the quartz extracts were obtained through the application of conventional sample preparation techniques. In order to possibly reduce the time necessary for quartz extraction, it was checked whether the heavy liquid density separation step in the sample preparation procedure could be omitted. For 12 OSL samples, quartz grains were extracted using both the complete and the shortened preparation procedure and subsequently compared. In a first test 6 aliquots of each OSL sample, 3 per preparation procedure, were stimulated with infrared to identify possible feldspar contamination. The purity of all extracts was confirmed by the absence of a significant infrared stimulated luminescence (IRSL) response at 60°C to a large (~50 Gy) regenerative β-dose. The sensitivity to infrared stimulation was defined as significant if the resulting signal amounted to more than 10% of the corresponding blue-light stimulated luminescence signal (Vandenberghe, 2004) or if the depletion ratio deviated more than 10% from unity (Duller, 2003). In a second test, equivalent doses and dose recovery ratios in twelve samples, prepared with and without the density separation, were compared; Figs. 6.4a and 6.4b illustrate the good agreement between the measurement results.

Based on the test results, quartz extracts from the remaining 45 samples were obtained by etching with HF only. Their purity was confirmed by the IR test outlined in the above on three separate aliquots of quartz and by the IR stimulation step included in the SAR protocol for equivalent dose estimation (see section 6.6.2).

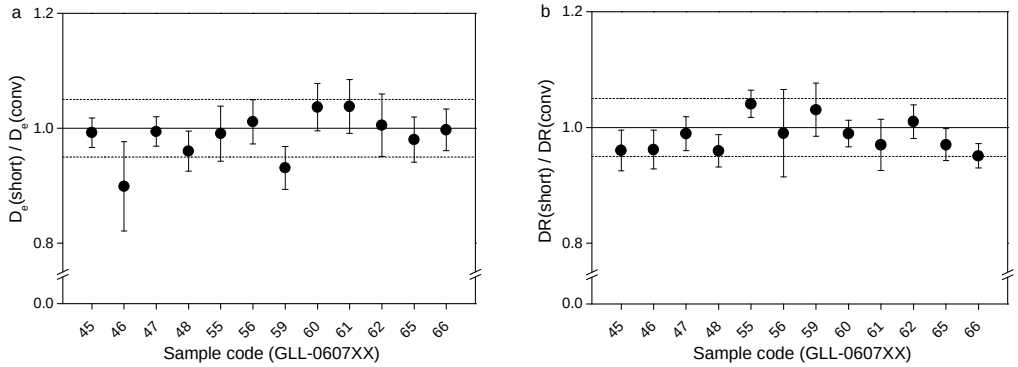

Fig. 6.4: Comparison of (a) equivalent doses, and (b) recovered to given doses obtained in samples that were prepared using the conventional sample preparation method and the shortened method in which the density separation using heavy liquids was omitted.

6.6.4. Luminescence characteristics

Representative luminescence decay and SAR growth curves for one aliquot from a coversand (GLL-060765) and a drift-sand (GLL-060752) sample are shown in Figs. 6.5a and 6.5b. The growth curves are well represented by single saturating exponential and linear functions, respectively. Fig. 6.5 illustrates the generally good behaviour of the samples in the SAR protocol. Recycling ratios are indistinguishable from unity, implying that sensitivity changes occurring throughout the measurement sequence (estimated to ~30% between the second and the first measurement cycle) are properly corrected for. Recuperation is generally less than 1% of the sensitivity corrected natural OSL signal, except for the drift-sands, which are characterised by recuperation values between 1 and 5%.

The net OSL signals were calculated from the initial 0.32 s of the decay curve, minus a background evaluated from (1) the 1.44 – 2.08 s interval (early background subtraction) and (2) the last 4 s of stimulation (late background subtraction). Whereas the latter is the originally applied method for calculating equivalent doses (Murray and Wintle, 2000), early background subtraction is thought to better isolate the part of the quartz luminescence signal that is dominated by the fast component (Cunningham and Wallinga, 2010). The integration interval for the early background (1.44 – 2.08 s) were chosen such that the resulting net signals and derived equivalent doses were associated with low uncertainties. In Fig. 6.6a, the ratio of the equivalent doses obtained using early and late background subtraction is plotted for the samples taken in profile 4; in Fig. 6.6b, the ratio of the dose recovery ratios is plotted for the same samples. From Fig. 6.6, it can be concluded that both methods yield consistent

doses; the recycling ratios and recuperation values are in agreement as well (data not represented here). This indicates that the quartz signals are dominated by the fast component. In all further calculations, the equivalent doses determined with the early background subtraction method were used, for the abovementioned reasons.

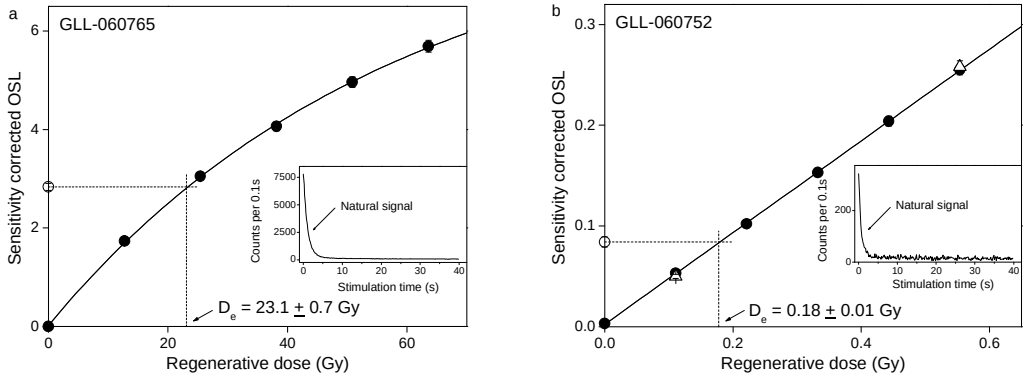

Fig. 6.5: Illustrative growth and luminescence decay curves of a representative (a) coversand sample GLL-060765 and (b) drift-sand sample GLL-060752. The filled circles show the responses to several regenerative doses, including a zero dose; the growth curves are obtained by fitting a single saturating exponential function (a) or a linear function (b) to these measurement points. The open triangles are obtained by a repeat measurement of the lowest and highest regenerative dose. The open circle is the natural luminescence signal; the equivalent dose De is determined by plotting the natural signal onto the growth curve.

The dose recovery results for all 57 samples are summarised in Fig. 6.7. Recovered to given dose ratios generally do not differ by more than 5% from unity; taking the analytical uncertainty (1 standard error) into account, all samples (except GLL-060735) are consistent with 1.00 ± 0.05. The deviating sample GLL-060735 has an average recovered to given dose ratio of 1.08 ± 0.02 (n=3); the associated average recycling ratio and recuperation value is 0.96 ± 0.1 and 0.13 ± 0.03%, respectively. The sensitivity change throughout the measurement cycle does not differ from that of the other samples; the same goes for the initial intensity of the luminescence signal. It is concluded that the causes of the deviation are not understood at present. The overall average recovered to given dose ratio is 0.997 ± 0.005 (n=203). The corresponding overall average recycling ratio is 0.979 ± 0.004, while the overall average recuperation amounts to 0.41 ± 0.09% of the sensitivity-corrected natural luminescence signal. The results from the dose recovery tests indicate that the applied SAR protocol is suitable to accurately measure equivalent doses.

Following the same measurement procedure, equivalent doses were determined in our samples. For each sample, 18 replicate measurements of the equivalent dose were made. The average D_e values (± 1 standard error) are synthesised in Table 6.2.

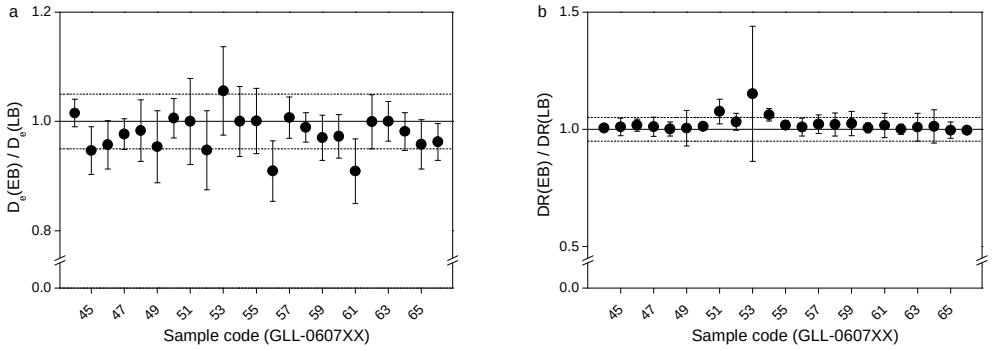

Fig. 6.6: Comparison of (a) equivalent doses and (b) dose recovery ratios obtained by subtracting a background evaluated from the 1.44 – 2.08 s interval (early background subtraction) and from the last 4 s of stimulation (late background subtraction) from the initial 0.32 s of the decay curve, respectively.

6.6.5. Dosimetry

The radionuclide activity concentrations determined with gamma-ray spectrometry were converted to dose rates using conversion factors derived from the nuclear energy releases tabulated by Adamiec and Aitken (1998). Based on Mejdahl (1979) and Aitken (1985), a factor of 0.9 (± 5% relative uncertainty) was adopted to correct the external beta dose rates for the effects of attenuation and etching. An internal dose rate of 0.010 ± 0.002 Gy ka^{-1} was assumed (Vandenberghe et al., 2008). The contribution of the surrounding sediment to the external dose rate shows some variability as a result of the difference in lithological features. More specifically, the silty beds and soil horizons intercalated within the aeolian sands have a higher radioactivity than the under- and overlying sand units. Seven samples (GLL-060722, -23, -46, -47, -48, -49 and -50) were corrected for the layer-to-layer variation in soil radioactivity according to the method discussed in Aitken (1985, Appendix H). The correction relates to the variations in the gamma radiation, which makes up about one third of the dose rate, and was performed here using the effective total moisture-corrected gamma-contribution determined in the bulk samples. It resulted in a correction of the original age by 1 – 3%, which appears to be negligible in comparison with the total uncertainty associated with the optical age. It should however be taken into account that some uncertainties may have been

introduced during the optical age correction, for example because of the use of bulk sample data, which may refer to sediments from more than one sedimentary unit (especially when this unit is thin, e.g. soil horizons).

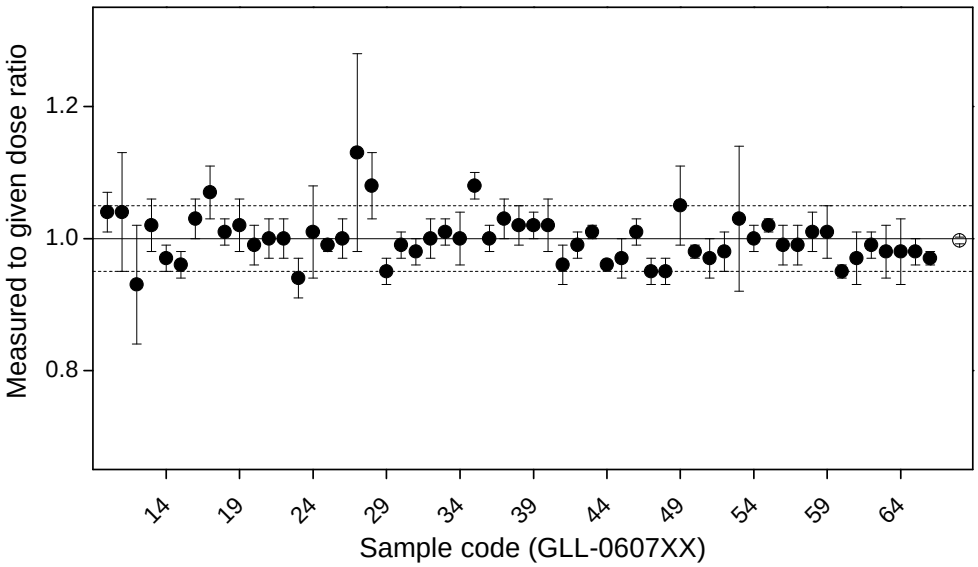

Fig. 6.7: Summary of the dose recovery test results. The solid line (eye guide) represents a measured to given dose ratio equal to unity; the dotted lines (eye guides) bracket a 5% deviation of the ratio from unity. The overall average recovered to given dose ratio (open circle) is 0.997 ± 0.005 (n=203).

Furthermore, the correction supposes that the radioactivity does not vary within an apparently homogeneous sediment unit, while it is observed that this is not necessarily the case (see later). The evaluation of the time-averaged moisture content and the associated correction of the dose rates were carried out following the procedure outlined in Aitken (1985). The water contents in fully saturated sediment were measured in the laboratory on the samples that were specifically collected for this purpose (see section 6.6.1). They were in the range of 16-22%. The time-averaged water content was then calculated from this value taking into account the sedimentological characteristics and the stratigraphical position of the samples. As such, time-averaged moisture contents varying between 9 ± 2% (e.g. for well-sorted drift-sands located at the top of the sedimentary sequence, ~3 to 6 m above the groundwater level) and 19 ± 5% (e.g. for silty sands near the groundwater table) were obtained. Increasing the water content with 1% increases the optical age by about 1% (or 10 years per ka).

Sample GLL-code	Depth (cm)	Unit	^{234}Th (Bq kg^{-1})	^{226}Ra (Bq kg^{-1})	^{210}Pb (Bq kg^{-1})	^{232}Th (Bq kg^{-1})	^{40}K (Bq kg^{-1})	Water content (%)	Total Dose rate (Gy ka^{-1})	D_e (Gy)	Age (ka)	σ_r (%)	σ_{sys} (%)	σ_{tot} (%)	σ_{tot} (ka)
060710	70	C	6.8 ± 0.6	7.1 ± 1.0	7.3 ± 1.2	6.9 ± 0.1	222 ± 2	9 ± 2	1.07 ± 0.02	0.33 ± 0.01	0.31	2.9	7.3	7.8	0.02
060711	135	C	8.0 ± 1.5	5.2 ± 1.1	6.1 ± 1.1	7.1 ± 0.1	234 ± 3	9 ± 2	1.07 ± 0.02	0.33 ± 0.01	0.30	2.6	7.3	7.7	0.02
060712	175	C	9.0 ± 0.9	6.4 ± 0.9	8.0 ± 0.9	8.3 ± 0.1	218 ± 2	9 ± 2	1.07 ± 0.01	0.31 ± 0.01	0.29	2.5	7.3	7.7	0.02
060713	200	C	8.6 ± 1.0	6.8 ± 1.1	9.0 ± 0.8	7.9 ± 0.2	217 ± 2	9 ± 2	1.07 ± 0.01	0.43 ± 0.04	0.40	8.2	7.3	11.0	0.04
060751	65	C	4.6 ± 0.9	3.1 ± 0.9	4.6 ± 1.0	5.1 ± 0.1	184 ± 3	10 ± 2	0.89 ± 0.02	0.18 ± 0.01	0.21	3.9	7.4	8.4	0.02
060752	65	C	4.6 ± 0.9	3.1 ± 0.9	4.6 ± 1.0	5.1 ± 0.1	184 ± 3	10 ± 2	0.89 ± 0.02	0.18 ± 0.01	0.20	3.5	7.4	8.2	0.02
060753	110	C	6.5 ± 1.7	6.7 ± 1.2	4.9 ± 0.8	6.0 ± 0.2	181 ± 3	10 ± 2	0.89 ± 0.01	0.19 ± 0.01	0.21	3.2	7.4	8.0	0.02
060754	170	C	4.0 ± 0.6	8.3 ± 0.7	5.7 ± 0.9	7.0 ± 0.1	224 ± 2	10 ± 2	1.01 ± 0.01	0.35 ± 0.01	0.35	3.6	7.4	8.3	0.03
060714	200	B *(YCII)*	10.2 ± 1.0	8.3 ± 1.1	8.1 ± 1.0	8.2 ± 0.2	243 ± 2	11 ± 3	1.17 ± 0.02	14.2 ± 0.3	12.2	2.7	7.1	7.6	0.9
060715	230	B *(YCII)*	5.9 ± 1.1	5.0 ± 1.2	4.9 ± 0.9	6.2 ± 0.1	201 ± 2	11 ± 3	0.94 ± 0.01	12.5 ± 0.3	13.3	2.8	7.1	7.6	1.0
060744	250	B *(YCII)*	5.2 ± 0.8	4.8 ± 1.1	5.9 ± 1.0	5.6 ± 0.1	231 ± 3	11 ± 3	1.03 ± 0.01	12.7 ± 0.2	12.3	2.2	7.8	8.1	1.0
060745	300	B *(YCII)*	6.3 ± 1.1	2.9 ± 1.0	4.9 ± 0.7	5.9 ± 0.1	216 ± 3	11 ± 3	0.97 ± 0.01	13.2 ± 0.3	13.6	2.5	7.8	8.2	1.1
060746	330	B *(YCII)*	6.4 ± 0.8	7.1 ± 1.2	7.6 ± 0.9	7.7 ± 0.1	240 ± 3	11 ± 3	1.11 ± 0.01	14.6 ± 0.4	13.2	2.7	7.8	8.3	1.1
060747	345	B *(Usselo)*	9.6 ± 0.7	11.2 ± 0.9	10.6 ± 1.2	10.8 ± 0.2	257 ± 4	12 ± 3	1.20 ± 0.02	16.4 ± 0.3	13.6	2.2	7.4	7.8	1.0
060748	380	B *(YCI)*	8.6 ± 1.0	5.3 ± 1.0	6.6 ± 0.7	7.5 ± 0.1	190 ± 3	9 ± 2	0.98 ± 0.01	14.5 ± 0.4	14.8	3.4	7.1	7.9	1.2
060722	25	B *(LLB)*	10.6 ± 1.4	9.8 ± 1.4	10.6 ± 1.2	10.9 ± 0.4	306 ± 8	16 ± 4	1.29 ± 0.03	20.2 ± 0.4	15.7	2.9	7.7	8.3	1.3
060749	405	B *(LLB)*	14.7 ± 1.0	14.9 ± 0.8	14.5 ± 0.9	14.6 ± 0.2	313 ± 3	16 ± 4	1.39 ± 0.02	19.6 ± 0.7	14.1	3.6	7.8	8.6	1.2

Sample GLL-code	Depth (cm)	Unit	^{234}Th (Bq kg^{-1})	^{226}Ra (Bq kg^{-1})	^{210}Pb (Bq kg^{-1})	^{232}Th (Bq kg^{-1})	^{40}K (Bq kg^{-1})	Water content (%)	Total Dose rate (Gy ka^{-1})	D_e (Gy)	Age (ka)	σ_r (%)	σ_{sys} (%)	σ_{tot} (%)	σ_{tot} (ka)
060716	270	B *(YCI – OCII)*	7.5 ± 1.2	5.7 ± 1.3	8.5 ± 0.9	7.8 ± 0.2	286 ± 3	16 ± 4	1.19 ± 0.01	16.5 ± 0.3	13.9	2.3	7.7	8.0	1.1
060717	300	B *(YCI – OCII)*	9.4 ± 1.3	8.0 ± 1.1	8.9 ± 0.7	8.7 ± 0.2	274 ± 2	16 ± 4	1.18 ± 0.01	16.2 ± 0.3	13.8	2.3	7.7	8.0	1.1
060718	325	B *(YCI – OCII)*	9.9 ± 1.0	6.7 ± 1.2	8.7 ± 0.9	8.6 ± 0.2	276 ± 3	18 ± 5	1.15 ± 0.01	15.0 ± 0.3	13	2.0	7.7	8.0	1.0
060719	360	B *(YCI – OCII)*	8.4 ± 0.9	6.5 ± 0.9	7.5 ± 1.0	6.4 ± 0.2	265 ± 3	19 ± 5	1.07 ± 0.01	15.4 ± 1.2	14.4	8.1	7.7	11.2	1.6
060720	405	B *(YCI – OCII)*	7.0 ± 1.3	2.9 ± 1.0	6.7 ± 1.0	5.7 ± 0.1	200 ± 2	19 ± 5	0.87 ± 0.01	10.9 ± 0.2	12.6	2.8	7.6	8.1	1.0
060721	435	B *(YCI – OCII)*	5.3 ± 1.0	4.4 ± 0.9	6.3 ± 0.9	4.8 ± 0.2	170 ± 2	19 ± 5	0.76 ± 0.01	12.1 ± 0.5	15.8	4.4	7.6	8.8	1.4
060723	40	B *(OCII)*	8.7 ± 1.3	6.6 ± 1.3	7.9 ± 1.3	7.8 ± 0.2	255 ± 2	12 ± 3	1.15 ± 0.02	17.0 ± 0.5	14.8	3.1	7.3	8.0	1.2
060724	75	B *(OCII)*	5.6 ± 0.9	7.6 ± 1.3	5.7 ± 1.4	6.4 ± 0.2	236 ± 3	13 ± 3	1.00 ± 0.02	13.4 ± 0.3	13.4	2.7	7.3	7.8	1.0
060725	125	B *(OCII)*	6.7 ± 0.8	6.0 ± 0.9	8.5 ± 0.8	6.6 ± 0.2	214 ± 2	14 ± 3	0.97 ± 0.01	14.0 ± 0.3	14.5	2.6	7.3	7.7	1.1
060726	155	B *(OCII)*	13.9 ± 1.1	13.4 ± 1.2	14.0 ± 0.9	10.1 ± 0.2	268 ± 3	14 ± 4	1.25 ± 0.01	16.6 ± 0.5	13.3	3.2	7.4	8.0	1.1
060727	155	B *(OCII)*	11.3 ± 1.8	12.9 ± 1.5	11.9 ± 1.6	10.0 ± 0.2	263 ± 2	14 ± 4	1.20 ± 0.02	17.0 ± 0.4	14.2	3.2	7.4	8.0	1.1
060729	135	B *(OCII)*	5.9 ± 1.3	7.2 ± 0.9	7.3 ± 1.0	7.9 ± 0.2	234 ± 3	14 ± 3	1.02 ± 0.02	14.8 ± 0.3	14.5	2.7	7.3	7.8	1.1
060730	165	B *(OCII)*	10.5 ± 1.2	10.7 ± 1.1	9.9 ± 0.6	9.3 ± 0.2	256 ± 2	14 ± 4	1.14 ± 0.01	15.6 ± 0.3	13.6	2.2	7.4	7.7	1.0
060737	75	B *(OCII)*	9.2 ± 1.0	7.6 ± 1.0	12.2 ± 1.0	7.7 ± 0.2	221 ± 3	14 ± 3	1.04 ± 0.02	13.2 ± 0.2	12.7	2.4	7.2	7.6	1.0
060750	430	B *(OCII)*	6.6 ± 0.9	6.8 ± 1.2	8.5 ± 0.9	7.0 ± 0.1	212 ± 3	12 ± 3	1.00 ± 0.01	15.1 ± 0.4	15.2	3.0	7.3	7.9	1.2
060755	375	B *(OCII)*	5.9 ± 0.7	7.3 ± 0.9	6.6 ± 0.7	6.8 ± 0.1	220 ± 2	12 ± 3	0.99 ± 0.01	14.9 ± 0.5	15	3.7	7.2	8.1	1.2
060756	445	B *(OCII)*	5.4 ± 0.9	5.8 ± 1.0	6.2 ± 0.8	5.8 ± 0.2	206 ± 3	12 ± 3	0.92 ± 0.01	12.5 ± 0.3	13.6	3.1	7.2	7.8	1.1
060757	505	B *(OCII)*	5.9 ± 0.4	6.9 ± 0.7	6.8 ± 0.6	6.4 ± 0.1	213 ± 2	12 ± 3	0.94 ± 0.01	12.8 ± 0.4	13.7	3.2	7.2	7.9	1.1
060758	595	B *(OCII)*	8.2 ± 1.1	6.6 ± 0.9	7.8 ± 1.0	6.5 ± 0.3	240 ± 2	13 ± 3	1.01 ± 0.02	13.4 ± 0.2	13.3	2.4	7.3	7.7	1.0
060759	635	B *(OCII)*	13.1 ± 0.9	11.9 ± 1.2	11.6 ± 0.7	10.3 ± 0.2	232 ± 2	14 ± 4	1.10 ± 0.01	13.6 ± 0.3	12.3	2.7	7.3	7.8	1.0
060760	635	B *(OCII)*	7.9 ± 1.1	9.1 ± 1.2	10.6 ± 0.7	7.9 ± 0.1	210 ± 2	14 ± 4	0.98 ± 0.01	13.5 ± 0.3	13.8	2.4	7.3	7.6	1.1

Sample GLL-code	Depth (cm)	Unit	^{234}Th (Bq kg^{-1})	^{226}Ra (Bq kg^{-1})	^{210}Pb (Bq kg^{-1})	^{232}Th (Bq kg^{-1})	^{40}K (Bq kg^{-1})	Water content (%)	Total Dose rate (Gy ka^{-1})	D_e (Gy)	Age (ka)	σ_r (%)	σ_{sys} (%)	σ_{tot} (%)	σ_{tot} (ka)
060731	180	A *(BGB)*	10.1 ± 0.8	7.2 ± 1.3	10.2 ± 1.2	8.2 ± 0.2	162 ± 3	15 ± 4	0.87 ± 0.02	18.0 ± 0.5	20.7	3.4	7.0	7.8	1.6
060732	180	A *(BGB)*	10.1 ± 0.8	7.2 ± 1.3	10.2 ± 1.2	8.2 ± 0.2	162 ± 3	15 ± 4	0.87 ± 0.02	20.3 ± 0.7	23.4	4.0	7.0	8.1	1.9
060733	180	A *(BGB)*	10.1 ± 0.8	7.2 ± 1.3	10.2 ± 1.2	8.2 ± 0.2	162 ± 3	15 ± 4	0.87 ± 0.02	19.3 ± 0.6	22.2	3.9	7.0	8.0	1.8
060761	645	A *(BGB)*	6.2 ± 0.9	6.2 ± 0.8	6.2 ± 0.8	5.6 ± 0.1	183 ± 2	15 ± 4	0.80 ± 0.01	12.9 ± 0.5	16.1	3.9	7.1	8.1	1.3
060763	665	A *(BGB)*	6.3 ± 0.7	6.4 ± 1.1	6.6 ± 1.0	6.5 ± 0.1	212 ± 2	15 ± 4	0.89 ± 0.01	17.9 ± 0.4	20.1	2.5	7.1	7.6	1.5
060764	685	A *(BGB)*	7.0 ± 0.6	6.7 ± 0.9	6.3 ± 0.6	6.7 ± 0.1	218 ± 2	15 ± 4	0.90 ± 0.01	18.3 ± 0.4	20.2	2.7	7.2	7.7	1.6
060728	185	B *(OCI)*	13.2 ± 1.4	14.1 ± 1.3	14.9 ± 1.1	12.8 ± 0.2	255 ± 3	17 ± 4	1.24 ± 0.02	27.7 ± 0.8	22.4	3.1	7.4	8.0	1.8
060734	190	B *(OCI)*	10.6 ± 1.0	11.6 ± 1.2	11.5 ± 0.9	11.6 ± 0.2	253 ± 2	17 ± 4	1.16 ± 0.01	27.6 ± 1.1	23.8	4.2	7.4	8.5	2.0
060735	210	B *(OCI)*	13.2 ± 1.2	10.7 ± 1.1	12.0 ± 1.0	12.4 ± 0.2	272 ± 2	17 ± 4	1.24 ± 0.02	28.4 ± 0.8	23.0	3.1	7.5	8.1	1.9
060736	250	B *(OCI)*	6.3 ± 0.7	8.5 ± 1.1	8.0 ± 1.1	8.1 ± 0.1	263 ± 2	17 ± 4	1.07 ± 0.01	23.8 ± 0.6	22.3	3.0	7.5	8.0	1.8
060738	100	B *(OCI)*	10.3 ± 1.3	9.4 ± 1.1	11.0 ± 0.8	8.7 ± 0.2	231 ± 3	15 ± 4	1.05 ± 0.01	21.0 ± 0.7	19.9	3.6	7.1	8.0	1.6
060739	100	B *(OCI)*	10.3 ± 1.3	9.4 ± 1.1	11.0 ± 0.8	8.7 ± 0.2	231 ± 3	15 ± 4	1.05 ± 0.01	21.1 ± 0.5	20.0	2.6	7.1	7.6	1.5
060740	130	B *(OCI)*	13.5 ± 1.2	10.1 ± 1.8	12.7 ± 1.7	10.4 ± 0.2	248 ± 3	15 ± 4	1.15 ± 0.02	25.4 ± 0.7	22.0	3.6	7.2	8.0	1.8
060741	165	B *(OCI)*	12.6 ± 1.2	12.9 ± 1.3	13.7 ± 1.5	11.1 ± 0.2	272 ± 2	15 ± 4	1.24 ± 0.02	27.4 ± 0.9	22.1	3.6	7.2	8.0	1.8
060742	215	B *(OCI)*	8.3 ± 1.0	12.1 ± 1.4	8.8 ± 1.0	9.6 ± 0.2	232 ± 3	15 ± 4	1.01 ± 0.01	24.8 ± 0.5	24.5	2.6	7.1	7.6	1.9
060743	245	B *(OCI)*	6.6 ± 0.7	6.1 ± 1.0	5.5 ± 1.1	6.0 ± 0.2	192 ± 2	15 ± 4	0.80 ± 0.02	20.2 ± 0.4	25.2	2.8	7.1	7.6	1.9
060762	650	B *(OCI)*	10.3 ± 1.0	4.8 ± 1.0	6.2 ± 1.2	7.4 ± 0.2	231 ± 2	15 ± 4	0.96 ± 0.02	22.5 ± 0.6	23.3	3.1	7.2	7.9	1.8
060765	690	B *(OCI)*	8.0 ± 0.7	9.2 ± 1.2	9.0 ± 1.1	8.8 ± 0.2	240 ± 2	15 ± 4	1.03 ± 0.02	22.8 ± 0.7	22.1	3.5	7.2	8.0	1.8
060766	710	B *(OCI)*	11.6 ± 1.1	12.8 ± 1.1	9.8 ± 1.0	11.2 ± 0.2	273 ± 2	15 ± 4	1.18 ± 0.01	25.1 ± 0.5	21.3	2.3	7.3	7.6	1.6

Table 6.2: Summary of the radionuclide activities, estimated time-averaged moisture contents, total dose rates, equivalent doses (D_e), optical ages, and random (σ_r), systematic (σ_{sys}) and total (σ_{tot}) uncertainties. The uncertainties mentioned with the dosimetry and De data are random; all uncertainties represent 1σ.

The contribution from cosmic radiation was calculated following Prescott and Hutton (1994), taking into account the depositional history of the aeolian sands, and amounted to 10-20% of the total dose rate. As a result of deflation of the top of the coversand profiles and redeposition of these sediments as drift-sands during historical times, the present-day cosmic radiation of the Late Weichselian sands does not reflect the average radiation dose through time. The time-averaged cosmic radiation of these aeolian sands was therefore calculated and compared for two scenarios. In a first scenario, the situation before the sand-drifting was reconstructed. The top of the podzol was thereby considered as the original surface and, in profiles 2 and 3 where part of the sediments was removed, an estimate of the original height of the surface was made to determine a better value for the cosmic radiation that has affected the sediments throughout most of the burial period.

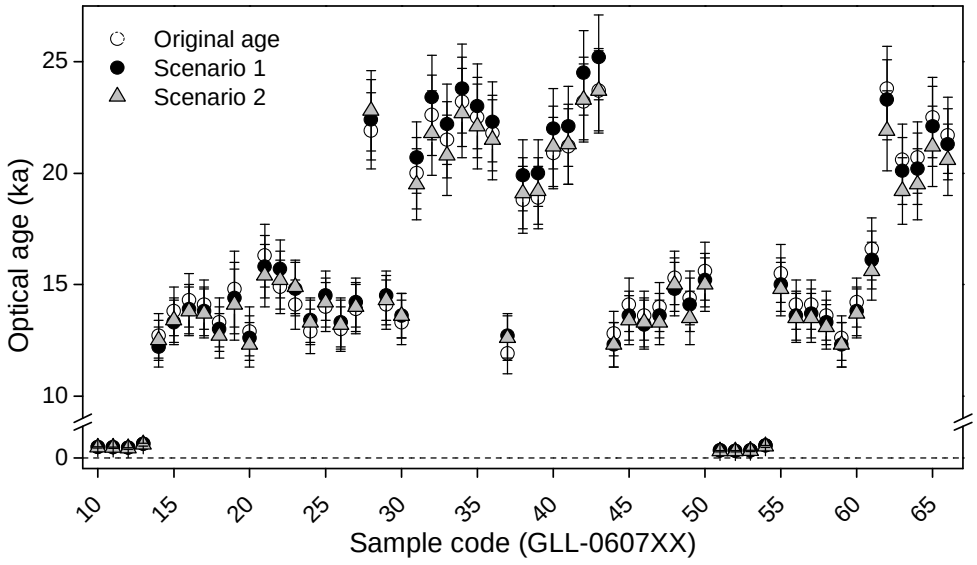

Fig. 6.8: Comparison of the optical ages, calculated on the basis of the present-day depth (open circles), on the basis of the estimated depth before sand-drifting events took place in the Lutterzand area (filled circles), and on the basis of the method outlined in Munyikwa (2000; grey triangles).

The resulting dose rates were up to ~7% lower in sequences situated in a deflation zone, and up to ~4% higher in profiles where drift-sands were recently deposited. In a second scenario, a multi-step episodic accumulation of sediments was assumed and corrected for (see

Munyikwa, 2000). In this respect, three major phases of (fluvio-)aeolian sedimentation were taken into account, corresponding to units A, B and C. The intervening 'stabilisation' phases were the deflation phase at the end of the Late Pleniglacial (assumed timing: 17 – 15 ka, based on the time boundaries for the Beuningen Gravel Bed determined by Kasse et al., 2007) and the Holocene podzolisation phase (assumed timing: 11.7 – 1.0 ka, based on the generally accepted timing for the onset of the Holocene, see e.g. Hoek, 2001, and the assumed onset of sand-drifting, see e.g. Castel et al., 1989). In Fig. 6.8, the original luminescence ages, determined using the present-day cosmic radiation, are compared with the ages obtained using the scenarios outlined in the above. It can be observed that the ages are generally in agreement within (total) uncertainty, but nevertheless the ages determined using the first scenario were the ones chosen to reconstruct the depositional history. A first reason for this choice is that the sand-drifting phase occurred fairly recently and its influence on the time-averaged cosmic radiation is negligible. By using the present-day cosmic radiation for calculating the optical ages, too much importance would be attached to the effect of sand-drifting. Secondly, it is impossible to reconstruct the timing of the stabilisation and deflation/erosion phases, their duration and their impact on the sediments. As such, these unknowns are sources of uncertainty in the age calculation on the basis of the second scenario.
The dosimetric information related to these ages is summarised in Table 6.2.

6.6.6. Optical ages

Table 6.2 summarises the optical ages, as well as the information relevant to the age and uncertainty calculation. Uncertainties on the luminescence ages were determined according to the error assessment system proposed by Aitken and Alldred (1972) and Aitken (1976). Additional information on the different sources of systematic uncertainty and their quantification can be found in Vandenberghe et al. (2004; see also Vandenberghe, 2004). The systematic uncertainty is generally dominant in the overall uncertainty on the ages and amounts to 7 – 8%. The ages of two samples (GLL-060713 and -19) are characterised by larger random than systematic uncertainties, due to the relatively large spread in equivalent doses. As the sources of systematic uncertainty are largely shared between the samples, only the random uncertainty, ranging between 2 and 4% for most samples, is taken into account to evaluate the internal consistency of the OSL dataset.

The optical ages of the fluvio-aeolian to aeolian sequence at Lutterzand range between 25.2 ± 0.7 ka and 0.20 ± 0.01 ka (Table 6.2 and Fig. 6.9). Two clear leaps in the OSL data can be identified, which closely correspond with the boundaries between the three sedimentary units (A, B and C) distinguished on the basis of their sedimentological characteristics (section 6.4). Within each sedimentary unit, there is some apparent variation in the optical ages, which is especially clear when the associated uncertainties are not taken into account. Horizontal variation is illustrated by samples GLL-060731, -32 and -33, yielding ages of 20.7 ± 0.7 ka, 23.4 ± 0.9 ka and 22.2 ± 0.9 ka. Although these ages are not significantely different within two sigma, some improvement could still be made in the age determination for these specific three samples. The above-mentioned ages were calculated on the basis of a single dose rate estimate obtained on the bulk sample that was collected from the sediment surrounding the three samples. Ages could also be calculated from the individual dose rate estimates for the samples, determined on the sediment collected from the outer ends of the sample tubes (Table 6.3). The dose rate results differ slightly from that obtained on the bulk sample. Using these results, indistinguishable ages of 24.0 ± 1.5 ka, 23.8 ± 0.9 ka and 23.8 ± 1.3 ka were obtained for GLL-060731, -32 and -33, respectively.

Sample GLL-code	^{234}Th (Bq kg^{-1})	^{226}Ra (Bq kg^{-1})	^{210}Pb (Bq kg^{-1})	^{232}Th (Bq kg^{-1})	^{40}K (Bq kg^{-1})	Total Dose rate (Gy ka^{-1})	Age (ka)	σ_r (%)	σ_{sys} (%)	σ_{tot} (%)	σ_{tot} (ka)
060731 (X1)	4.8 ± 1.0	4.8 ± 0.4	7.4 ± 0.5	5.7 ± 0.3	131 ± 3	0.69 ± 0.01	26.0	3.3	7.0	7.7	2.0
060731 (X2)	8.6 ± 1.4	6.1 ± 0.4	7.5 ± 0.9	6.8 ± 0.2	162 ± 3	0.80 ± 0.02	22.3	3.4	7.0	7.8	1.7
060731 (average)	6.7 ± 1.9	5.5 ± 0.7	7.4 ± 0.1	6.2 ± 0.6	146 ± 15	0.75 ± 0.04	24.0	6.3	7.0	9.4	2.3
060732 (X1)	6.0 ± 1.1	6.0 ± 0.3	7.1 ± 0.5	6.9 ± 0.2	175 ± 2	0.83 ± 0.01	24.5	3.7	7.0	7.9	1.9
060732 (X2)	6.4 ± 0.6	6.3 ± 0.3	8.0 ± 0.8	7.9 ± 0.2	184 ± 2	0.88 ± 0.01	23.1	3.7	7.0	8.0	1.8
060732 (average)	6.2 ± 0.2	6.1 ± 0.2	7.6 ± 0.4	7.4 ± 0.5	180 ± 4	0.85 ± 0.01	23.8	3.9	7.0	8.0	1.9
060733 (X1)	6.6 ± 1.2	5.7 ± 0.3	7.5 ± 0.7	7.3 ± 0.2	156 ± 2	0.79 ± 0.01	24.4	3.7	7.0	7.9	1.9
060733 (X2)	6.3 ± 1.2	5.6 ± 0.3	6.1 ± 0.8	6.6 ± 0.2	182 ± 2	0.83 ± 0.01	23.3	3.7	7.0	8.0	1.9
060733 (average)	6.4 ± 0.1	5.69 ± 0.04	6.8 ± 0.7	7.0 ± 0.3	169 ± 13	0.81 ± 0.04	23.8	5.5	7.0	8.9	2.1

Table 6.3: Radionuclide activities and derived total dose rates and ages for the samples taken at the outer ends of each OSL sample cylinder. X1 is the cylinder end that was hammered into the sediment profile, X2 is the end that was closest to the surface.

Generally the fluvio-aeolian and aeolian sediments can be considered as well bleached. For the fluvial sediments in the lower part of Unit A2, however, this cannot be unequivocally

concluded; in this respect, dose distribution analyses could give a more decisive answer. The nature of the transport process (e.g. depth of the water column, flow regime) is the main determining factor for the degree of bleaching in a fluvial environment (Murray and Olley, 2002). For profile 2, in which the fluvial deposit reaches a thickness of not more than a few cm and is relatively coarse-grained, it could be assumed that the sediment was transported in a shallow water column. As such, the possibility for the coarse sand grains to be exposed to daylight and hence to be completely bleached may have been larger in profile 2 than in profile 4, where the deposit is markedly thicker. The degree of bleaching is also dependent on the grain size of the investigated sediments. Vandenberghe et al. (2007) reported this grain size dependency for recent floodplain deposits in the Ardenne region (S Belgium) and concluded that the coarsest grain size yielded the lowest equivalent doses, i.e. it was more completely bleached. In this research, a relatively coarse grain size fraction was chosen to determine equivalent doses, so it could be expected that the sediment grains were relatively well-bleached. This is confirmed by the fact that the equivalent doses (measured in large aliquots) in the fluvial samples do not show a large variation. Nevertheless, it should be kept in mind that the derived OSL ages may represent maximum ages for the fluvial sediments at the base of Unit A2.

It can be concluded that the ages within each profile are consistent with the stratigraphic position of the samples and that the OSL dataset is internally consistent. None of the optical ages could be identified as an outlier on the basis of the Q test (Dean and Dixon, 1951).

6.7. DISCUSSION ON THE TIMING OF THE COVERSAND DEPOSITION

This study provides the most detailed set of optical ages currently available at the type locality for the Late Weichselian in the E Netherlands. They can be compared and correlated with other chronological records (based on e.g. previously obtained luminescence ages, radiocarbon ages, pollen analysis), determined for the same and equivalent deposits in the NW European lowlands. To facilitate this comparison, all optical ages in the following are mentioned with their total (1 σ) uncertainty and they are related to the commonly adopted lithostratigraphy for the Late Weichselian and Holocene, as established by Van der Hammen and Wijmstra (1971). On the whole, the following discussion seeks to provide a reliable chronological framework for the environmental changes during the Weichselian-Holocene transition in NW Europe.

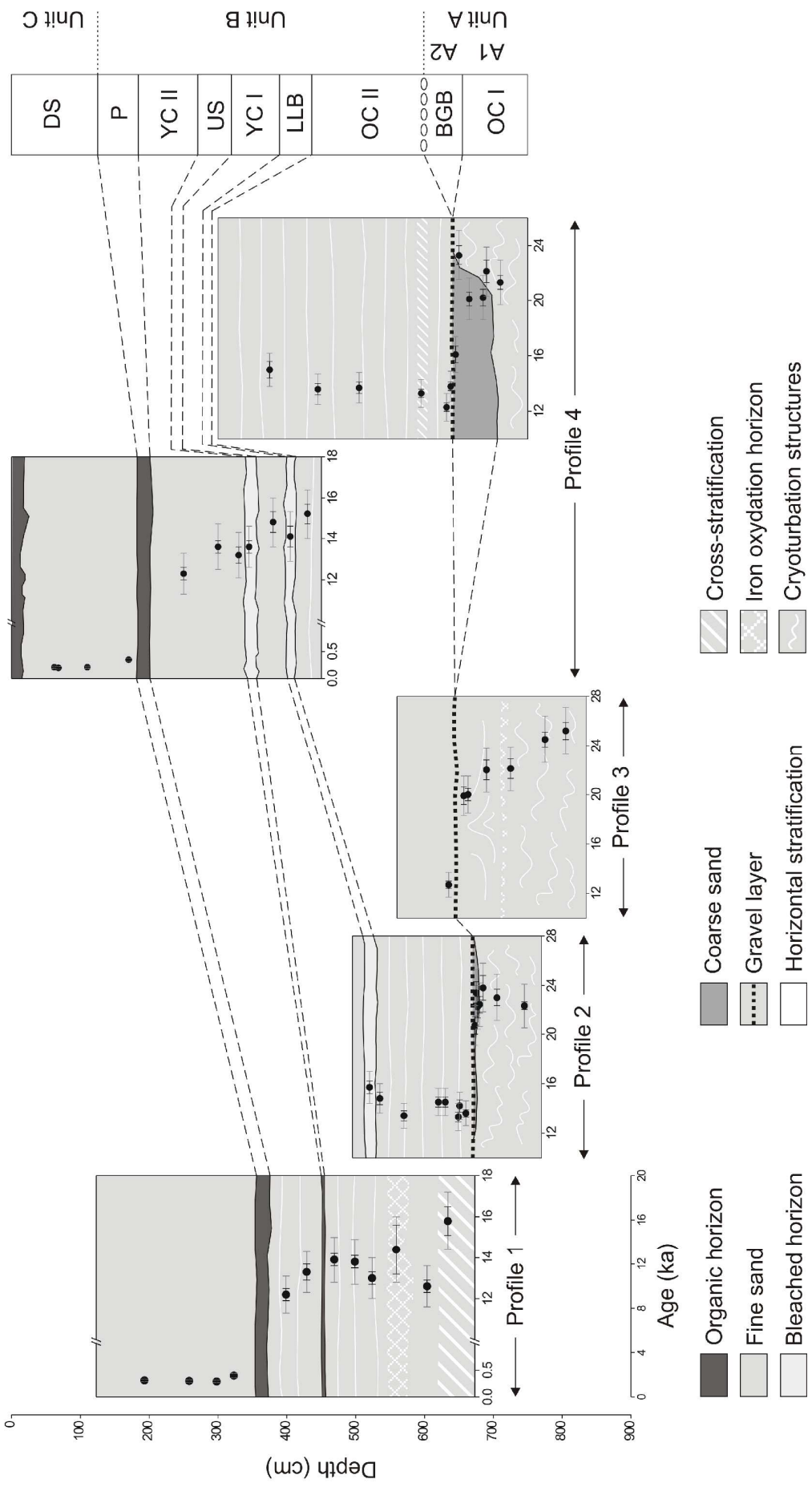
Unit C
Unit B
Unit A
A2
A1
DS
P
YC II
US
YC I
LLB
OC II
BGB
OC I
Profile 1
Profile 2
Profile 3
Profile 4
Depth (cm)
Age (ka)
Organic horizon
Fine sand
Bleached horizon
Coarse sand
Gravel layer
Horizontal stratification
Cross-stratification
Iron oxydation horizon
Cryoturbation structures

Fig. 6.9: Synthesis of the optical ages, plotted on the schematic profiles shown in Fig. 6.2. The black error bars represent the random uncertainty and can be used to evaluate the internal consistency of the OSL dataset, as the sources of systematic uncertainty are generally shared. The grey error bars represent the total uncertainty on the ages. To facilitate the evaluation of the OSL ages in view of the depositional history and landscape evolution, the stratigraphy of each profile is schematically indicated on the figure.

6.7.1. Unit A (fluvial and fluvio-aeolian sands)

As discussed in section 6.4.1, Unit A can be subdivided into two subunits: (1) fluvio-aeolian Unit A1, consisting of silty, fine-grained sands and equivalent to the Older Coversand I unit, and (2) Unit A2, comprising medium to coarse-grained fluvial sands that are truncated by a gravel string. This gravel layer is commonly interpreted as a desert pavement; the complete unit A2 is considered to be equivalent to the Beuningen Gravel Bed. For Unit A1, or the Older Coversand I, our OSL ages range from 25.2 ± 1.9 ka to 19.9 ± 1.6 ka. As the base of this silty sand unit could not be sampled due to its location underneath the groundwater level, the age of 25.2 ± 1.9 ka should be regarded as a minimum age for the onset of its deposition. Similarly, as the top of Unit A1 was truncated by the Beuningen Gravel Bed (Unit A2), the age of 19.9 ± 1.6 ka should be regarded as a minimum age for the end of its deposition. The fluvial part of Unit A2 yielded ages between 23.4 ± 1.9 ka and 16.1 ± 1.3 ka.

No independent age control is available for Unit A at Lutterzand. According to Kolstrup (1980), the deposition of the Older Coversand I (Unit A1) took place after approximately 28 – 27 ka ^{14}C BP (~32-31 ka calBP) and before ca. 19,100 ± 180 ^{14}C BP (23.2 – 23.1 ka calBP (5.2%), 23.0 – 22.5 ka calBP (63.0%)). The latter age was obtained on a humic extract from an organic gully filling at Staphorst (some 70 km to the west of Lutterzand), which was thought to represent the lateral equivalent of the Beuningen Gravel Bed (Kolstrup, 1980). Our ages for Unit A are not inconsistent with this radiocarbon age and with the age range postulated by Kolstrup (1980), although the optical ages point out that sediment deposition continued till after 23.0 – 22.5 ka calBP (63.0%; Kolstrup, 1980) in the Lutterzand area.

Unit A reveal a fining-upwards sequence (Unit A1), unconformably overlain by the coarse-grained sands of Unit A2. The fining-upwards sequence reflects the increasing influence of fluvio-aeolian and aeolian sedimentation during the Late Pleniglacial (Vandenberghe and Van Huissteden, 1988; Van Huissteden, 1990), subsequent to the dominant fluvial sedimentation during the Middle Pleniglacial. The upward decrease of fluvial activity followed by fluvio-aeolian deposition is regionally recognised in river valleys of the NW European lowlands (see

Kasse et al., 2007, and references therein); Kasse et al. (2007) therefore attributed it to external forcing, presumably caused by the increasing climate aridity during the Late Pleniglacial. In the Lutterzand area, this phase was dated between 25.2 ± 1.9 ka and 19.9 ± 1.6 ka. Comparable ages between 25.2 ± 2.0 and 17.2 ± 1.2 ka were obtained at the type locality Grubbenvorst in the S Netherlands (Kasse et al., 2007).

The sediments of Unit A1 are strongly affected by periglacial phenomena, such as cryoturbation, the formation of large-scale loading structures, and thermal contraction features. Despite this, the ages obtained for Unit A1 appear to increase rather well with depth (profile 3), which leads us to conclude that cryoturbation did not greatly disturb the OSL age pattern. Unit A1 appears to represent a phase of maximum cold and continuous permafrost conditions during the Late Pleniglacial. Frost cracks that extend from the overlying Beuningen Gravel Bed (Unit A2) downwards indicate that the landscape could probably be classified as a 'polar desert' (Van der Hammen and Wijmstra, 1971). In Unit B, periglacial features are not generally present, although at Lutterzand and at some localities in the NW European lowlands, for instance at the site of Arendonk-*Korhaan* (NE Belgium; Derese et al., in press), frost cracks resulting from deep seasonal frost have been found within Late Dryas sands. The general presence of periglacial phenomena in the sediments underlying the Beuningen Gravel Bed and their absence in the sediments covering this unit are widely seen as indications that the formation of the Beuningen Gravel Bed was contemporaneous with a marked amelioration of the palaeoclimatic and -environmental conditions, leading to permafrost degradation.

At many sites in NW Europe, the fluvial part of the Beuningen Gravel Bed is absent. The widespread desert pavement at its top is then considered as the lithostratigraphic marker horizon for the change in the palaeoclimate and –environment and hence for permafrost degradation and aeolian deflation. Bateman and Van Huissteden (1999) constrained this desert pavement between 21.9 ± 1.9 ka and 17.5 ± 2.6 ka in the Lutterzand area. In Grubbenvorst (S Netherlands), it was bracketed between 17.2 ± 1.2 ka and 15.3 ± 1.0 ka (Kasse et al., 2007). At Rotem (NE Belgium), the age range for the pebbly deflation horizon separating the fluvio-aeolian and aeolian sediments was established at 18.2 ± 1.3 ka to 15.9 ± 1.1 ka (Vandenberghe et al., 2009). In our study, the Beuningen Gravel Bed (Unit A2) is present within three profiles (2, 3 and 4), either as a fluvial unit truncated by a gravel string or as a gravel string only. In profile 1, only an estimate for the upper time boundary for this phase could be made, as the lowermost sediment unit in this profile is assumed to be situated in a stratigraphically higher position than unit A2. The Beuningen Gravel Bed was there covered by sediments of Unit B from at least 15.8 ± 1.4 ka onwards.

In order to allow a comparison between our results and those obtained at other localities within the NW European lowlands, a clear distinction should be made between the two abovementioned facies of the Beuningen Gravel Bed. A comparison with the other sites is only possible for those profiles where the Beuningen Gravel Bed is represented by the desert pavement only, i.e. in profile 3 and partly in profile 4. In profile 3, the Beuningen Gravel Bed is constrained between 19.9 ± 1.1 ka (n=2; top OCI) and 12.7 ± 1.0 ka (n=1; base OCII). In profile 4, the desert pavement is bracketed between 23.3 ± 1.8 ka (GLL-060762) and 12.3 ± 1.0 ka (GLL-060759). The upper time boundary of the Beuningen Gravel Bed (Unit A2) and of the aeolian deflation period at Lutterzand is estimated at 13.3 ± 1.0 (n=6; base OCII). These age limits, especially the upper one, are slightly different from those obtained by Bateman and Van Huissteden (1999), Kasse et al. (2007) and Vandenberghe et al. (2009). However, it should be pointed out that Bateman and Van Huissteden (1999) applied a different single-aliquot protocol to determine equivalent doses, namely the so-called preheat correction method (Duller, 1994). Furthermore, the lower time boundary for the Beuningen Gravel Bed was based on a single age of 21.9 ± 1.9 ka determined for the Older Coversand I (Unit A1), whereas the upper time boundary for this desert pavement was chosen to be equal to the maximum age of 17.6 ± 2.6 ka obtained for the Older Coversand II and/or Younger Coversand I (Unit B). This maximum age was determined on a sample collected from the top of Unit B in the northern section (our profile 1), where the Beuningen Gravel Bed was not observed. The sample from Unit B immediately overlying the gravel bed in the southern section (our profile 4) yielded an age of 13.9 ± 1.3 ka (Bateman and Van Huissteden, 1999), which is consistent with our age of 13.1 ± 1.0 ka (n=2) for the sediments overlying the gravel layer. The difference in time-brackets of the Beuningen Gravel Bed obtained at different localities in the NW European lowlands does not unequivocally suggest that the phase of aeolian deflation had a different timing and duration at these localities. However, it does indicate that local environmental parameters (e.g. geomorphological setting, vegetation density, wetness) presumably influenced the accumulation and preservation potential of the sediments under- and overlying the Beuningen Gravel Bed.

The occurrence at Lutterzand of the Beuningen Gravel Bed as a fluvial unit truncated by the widespread desert pavement (in profiles 2 and 4) gives us the unique possibility to derive direct ages for this lithostratigraphic horizon. The coarse-grained fluvial sediments of Unit A2 were found to be deposited between approximately 23.4 ± 1.9 ka and 16.1 ± 1.3 ka. Their discontinuous occurrence within the Lutterzand sections suggests that the sediments were deposited in channels, which did not necessarily develop synchronously over the whole area.

In profile 2, they accumulated during a short phase around 22.1 ± 1.6 ka (n=3). In profile 4, where the fluvial unit is more developed, the sediments seem to have accumulated from 20.2 ± 1.6 ka to 16.1 ± 1.3 ka. The desert pavement itself can, on the basis of the optical ages of the fluvial deposit, be more narrowly bracketed than at locations where the fluvial unit is not present. In profile 4, the desert pavement represents the most stringent time interval, between 16.1 ± 1.3 ka (see above) and 13.8 ± 1.1 ka (GLL-060760).

6.7.2. Unit B (aeolian sands)

Unit B encompasses several of the lithostratigraphic units differentiated by Van der Hammen and Wijmstra (1971): Older Coversand II, Lower Loamy Bed, Younger Coversand I, Usselo Soil and Younger Coversand II. The sedimentological characteristics of the coversand units are generally very uniform and the main criterion to distinguish between them is the presence of intercalated silty sand units (Lower Loamy Bed and Usselo Soil) or their organic equivalents. The horizontal stratification of the coversands, which can be followed over considerable distances, indicates their aeolian nature; the absence of any cryoturbation structures and thermal contraction features provides evidence for the climatic amelioration and the absence of permafrost conditions during the deposition of these sediments. Unit B yields ages between 15.8 ± 1.4 ka and 12.2 ± 0.9 ka. The ages for this unit increase slowly with depth in profile 1 and in the upper part of profile 4, but do not show such an increase in profile 2 and in the lower part of profile 4. Some variability is present within the OSL datasets. Such a variability has been noted before (see e.g. Derese et al., 2009; in press) and appears to be inherent to the OSL dating technique; its causes are presently unknown. In profiles 2, 3 and 4, the Older Coversand II has been dated between 15.2 ± 1.2 ka and 12.3 ± 1.0 ka. For this particular unit, the optical ages do not increase with depth but seem to be spread around an average of 13.8 ± 1.0 ka (n=15), suggesting that the sediments may have been deposited during a relatively short time interval.

In profile 1, the stratigraphic interpretation of the sediments in which samples GLL-060716 to -21 were collected is not completely clear. This is partly due to the fact that the only lithostratigraphic markers present within the profile are a peat layer, thought to represent the lateral variant of the Usselo Soil, and a podzol. A second factor of uncertainty is related to the sedimentological features of this specific deposit (see section 6.4.2), which appear to reflect a upward transition from a fluvial sediment to an aeolian deposit. As such, this sediment unit

shows some similarities with the depositional character of Unit A1 (see section 6.4.1). The optical ages determined for this unit range from 15.8 ± 1.4 ka to 12.6 ± 1.0 ka, with an average of 13.8 ± 1.1 ka (n=6). The OSL ages thus indicate that the sediments in profile 1 presumably accumulated after the formation of the Beuningen Gravel Bed; they are therefore thought to represent the Older Coversand II and/or Younger Coversand I.

The Lower Loamy Bed has been dated between 14.1 ± 1.2 ka and 15.7 ± 1.3 ka, with an average of 14.9 ± 1.2 ka (n=2). A single age of 14.8 ± 1.2 ka has been obtained for the Younger Coversand I. The Usselo Soil yielded an age of 13.6 ± 1.0 ka (n=2), and the Younger Coversand II was dated between 13.6 ± 1.1 ka and 12.2 ± 0.9 ka, with an average of 12.9 ± 1.0 ka (n=5). These ages are in agreement with the previously established radiocarbon chronology, with the newly obtained AMS radiocarbon ages of 12.6 – 12.4 ka calBP (profile 1) and 13.2 – 12.9 ka calBP (profile 4) for the Usselo Soil, and with the generally accepted ^{14}C-based chronostratigraphy for the Late Glacial.

In general, the optical ages indicate that the deposition of Unit B probably started during the final phase of the Late Pleniglacial and continued throughout the Late Glacial. Phases of landscape stabilisation (Bølling and Allerød interstadials) are not clearly reflected in the OSL ages because they represent fairly short periods in time in comparison to the uncertainty on the optical ages (~1 ka). This illustrates the limit on the time resolution that can be achieved with optically stimulated luminescence dating.

Overall, the OSL dataset suggests that sand-sheet deposition went on during the climatic improvement around the Late Pleniglacial / Late Glacial transition (~14.7 ka calBP, or the onset of the Bølling interstadial). It has been argued that the widespread sand-sheet deposition and preservation is the short-term response to this climatic warming (Kasse, 1997). Continuation of the aeolian deposition across the Late Pleniglacial / Late Glacial boundary has been observed before at the sites of Ossendrecht (Vandenberghe et al., 2004), Grubbenvorst (S Netherlands; Kasse et al., 2007), Lommel-*Maatheide* and Arendonk-*Korhaan* (NE Belgium; Derese et al., in press). This observation was not only based on the absence of hiatuses around 14.7 ka in the OSL dataset, but also on the general scarcity of Bølling age organics and soils within the sediments in comparison with the more frequent Allerød soils and peats. Our OSL ages also seem to point to fairly continuous sedimentation of Unit B during the Late Glacial, over the whole Lutterzand area. The presence of organic and bleached soil horizons interbedded within the coversands shows that this deposition decreased or was interrupted due to vegetation growth and landscape stabilisation, probably related to climate amelioration during interstadial periods. The Lower Loamy Bed does not

show clear signs of soil formation or organic material accumulation, and its more silty character is due to a slowing down of the aeolian deposition. The Usselo Soil or peat bed of Allerød age, however, reveals clear evidence for vegetation growth and landscape stabilisation.

So far, the clastic components of the Usselo Soil and the Lower Loamy Bed have rarely been directly dated. At Lutterzand, we have obtained ages between 14.1 ± 1.2 ka and 15.7 ± 1.3 ka (average: 14.9 ± 1.2 ka, n=2) for the sediments composing the Lower Loamy Bed and 13.6 ± 1.0 ka for those composing the Usselo Soil. At Arendonk-*Korhaan* and Lommel-*Maatheide*, optical ages for the bleached Usselo Soil of 15.2 ± 1.3 ka and of 10.5 ± 0.8 and 12.2 ± 0.9 ka have been obtained, respectively (Derese et al., in press). In their study concerning the characteristics of the Usselo Soil, Kaiser et al. (2009) show that the OSL dating of the clastic component of soil horizons is not straightforward. The optical age results may reflect the depositional age of the parent material of the palaeosol and hence pre-date the soil formation. Equally the samples from within the palaeosol may show younger ages as a result of bioturbation. Kaiser et al. (2009) conclude that the most reliable ages are those obtained for the sediments covering the palaeosol, as their stratigraphic position is best known. In accordance with the conclusions of Kaiser et al. (2009), we achieved the following time boundaries for the Usselo Soil and Lower Loamy Bed, based on the OSL results of the sediments under- and overlying these horizons: (1) the Lower Loamy Bed formed after 14.0 ± 1.0 ka (n=7) in profile 2 and between 13.8 ± 1.0 ka (n=7) and 14.8 ± 1.2 ka (n=1) in profile 4, and (2) the Usselo Soil formed between 13.8 ± 1.1 (n=6) and 12.7 ± 0.9 (n=2) in profile 1 and between 14.8 ± 1.2 ka (n=1) and 13.0 ± 1.0 (n=3) in profile 4. Based solely on these time boundaries, it would appear that both horizons date from the Allerød interstadial. A similar situation has been reported at Opgrimbie (NE Belgium; Derese et al., 2009). There, two bleached horizons, one previously assigned to the Bølling period and one to the Allerød, were thought to belong to the same soil complex that formed during the Allerød interstadial on the basis of optical dating. The optical age information obtained for the Usselo Soil at Lutterzand is not only in agreement with independent age information (see above), but also with the OSL ages obtained at other localities within the NW European lowlands. Bateman and Van Huissteden (1999) dated the Usselo Soil at Lutterzand between 15.8 ± 1.8 ka (n=3) and 12.5 ± 1.1 ka (n=2). Similarly, Vandenberghe et al. (2004) obtained ages between 14.7 ± 0.6 ka (n=3) and 12.3 ± 0.8 ka (n=3) for the equivalent unit at Ossendrecht (S Netherlands). At the type locality Grubbenvorst (S Netherlands,) this unit was dated between 15.3 ± 1.0 ka (n=4) and 13.8 ± 1.0 ka (n=1).

6.7.3. Unit C (drift-sands)

The investigated profiles in the Lutterzand area can be classified into different types of drift-sand areas, based on their mainly erosional or accumulational character and the presence or absence of a buried soil profile: (1) profile 4 can be considered as a "blown-over" area, where drift-sand sedimentation occurred on top of the original surface (podzol) without any previous deflation, (2) profile 1 can be identified as a "blown-on" area, as the original top of the podzol was deflated and subsequently covered by drift-sands, and (3) profiles 2 and 3 can be described as "blown-out" parts, where the original surface (podzol) was removed by deflation (Castel et al., 1989). This classification has been achieved on the basis of field observations. Based on the thicknesses of the drift and coversands in profiles 1 and 4, it is estimated that around 1.5 m and 3.3 m of sediment was deflated from profiles 2 and 3, respectively.

The drift-sands of Unit C can be differentiated from the underlying coversands by their stratigraphical position, slightly humic character due to the uptake of the deflated Holocene podzolic soil, better sorting and loose consistency. The textural properties of the drift and coversands are very similar, which suggests that the drift-sands originate with the transport and resedimentation of the latter; this has been argued before by Castel et al. (1989). In profiles 1 and 4, the 8 drift-sands samples yield ages between 0.40 ± 0.04 ka and 0.20 ± 0.02 ka; consistent results are obtained for both profiles, and the ages are in agreement with the stratigraphic position of the samples. Moreover, the optical ages are consistent with the location of the drift-sands on top of the podzol, which has been dated at 1.52 – 1.46 ka calBP (38.2%), 1.45 – 1.39 ka calBP (30.0%) using radiocarbon dating (profile 4). The OSL ages for the drift-sands indicate that sedimentation of Unit C sands in profiles 1 and 4 took place during a fairly short period; around 1.5 to 2 m of drift-sands was deposited in the course of ~200 years.

In their description of the Late Quaternary depositional history, Van der Hammen and Wijmstra (1971) state that natural river dunes already occurred during the Middle Holocene in the Lutterzand area, but that the major expanse of inland dunes took place from the Middle Ages onwards. They attributed this to the damage done to the heath vegetation, as a result of sod-cutting ~1.2 – 1.0 ka onwards. Castel et al. (1989, and references therein) place the initial phase of major sand-drifting in The Netherlands around 1.1 – 0.9 ka, although they agree that minor drift-sand sedimentation might have occurred before. At Pulle (NE Belgium), for example, the average optical age of 1.2 ± 0.1 ka (n=7) for a ~2 m high drift-sand dune

indicates that human cultural activities could exceed the capacity of the local environment before 1.1 ka (Derese et al., 2010). At Weerterbergen (SE Netherlands), several phases of sand-drifting have been identified on the basis of OSL dating, namely between 5.8 0.5 ka and 4.7 ± 0.4 ka, between 1.3 ± 0.1 ka and 0.35 ± 0.03 ka, and from 0.10 ± 0.01 ka to present (van Mourik et al., 2010). It is not clear when sand-drifting events started to take place in the Lutterzand area and whether multiple phases of sand-drifting occurred. Bateman and Van Huissteden (1999) determined an age of 0.60 ± 0.10 ka for the drift-sands in profile 1. Our optical ages of 0.40 ± 0.04 ka to 0.20 ± 0.02 ka indicate that sand-drifting has continued until very recently.

6.8. CONCLUSIONS

In this study a detailed set of optical ages is presented for the fluvial, fluvio-aeolian and aeolian events at the type locality Lutterzand in the E Netherlands. Based on the lithostratigraphical and sedimentological characteristics of the sedimentary sequence and the age determinations with optically stimulated luminescence dating, the following major conclusions concerning the landscape evolution could be drawn:

From at least 25.2 ± 1.9 ka onwards, a transition from fluvial to fluvio-aeolian sedimentation took place. This change has also been noted in other European river systems and has been related to increased climate aridity. Fluvio-aeolian deposition (Older Coversand I) continued at least until 19.9 ± 1.6 ka. The fluvial and fluvio-aeolian deposits are characterised by the occurrence of periglacial features, such as large-scale cryoturbation and frost cracks, which point to continuous permafrost conditions. They are overlain by the Beuningen Gravel Bed, which at Lutterzand consists of a discontinuous fluvial unit of coarse sands and a widespread gravel layer (desert pavement) truncating all underlying deposits. The Beuningen Gravel Bed is considered as the lithostratigraphic marker for the climatic amelioration, permafrost degradation and extensive aeolian deflation at the end of the Late Pleniglacial. Fluvial deposition in shallow channels occurred between approximately 23.4 ± 1.9 ka and 16.1 ± 1.3 ka and was strongly dependent on local variables. The overlying desert pavement was bracketed most narrowly between 16.1 ± 1.3 ka and 13.8 ± 1.1 ka on the basis of the age information determined for the immediately under- and overlying sediments. The age range obtained at Lutterzand is slightly different than at other localities in the NW European lowlands, which illustrates the influence of local environmental parameters on the

accumulation and preservation potential of the sandy deposits below and above the Beuningen Gravel Bed. In the E Netherlands, sedimentation may have started later after the phase of aeolian deflation and formation of the desert pavement.

The Late Pleniglacial and Late Glacial aeolian sediments yield ages between 15.8 ± 1.4 ka and 12.2 ± 0.9 ka. Some variability is present within the OSL dataset, illustrating the importance of determining more than one age estimate per sedimentary unit. The resolution of optical dating does not allow identifying landscape stabilisation phases within the Late Glacial. Hence the optical ages seem to indicate that sedimentation may have been fairly continuous throughout the Late Glacial. The presence of the Lower Loamy Bed and the Usselo Soil, however, indicate that the aeolian activity decreased or even stopped during the interstadial phases, but apparently only during a fairly short period of time (shorter than ~1 ka). Based on the OSL dataset, the Lower Loamy Bed cannot unequivocally be ascribed to the Bølling interstadial. Further research is necessary to resolve this matter. OSL dates of the Usselo Soil, however, confirm its Allerød age.

Between 0.40 ± 0.04 ka and 0.20 ± 0.02 ka, sand-drifting took place. It is unclear when sand-drifting has started or whether multiple phases of sand-drifting have occurred. Sand-drifting is thought to have been initiated as a result of forest degradation and sod-cutting since 1.2 – 1.0 ka. In the major part of the Lutterzand area, these drift-sands have now been stabilised by afforestation with pine trees.

This study illustrates how luminescence dating may contribute to an improved understanding of the landscape dynamics during the Weichselian-Holocene transition. The chronological framework established here for the classic type locality of the Late Weichselian fluvial and aeolian deposits, even with its limited precision, undoubtably forms a valuable step towards better chronostratigraphic correlation between equivalent deposits in the European coversand belt in general and the NW European lowlands in particular.

Chapter 7

Interpretations and conclusions

CHAPTER 7. INTERPRETATIONS AND CONCLUSIONS

This PhD thesis reports on the application of quartz SAR-OSL dating to six Late Weichselian and Holocene sandy sequences in N Belgium and The Netherlands. In the following paragraphs, the results of this research are discussed in terms of (1) the luminescence characteristics of the investigated sediments, (2) the precision of the resulting OSL ages, (3) their accuracy, and (4) their interpretation with reference to the changes in the sedimentary environments through time. Finally some methodological challenges and future applications on equivalent deposits in the NW European lowlands are highlighted.

7.1. LUMINESCENCE CHARACTERISTICS OF THE INVESTIGATED SEDIMENTS

Vandenberghe (2004; see also Vandenberghe et al., 2004) investigated and compared a number of measurement protocols (multiple-aliquot additive dose or MAAD, single-aliquot additive dose or SAAD, single-aliquot regenerative dose or SAR) in order to find the most suitable protocol for determining the equivalent dose in coversands from the southern Netherlands. Both the SAAD and the MAAD protocols were excluded from further investigation at an early stage, the SAAD because the OSL decay could not be characterised by a single exponential function and there was some sensitivity increase during the measurement cycle, and the MAAD because it uses an average growth curve and therefore was thought to average out the equivalent doses, possibly leading to the wrong answer. The SAR protocol, on the other hand, was found to be suitable for the coversand samples. Moreover, a small laboratory intercomparison on SAR equivalent dose determination yielded an acceptable overall agreement, thus giving confidence in the implementation of the technique and the results obtained. The consistency between the SAR-OSL ages and radiocarbon ages for the sequence in the southern Netherlands demonstrated that the SAR protocol yielded accurate results (Vandenberghe, 2004; Vandenberghe et al., 2004). Hence, this measurement protocol was used in further investigations on the NW European coversands (e.g. Kasse et al., 2007; Vandenberghe et al., 2009) and it was also the technique of choice in this thesis research.

Initially, the following measurement parameters were adopted (e.g. for dune sands at Opgrimbie; see Chapter 3): (1) a preheat temperature of 240°C, (2) a cutheat temperature of

160°C, and (3) a test dose amounting to ~50% of the estimated natural dose. However, for the coversands at Heidebos (Chapter 5) and at Lutterzand (Chapter 6), dose recovery tests indicated that adopting a higher cutheat (180°C and 220°C for Heidebos and Dinkel, respectively) resulted in a better recovery of the laboratory dose (i.e. more precise and accurate results). In the case of very young deposits, such as the drift sands at Pulle (Chapter 2), the use of the aforementioned parameters could have led to (1) an overestimation of the equivalent dose as a result of unwanted charge transfer in response to the high preheat temperature of 240°C, and (2) imprecise results due to the high contribution of the (weak) test dose signal to the measurement precision. In order to reduce the effects of preheat temperature and test dose, it was chosen to reduce the preheat temperature as much as possible, bearing in mind that it should be higher than the cutheat temperature of 160°C, and to increase the test dose. A preheat temperature of 180°C was chosen, as preheat plateau and thermal transfer tests did not show a marked charge transfer for this temperature, and the test dose was increased to ~3 Gy (or ~300% of the estimated natural dose).

All sediments investigated here show satisfactory luminescence characteristics in terms of brightness (clearly distinguishable from background), OSL decay (dominated by the fast component), recycling ratios (consistent with unity), recuperation (generally less than 5% of the sensitivity-corrected natural OSL signal), and dose recovery (dose recovery ratios within 10% of unity). It is therefore concluded that the chosen SAR measurement protocols were suitable for determining equivalent doses in the sandy sediments studied in the frame of this thesis. Equivalent dose distributions, such as those obtained for a dune sand sample at Opgrimbie (NE Belgium; see Chapter 3) and at other localities (e.g. Ossendrecht, Rotem; see Vandenberghe et al., 2004; 2009), indicate that the coversands are generally well-bleached and undisturbed by post-depositional mixing. For the fluvial sediments of the Beuningen Gravel Bed at Lutterzand (see Chapter 6), it cannot be unequivocally concluded that they were completely bleached. However, as the sediments are thought to have been deposited in shallow channels with sufficient energy to transport the coarse-grained sands and gravels and thus also to let them be exposed to daylight, and a relatively coarse-grained sand fraction (180-212 µm) was analysed, it is expected that they are sufficiently bleached. In the whitish horizons intercalated between the sand units at Arendonk, Lommel (see Chapter 4) and Lutterzand (see Chapter 6), some macroscopic evidence of bioturbation processes could be observed. Most notably, traces of burrowing by dung beetles were found in the bleached Usselo horizon at Lutterzand. Although the OSL age of 13.6 ± 1.0 ka derived for this horizon

matches the presumed (Allerød) age of the Usselo layer, it is concluded that the most reliable ages for this and other palaeosols are those determined for the overlying sediments.

7.2. PRECISION OF THE OPTICAL AGES

The OSL dataset is typically characterised by some variability, which can be larger than expected from the individual (random) uncertainties. For instance, at Arendonk-*Korhaan* (NE Belgium; see Chapter 4) a deviating age of 13.0 ± 0.4 ka was determined for a sediment unit generally yielding ages between 15.0 ± 0.5 and 16.2 ± 0.6 ka. The causes for the variability within the OSL dataset are not fully understood at present. Based on the interpretation of the equivalent dose distributions (see section 7.1), they appear not to be related to incomplete bleaching or turbation processes. It also seems unlikely that experimental errors introduced during the measurement or data processing are at the base of the variations, as the internal tests (recycling, recuperation) included in the SAR protocol and the dose recovery tests yielded good results. It can be suggested that the (fluvio-)aeolian sediments, although for the most part consisting of quartz grains, may have a larger heterogeneity in mineral composition than expected, resulting in variations of the dose rate and thus of the optical age. Variations in the dose rate within the same stratigraphical horizon have been reported by Vandenberghe et al. (2009) for sandy sequences at Rotem (NE Belgium) and have been related to significant differences in the K and Th content. Further possible causes of the variability in the OSL dataset should be investigated in future.

The optical ages obtained in this thesis are characterised by total (1 σ) uncertainties of ~8-10%, in which the systematic uncertainty (~7-8%) is generally dominant. Within the investigated timeframe (~25 ka to present), the resolution of quartz SAR-OSL dating is limited to ~2 ka for the Late Pleniglacial, ~1 ka for the Late Glacial and ~0.1 ka for the Late Holocene, i.e. sedimentation phases of shorter duration cannot be unequivocally distinguished. This implies that short-lived phases during the Late Glacial, such as the Early Dryas (14.1 – 14.0 ka calBP, according to Hoek, 2001), cannot be differentiated with OSL dating but only on the basis of lithostratigraphic evidence supported by independent chronological information of sufficient precision. The sources of systematic uncertainty, related either to the instrumentation (e.g. calibration of beta source and gamma-spectrometer, conversion parameters) or to environmental variables (e.g. estimation of cosmic radiation and internal dose rate, and time-averaged moisture content determination) are largely correlated between

the OSL samples from a single site. For the evaluation of the internal consistency of the OSL dataset at a certain locality and for the interpretation in terms of sedimentation rates and episodic deposition events on the basis of the OSL ages only, the systematic uncertainty can be omitted and the ages can be mentioned with their random uncertainties (amounting to ~3-4% of the OSL age). In this respect, the term 'depositional event' does not refer to a sedimentation pulse, i.e. continuous rapid sedimentation over a short (~10 to 100 years) period of time, as this cannot be distinguished with OSL. In luminescence dating, a 'depositional event' is considered as a single phase of sedimentation, not necessarily characterised by continuous deposition, that cannot be subdivided due to the limited resolution of the dating method. Here we identified such phases roughly when the OSL ages obtained for a certain sedimentary unit are spread closely around a central value (e.g. the average of all OSL ages); more accurately they could be determined on the basis of statistical methods (such as Bayesian analysis). At Pulle (see Chapter 2), for instance, the OSL ages for all samples taken in a ~2.5 m thick drift-sand sequence were indistinguishable from their average of 1.2 ± 0.1 ka (n=7). It was concluded that sand-drifting occurred during a single, fairly short (~100-200 years, based on the uncertainties associated with the OSL ages) event in the Early Middle Ages. At Opgrimbie (NE Belgium; see Chapter 3 and Derese et al., 2009), a Late Glacial dune sequence yielded average ages of 12.9 ± 0.2 ka (n=6) and 13.0 ± 0.2 ka (n=3) for the sediments above and below a bleached horizon, respectively. The optical ages suggest that it was deposited fairly rapidly during one event. At Heidebos (see Chapter 5), the OSL dataset could be looked at in two ways: (1) when considering all ages for the uppermost 6 m, ranging from 13.3 ± 0.5 ka to 11.0 ± 0.4 ka and spread around an average of 12.3 ± 0.1 ka (n=9), this sedimentary unit may have been deposited during a single event in the Late Dryas, and (2) when considering all ages of the sedimentary sequence, ranging between 17.3 ± 0.8 ka and 11.0 ± 0.4 ka, a gradual semi-continuous sedimentation from the Late Pleniglacial until the Holocene could be assumed. Drawing conclusions about the sedimentation rate and the occurrence of episodes of sand deposition is only possible when multiple age estimates are available per lithostratigraphic unit. This illustrates the importance of adopting a closely spaced sampling strategy, while at the same timing taking into account that sampling a section in greater resolution than can discussed by the dating technique applied is a waste of effort. This was the strategy adopted in this research: the samples were collected along a well-defined vertical (~every 20-30 cm) and lateral (multiple samples per horizontal level) profile. It should be noted that, while choosing the exact sample location within a profile, the lithostratigraphy was taken into account, i.e. all units were sampled,

samples were particularly collected at the lithostratigraphic boundaries or along horizons where a marked difference in lithology could be observed. A 'blind' high-resolution sampling, i.e. taking samples at equal distances without taking into account the stratigraphical evidence, is only useful within profiles that do not show macroscopic sedimentological or other lithological differences (such as loess profiles).

7.3. ACCURACY OF THE OPTICAL AGES

The accuracy of the quartz SAR-OSL ages can be investigated by comparing them with independent age information, which for the investigated period (~25 ka to present) and sediments mostly comes from radiocarbon dating. It should thereby be taken into consideration that both OSL and ^{14}C dating are characterised by specific limitations and factors of uncertainty.

Some of the uncertainties that are typically related with OSL dating have been elaborately discussed in the other chapters of this thesis and are therefore only briefly discussed in this section. They can be subdivided into two groups: (1) those that mainly have an influence on the equivalent dose, and (2) those that mainly affect the dose rate determination. To the first group belong, among other processes, incomplete bleaching and post-depositional mixing. As the luminescence signal is bleached out during the exposure to daylight, the transport mechanism is the determining factor for the degree of bleaching. In general, aeolian sediments will be more easily and more homogeneously bleached than sediments transported by water or glaciers, as both water and ice can attenuate and scatter the UV rays. Even when transported over short distances, the aeolian sands investigated here will have a relatively high possibility to be completely bleached. The luminescence signal in the fluvial sediments, on the other hand, may not have been completely zeroed upon burial; it follows that their OSL ages may show an overestimation. Post-depositional mixing due to penetrating plant roots, burrowing animals, cryoturbation, loading processes etc. may result in the transport of both under- and overlying sediment grains to the sediment unit under investigation. Because of this, it is not always straightforward to estimate the effect of post-depositional mixing on the equivalent doses. The dose rate determination is mostly hampered by layer-to-layer variations in radioactivity and in moisture content, by the occurrence of uranium disequilibria due to especially radon or radium escape, by the occurrence of erosional phases affecting the contribution of cosmic radiation through time, and by variations in internal radioactivity. As

has been shown for Lutterzand (see Chapter 6), layer-to-layer variations can be modelled according to the method outlined in Aitkin (1985, Appendix H) and the sedimentation history can be taken into account using models such as that discussed by Munyikwa (2000). The influence of the internal dose will be almost negligible in quartz grains, while the occurrence of uranium disequilibria might be identified based on the gamma-ray spectrometry results. Hence it can be concluded that the most significant unknown is the moisture content. The time-averaged water content is always assessed on the basis of field indicators (e.g. sediment type, sediment structures, presence of peat) and is associated with an uncertainty of 10-25%; nevertheless it should always be borne in mind that 1% increase in the water content has an effect of ~1% increase in the optical age.

Radiocarbon dating, although the standard technique for dating organic material from the Late Quaternary, is subjected to some uncertainties as well. Until a decade ago, conventional radiocarbon dating was usually applied to bulk samples of, for example, peat. It is now widely accepted that ^{14}C ages of bulk organic sediment samples may be affected by a number of error sources, such as the botanical contamination of peats due to the vertical penetration of (younger) roots, errors induced due to the hardwater effect and fluvial or aeolian input of older reworked organic debris (see e.g. Olsson, 1986; Törnqvist, 1992; Shore et al., 1995; Lowe and Walker, 1997; 2000). As a result, these bulk ages may be either too young or too old. Van Mourik et al. (2010) illustrate that not only peat, but organic soil matter from buried humic horizons may be difficult to date accurately, as a result of its complicated chemical composition. Fractionated radiocarbon dating at Weerterbergen (SE Netherlands) showed that: (1) the humic acids yield ages close to the moment of fossilisation (burial) of the soil, (2) the humin fraction has ages that generally overestimate the time of fossilisation as this fraction accumulates over the whole period of soil development, and (3) the fulvic acids are unreliable for dating purposes as they easily migrate through the soil profile or leach away.

At present, accelerator mass spectrometry (AMS) is used to determine the ^{14}C content. This technique allows accurately measuring very small samples containing only a few milligrams of carbon, so that samples can be more selectively chosen. Nevertheless, some variables may influence the ^{14}C content of organic matter in nature. Uncertainties are also introduced during the calibration of the radiocarbon ages. The calibration curves, the most recent one for the northern hemisphere being that of Reimer et al. (2009), are based on ^{14}C measurements of tree rings until about 12 ka calBP and of foraminifera and corals until about 26 ka calBP, and are valid for one hemisphere. Although the calibration curves are regularly updated, they are characterised by a number of wiggles and radiocarbon ‘plateaus’ that complicate the accurate

calibration of radiocarbon ages. In the relevant timeframe of this study (~25 ka until present), 'plateau' regions occur around 10-12.5 ka calBP ('Younger Dryas plateau') and around 13.8-15 ka calBP ('Older Dryas plateau'; Kitagawa and van der Plicht, 1998).

When comparing ^{14}C and OSL ages, not only the above-mentioned factors of uncertainty should be taken into account, but it should also be borne in mind that different types of material are being dating using the two techniques. The ^{14}C and OSL ages do generally not represent the same event. Nevertheless, a comparison is useful in order to assess the reliability of both datasets. In this study, the age information derived with OSL and radiocarbon dating is generally consistent. At Pulle (see Chapter 2), the average age of the drift sand samples (1.2 ± 0.1 ka) is younger than the radiocarbon ages of ca. 1.5 ka for wooden fragments found in the habitation level below them. At Arendonk (see Chapter 4), the peat layer yielded radiocarbon ages of ca. 13.9 – 12.8 ka, while the overlying sediments were OSL dated around 11.4 ± 0.8 ka (n=5). At Lutterzand (see Chapter 6), the Usselo layer was characterised by radiocarbon ages of ca. 12.4 ka and 13.0 ka. The over- and underlying OSL ages were 13.3 ± 1.0 ka and 13.9 ± 1.1 ka in profile 1 and 13.2 ± 1.1 ka and 14.8 ± 1.2 ka in profile 4, respectively. Only at Opgrimbie (see Chapter 3), a deviation was found between the optical ages of the lowermost sediment unit (overall average: 13.0 ± 0.8 ka; n=3) and the bulk radiocarbon age of the overlying sandy peat layer (15.2-14.5 ka calBP). Both problems with the OSL dating of the dune sands (e.g. unaccurate dose rate determination, post-depositional mixing) and with ^{14}C dating of peat bulk samples were proposed to explain this discrepancy, but it was concluded that the causes are not fully understood at present and should be further investigated. It was however pointed out that there were no sound reasons to doubt the accuracy of the OSL dataset. On the basis of the aforementioned comparison of radiocarbon and OSL measurements, it appears that the OSL ages do not systematically deviate from the radiocarbon ages. As there are no indications that the radiocarbon ages can be seen as inaccurate, the OSL ages may be considered to be reliable as well. This conclusion is in line with the studies by Murray and Olley (2002) and Madsen and Murray (2009). These authors extensively reviewed OSL ages from a range of sedimentary environments, such as aeolian, fluvial/lacustrine, marine and glacio-fluvial/lacustrine, and found no evidence for systematic errors over a time period from the last century to at least 350 ka. It is however pointed out that – because of the general lack of suitable organic matter within the NW European coversands – the radiocarbon dataset used for comparison is relatively small. To draw final conclusions concerning the accuracy of OSL ages, a more elaborate comparison should be carried out, not

only with radiocarbon dating, but also with other chronological tools that are applicable to the Late Quaternary.

7.4. REGIONAL CHRONOLOGY FOR THE LATE WEICHSELIAN TO HOLOCENE SANDS

The optical ages determined during this research can be compared with those previously obtained at some other sites in N Belgium and The Netherlands (see summary in Table 7.1 and in Figs. 7.1 and 7.2). The ages are assembled according to the sedimentological units that have been distinguished at Lutterzand (see Chapter 6) and their relation to the lithostratigraphy defined by Van der Hammen and Wijmstra (1971). At some localities, there are no lithostratigraphic marker horizons that allow assigning a certain sediment to one of the generally used lithostratigraphic horizons (e.g. the coversands below the habitation level at Pulle; see Chapter 2). This complicates the comparison of its OSL ages with other geochronological information. For the fluvio-aeolian sands below the Beuningen Gravel Bed, ages have been obtained between 14.3 ± 1.1 ka and 22.6 ± 1.7 ka at Rotem (NE Belgium), between 17.2 ± 1.2 ka and 23.7 ± 1.7 ka at Grubbenvorst (SE Netherlands) and between 19.9 ± 1.6 and 25.2 ± 1.9 ka at Lutterzand (E Netherlands). At Lutterzand, fluvial sediments of the Beuningen Gravel Bed– with OSL ages between 16.1 ± 1.3 ka and 23.4 ± 1.9 ka – covered these sands; this might have been the case at the other localities also, but then this unit has been completely removed during the subsequent aeolian deflation phase. In any case, within the total uncertainties associated with the OSL ages (~8-10%), it appears that this unit was more or less deposited simultaneously at the investigated sites in Belgium and The Netherlands. At Heidebos (N Belgium) and Pulle (NE Belgium), the lowermost sediment unit does not have a clear lithostratigraphic interpretation, i.e. it could belong to Unit A or Unit B. Ages of 15.5 ± 1.1 and 17.3 ± 1.3 ka (Heidebos) and of 15.1 ± 1.4 ka and 17.7 ± 1.6 ka (Pulle) have been obtained. For the lower part of Unit B (below the widespread Usselo soil), ages have been determined at Heidebos (N Belgium) between ca. 12.4 ± 1.1 ka and 13.3 ± 0.9 ka (or perhaps 17.3 ± 1.3 ka; see above), at Arendonk (NE Belgium) between 13.0 ± 1.0 ka and 16.2 ± 1.4 ka, at Lommel (NE Belgium) between 12.4 ± 0.9 ka and 15.3 ± 1.1 ka, at Rotem (E Belgium) between 15.1 ± 1.1 ka and 16.5 ± 1.3 ka, at Ossendrecht (S Netherlands) between 14.6 ± 0.9 ka and 15.3 ± 0.9 ka, at Grubbenvorst (SE Netherlands) between 12.7 ± 0.9 ka and 16.3 ± 1.1 ka and at Lutterzand (E Netherlands) between 12.3 ± 1.0 ka and 15.8 ± 1.4 ka.

Unit	Lutterzand (1)	Lutterzand (2)	Grubben-vorst (3)	Ossen-drecht (4)	Defensiedijk (5)	Pulle (6)	Arendonk (7,8)	Lommel (8)	Rotem (9)	Opgrimbie (10)	Heidebos (11)
C	0.60 ± 0.1	0.31 ± 0.02			0.082 ± 0.008	1.2 ± 0.1					
C		0.30 ± 0.02			0.10 ± 0.01	1.2 ± 0.1					
C		0.29 ± 0.02			0.09 ± 0.01	1.2 ± 0.1					
C		0.40 ± 0.04			0.35 ± 0.03	1.2 ± 0.1					
C		0.21 ± 0.02			0.59 ± 0.05	1.3 ± 0.1					
C		0.20 ± 0.02			0.67 ± 0.06	1.3 ± 0.1					
C		0.21 ± 0.02			1.3 ± 0.1	1.3 ± 0.1					
C		0.35 ± 0.03			5.8 ± 0.5						
C					4.7 ± 0.4						
C					9.2 ± 0.8						
B (YCII)	13.27 ± 0.9	12.2 ± 0.9	13.8 ± 1.0	12.2 ± 0.7			13.0 ± 1.0	12.0 ± 0.9			12.6 ± 1.2
B (YCII)	11.72 ± 1.5	13.3 ± 1.0		13.1 ± 0.9			12.7 ± 1.0	11.6 ± 0.8			11.9 ± 1.1
B (YCII)		12.3 ± 1.0		11.5 ± 0.7			11.1 ± 0.8	11.7 ± 0.8			12.4 ± 1.1
B (YCII)		13.6 ± 1.1					11.1 ± 0.8	12.3 ± 0.8			
B (YCII)		13.2 ± 1.1					11.8 ± 0.9	11.0 ± 0.7			
B (YCII)							11.4 ± 0.8	11.5 ± 0.8			
B (YCII)							12.8 ± 1.1				
B (YCII)							11.7 ± 0.9				
B (Usselo)	13.6 ± 1.0						15.2 ± 1.3	10.6 ± 0.7			
B (Usselo)								12.4 ± 0.9			
B (YCI - OCII)		13.9 ± 1.1	12.7 ± 0.9	14.6 ± 0.9			16.1 ± 1.3	13.3 ± 1.0	15.5 ± 1.2	13.1 ± 1.0	12.4 ± 1.1
B (YCI - OCII)		13.8 ± 1.1	14.1 ± 1.0	15.3 ± 0.9			16.2 ± 1.4	15.3 ± 1.1	15.1 ± 1.1	13.9 ± 1.2	12.5 ± 1.1
B (YCI - OCII)		13.0 ± 1.0	15.5 ± 1.0	14.6 ± 0.9			13.0 ± 1.0	12.4 ± 0.9	16.4 ± 1.2	13.0 ± 1.0	13.0 ± 1.1
B (YCI - OCII)		14.4 ± 1.6	15.4 ± 1.1				15.4 ± 1.2	14.0 ± 1.0	15.9 ± 1.2	12.3 ± 0.9	13.3 ± 0.9

Unit	Lutterzand (1)	Lutterzand (2)	Grubben-vorst (3)	Ossen-drecht (4)	Defensiedijk (5)	Pulle (6)	Arendonk (7,8)	Lommel (8,*)	Rotem (9)	Opgrimbie (10)	Heidebos (11)
B (YCI - OCII)		12.6 ± 1.0	16.3 ± 1.1				15.0 ± 1.2	13.7 ± 1.0	16.5 ± 1.3	12.9 ± 1.0	
B (YCI - OCII)		15.8 ± 1.4						14.5 ± 1.1		12.3 ± 0.9	
B (YCI - OCII)		12.7 ± 1.0						12.7 ± 0.9		12.2 ± 0.9	
B (YCI - OCII)								13.3 ± 0.9		13.0 ± 0.9	
B (YCI - OCII)										13.7 ± 1.0	12.1 ± 0.8
B (YCI - OCII)										13.7 ± 1.0	11.0 ± 0.8
B (YCI)		14.8 ± 1.2									
B (LLB)		15.7 ± 1.3									
B (LLB)		14.1 ± 1.2									
B (OCII)	17.55 ± 2.6	14.8 ± 1.2									
B (OCII)	16.08 ± 1.9	13.4 ± 1.0									
B (OCII)	13.90 ± 1.3	14.5 ± 1.1									
B (OCII)		13.3 ± 1.1									
B (OCII)		14.2 ± 1.1									
B (OCII)		14.5 ± 1.1									
B (OCII)		13.6 ± 1.0									
B (OCII)		15.0 ± 1.2									
B (OCII)		13.6 ± 1.1									
B (OCII)		13.7 ± 1.1									
B (OCII)		13.3 ± 1.0									
B (OCII)		12.3 ± 1.0									
B (OCII)		13.8 ± 1.1									
A (BGB)		20.7 ± 1.6									
A (BGB)		23.4 ± 1.9									

Unit	Lutterzand (1)	Lutterzand (2)	Grubbenvorst (3)	Ossendrecht (4)	Defensiedijk (5)	Pulle (6)	Arendonk (7,8)	Lommel (8)	Rotem (9)	Opgrimbie (10)	Heidebos (11)
A (BGB)		22.2 ± 1.8									
A (BGB)		16.1 ± 1.3									
A (BGB)		20.1 ± 1.5									
A (BGB)		20.2 ± 1.6									
A (OCI-OCII)						15.1 ± 1.4					15.5 ± 1.1
A (OCI-OCII)						17.7 ± 1.6					17.3 ± 1.3
A (OCI)	21.94 ± 0.1	22.4 ± 1.8	17.2 ± 1.2						22.6 ± 1.7		
A (OCI)		23.8 ± 2.0	19.8 ± 1.4						18.8 ± 1.5		
A (OCI)		23.0 ± 1.9	19.7 ± 1.4						18.4 ± 1.4		
A (OCI)		22.3 ± 1.8	19.4 ± 1.4						18.3 ± 1.4		
A (OCI)		19.9 ± 1.6	18.9 ± 1.3						14.3 ± 1.1		
A (OCI)		20.0 ± 1.5	23.5 ± 1.7						18.8 ± 1.3		
A (OCI)		22.0 ± 1.8	20.9 ± 1.5						16.7 ± 1.3		
A (OCI)		22.1 ± 1.8	21.8 ± 1.5						22.6 ± 1.7		
A (OCI)		24.5 ± 1.9	22.0 ± 1.6								
A (OCI)		25.2 ± 1.9	23.7 ± 1.7								
A (OCI)		23.3 ± 1.8	25.2 ± 2.0								
A (OCI)		22.1 ± 1.8									
A (OCI)		21.3 ± 1.6									

Table 7.1: Comparison of the optically stimulated luminescence ages obtained for some NW European coversand and drift sand sites by: (1) Bateman and Van Huissteden (1999); (2) Derese et al. (in prep.); (3) Kasse et al. (2007); (4) Vandenberghe et al. (2004); (5) Van Mourik et al. (2010); (6) Derese et al. (2010(a)); (7) Derese et al. (2011); (8) Derese et al. (in press); (9) Vandenberghe et al. (2009); (10) Derese et al. (2009); (11) Derese et al. (2010(b)). The subdivision between Units A, B and C is based on that made for the Lutterzand sections (see Chapter 6): Unit C comprises the drift sands, Unit B the aeolian sands overlying the Beuningen Gravel Bed and underlying the Holocene podzol (i.e. Younger Coversands (YC) I and II, Usselo Soil, Lower Loamy Bed (LLB) and Older Coversands (OC) II), and Unit A the Beuningen Gravel Bed (BGB) and underlying fluvio-aeolian sands (Older Coversands (OC) I).

The ages at Opgrimbie (E Belgium) have not been included in this comparison, as their lithostratigraphic interpretation is not clear. However, the OSL ages from the other sites show some variability, i.e. at Heidebos they might be slightly younger (if they were deposited from ca. 13.3 ka onwards), and at Rotem and Ossendrecht they might represent the lower part of the age range obtained at the other sites. Nevertheless, the ages obtained at different localities cannot be unequivocally considered as different on the basis of the optical ages. For the upper part of Unit B (above the Usselo horizon), the OSL ages show a great similarity at all investigated sites and span the time interval from ca. 11 to 13 ka. The drift sands (Unit C), on the other hand, appear to have been deposited during very distinct periods of time. At Defensiedijk (S Netherlands), several phases of sand-drifting have been identified in the time interval between 0.082 ± 0.008 ka and 9.2 ± 0.8 ka. At Pulle (NE Belgium), the sand-drifting took place around 1.2 ± 0.1 ka and, at Lutterzand (E Netherlands), between 0.20 ± 0.02 ka and 0.40 ± 0.04 ka (0.60 ± 0.1 ka, according to Bateman and Van Huissteden, 1999).

The age differences between the phases of sand-drifting at different sites can be explained by the fact that they are thought to be caused mainly by anthropogenic processes (deforestation) or perhaps local climatic or environmental factors, and not by regional climatic and environmental changes. As shown before, the ages of the different coversand units seem to be generally in agreement and a distinction between the sedimentation processes in the Belgian and Dutch coversand regions cannot be made on the basis of OSL ages. The age information obtained here suggests the occurrence of regional phases of aeolian activity during the past ~25 ka in the NW European lowlands. It should be pointed out that this observation may be due to the limits on the resolution of the OSL dating technique (see section 7.2). The sedimentary profiles show that local differences in e.g. geomorphology, vegetation density and hydrology have influenced the accumulation and preservation of sediments and intercalated soil horizons at a certain site, and it is therefore most likely that the resulting

sediment units have distinct ages. The latter was also concluded by Kolstrup (2007) on the basis of pollen analyses and radiocarbon dating at a number of coversand sites in NW Europe. She states that localities with accumulation and preservation of both organic material and coversand represent locally moist/wet conditions. This agrees with the observations done in this thesis: at Arendonk-*Korhaan* (see Chapter 4), for instance, the transition between a bleached Usselo horizon and a (> 0.5 m) thick peat layer appears to be related to the difference in elevation and presence of moisture (i.e. top of the sand ridge, as opposed to the wet depression at the base of the ridge, respectively). At Lommel-*Maatheide* (see Chapter 4), a similar transition between a bleached and a peaty horizon has been observed. The investigated section is however located on a nearly flat area, and both the bleached horizon and the peat seem to have developed and preserved in moist conditions.

Based on the OSL dataset, four main phases of (fluvio-)aeolian deposition can be distinguished in Belgium and the Netherlands, during the Late Pleniglacial, the pre-Allerød Late Glacial, the Late Dryas and the Late Holocene, respectively. The sedimentation rate during these four phases was clearly different. During the Late Pleniglacial, the sedimentation was generally gradual. At Lutterzand (see Chapter 6), for example, about 2 m of sediment was deposited in the course of ~5 ka. During the Late Glacial and the Late Dryas, sedimentation events could be recognised (see also above): at Lutterzand, deposition of the Older Coversand II (reaching thicknesses of ~3 m) took place around ~13.8 ka and of Younger Coversand II (up to 1.5 m thick) around ~12.9 ka. The drift-sands are most rapidly deposited. At Lutterzand ~2 m of drift-sand has accumulated in the course of ~0.2 ka.

The first phase, roughly dated between 25 and 17 ka, was characterised by extensive fluvio-aeolian sedimentation. The sediments are often characterised by the presence of indistinct horizontal bedding of fine sand with an alternation of silty laminae and lenses of coarse sand, small-scale current ripple lamination and clayey-silty drapes indicative of fluvial deposition. They frequently bear traces of cryoturbation and other periglacial phenomena, such as a crinkly or wavy appearance, massive bedding, ice-wedge casts and vertical platy structures (Kasse, 2002). According to Kasse (2002), this type of sediment is usually restricted to valleys. So far, this seems to be consistent with the results of optically stimulated luminescence (Table 7.1), which point to the occurrence of sediments from this first phase of aeolian activity at Lutterzand, Grubbenvorst and Rotem, all situated in a valley context (of the Dinkel and the Meuse, respectively). At the other investigated sites, these sediments are either not present or not yet sampled for optically stimulated luminescence; this needs to be further

investigated. The end of the Late Pleniglacial was marked by a phase dominated by permafrost degradation, shallow channelling and aeolian deflation in a desert environment, associated with the formation of the Beuningen Gravel Bed (BGB). The latter is a widespread lithostratigraphic marker horizon in the NW European lowlands (see e.g. Van Huissteden, 1990). According to Kolstrup (1980), the BGB acknowledged a two-phase development, with a first phase dominated by fluvial activity, and a second phase characterised by strong wind activity due to the increased drought. Kasse et al. (2007) questioned this hypothesis and pointed out that (1) the 'fluvial' phase is often not present, and (2) desert environments can be characterised by ephemeral fluvial activity during (rare) storm events. In this research, the fluvial part of the BGB was only discerned in two exposures along the Dinkel river (Lutterzand) and was there dated between ~16 and 23 ka. The period of permafrost degradation, deflation and formation of the BGB was constrained between ~17 and 15 ka at Grubbenvorst (Kasse et al., 2007), between ~18 and 16 ka at Rotem (Vandenberghe et al., 2009) and between ~20 to 13 ka at Lutterzand, for those profiles where the fluvial phase is not present (~22 to 17 ka, according to Bateman and Van Huissteden, 1999). Where the fluvial phase is present (at Lutterzand), the deflation phase could be more stringently bracketed between ~16 and 14 ka. The difference in time boundaries for the Beuningen Gravel Bed appears to indicate that local environmental conditions seem to have had an influence on the accumulation and preservation potential of the sediments under- and overlying the BGB. In this research, it was also suggested that part of the deflated sand may have accumulated in N Belgium, where it formed the basal part of a prominent geomorphological feature, known as the Maldegem-Stekene coversand ridge.

The second phase of aeolian activity yielded OSL ages between ca. 17 and 13 ka, depending on the locality. The sediments are usually characterised by alternating bedding of fine sand and silty sand, as a result of deposition and adhesion of sediment on an alternating dry and wet surface (Schwan, 1986; Kasse, 2002). The lamination can usually be followed over considerable distances, suggesting that these sediments "covered" the pre-existing morphology (hence "coversands"). They do not show any periglacial features.

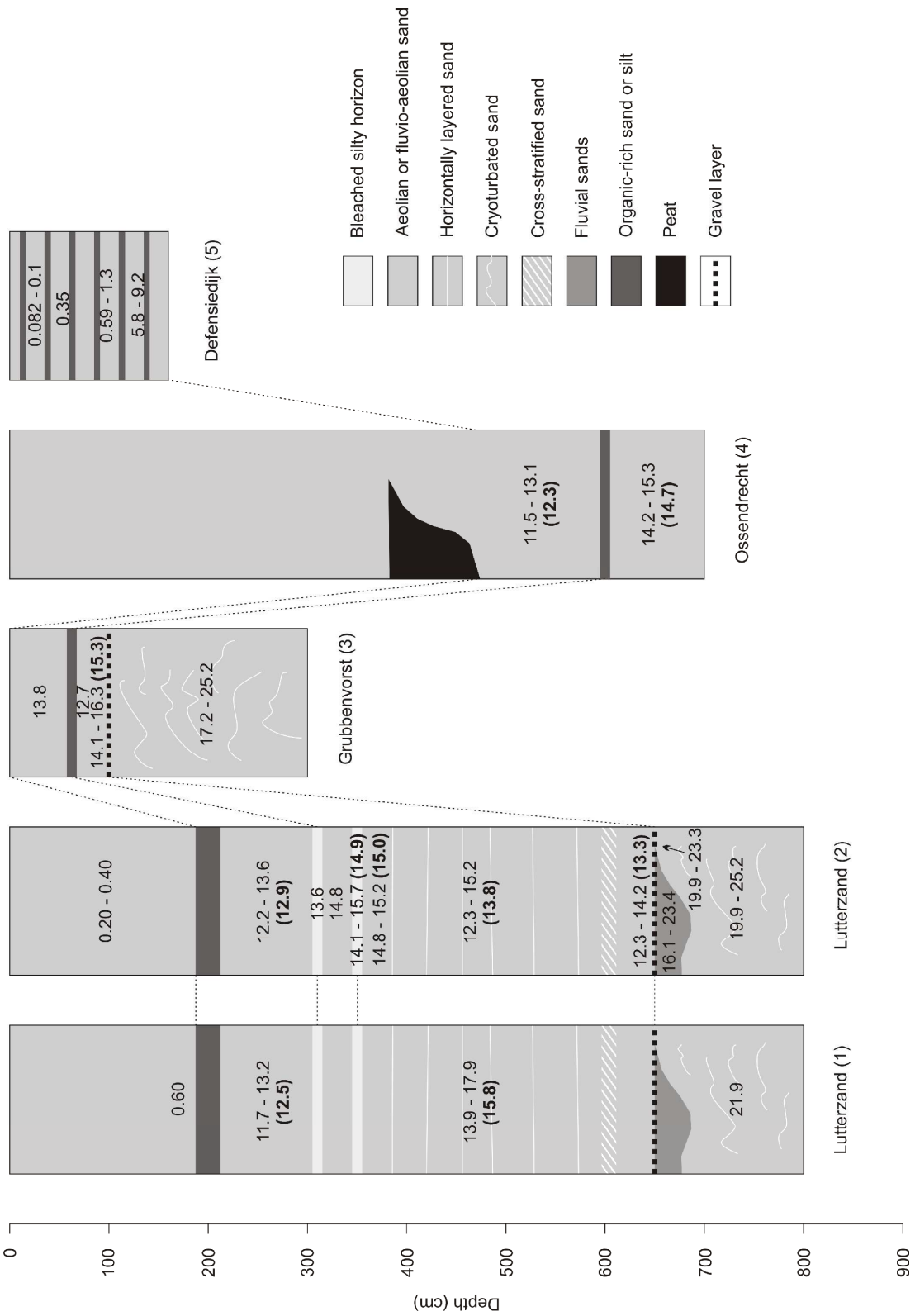

Figure 7.1: Simplified sedimentary profiles and age ranges (average ages between brackets, when applicable) for the coversand sites dated with OSL in the Netherlands. The OSL have been determined by (1) Bateman and Van Huissteden (1999); (2) Derese et al. (in prep.); (3) Kasse et al. (2007); (4) Vandenberghe et al. (2004); and (5) Van Mourik et al. (2010). All depths are indicated in cm below ground level.

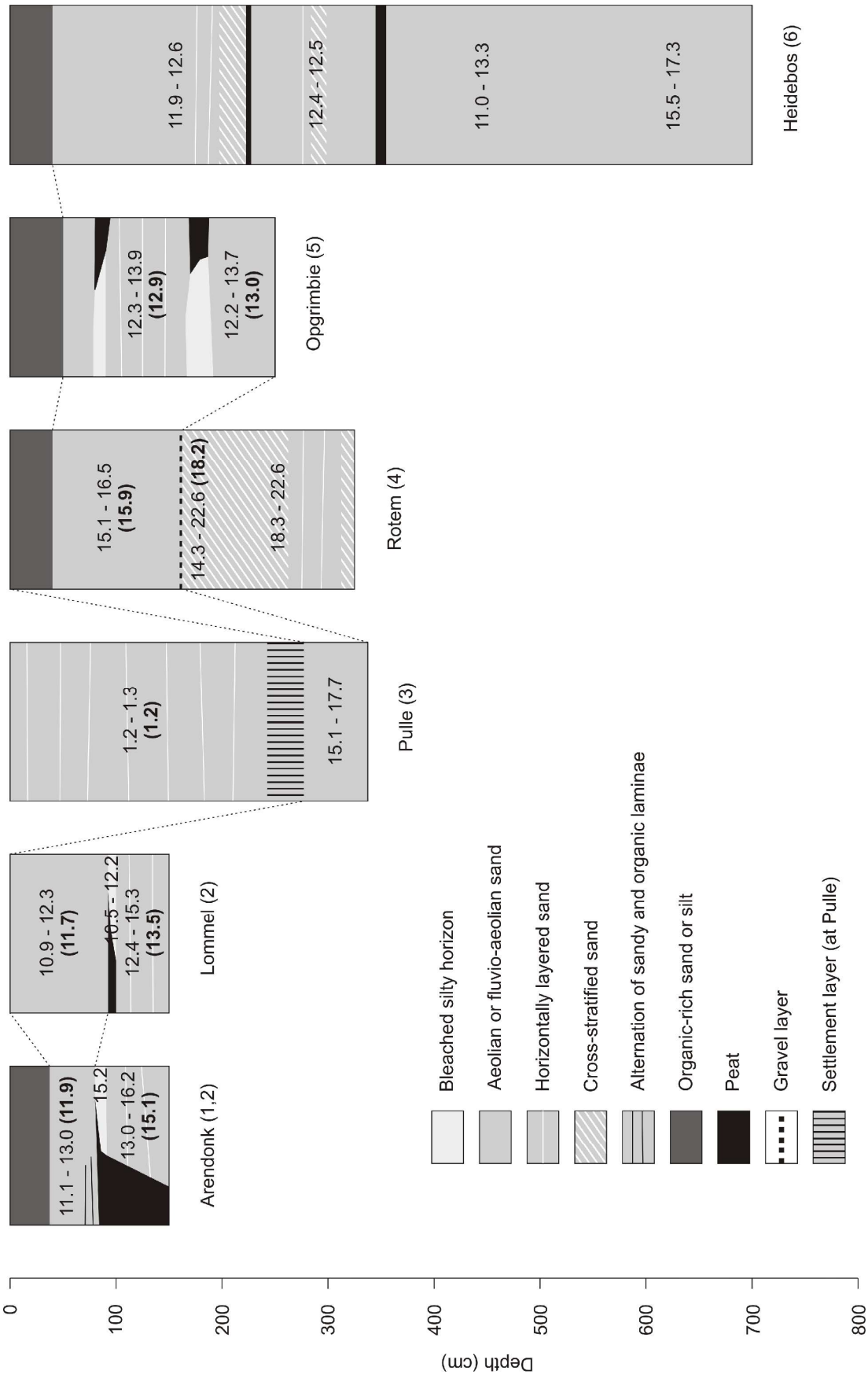
Arendonk (1,2)
11.1 - 13.0 (11.9)
15.2
13.0 - 16.2 (15.1)
Lommel (2)
10.9 - 12.3 (11.7)
10.5 - 12.2
12.4 - 15.3 (13.5)
Pulle (3)
1.2 - 1.3 (1.2)
15.1 - 17.7
Rotem (4)
15.1 - 16.5 (15.9)
14.3 - 22.6 (18.2)
18.3 - 22.6
Opgrimbie (5)
12.3 - 13.9 (12.9)
12.2 - 13.7 (13.0)
Heidebos (6)
11.9 - 12.6
12.4 - 12.5
11.0 - 13.3
15.5 - 17.3
Bleached silty horizon
Aeolian or fluvio-aeolian sand
Horizontally layered sand
Cross-stratified sand
Alternation of sandy and organic laminae
Organic-rich sand or silt
Peat
Gravel layer
Settlement layer (at Pulle)
Depth (cm)
0
100
200
300
400
500
600
700
800

Figure 7.2: Simplified sedimentary profiles and age ranges (average ages between brackets, when applicable) for the coversand sites dated with OSL in N Belgium. The OSL have been determined by (1) Derese et al. (2011); (2) Derese et al. (in press); (3) Derese et al. (2010(a)) (4) Vandenberghe et al. (2009); (5) Derese et al. (2009); and (6) Derese et al. (2010(b)). All depths are indicated in cm below ground level.

It is striking that, despite the pronounced climatic oscillations during the Late Glacial, the OSL datasets do not seem to point to clear breaks in the aeolian sedimentation. As it has been stated in the above, local breaks in sedimentation could be masked by the large uncertainties associated with the OSL ages. However, the OSL data could also point to semi-continuous aeolian activity throughout this period. This is in agreement with the suggestion of Kasse (1997; 2002) that aeolian deposition continued during the Bølling interstadial, although perhaps with a decreased intensity. Both Hoek (2001) and Kasse et al. (2007) suggested that the persistence of aeolian activity around 14.7 ka was related to the delayed response of the vegetation, as a result of the relatively slow and discontinuous migration of the plants to the periglacial zone, the lack of available nutrients and soils, and the occurrence of deep seasonal frost and strong winds at the onset of the Late Glacial. A decrease of the aeolian activity, resulting in loam deposition or peat formation, could only occur in local wet environments (e.g. seepage zones, wet depressions; Kasse, 2002; Kasse et al., 2007).

During the Allerød interstadial, the aeolian activity appears to have stopped at many locations within the NW European lowlands. Bleached Usselo horizons and peat layers dating from this period are found at e.g. Ossendrecht, Grubbenvorst, Opgrimbie, Arendonk, Lommel and Lutterzand. At the latter three sites, the quartz from the bleached horizon was dated between ca. 15 and 11 ka. The interpretation of these age results is difficult, as they may relate to the age of the sediments in which the Usselo horizon developed, to the soil development itself or to any time in between (in the case of incomplete bleaching during post-depositional mixing; see e.g. Kaiser et al., 2009). Radiocarbon dating is not always an alternative to OSL dating for the bleached horizons. Firstly, suitable organic matter cannot always be found within these horizons, and secondly, the organic fragments may be recent, assimilated in the horizon by bioturbation. Hence, the most reliable ages for the bleached horizon can be obtained by (1) radiocarbon dating the adjacent peat layers, where present (e.g. Lommel, Arendonk) and (2) OSL dating the over- and underlying deposits. The OSL time boundaries of this horizon are generally thought to provide a good estimate of the timing and duration of the landscape stabilisation and soil development. They vary between the different localities: at Lutterzand the Usselo horizon was dated between ~13.8 ka and 12.9 ka (see Chapter 6), at Grubbenvorst

between ~12.7 ka and 13.8 ka (Kasse et al., 2007), at Ossendrecht between ~14.7 ka and 12.3 ka (Vandenberghe et al., 2004), at Arendonk-*Korhaan* between ~15.1 ka and 12.8 ka (see Chapter 4) and at Lommel-*Maatheide* between ~13.5 ka and 11.3 ka (see Chapter 4). This is either due to the fact that the sediments under- and overlying the Usselo horizon were not deposited at the exact same time or because the soil horizons did not develop synchronously. In this respect, Kolstrup (2007) questions the classic assumption of a stillstand in aeolian deposition during the Allerød and the synchronism of the peat layers and bleached horizons. Both in Denmark and in the UK, 'Allerød' peat horizons were found to be of both Allerød and Late Dryas age. Kolstrup (2007) therefore suggests that areas with a discontinuous vegetation cover must have existed contemporaneously with more densely vegetated areas.

According to the OSL results, the third phase of aeolian sedimentation took place between ~13 and 11 ka. The deposited sands are characterised by horizontal to low-angle bedding that is probably related to the formation of low dunes. According to Kolstrup (2007), the sands usually have a local origin. Sediments from this period are found in most investigated localities and can reach considerable thicknesses (more than 2 m at Heidebos, Arendonk and Lommel). The optical ages indicate that they seem to form the bulk part of sand ridges in N Belgium (e.g. at Heidebos, Arendonk and Lommel). From the OSL datasets, it cannot be unequivocally concluded whether or not the aeolian activity continued into the Holocene. First of all, the top of Late Glacial profiles was generally not sampled because: (1) a Holocene podzolic soil had developed in the top of the sediments and this development was probably associated with bioturbation, (2) the top of the Late Glacial sediments was missing as a result of later sand-drifting events, or (3) the top was situated at surface level and was not sampled in order to avoid having to take into account the soft component of the cosmic radiation. Secondly, the resolution of quartz SAR-OSL dating does not allow establishing whether sediments were deposited at the end of the Late Dryas or at the beginning of the Holocene. Both Kasse (2002) and Kolstrup (2007) however suggest that aeolian sedimentation, perhaps locally, may have continued during the Early Holocene, until the vegetation cover was sufficiently dense to prevent deflation.

During the Late Holocene, a final phase of sand transportation and deposition took place. Unlike the other phases of aeolian activity, which seem to have had a regional importance on the basis of the OSL results and have been related to climatic changes, this phase of so-called sand-drifting had a local origin, i.e. it is generally ascribed to deforestation of the coversand

landscape by man. It is difficult to assess whether the climate had an influence on sand-drifting as well. The timing and duration of the sand-drifting differed from place to place (Table 7.1, and Figs. 7.1 and 7.2). Although it is generally assumed that major sand-drifting events in the NW European lowlands started in the 10^{th}-12^{th} century (Castel et al., 1989; Koster et al., 1993), the OSL ages indicate that sand-drifting may have occurred during earlier times as well. At Pulle, ages of ~1.2 – 1.3 ka were obtained for a more than 2 m high drift-sand dune (see Chapter 2). At Defensiedijk, three different phases of drift-sand formation have been distinguished, around 5 – 4.5 ka, around 1.2 – 0.35 ka and from 0.1 ka to present (van Mourik et al., 2010). At both Defensiedijk and Lutterzand, the OSL ages indicate that sand-drifting events took place until very recently.

7.5. CONCLUSIONS

In this PhD thesis we have investigated how quartz SAR-OSL dating can contribute to establishing an absolute chronological framework for the (Late) Weichselian to Holocene fluvio-aeolian and aeolian sandy deposits in N Belgium and The Netherlands. In connection to this, it was also shown to which extent the dating method can provide useful time information with respect to the reconstruction of changes in the sedimentary environments in relation to palaeoclimatic changes and human settlement dynamics.

In our study we have pointed out some of the limitations of the dating method for application on Late Weichselian and Holocene sandy sediments. First of all, the OSL datasets are marked by a certain degree of variability that is sometimes larger than expected from the individual uncertainties on the OSL ages. This shows that conclusions concerning the depositional age of a certain sediment unit should not be based on a single OSL age estimate for this unit, and that, as a consequence, a correlation based on single age determinations obtained for separate sites may be largely erroneous. Indeed, the results of this thesis illustrate the importance of obtaining multiple age estimates per sedimentary unit, thereby bearing in mind that there is no point in analysing samples that are too closely spaced to be resolved in time by the dating technique. The relative precision associated with quartz SAR-OSL dating is in the range of 8-10% of the OSL age. This limits the possibility to unequivocally distinguish phases of sediment deposition and phases of landscape stabilisation and vegetation growth during the timeframe investigated in this thesis, because either these phases may have a local character (e.g. the fluvial part of the Beuningen Gravel Bed from the Late Pleniglacial, and the Lower

Loamy Bed or organics from the Bølling interstadial) or a relatively too short duration in comparison to the uncertainties on the OSL ages (e.g. the Usselo Soil from the Allerød interstadial). In addition, bioturbation may have disturbed the sediments (e.g. at Rotem and at Defensiedijk; van Mourik et al., 2010; Vandenberghe et al., 2009). Therefore, the most reliable and detailed chronologies are obtained when OSL age information is combined with independent information from e.g. radiocarbon dating, lithostratigraphy and pollen analyses. An asset of OSL dating for Quaternary geochronology is that the technique allows directly determining the time of sediment deposition and therefore sedimentation rates. As a result, it allows recognising gradual semi-continuous sedimentation, as opposed to episodic sediment deposition.

Further advances can be made on the luminescence dating technique in terms of precision, for instance by addressing the causes of the variability that characterises the OSL datasets, and of accuracy, for example by further investigating the effects of bioturbation or by making an extensive comparison with radiocarbon dating and other time indicators, taking into account all of their associated uncertainties. In order to draw more definite conclusions concerning the influence of regional climatic and environmental changes and the impact of human activities on the NW European coversand belt landscape, more sites need to be investigated using OSL dating in combination with other relative and absolute chronologic methods and proxy indicators. Furthermore, the optical dates presented in this thesis could be used in statistical analysis to more accurately determine sedimentation rates, internal consistency of the datasets and duration of phases with aeolian activity. In general, however, it can be concluded from this research that, notwithstanding its limitations, quartz SAR-OSL dating is a useful tool for establishing an absolute chronological framework for the Late Weichselian coversands and Holocene drift-sands in the NW European lowlands.

Summary - Samenvatting

SUMMARY

Optically stimulated luminescence (OSL, or optical) dating is a reliable dating method that is increasingly applied in Quaternary studies. The technique determines when sediments were last exposed to sunlight. The major advantages of optical dating over other Quaternary dating methods, such as radiocarbon dating, are that it allows determining direct ages for the mineral components of the sediments (quartz, feldspar) and that it does not require calibration to yield ages in calendar years. In the Ghent Luminescence Laboratory, optical dating was introduced about a decade ago and first applied to quartz extracts from cover- and drift-sands in the southern Netherlands (Ossendrecht, Grubbenvorst, Defensiedijk). Since then, our laboratory successfully dated samples from a variety of sedimentary context (e.g. aeolian, fluvial) all over the world, generally in the frame of multidisciplinary research projects combining geological, sedimentological, geoarchaeological and other data.
In this research project, the potential of OSL for dating Late Weichselian to Holocene fluvio-aeolian and aeolian sands was further investigated. On the basis of dating results from six sites in N Belgium and The Netherlands, including the classic type locality for the Late Weichselian lithostratigraphy in NW Europe at Lutterzand (E Netherlands), a chronological framework was established for the changes in the physical landscape over the past ~25 ka.

Optical ages are calculated by simply dividing two parameters: (1) the equivalent dose, or the total dose of energy from nuclear radiation that is absorbed by mineral grains since they were last exposed to sunlight, and (2) the dose rate, or the rate of energy absorption through time. In this PhD thesis, use was made of the single-aliquot regenerative-dose (SAR) measurement protocol to coarse (125-180 µm and 180-212µm) quartz grains to determine the equivalent dose. Several tests were carried out to evaluate whether the applied SAR procedure was suitable for measuring equivalent doses in our samples, i.e. to check the luminescence characteristics of our samples. The dose rate was obtained using high-resolution low-background gamma-ray spectrometry in the laboratory.

A first application of quartz SAR-OSL dating concerned a drift-sand dune at an archaeological site near Pulle (N Belgium). There, exploratory archaeological trenching resulted in the discovery of a dense spread of building structures and ceramics indicating human occupation during the Iron Age and Early Middle Ages (roughly from the 6th to the 1st

century BC and from the 6th to the 9th century AD, respectively). The remains were partly covered by a ~2.5 m high drift-sand dune, suggesting that the accumulation of these aeolian deposits resulted in the deterioration of the living conditions and eventually in the abandonment of the site. OSL dating was carried out to deliver information concerning the onset and rate (or periodicity) of the sand-drifting, as this could contribute significantly to the understanding of the occupational history of the site.

The sands underlying the settlement level were dated at 15.1 ± 1.4 ka and 17.7 ± 1.6 ka, indicating that the settlement was located on a sequence of coversands deposited during the Weichselian Late Pleniglacial. The optical ages for the drift-sand dune varied between 1.2 ± 0.1 ka and 1.3 ± 0.1 ka (overall average: 1.2 ± 1.0 ka; n=7); these ages are in agreement with the radiocarbon dates of the wooden shuttering of two wells from the underlying settlement level (AD 430-600, AD 640-780 and AD 770-900). It was concluded that sand-drifting occurred during a single, fairly short event in the Early Middle Ages. As no archaeological evidence from the post-sand-drifting period was found, it is most likely that the sand-drifting put an end to the human occupation at Pulle.

A second application focussed on the dune complex at Opgrimbie (NE Belgium). A previous study using sedimentology, palynology and radiocarbon dating had indicated the presence of both Bølling and Allerød peat at the site, laterally grading into bleached layers. As Bølling organics and soils are generally lacking within the aeolian sequences in the NW European lowlands, this site was considered as a type section for the aeolian sand deposition in NW Europe. The original study however did not provide direct ages for the sediment units. The site was therefore reinvestigated in the frame of this PhD project.

Quartz SAR-OSL dating yielded average ages of 12.9 ± 0.9 ka (n=6) and 13.0 ± 0.8 ka (n=3) for the dune sands over- and underlying the lowermost bleached horizon of presumed Bølling age, respectively. The age of 12.9 ± 0.9 ka is in agreement with the previously determined bulk radiocarbon age of 14.0-13.6 ka calBP and with the recently determined AMS radiocarbon ages of 13.9-13.7 ka calBP and 13.2-13.0 ka calBP for the overlying peat / bleached horizon. However, the OSL age of 13.0 ± 0.8 ka is significantly younger than the bulk ^{14}C age of 15.2-14.5 ka calBP for the overlying sandy peat. A study of the parameters influencing the OSL ages, e.g. time-averaged moisture content, internal dose and post-depositional mixing of the sediments, showed that none of them were able to cause the OSL ages to be significantly and systematically in error. Hence it was suggested that the bulk ^{14}C age could be inaccurate. On the basis of the optical age results, it was concluded that the two

bleached horizons may belong to a single soil complex that formed during the Allerød interstadial. It follows that a significant part of the dune sequence may have accumulated subsequent to the Bølling period and that the dune complex at Opgrimbie possibly can not longer be retained as a key sequence for the Late Glacial in the southernmost part of the NW European coversand belt. At the very least, the OSL and AMS results point to significant aeolian deposition and fairly rapid sand accumulation during the pre-Allerød period of the Late Glacial.

The archaeological sites of Arendonk-*Korhaan* and Lommel-*Maatheide* (NE Belgium) are characterised by sandy sequences in which the Final Palaeolithic and Early Mesolithic settlement phases are stratigraphically separated. As such, they offer a unique means to study the possible relation between human occupation patterns and environmental changes during the Weichselian-Holocene transition in the Campine region. The chronological framework was provided by quartz SAR-OSL dating.

Both sites present a similar stratigraphy, consisting of two sandy units (Unit 1 and 3) and an intercalated bleached horizon (Unit 2) laterally grading into a peat layer. Unit 1 yielded optical ages between 16.2 ± 1.4 ka and 13.0 ± 1.0 ka at Arendonk-*Korhaan* and between 15.3 ± 1.1 ka and 12.4 ± 0.9 ka at Lommel-*Maatheide*. The bleached clastic horizon (Unit 2) was dated to 15.2 ± 1.3 ka at Arendonk-*Korhaan* and to 12.4 ± 0.9 ka and 10.6 ± 0.7 ka at Lommel-*Maatheide*. The time boundaries for this Unit 2 are considered to be more reliable than the direct ages and are between 15.1 ± 1.1 ka (n=5) and 12.8 ± 1.0 ka (n=2) at Arendonk-*Korhaan* and between 13.5 ± 0.9 ka (n=4) and 11.3 ± 0.8 ka (n=2) at Lommel-*Maatheide*. For Unit 3, ages between 12.3 ± 0.8 ka and 11.0 ± 0.7 ka were obtained at Lommel-*Maatheide* and between 13.0 ± 1.0 ka and 11.1 ± 0.8 ka at Arendonk-*Korhaan*. The SAR-OSL results indicate that aeolian sedimentation at Arendonk-*Korhaan* was already going on during the Late Pleniglacial and continued across the Late Pleniglacial/Late Glacial boundary. At Lommel-*Maatheide*, it cannot be excluded that sand deposition was confined to the Late Glacial. At none of both sites, there are clear indications in the lithostratigraphic and chronological record that the aeolian activity was interrupted prior to the Allerød interstadial. The decreasing aeolian activity during the Allerød promoted the development of a bleached horizon, i.e. the Usselo horizon, and an adjacent peat layer. Aeolian sand deposition resumed during the Late Dryas and eventually stopped during the Holocene, mainly as a result of the expansion of the vegetation cover. From the OSL ages, it was concluded that human settlement at both sites was presumably constrained to phases of landscape stability, i.e.

periods without strong aeolian activity such as the Allerød interstadial and the Early Holocene. There appears to have been a clear interaction between the human occupation patterns and the changes in the environmental context.

A last application of OSL dating in N Belgium dealt with a sedimentary core taken at the locality of Heidebos, near the top of the Maldegem-Stekene coversand ridge and to the north of a large Late Glacial palaeolake known as the 'Moervaart depression'. The area around the Moervaart depression including the coversand ridge is considered as a key-site for human occupation during the Late Glacial and the Early Holocene owing to the many sites and site-complexes along the borders of the lake and on the coversand ridge. The area was studied to reconstruct the evolution of the former landscape, and the interaction between past human societies and their natural environment.
In the core, consisted of ~7 m laminated and massive sands intercalated by several organic layers and capped by a podzol, samples for OSL dating were taken above and below lithological contacts. From the OSL dataset, with ages between 17.3 ± 1.3 ka and 11.0 ± 0.8 ka, it could not be unequivocally concluded whether the coversand ridge developed during (at least) two distinct phases of aeolian activity, one during the Late Pleniglacial (around 16.3 ka) and one during the Late Dryas (around 12.3 ka), or as a result of semi-continuous coversand deposition from the final phase of the Late Pleniglacial until the Late Dryas or perhaps the Holocene. The average age of 16.3 ± 1.1 ka (n=2) for the lowermost 1 m of sediment matches the age bracket for the Beuningen Gravel Bed, a widespread lithostratigraphic marker horizon within the NW European coversand sequences that is generally correlated with a large-scale deflation event at the end of the Late Pleniglacial. It is therefore suggested that this sandy unit may represent the time-equivalent of the gravel bed. The bulk of the coversand ridge was probably deposited during the Allerød interstadial and/or the Late Dryas stadial. During the Allerød interstadial, the palaeolake to the south of the coversand ridge reached its maximum extension; this may have favoured human settlement in the area despite the possible continuation of aeolian activity at that time. At some stage during the Allerød and/or Late Dryas, the sand deposition intensified dramatically; simultaneously the palaeolake started to dry out. Probably these events had a considerable impact on human life so that the area was abandoned until the Early Holocene.

The last application of quartz SAR-OSL dating in this thesis concerned the classic type locality for the Late Weichselian lithostratigraphy in the NW European coversand belt at

Lutterzand (E Netherlands). There, natural exposures along the Dinkel river comprise the following sedimentary sequence, which is thought to reflect the rapid climatic and environmental changes during the Late Weichselian and the Late Weichselian-Holocene transition: Older Coversand I, Beuningen Gravel Bed, Older Coversand II, Lower Loamy Bed, Younger Coversand I, Usselo Soil and Younger Coversand II. At some point during the (Late) Holocene, the area underwent sand-drifting. Four profiles were sampled into detail, resulting in a total of 57 samples for OSL dating.

Ages between 25.2 ± 0.7 ka and 0.20 ± 0.01 ka were obtained. The lowermost unit of cryoturbated fluvio-aeolian sands, formerly described as the Older Coversand I, was deposited from at least 25.2 ± 1.9 ka to 19.9 ± 1.6 ka during the final phase of the Late Pleniglacial. The overlying coarse-grained fluvial sands in the lower part of the Beuningen Gravel Bed, which occur discontinuously in the Lutterzand profiles and are thus considered to be deposited in local shallow channels, were dated between 23.4 ± 1.9 ka and 16.1 ± 1.3 ka. The desert pavement at the top of the Beuningen Gravel Bed is generally related to a phase of permafrost degradation and extensive aeolian deflation at the end of the Late Pleniglacial; at Lutterzand, this phase was most narrowly bracketed between 16.1 ± 1.3 ka and 13.8 ± 1.1 ka. A second period of aeolian activity, resulting in the deposition of sand sheets, took place between 15.8 ± 1.4 ka and 12.2 ± 0.9 ka. The optical ages thus indicate that the sedimentation occurred already during the final phase of the Late Pleniglacial and continued throughout the Late Glacial, also during the climatic amelioration around ~14.7 ka. It was only interrupted during short (interstadial) phases that can be distinguished in the lithostratigraphic record. These sediments were affected by sand-drifting. It has been suggested that natural river dunes already occurred during the Middle Holocene in the Lutterzand area and that the major expanse of inland dunes took place from the Middle Ages onwards. As OSL only allows dating the last depositional event, which appears to have taken place between 0.40 ± 0.04 ka and 0.20 ± 0.02 ka, this hypothesis cannot be verified. OSL dating however shows that sand-drifting continued until very recently in the area.

From the thesis research, it can be concluded that the fluvio-aeolian and aeolian sands in N Belgium and The Netherlands dispose of satisfactory luminescence characteristics. Moreover, they are generally well-bleached and not significantly affected by post-depositional mixing processes. Some variability is present within the obtained OSL datasets and its causes are not fully understood at present. It is suggested that the sands may be characterised by a larger heterogeneity in mineral composition and sedimentological characteristics than expected,

resulting in dose rate and thus optical age variations. Further research is required to confirm this. The optical ages are marked by total (1 σ) uncertainties of ~8-10%, in which the systematic uncertainty is generally dominant. Hence it is difficult to unequivocally distinguish between the different periods of the Late Glacial on the basis of OSL dating alone; it is more useful to combine OSL ages with lithostratigraphic evidence and independent age information. In comparison to, for example, radiocarbon dating (which determines ages of associated organic material), optical dating does allow calculating sedimentation rates and interpreting the depositional history of a certain sedimentary sequence in terms of semi-continuous gradual sedimentation and sedimentation 'events'. This however requires that multiple age estimates are obtained per sedimentary unit and thus illustrates the importance of applying a high-resolution sampling strategy.

In general, the OSL ages determined in the frame of this PhD research are in agreement with independent age information, taking into account the specific uncertainties associated with the different dating techniques. Based on the optical age results obtained in this thesis and previously at the same and equivalent sites in Belgium and The Netherlands, four main phases of (fluvio-)aeolian deposition can be differentiated:

From at least ~25 and 17 ka, a phase of fluvio-aeolian sedimentation took place under permafrost conditions, resulting in silty sands that are frequently marked by cryoturbation and other periglacial phenomena. So far, these sands have been mainly identified and dated in valley contexts (Grubbenvorst, Lutterzand). The end of the Late Pleniglacial is usually associated with a phase dominated by permafrost degradation, shallow channelling and aeolian deflation in a desert environment, resulting in the formation of the Beuningen Gravel Bed. The coarse-grained fluvial variant of this gravel bed has only been discerned in two profiles along the Dinkel river in this research, where it shows a discontinuous occurrence pointing to its local character. It was dated between ~23 and 16 ka. The phase of permafrost degradation, aeolian deflation and formation of the desert pavement was bracketed between ~16 and 14 ka. At other localities in the NW European lowlands, different time brackets were obtained, e.g. ~17 to 15 ka at Grubbenvorst and ~18 to 16 ka at Rotem. This shows that the accumulation and preservation potential of sediments at a certain site was probably influenced by local differences in - for instance - geomorphology, vegetation density and hydrology.

A second phase of aeolian activity was dated between ~17 and 13 ka and resulted in laminated fine sands to silty sands, as a result of deposition and adhesion of the sediments on an alternating dry and wet surface. The climatic amelioration around ~14.7 ka has not been

recognised in the lithostratigraphic record, indicating that it was not accompanied by a general stabilisation of the land surface in the NW European lowlands. The climatic improvement around ~14 ka however did result in landscape stability and the development of bleached soil horizons and peats. The clastic component of the bleached horizon was dated between ~15 and 11 ka, but the interpretation of these OSL dates is difficult as they may refer either to the age of the sediments in which the bleached horizon developed or to the timing of the soil development.

A third phase of aeolian deposition took place between ~13 and 11 ka. The resulting sands are characterised by horizontal to low-angle bedding that is probably related to the formation of low dunes. Due to the limited resolution of the OSL ages, it cannot be unequivocally concluded whether the aeolian sedimentation continued across the Late Glacial-Early Holocene boundary.

A final phase of sand transportation and deposition occurred during the Late Holocene and was of local importance, as it is related to deforestation of the coversand landscape by humans. The timing and duration of this sand-drifting period differed from place to place. In the southern Netherlands, several phases of sand-drifting were recognised, the first starting around 5 ka. In NE Belgium, a sand-drifting event occurred around 1.2 ka, and in the eastern Netherlands, sand-drifting went on until ~0.2 ka.

This research has illustrated how quartz SAR-OSL dating may contribute to establishing an accurate and robust chronological timeframe for the (fluvio-)aeolian deposition in Belgium and The Netherlands, and thus to reconstructing the changes in the sedimentary environments in relation to palaeoclimatic changes and human settlement dynamics. It has also indicated some of the limitations of optical dating for application on Late Weichselian and Holocene sandy deposits and shows where further methodological advances may be needed, i.e. improvement of precision and accuracy.

SAMENVATTING

Optisch gestimuleerde luminescentiedatering (OSL, of optische datering) is een betrouwbare dateringsmethode die meer en meer wordt aangewend in de studie van het Quartair. De techniek bepaalt wanneer sedimenten voor het laatst aan zonlicht werden blootgesteld. De belangrijkste voordelen van optische datering ten opzichte van andere dateringsmethoden voor het kwartair, zoals radiokoolstofdatering (^{14}C), zijn dat, ten eerste, de techniek toelaat om directe ouderdomsinformatie te bekomen voor de minerale componenten van sedimenten (o.a. kwarts, veldspaat) en, ten tweede, de methode geen calibratie vergt om ouderdommen in kalenderjaren te verkrijgen. OSL datering werd een tiental jaar geleden geïntroduceerd in het Gentse luminescentielaboratorium en initieel toegepast op kwartsextracten van dekzanden en stuifzanden uit Zuid-Nederland (Ossendrecht, Grubbenvorst, Defensiedijk). Sindsdien werden in het laboratorium monsters uit verschillende sedimentaire contexten (o.a. eolisch, fluvial) van overal ter wereld gedateerd, over het algemeen in het kader van multidisciplinaire onderzoeksprojecten die data uit geologie, sedimentologie, geo-archeologie en andere wetenschapsdomeinen met elkaar combineren.

In dit onderzoeksproject werd het potentieel van OSL voor de datering van laat-weichsel en holocene (fluvio-)eolische zanden verder onderzocht. Op basis van de dateringsresultaten van zes sites in Noord-België en Nederland, waaronder de klassieke typelocaliteit voor de laat-weichsel lithostratigrafie in Noordwest-Europa te Lutterzand (Oost-Nederland), werd een chronologisch kader voor de landschapsveranderingen tijdens de laatste 25.000 jaar uitgebouwd.

OSL ouderdommen worden berekend op basis van twee meetparameters: (1) de equivalente dosis, en (2) het dosistempo. De equivalente dosis komt overeen met de totale dosis energie afkomstig van nucleaire straling die geabsorbeerd werd door de mineraalkorrels sinds deze voor het laatst aan zonlicht werden blootgesteld. Het dosistempo is een maat voor de hoeveelheid energie die geabsorbeerd werd per tijdseenheid. In deze doctoraatsthesis werd gebruik gemaakt van het single-aliquot regenerative-dose (SAR) meetprotocol voor het bepalen van de equivalente dosis in grove kwartskorrels (diameter: 125-180 µm of 180-212 µm). Verscheidene testen werden uitgevoerd om de geschiktheid van de gebruikte SAR prodecure te evalueren, m.a.w. om de luminescentiekarakteristieken van onze monsters te

achterhalen. Het dosistempo werd gemeten met behulp van hoge-resolutie lage-achtergrond gammaspectrometrie in het laboratorium.

Een eerste toepassing van kwarts SAR-OSL datering in het kader van dit onderzoek had betrekking op een stuifzandduin op een archeologische site nabij Pulle (Noord-België). Het graven van proefputten op de locatie resulteerde in de ontdekking van een dicht netwerk van bouwstructuren en ceramiek, wijzend op menselijke bewoning tijdens de IJzertijd en de vroege Middeleeuwen (dus ruwweg van de 6de tot de 1^{e} eeuw vC. en van de 6de tot de 9de eeuw nC.). De overblijfselen werden deels bedekt door een ongeveer 2,5 m hoge stuifzandduin. Dit suggereerde dat de opeenhoping van deze eolische sedimenten mogelijk leidde tot een verslechtering van de leefomstandigheden en uiteindelijk tot het verlaten van de site. OSL datering werd toegepast om informatie betreffende het begintijdstip en de snelheid (of de periodiciteit) van de zandverstuiving te verschaffen, aangezien dit een bijdrage kon leveren tot het reconstrueren van de bewoningsgeschiedenis op de site.
De zanden onder het bewoningsniveau werden gedateerd op 15,1 ± 1,4 ka en 17,7 ± 1,6 ka. De nederzetting werd dus gebouwd op een sequentie van Laat-Pleniglaciale dekzanden. De ouderdommen voor de stuifzandduin zelf varieerden tussen 1,2 ± 0,1 ka en 1,3 ±0,1 ka, met een gemiddelde van 1,2 ± 1,0 ka (n=7). Deze ouderdommen komen overeen met de radiokoolstofouderdommen van AD 430-600, AD 640-780 en AD 770-900, bepaald voor de houten beschutting van twee waterputten uit het onderliggende bewoningsniveau. Er werd geconcludeerd dat de zandverstuiving plaatsvond gedurende één vrij korte gebeurtenis tijdens de vroege Middeleeuwen. Omdat er geen archeologische vondsten van de periode na de verstuiving werden aangetroffen, kon eveneens worden besloten dat de zandverstuiving waarschijnlijk een einde maakte aan de menselijke bewoning te Pulle.

Een tweede toepassing werd uitgevoerd op het duincomplex te Opgrimbie (Noordoost-België). Een eerdere studie gesteund op sedimentologie, palynologie en radiokoolstofdatering had uitgewezen dat veen uit zowel de Bøllingperiode als de Allerødperiode aanwezig was op de site. Deze veenpakketten gingen lateraal over in gebleekte horizonten, naar de top van het duincomplex toe. Vermits organisch materiaal en bodems uit het Bølling slechts zelden worden aangetroffen in de zandafzettingen van de Noordwest-Europese laaglanden werd deze site beschouwd als een typelocaliteit voor de eolische zandafzetting in Noordwest-Europa. De pilootstudie vermeldde echter geen directe ouderdommen voor het sediment zelf.

Kwarts SAR-OSL datering resulteerde in gemiddelde ouderdommen van respectievelijk 12,9 ± 0,9 ka (n=6) en 13,0 ± 0,8 ka (n=3) voor de duinzanden boven en onder de onderste gebleekte horizont met een vermoedelijke Bøllingouderdom. De ouderdom van 12,9 ± 0,9 ka is consistent met de eerder bepaalde bulk ^{14}C datering van 14,0-13,6 ka calBP en met de recent bepaalde AMS ^{14}C ouderdommen van 13,9-13,7 ka calBP en 13,2-13,0 ka calBP voor de bovenliggende veenlaag / gebleekte horizont. De OSL ouderdom van 13,0 ± 0,8 ka is echter significant jonger dan de bulk ^{14}C ouderdom van 15,2-14,5 ka calBP voor het bovenliggende zandige veen. Een studie van de verschillende parameters die invloed hebben op de uiteindelijke OSL-ouderdommen, zoals het tijdsgemiddelde vochtgehalte, de interne dosis van de kwartskorrels en bioturbatie van het sediment, toonde aan dat geen enkele van deze factoren in staat was om significante en systematische fouten in de OSL dateringen te kunnen introduceren. Daarom werd geopperd dat de bulk ^{14}C ouderdom van het veen misschien inaccuraat is. Op basis van de OSL resultaten werd geconcludeerd dat de twee gebleekte horizonten mogelijk deel uitmaken van één bodemcomplex dat zich ontwikkelde tijdens het Allerød interstadiaal. Hieruit volgt dat een groot gedeelte van de duin mogelijk afgezet werd na de Bøllingperiode en dat het duincomplex te Opgrimbie misschien niet langer weerhouden kan worden als een sleutelsectie voor het Laat-Glaciaal in het zuidelijkste gedeelte van de Noordwest-Europese dekzandgordel. In elk geval duiden zowel de OSL als de AMS resultaten op belangrijke eolische sedimentatie en een vrij snelle zandafzetting tijdens de pre-Allerød fase van het Laat-Glaciaal.

De archeologische sites Lommel-*Maatheide* en Arendonk-*Korhaan* in Noordoost-België worden gekenmerkt door zandige sequenties waarin de Finaal-Paleolithische en Vroeg-Mesolitische bewoningsfasen stratigrafisch gescheiden voorkomen. Daardoor laten ze toe om de mogelijke relatie tussen de menselijke bewoningspatronen en de veranderingen in het milieu tijdens de Weichsel-Holoceen overgang in de Kempen te onderzoeken. Het chronologische kader werd aangeleverd door kwarts SAR-OSL datering.

De twee sites hebben een vergelijkbare stratigrafie, bestaande uit twee zandige sedimenteenheden (Eenheid 1 en 3) en een tussenliggende gebleekte horizont (Eenheid 2), die lateraal overgaat in een veenpakket. Voor Eenheid 1 werden ouderdommen bekomen tussen 16,2 ± 1,4 ka en 13,0 ± 1,0 ka te Arendonk-*Korhaan* en tussen 15,3 ± 1,1 ka en 12,4 ± 0,9 ka te Lommel-*Maatheide*. De gebleekte klastische horizont (Eenheid 2) werd gedateerd op respectievelijk 15,2 ± 1,3 ka te Arendonk-*Korhaan* en 12,4 ± 0,9 ka en 10,6 ± 0,7 ka te Lommel-*Maatheide*. De tijdsgrenzen voor deze Eenheid 2 worden echter meer betrouwbaar

geacht dan de directe ouderdommen en zijn tussen 15,1 ± 1,1 ka (n=5) en 12,8 ± 1,0 ka (n=2) te Arendonk-*Korhaan* en tussen 13,5 ± 0,9 ka (n=4) en 11,3 ± 0,8 ka (n=2) te Lommel-*Maatheide*. De bovenste zandeenheid (Eenheid 3) resulteerde in ouderdommen tussen 12,3 ± 0,8 ka en 11,0 ± 0,7 ka te Lommel-*Maatheide* en tussen 13,0 ± 1,0 ka en 11,1 ± 0,8 ka te Arendonk-*Korhaan*. De SAR-OSL resultaten tonen aan dat de afzetting van eolische sedimenten te Arendonk-*Korhaan* reeds plaatsvond tijdens het Laat-Pleniglaciaal en zich voortzette over de Laat-Pleniglaciaal / Laat-Glaciaal grens. Voor Lommel-*Maatheide* valt het niet uit te sluiten dat de zandafzetting zich beperkte tot het Laat-Glaciaal. Op geen van beide sites zijn er duidelijke aanwijzingen in het lithostratigrafische en chronologische archief dat de zandafzetting werd onderbroken vóór het Allerød interstadiaal. De verminderende eolische activiteit tijdens het Allerød bevorderde de ontwikkeling van een gebleekte horizont, met name de Usselo-horizont, en een aangrenzende veenlaag. Eolische zandafzetting ging opnieuw verder tijdens het Laat-Dryas en stopte uiteindelijk tijdens het Holoceen, voornamelijk als een gevolg van de uitbreiding van de vegetatie. Uit de OSL data kon worden afgeleid dat de bewoning op beide sites zich beperkte tot de fases met landschapsstabilisatie, d.w.z. periodes zonder sterke eolische activiteit zoals het Allerød interstadiaal en het Vroeg-Holoceen. Het lijkt erop dat er een duidelijke interactie was tussen de menselijke bewoningspatronen en de veranderingen in de milieucontext.

Een laatste toepassing van OSL datering in Noord-België handelde over een sedimentkern genomen te Heidebos, nabij de top van de dekzandrug van Maldegem-Stekene en ten noorden van een groot Laat-Glaciaal paleomeer (de ‘Moervaart depressie’). De omgeving van de Moervaart depressie, met inbegrip van de dekzandrug, wordt beschouwd als een belangrijke locatie voor de studie van menselijke bewoning tijdens het Laat-Glaciaal en het Holoceen dankzij de vele sites en sitecomplexen die werden aangetroffen op de oevers van het meer en op de dekzandrug. De regio werd onderzocht ter reconstructie van de evolutie van het vroegere landschap en van de interactie tussen vroegere bewoningsgemeenschappen en hun natuurlijke omgeving.

De sedimentkern te Heidebos bestond uit een zevental meter gelamineerde en massieve zanden geïntercaleerd door verschillende organische lagen en bedekt door een podzol. De monsters gekozen voor OSL datering werden genomen boven en onder lithologische contacten en werden gekenmerkt door ouderdommen tussen 17,3 ± 1,3 ka en 11,0 ± 0,8 ka. Uit de OSL dataset kan niet eenduidig worden opgemaakt of de dekzandrug te Heidebos zich ontwikkelde tijdens (minstens) twee afzonderlijke fasen van eolische activiteit (één tijdens het

Laat-Pleniglacial rond 16,3 ka en één tijdens het Laat-Dryas rond 12,3 ka) of dat de dekzandrug zich vormde als een gevolg van semi-continue zandafzetting vanaf de laatste fase van het Laat-Pleniglaciaal tot het Laat-Dryas of zelfs Holoceen. De gemiddelde ouderdom van 16,3 ± 1,1 ka (n=2) voor de onderste meter sediment is in overeenstemming met de tijdsgrenzen van de Beuningen grintlaag, een wijdverbreide lithostratigrafische 'marker' horizont in de Noordwest-Europese dekzandsequenties die algemeen gerelateerd wordt aan grootschalige deflatie op het einde van het Laat-Pleniglaciaal. Daarom wordt geopperd dat het basale zand misschien het tijdsequivalent vormt van de Beuningen grintlaag. Het grootste gedeelte van de dekzandrug werd vermoedelijk afgezet tijdens het Allerød interstadiaal en/of het Laat-Dryas stadiaal. Tijdens het Allerød bereikte het paleomeer ten zuiden van de dekzandrug zijn maximale omvang. Dit zou de oprichting van menselijke nederzettingen in de omgeving hebben kunnen bevorderen, ondanks de mogelijke verderzetting van de eolische activiteit. Op een zeker ogenblik tijdens het Allerød en/of Laat-Dryas nam de intensiteit van de zandafzetting dramatisch toe, en tegelijkertijd begon het paleomeer in te krimpen door uitdroging. Waarschijnlijk hadden deze beide gebeurtenissen een aanzienlijke impact op de leefomstandigheden zodat de regio verlaten werd tot in het Vroeg-Holoceen.

De laatste toepassing van kwarts SAR-OSL datering in deze thesis handelde over de klassieke typelocaliteit voor de Laat-Weichsel lithostratigrafie in de Noordwest-Europese dekzandgordel te Lutterzand (Oost-Nederland). Op deze locatie bevatten de natuurlijke ontsluitingen langsheen de Dinkel rivier de volgende sedimentaire opeenvolging: Oud Dekzand I, Beuningen grintlaag, Oud Dekzand II, Onderste Lemige Laag, Jong Dekzand I, Usselo bodem en Jong Dekzand II. Deze afwisseling van dekzanden, een grintlaag en bodemhorizonten werd gerelateerd aan de snelle klimaats- en omgevingsveranderingen tijdens het Laat-Weichsel en de overgang tussen het Laat-Weichsel en het Holoceen. Op een bepaald ogenblik tijdens het (Laat-)Holoceen werd de regio eveneens gekenmerkt door zandverstuiving. Vier profielen werden in detail bemonsterd; dit resulteerde in 57 OSL monsters.

De toepassing van OSL datering resulteerde in ouderdommen tussen 25,2 ± 0,7 ka en 0,20 ± 0,01 ka. De onderste sedimenteenheid, bestaande uit gecryoturbeerde fluvio-eolische zanden die vroeger werden toegeschreven aan het Oud Dekzand I, werd afgezet tussen (ten laatste) 25,2 ± 1,9 ka en 19,9 ± 1,6 ka, m.a.w. tijdens de laatste fase van het Laat-Pleniglaciaal. De bovenliggende grove fluviatiele zanden uit het onderste gedeelte van de Beuningen grintlaag werden gedateerd tussen 23,4 ± 1,9 ka en 16,1 ± 1,3 ka. Vermits deze zanden slechts

discontinu voorkomen in enkele Lutterzand-profielen, wordt gedacht dat ze werden afgezet in lokale ondiepe kanaaltjes. Het 'desert pavement' in de top van de Beuningen grintlaag wordt wel in alle profielen aangetroffen. Het wordt typisch gerelateerd aan een fase van permafrostdegradatie en grootschalige eolische deflatie op het einde van het Laat-Pleniglaciaal, een fase die hier werd gedateerd tussen 16,1 ± 1,3 ka en 13,8 ± 1,1 ka. Een tweede fase van eolische activiteit (15,8 ± 1,4 ka tot 12,2 ± 0,9 ka) resulteerde in de afzetting van zogenaamde 'sand sheets' vanaf de finale fase van het Laat-Pleniglaciaal en gedurende het Laat-Glaciaal. De OSL-ouderdommen wijzen er dus op dat de sedimentatie ook doorging tijdens de fase van klimaatsverbetering rond ~14,7 ka en enkel werd onderbroken tijdens korte (interstadiale) perioden die terug te vinden zijn het lithostratigrafisch archief. De top van de sedimenten werd op sommige plaatsen weggeblazen als een gevolg van zandverstuiving, terwijl deze op andere plaatsen bedekt werd door tientallen cm stuifzand. In de literatuur werd gesuggereerd dat natuurlijke rivierduinen reeds voorkwamen vanaf het Mid-Holoceen te Lutterzand en dat de belangrijkste uitbreiding van deze duinen plaatsvonden vanaf de Middeleeuwen. Het is echter zo dat OSL enkel toelaat om de laatste fase van afzetting en begraving te dateren. Daarom kan deze hypothese uit de literatuur niet worden geverifieerd. De ouderdommen van de stuifzanden variëren tussen 0,40 ± 0,04 ka en 0,20 ± 0,02 ka, wat erop wijst dat zandverstuiving nog steeds voorkwam tijdens het zeer recente verleden in de Lutterzand regio.

Uit dit thesisonderzoek kan worden afgeleid dat de fluvio-eolische en eolische zanden in Noord-België en Nederland beschikken over goede luminescentiekarakteristieken. Bovendien zijn ze over het algemeen goed gebleekt en niet sterk beïnvloed door post-depositionele mengprocessen. Binnen de OSL datasets kan een zekere mate van variabiliteit worden waargenomen, waarvan de oorzaken niet volledig gekend zijn. In deze thesis werd gesuggereerd dat de zanden misschien gekenmerkt worden door een grotere heterogeniteit in minerale samenstelling en in textuur dan verwacht en dat dit zou leiden tot de variaties in het dosistempo en in de ouderdom. Vervolgonderzoek zal uitwijzen of deze hypothese klopt. De optische ouderdommen zijn geassocieerd met totale (1 σ) onzekerheden van 8 à 10%. De systematische onzekerheid is hierin dominant. Daarom is het moeilijk om ondubbelzinnig een onderscheid te maken tussen de verschillende periodes van het Laat-Glaciaal op basis van OSL datering. Het is zinvoller om de OSL-ouderdommen te combineren met het lithostratigrafische bewijs en met onafhankelijke ouderdomsinformatie. In vergelijking met bijvoorbeeld radiokoolstofdatering (bepaalt ouderdommen voor geassocieerd organisch

materiaal) laat optische datering ook toe om sedimentatiesnelheden te berekenen en de afzettingsgeschiedenis te interpreteren in termen van geleidelijke semi-continue sedimentatie of afzettings'events'. Dit vereist echter dat verschillende ouderdommen bepaald worden per sedimenteenheid: dit illustreert het belang van de toepassing van een hoge-resolutie monsternamestrategie.

Over het algemeen komen de OSL-resultaten uit dit doctoraatsonderzoek overeen met onafhankelijke ouderdomsinformatie als de specifieke onzekerheden van de verschillende dateringsmethoden in rekening gebracht worden. Op basis van de resultaten van optische datering bepaald tijdens deze studie en in de literatuur teruggevonden voor dezelfde en equivalente afzettingen in België en Nederland kunnen vier belangrijke fasen van (fluvio-) eolische afzetting worden onderscheiden:

Vanaf ten laatste 25 ka tot ongeveer 17 ka vond fluvio-eolische afzetting plaats in de regio. De bodem werd gekenmerkt door permafrost, waardoor de resulterende siltige zanden vaak sporen van cryoturbatie en andere periglaciale fenomenen vertonen. Tot nu toe werden deze zanden voornamelijk herkend en gedateerd in vallei-omgevingen, zoals Grubbenvorst en Lutterzand. Het einde van het Laat-Pleniglaciaal wordt over het algemeen aanzien als een fase die gedomineerd wordt door permafrostdegratatie, ondiepe kanaalvorming en eolische deflatie in een koude woestijnomgeving, culminerend in de vorming van de Beuningen grintlaag. De grofkorrelige fluviatiele variant van deze grintlaag werd tijdens dit onderzoek enkel teruggevonden in twee profielen langsheen de Dinkel rivier, waarin het een discontinu patroon voorkomen vertoont dat wijst op het lokale karakter van deze afzetting. Deze sedimenteenheid werd gedateerd tussen ~23 en 16 ka. De fase van permafrostdegradatie, eolische deflatie en de vorming van het 'desert pavement' werd toegewezen aan de periode 16-14 ka in Lutterzand. Op andere plaatsen in de Noordwest-Europese laaglanden werden andere tijdsgrenzen teruggevonden, o.a. 17-15 ka te Grubbenvorst en 18-16 ka te Rotem. Dit toont aan dat het accumulatie- en preservatiepotentieel van sedimenten op een bepaalde site waarschijnlijk beïnvloed werd door plaatselijke verschillen in bijvoorbeeld geomorfologie, vegetatiedensiteit en hydrologie.

Een tweede fase van eolische activiteit werd gedateerd tussen ongeveer 17 en 13 ka. Deze resulteerde in de sedimentatie van gelamineerde fijne zanden tot siltige zanden, als een gevolg van afzetting en adhesie van de sedimenten op een afwisselend droog en nat oppervlak. Hierbij kan opgemerkt worden dat de klimaatsverbetering rond ~14,7 ka blijkbaar weinig sporen nagelaten heeft in de terrestrische afzettingen, terwijl deze in bijvoorbeeld de ijskernen

wel duidelijk te identificeren is. Dit toont aan dat deze klimaatsverbetering niet geleid heeft tot een algemene stabilisatie van het oppervlak in de Noordwest-Europese laaglanden. Dit in tegenstelling tot de klimaatsverbetering rond 14 ka, die wel leidde tot een stilstand in sedimentatie, landschapsstabilisatie en ontwikkeling van gebleekte bodemhorizonten en veenpakketten. De klastische component van deze gebleekte horizonten werd gedateerd tussen 15 en 11 ka. De interpretatie van deze OSL resultaten is echter moeilijk, vermits ze zowel kunnen refereren naar de ouderdom van de sedimenten waarin de gebleekte horizonten zich ontwikkelden als naar het tijdstip van de bodemvorming.
Een derde fase van eolische afzetting vond plaats tussen ~13 en 11 ka. De zanden worden gekarakteriseerd door horizontale tot licht-schuine gelaagdheid die vermoedelijk in verband staat met de vorming van lage duinen. Als een gevolg van de limiet op de tijdsresolutie van de OSL ouderdommen kan niet eenduidig worden geconcludeerd of de eolische sedimentatie wel dan niet voortgezet werd tijdens de Laat-Glaciaal/Vroeg-Holoceen grens.
Een laatste fase gekenmerkt door het transport en de afzetting van zand trad op tijdens het Laat-Holoceen en was enkel plaatselijk belangrijk. Deze fase is gerelateerd aan de ontbossing van het dekzandlandschap door mensen en resulteerde in zandverstuiving. Het tijdstip en de duur van de zandverstuivingen varieerden van plaats tot plaats: in Zuid-Nederland werden verschillende fasen van zandverstuiving aangetroffen vanaf 5 ka, in Noordoost-België trad zandverstuiving op rond 1,2 ka en in Oost-Nederland gingen de verstuivingen door tot ca. 0,2 ka.

Dit onderzoek illustreert hoe optisch gestimuleerde luminescentiedatering een bijdrage kan leveren tot de uitbouw van een accuraat en robuust tijdskader voor de (fluvio-)eolische afzetting in België en Nederland en bijgevolg tot de reconstructie van de veranderingen in de sedimentaire omgevingen in relatie tot de paleoklimatologische veranderingen en de menselijke bewoningsdynamiek. De studie heeft ook enkele beperkingen van de OSL dateringsmethode aan het licht gebracht in het kader van de toepassing op Laat-Weichsel zanden en toont zo aan op welke vlakken methodologische vooruitgang kan worden verwezenlijkt (voornamelijk op het vlak van precisie en accuraatheid).

References

REFERENCES

Adamiec, G., Aitken, M., 1998. Dose-rate conversion factors: update. Ancient TL 16, 37-50.

Aitken, M.J., 1976. Thermoluminescence age evaluation and assessment of error limits: revised system. Archaeometry 18, 233-238.

Aitken, M.J., 1985. Thermoluminescence dating. Academic Press Inc., London. 359 pp.

Aitken, M.J., 1998. An introduction to optical dating. The dating of Quaternary sediments by the use of photon-stimulated luminescence. Oxford University Press, Oxford. 267 pp.

Aitken, M.J., Alldred, J.C., 1972. The assessment of error limits in thermoluminescence dating. Archaeometry 14, 257-267.

Antoine, P., Munaut, A.V., Limondin-Lozouet, N., Ponel, Ph., Dupéron, J., Dupéron, M., 2003. Response of the Selle river to climatic modifications during the Lateglacial and Early Holocene (Somme Basin-Northern France). Quaternary Science Reviews 22, 2061-2076.

Baales, M., 2001. From lithics to spacial and social organization: Interpreting the lithic distribution and raw material composition at the Final Palaeolithic site of Kettig (Central Rhineland, Germany). Journal of Archaeological Science 28, 127-141.

Baales, M., 2006. Final Palaeolithic environment and archaeology in the Central Rhineland (Rhineland-Palatinat, western Germany): conclusions of the last 15 years of research. L'anthropologie 110, 418-444.

Baeté, H., Christiaens, B., De Keersmaeker, L., Esprit, M., Van De Kerckhove, P., Vandekerkhove, K., Walleyn, R., 2004. Bosreservaat De Heirnisse: basisrapport: situering, standplaats, historiek en onderzoek. Rapporten van het instituut voor bosbouw en wildbeheer - sectie bosbouw 18. Instituut voor Bosbouw en Wildbeheer (Geraardsbergen), 108 pp.

Baeyens, L., 1971. Verklarende tekst bij het kaartblad Grobbendonk 29E. Centrum voor Bodemkartering, Gent.

Ballarini, M., Wallinga, J., Murray, A.S., van Heteren, S., Oost, A.P., Bos, A.J.J., van Eijk, C.W.E., 2003. Optical dating of young coastal dunes on a decadal time scale. Quaternary Science Reviews 22, 1011-1017.

Bateman, M.D., 1995. Thermoluminescence dating of the British coversand deposits. Quaternary Science Reviews 14, 791-797.

Bateman, M.D., 2008. Luminescence dating of periglacial sediments and structures. Boreas 37, 574-588.

Bateman, M.D., Van Huissteden, J., 1999. The timing of last-glacial periglacial and aeolian events, Twente, eastern Netherlands. Journal of Quaternary Science 14, 277-283.

Bats, M., De Reu, J., De Smedt, P., Antrop, M., Bourgeois, J., Court-Picon, M., De Meyer, P., Finke, P., Van Meirvenne, M., Verniers, J., Werbrouck, I., Zwertvaegher, A., Crombé, P., 2009. Geoarchaeological research of the large palaeolake of the Moervaart (municipalities of Wachtebeke and Moerbeke-Maas, East Flanders, Belgium). From Late Glacial to Early Holocene. Notae Praehistoricae 29, 105-112.

Bats, M., De Reu, J., De Smedt, P., Antrop, M., Bourgeois, J., Court-Picon, M., De Meyer, P., Finke, P., Van Meirvenne, M., Verniers, J., Werbrouck, I., Zwertvaegher, A., Crombé, P., 2010. Continued geoarchaeological research of the large palaeolake of the Moervaart: a preliminary report of the 2010 campaign. Notae Praehistoricae 30, 15-21.

Bender, M., Sowers, T., Dickson, M.-L., Orchardo, J., Grootes, P., Mayewski, P., Meese, D., 1994. Climate correlations between Greenland and Antarctica during the last 100,000 years. Nature 372, 663-666.

Bogemans, F., 2005. Toelichting bij de Quartairgeologische kaart. Kaartblad 3-6, Arendonk-Maarle. Vlaamse Overheid Dienst Natuurlijke Rijkdommen, Brussel.

Bogemans, F., Vandenberghe, D., submitted. OSL dating of an inland dune along the lower River Scheldt near Schellebelle (East Flanders – Belgium). Netherlands Journal of Geosciences.

Bokhorst, M.P., Beets, C.J., Marković, S.B., Gerasimenko, N.P., Matviishina, Z.N., Frechen, M., 2009. Pedo-chemical climate proxies in Late Pleistocene Serbian-Ukranian loess sequences. Quaternary International 198, 113-123.

Bøtter-Jensen, L., Andersen, C.E., Duller, G.A.T., Murray, A.S., 2003. Developments in radiation, stimulation and observation facilities in luminescence measurements. Radiation Measurements 37, 535-541.

Bos, J.A.A., Janssen, C.R., 1996. Local impact of Palaeolithic man on the environment during the end of the Last Glacial in the Netherlands. Journal of Archaeological Science 23, 731-739.

Bronk Ramsey, C., 1995. Radiocarbon calibration and analysis of stratigraphy: The OxCal program. Radiocarbon 37, 425-430.

Bronk Ramsey, C., 2001. Development of the radiocarbon calibration program OxCal. Radiocarbon 43, 355-363.

Bronk Ramsey, C., 2009. Bayesian analysis of radiocarbon dates. Radiocarbon 51, 337-360.

Buylaert, J.-P., Ghysels, G., Murray, A.S., Thomsen, K.J., Vandenberghe, D., De Corte, F., Heyse, I., Van den haute, P., 2009. Optical dating of relict sand wedges and composite-wedge pseudomorphs in Flanders, Belgium. Boreas 38, 160-175.

Castel, I., Koster, E., Slotboom, R., 1989. Morphogenetic aspects and age of Late Holocene eolian drift-sands in Northwest Europe. Zeitschrift für Geomorphologie 33, 1-26.

Chen, F.H., Bloemendal, J., Wang, J.M., Li, J.J., Oldfield, F., 1997. High-resolution multi-proxy climate records from Chinese loess: evidence for rapid climatic changes over the last 75 kyr. Palaeogeography, Palaeoclimatology, Palaeoecology 130, 323-335.

Crombé, Ph., Cauwe, N., 2001. The Mesolithic. In: Cauwe, N., Hauzeur, A., van Berg, P.-L. (eds.). Prehistory of Belgium. Special issue on the occasion of the XIVth Congress of the International Union for Prehistoric and Protohistoric Sciences. Bulletin de la Société royale belge d'Anthropologie et de Préhistoire 112: 49-62.

Crombé, Ph., Verbruggen, C., 2002. The Lateglacial and early Postglacial occupation of northern Belgium: the evidence from Sandy Flanders. In: Eriksen, B.V., Bratlund, B (eds.). Recent studies in the Final Palaeolithic of the European plain. Proceedings of a UISPP Symposium, Stockholm 1999. Jutland Archaeological Society Publications, 165-180.

Cunningham, A.C., Wallinga, J., 2010. Selection of integration time intervals for quartz OSL decay curves. Quaternary Geochronology 5, 657-666.

Dansgaard, W., Johnsen, S.J., Clausen, H.B., Dahl-Jensen, D., Gundestrup, N.S., Hammer, C.U., Hvidberg, C.S., Steffensen, J.P., Sveinbjörnsdóttir, A.E., Jouzel, J., Bond, G., 1993. Evidence for general instability of past climate from a 250-kyr ice core record. Nature 364, 218-220.

Dean, R.B., Dixon, W.J., 1951. Simplified statistics for small numbers of observations. Analytical Chemistry 23, 636-638.

De Bie, M., 1997. L'industrie à Federmesser de Rekem (Belgique): datation, technologie lithique et répartition spatiale. In: Fagnart, J.P., Thévenin, A. (Eds.), Chronostratigraphie et environnement des occupations humaines du Tardiglaciaire et du début de l'Holocène en Europe du Nord-Ouest. Editions du CTHS, 381-396.

De Bie, M., Caspar, J.-P., 2000. Rekem, a Federmesser camp on the Meuse river bank. Archeologie in Vlaanderen 3 & Acta Archaeologica Lovaniensa 10, Asse-Zellik and Leuven.

De Bie, M., Van Gils, M., 2004. Steentijdsites op de Maatheide te Lommel. Archeologisch waarderingsonderzoek 2003. Intern rapport VIOE, Brussel.

De Bie, M, Van Gils, M., 2009. Mesolithic settlement and land use in the Campine region (Belgium). In: McCartan, S., Schulting, R., Warren, G., Woodman, P. (Eds.). Mesolithic Horizons. Papers presented at the Seventh International Conference on the Mesolithic in Europe, Belfast 2005. Oxbow, Oxford, pp. 282-287.

De Bie, M., Van Gils, M., Deforce, K., 2009. Human occupation in a Late Glacial landscape: The Federmessergruppen site complex at Lommel Maatheide (Belgium). In: Street, M., Barton, N., Terberger, T. (eds.). Humans, environment and chronology of the Late Glacial of the North European Plain. Proceedings of Workshop 14 (Commission XXXII) of the 15th U.I.S.P.P. Congress, Lisbon. RGZM-Tagungen 6, Mainz, 77-87.

De Bie, M., Vermeersch, P.M., 1998. Pleistocene-Holocene transition in Benelux. Quaternary International 49/50, 29-43.

De Corte, F., Vandenberghe, D., De Wispelaere, A., Buylaert, J.-P., Van den haute, P., 2006. Radon loss from encapsulated sediments in Ge gamma-ray spectrometry for the annual radiation dose determination in luminescence dating. Czech Journal of Physics 56, D183-D194.

Deeben, J., Rensink, E., 2005. Het Laat-Paleolithicum in Zuid-Nederland. In: Deeben, J., Drenth, E., van Oorsouw, M.-F., Verhart, L. (eds.). De Steentijd van Nederland. Archeologie 11/12, 171-199.

De Klerk, P., 2004. Confusing concepts in Lateglacial stratigraphy and geochronology: origin, consequences, conclusions (with special emphasis on the type locality Bøllingsø). Review of Palaeobotany and Palynology 129, 265-298.

De Moor, G., 1963. Bijdrage tot de kennis van de fysische landschapsvorming in Binnen-Vlaanderen. Tijdschrift van de Belgische Vereniging voor Aardrijkskundige Studies 32, 329-433.

De Moor, G., Heyse, I., 1978. De morfologische evolutie van de Vlaamse Vallei. De Aardrijkskunde 4, 343-375.

Derese, C., Vandenberghe, D.A.G., Kasse, C., Van den haute, P., in prep. Late Weichselian (fluvio-) aeolian sediments and Holocene drift-sands of the classic type locality in Twente (E Netherlands): A high-resolution dating study using optically stimulated luminescence.

Derese, C., Vandenberghe, D., Paulissen, E., Van den haute, P., 2009. Revisiting a type locality for Late Glacial aeolian sand deposition in NW Europe: Optical dating of the dune complex at Opgrimbie (NE Belgium). Geomorphology 109, 27-35.

Derese, C., Vandenberghe, D., Eggermont, N., Bastiaens, J., Annaert, R., Van den haute, P., 2010(a). A medieval settlement caught in the sand: Optical dating of sand-drifting at Pulle (N Belgium). Quaternary Geochronology 5, 336-341.

Derese, C., Vandenberghe, D.A.G., Van Gils, M., Mees, F., Paulissen, E., Van den haute, P., in press. Final Palaeolithic settlements of the Campine region (NE Belgium) in their environmental context: optical age constraints. Quaternary International, doi: 10.1016/j.quaint.2011.03.023.

Derese, C., Vandenberghe, D.A.G., Van Gils, M., Vanmontfort, B., Meirsman, E., Mees, F., Van den haute, P., 2011. Establishing a chronology for landscape evolution around a Final Palaeolithic site at Arendonk-*Korhaan* (NE Belgium): First results from optically stimulated luminescence dating. Mediterranean Archaeology and Archaeometry 10, 43-51.

Derese, C., Vandenberghe, D.A.G., Zwertvaegher, A., Court-Picon, M., Crombé, Ph., Verniers, J., Van den haute, P., 2010(b). The timing of aeolian events near archaeological settlements around Heidebos (Moervaart area, N Belgium). Netherlands Journal of Geosciences 89, 173-186.

Dijkmans, J.W.A., Wintle, A.G., 1991. Methodological problems in thermoluminescence dating of Weichselian coversand and late Holocene drift-sand from the Lutterzand area, E. Netherlands. Geologie en Mijnbouw 70, 21-33.

Dijkmans, J.W.A., Wintle, A.G., Mejdahl, V., 1988. Some thermoluminescence properties and dating of eolian sands from The Netherlands. Quaternary Science Reviews 7, 349-355.

Dijkmans, J.W.A., van Mourik, J.M., Wintle, A.G., 1992. Thermoluminescence dating of aeolian sands from polycyclic soil profiles in the southern Netherlands. Quaternary Science Reviews 11, 85-92.

Duller, G.A.T., 1994. Luminescence dating using single aliquots: new procedures. Quaternary Geochronology (Quaternary Science Reviews) 13, 149-156.

Duller, G.A.T., 2003. Distinguishing quartz and feldspar in single grain luminescence measurements. Radiation Measurements 37, 161-165.

Eggermont, N., Annaert, R., Bastiaens, J., Derese, C., Vandenberghe, D., Van den haute, P., Haneca, K., Van Strydonck, M., 2008. Nederzettingssporen uit de ijzertijd en de vroege middeleeuwen onder een stuifduin langs de Keulsebaan te Pulle (gem. Zandhoven, prov. Antwerpen). Intern rapport VIOE, Brussel, Belgium.

Fagnart, J.-P., Coudret, P., 2000. Données récentes sur le Tardiglaciaire du basin de la Somme. In : Pion, G. (ed.). Le Paléolithique supérieur récent. Nouvelles données sur le peuplement et l'environnement : Actes de la Table ronde de Chambéry, 12-13 mars 1999. Mémoire de la Société Préhistorique Française, 113-126.

Frenchen, M., Van den Berg, M.W., 2002. The coversand and timing of Late Quaternary earthquake events along the Peel Boundary Fault in the Netherlands. Geologie en Mijnbouw / Netherlands Journal of Geosciences 81, 61-70.

Frechen, M., Oches, E.A., Kohfeld, K.E., 2003. Loess in Europe – mass accumulation rates during the Last Glacial Period. Quaternary Science Reviews 22, 1835-1857.

Frechen, M., Vanneste, K., Verbeeck, K., Paulissen, E., Camelbeeck, T., 2001. The deposition history of the coversands along the Bree Fault escarpment, NE Belgium. Netherlands Journal of Geosciences / Geologie en Mijnbouw 80, 171-185.

Folz, E., Bodu, P., Bonte, Ph., Joron, J.-L., Mercier, N., Reyss, J.-L., 2001. OSL dating of fluvial quartz from Le Closeau, a Late Paleolithic site near Paris – comparison with ^{14}C chronology. Quaternary Science Reviews 20, 927-933.

Galbraith, R.F., Roberts, R.G., Laslett, G.M., Yoshida, H., Olley, J.M., 1999. Optical dating of single and multiple grains of quartz from Jinmium rock shelter, Northern Australia: Part I, experimental design and statistical models. Archaeometry 41, 339-364.

Gibbard, P.L., Head, M.J., Walker, M.J.C., the Subcommission on Quaternary Stratigraphy, 2010. Formal ratification of the Quaternary System/Period and the Pleistocene Series/Epoch with a base at 2.58 Ma. Journal of Quaternary Science 25, 96-102.

Guiter, F., Andrieu-Ponel, V., de Beaulieu, J.-L., Cheddadi, R., Calvez, M., Ponel, Ph., Reille, M., Keller, T., Goeury, C., 2003. The last climatic cycles in Western Europe: a comparison between long continuous lacustrine sequences from France and other terrestrial records. Quaternary International 111, 59-74.

Gullentops, F., Bogemans, F., De Moor, G., Paulissen, E., Pissart, A., 2001. Quaternary lithostratigraphic units (Belgium). In: Bultynck, P., Dejonghe, L. (Eds.), Guide to a revised lithostratigraphic scale of Belgium, Geologica Belgica 4/1-2, pp. 153-164.

Heusser, L., Morley, J., 1997. Monsoon fluctuations over the past 350 kyr: high-resolution evidence from Northeast Asia/Northwest Pacific climate proxies (marine pollen and radiolarians). Quaternary Science Reviews 16, 565-581.

Heyse, I., 1979. Bijdrage tot de geomorfologische kennis van het noordwesten van Oost-Vlaanderen (België). Verhandelingen van de Koninklijke Academie voor Wetenschappen, Letteren en Schone Kunsten van België 40, 217 pp.

Hoek, W.Z., 1997. Atlas to Palaeogeography of Lateglacial vegetations; Maps of Lateglacial and Early Holocene landscape and vegetation in The Netherlands, with an extensive review of available palynological data. Ph.D. thesis, Vrije Universiteit Amsterdam, 165 pp.

Hoek, W.Z., 2000. Abiotic landscape and vegetation patterns in the Netherlands during the Weichselian Late Glacial. Geologie en Mijnbouw/Netherlands Journal of Geosciences 79, 497-509.

Hoek, W.Z., 2001. Vegetation response to the ~14.7 and ~11.5 ka cal.BP climate transitions: is vegetation lagging climate? Global and Planetary Change 30, 103-115.

Hoek, W.Z., Bohncke, S.J.P., 2002. Climatic and environmental events over the Last Termination, as recorded in The Netherlands: a review. Netherlands Journal of Geosciences /Geologie en Mijnbouw 81, 123-137.

Hossain, S.M., 2003. A critical comparison and evaluation of methods for the annual radiation dose determination in the luminescence dating of sediments. PhD-thesis Universiteit Gent.

Hijszeler, C.C.W.J., 1947. De oudheidkundige opgravingen in Twente in de laatste jaren. In: Van Gelder, H.E., Glazema, P., Bontekoe, G.A. (eds.). Een kwart eeuw oudheidkundig bodemonderzoek in Nederland. Gedenkboek A.E. van Giffen. J.A. Boom & Zoon, Meppel, 327-349.

Hijszeler, C.C.W.J., 1957. Late-glacial human cultures in the Netherlands. Geologie en Mijnbouw 19, 288-302.

Huijzer, B., Vandenberghe, J., 1998. Climatic reconstruction of the Weichselian Pleniglacial in northwestern and central Europe. Journal of Quaternary Science 13, 391-417.

Jain, M., Murray, A.S., Bøtter-Jensen, L., 2004. Optically stimulated luminescence dating: how significant is incomplete light exposure in fluvial environments? Quaternaire 15, 143-157.

Kaiser, K., Hilgers, A., Schlaak, N., Jankowski, M, Kühn, P., Bussemer, S., Przegiętka, K., 2009. Palaeopedological marker horizons in northern central Europe: characteristics of Lateglacial Usselo and Finow soils. Boreas 38, 591-609.

Kasse, C., 1997. Cold-climate aeolian sand-sheet formation in North-Western Europe (c. 14 – 12.4 ka); a response to permafrost degradation and increased aridity. Permafrost and Periglacial Processes 8, 295-311.

Kasse, C., 1999. Late Pleniglacial and Lateglacial aeolian phases in The Netherlands. In: Schirmer, W. (Ed.), Dunes and fossil soils. GeoArchaeoRhein 3, 61-82.

Kasse, C., 2002. Sandy aeolian deposits and environments and their relation to climate during the Last Glacial Maximum and Lateglacial in northwest and central Europe. Progress in Physical Geography 26, 507-532.

Kasse, C., Vandenberghe, D., De Corte, F., Van den haute, P., 2007. Late Weichselian fluvio-aeolian sands and coversand of the type locality Grubbenvorst (southern Netherlands): sedimentary environments, climate record and age. Journal of Quaternary Science 22, 695-708.

Kitagawa, H., van der Plicht, J., 1998. Atmospheric radiocarbon calibration to 45,000 yr B.P.: Late Glacial fluctuations and cosmogenic isotope production. Science 279, 1187-1190.

Kiyak, N.G., Canel, T., 2006. Equivalent dose in quartz from young samples using the SAR protocol and the effect of preheat temperature. Radiation Measurements 41, 917-922.

Kolstrup, E., 1980. Climate and Stratigraphy in Northwestern Europe between 30,000 B.P. and 13,000 B.P., with special reference to The Netherlands. Mededelingen Rijks Geologische Dienst 32, 181-253.

Kolstrup, E., 2007. Lateglacial older and younger coversand in northwest Europe: chronology and relation to climate and vegetation. Boreas 36, 65-75.

Kolstrup, E., Heyse, I., 1980. A different Late-Glacial vegetation and its environment in Flanders (Belgium). Pollen et Spores 22, 469-481.

Kolstrup, E., Wijmstra, T.A., 1977. A palynological investigation of the Moershoofd, Hengelo, and Denekamp interstadials in the Netherlands, Geologie en Mijnbouw 58, 377–380.

Kolstrup, E., Murray, A., Possnert, G., 2007. Luminescence and radiocarbon ages from laminated Lateglacial aeolian sediments in western Jutland, Denmark. Boreas 36, 314-325.

Koster, E.A., 1982. Terminology and lithostratigraphic division of (surficial) sandy eolian deposits in The Netherlands: an evaluation. Geologie en Mijnbouw 61, 131-129.

Koster, E.A., 2005. Recent advances in luminescence dating of Late Pleistocene (cold-climate) aeolian sand and loess deposits in Western Europe. Permafrost and Periglacial Processes 16, 131-143.

Koster, E.A., Castel, I.I.Y., Nap, R.L., 1993. Genesis and sedimentary structures of late Holocene aeolian drift-sands in northwest Europe. In: Pye, K. (Ed.), The Dynamics and Environmental Context of Aeolian Sedimentary Systems. Geological Society Special Publication No. 72, London, United Kingdom, pp. 247-267.

Kühn, P., Aguilar, J., Miedema, R., 2010. Textural features and related horizons. In: Stoops, G., Marcelino, V., Mees, F. (Eds.), Interpretation of Micromorphological Features of Soils and Regoliths. Elsevier, Amsterdam, in press.

Lorius, C., Jouzel, J., Ritz, C., Merlivat, L., Barkov, N.I., Korotkevich, Y.S., Kotlyakov, M., 1985. A 150,000-year climatic record from Antarctic ice. Nature 316, 591-596.

Lowe, J.J., Walker, M.J.C., 1997. Reconstructing Quaternary environments. Second edition. Addison Wesley Longman Limited, Harlow. 446 pp.

Lowe, J.J., Walker, M.J.C., 2000. Radiocarbon dating the Last Glacial-Interglacial transition (Ca. 14-9 ^{14}C ka BP) in terrestrial and marine records: the need for new quality assurance protocols. Radiocarbon 42, 53-68.

Lyell, C.,1830. Principles of Geology. John Murray, London.

Madsen, A.T., Murray, A.S., 2009. Optically stimulated luminescence dating of young sediments: A review. Geomorphology 109, 3-16.

Magny, M., 2001. Palaeohydrological changes as reflected by lake-level fluctuations in the Swiss Plateau, the Jura Mountains and the northern French Pre-Alps during the Last Glacial-Holocene transition: a regional synthesis. Global and Planetary Change 30, 85-101.

Maréchal, R., 1992. Géologie du Quaternaire, lithologie des terrains superficiels. Deuxième Atlas de Belgique. National Institute of Geography, Commission of the National Atlas, Brussels, 25p.

Meirsman, E., Van Gils, M., Vanmontfort, B., Paulissen, E., Bastiaens, J., Van Peer, P., 2008. Landschap De Liereman herbezocht. De waardering van een gestratifieerd finaalpaleolithisch en mesolithisch sitecomplex in de Noorderkempen (gem. Oud-Turnhout en Arendonk), Notae Praehistoricae 28, 33-41.

Mejdahl, V., 1979. Thermoluminescence dating: beta-dose attenuation in quartz grains. Archaeometry 21, 61-72.

Munyikwa, K., 2000. Cosmic ray contribution to environmental dose rates with varying overburden thickness. Ancient TL 18, 27-34.

Murray, A.S., Olley, J.M., 2002. Precision and accuracy in the optically stimulated luminescence dating of sedimentary quartz: a status review. Geochronometria 21, 1-16.

Murray, A.S., Wintle, A.G., 2000. Luminescence dating of quartz using an improved single-aliquot regenerative-dose protocol. Radiation Measurements 32, 57-73.

Murray, A.S., Wintle, A.G., 2003. The single aliquot regenerative dose protocol: potential for improvements in reliability. Radiation Measurements 37, 377-381.

Olsson, I.U., 1986. A study of errors in ^{14}C dates of peat and sediment. Radiocarbon 28, 429-435.

Paepe, R., Vanhoorne, R., 1967. The stratigraphy and palaeobotany of the Late Pleistocene in Belgium. Toelichtende Verhandelingen voor de Geologische Kaart en Mijnkaart van België 8, 96 pp.

Paulissen, E., Munaut, A.V., 1969. Un horizon blanchâtre d'age Bølling à Opgrimbie. Acta Geographica Lovaniensia 7, 65-91.

Prescott, J.R., Hutton, J.T., 1994. Cosmic ray contributions to dose rates for luminescence and ESR dating: large depths and long-term time variations. Radiation Measurements 23, 497-500.

Porter, S.C., An, Z., 1995. Correlation between climate events in the North Atlantic and China during the last glaciation. Nature 375, 305-308.

Rasmussen, S.O., Seierstad, I.K., Andersen, K.K., Bigler, M., Dahl-Jensen, D., Johnsen, S.J., 2008. Synchronization of the NGRIP, GRIP, and GISP2 ice cores across MIS 2 and palaeoclimatic implications. Quaternary Science Reviews 27, 18-28.

Reimer, P.J., Baillie, M.G.L., Bard, E., Bayliss, A., Beck, J.W., Bertrand, C., Blackwell, P.G., Buck, C.E., Burr, G., Cutler, K.B., Damon, P.E., Edwards, R. L., Fairbanks, R. G., Friedrich, M., Guilderson, T.P., Hughen, K.A. , Kromer, B., McCormac, F.G., Manning, S., Bronk Ramsey, C., Reimer, R.W., Remmele, S., Southon, J.R., Stuiver, M., Talamo, S., Taylor, F.W., van der Plicht, J., Weyhenmeyer, C.E., 2004. IntCal04 Terrestrial Radiocarbon Age Calibration, 0-26 Cal Kyr BP. Radiocarbon 46, 1029-1058.

Reimer, P.J., Baillie, M.G.L., Bard, E., Bayliss, A., Beck, J.W., Blackwell, P.G., Bronk Ramsey, C., Buck, C.E., Burr, G.S., Edwards, R.L., Friedrich, M., Grootes, P.M., Guilderson, T.P., Hajdas, I., Heaton, T.J., Hogg, A.G., Hughen, K.A., Kaiser, K.F., Kromer, B., McCormac, F.G., Manning, S.W., Reimer, R.W., Richards, D.A., Southon, J.R., Talamo, S., Turney, C.S.M., van der Plicht, J., Weyhenmeyer, C.E., 2009. IntCal09 and Marine09 radiocarbon age calibration curves, 0-50,000 years cal BP. Radiocarbon 51, 1111-1150.

Renssen, H., Kasse, C., Vandenberghe, J., Lorenz, S.J., 2007. Weichselian Late Pleniglacial surface winds over northwest and central Europe: a model-data comparison. Journal of Quaternary Science 22, 281-293.

Schokker, J., de Lang, F.D., Weerts, H.J.T., den Otter, C., 2003. Formatie van Boxtel. In: TNO-NITG. Lithostratigrafische nomenclator ondiepe ondergrond Netherland (online). Available from: www.nitg.tno.nl/nomenclatorShallow/nl/overig/boxtel/index.html (Accessed 15 October 2010).

Schokker, J., de Lang, F.D., Weerts, H.J.T., den Otter, C., 2003. Formatie van Boxtel. In: TNO-NITG. Lithostratigrafische nomenclator ondiepe ondergrond Netherland (online). Available from: www.nitg.tno.nl/nomenclatorShallow/nl/overig/boxtel/index.html (Accessed 15 October 2010).

Schokker, J., Cleveringa, P., Murray, A.S., Wallinga, J., Westerhoff, W.E., 2005. An OSL dated Middle and Late Quaternary sedimentary record in the Roer Valley Graben (southeastern Netherlands). Quaternary Science Reviews 24, 2243-2264.

Schokker, J., Weerts, H.J.T., Westerhoff, W.E., Berendsen, H.J.A., den Otter, C., 2007. Introduction of the Boxtel Formation and implications for the Quaternary lithostratigraphy of the Netherlands. Netherlands Journal of Geosciences 86, 197-210.

Schwabedissen, H., 1954. Die Federmesser-Gruppen des nordwesteuropäischen Flachlandes. Zur Ausbreitung des Spät-Magdalénien. Offa Bücher 9, Neumünster, 104 pp.

Schwan, J., 1986. The origin of horizontal alternating bedding in Weichselian aeolian sands in northwestern Europe. Sedimentary Geology 49, 73-108.

Schwan, J., 1988. The structure and genesis of Weichselian to Early Holocene aeolian sand sheets in western Europe. Sedimentary Geology 55, 197-232.

Sergant, J., Crombé, Ph., Perdaen, Y., 2009. Mesolithic territories and land-use systems in north-western Belgium. In: McCartan, S.B., Schulting, R., Warren, G., Woodman, P. (eds.). Mesolithic Horizons. Papers presented at the Seventh International Conference on the Mesolithic in Europe, Belfast 2005, Oxbow Books (Oxford), 277-281.

Shore, J.S., Bartley, D.D., Harkness, D.D., 1995. Problems encountered with the ^{14}C dating of peat. Quaternary Science Reviews (Quaternary Geochronology) 14, 373-383.

Spiers, V., 1986. Mineralogisch en petrografisch onderzoek van de kalkrijke sedimenten van de Moervaartdepressie. Licentiaatsverhandeling, Rijksuniversiteit Gent (Gent), 61 pp.

Stokes, S., 1991. Quartz-based optical dating of Weichselian coversands from the eastern Netherlands. Geologie en Mijnbouw 70, 327-337.

Stoops, G., 2003. Guidelines for Analysis and Description of Soil and Regolith Thin Sections. Soil Science Society of America, Madison, Wisconsin.

Street, M., 1998. The archaeology of the Pleistocene-Holocene transition in the northern Rhineland, Germany. Quaternary International 49/50, 45-67.

Smith, B.W., Rhodes, E.J., Stokes, S., Spooner, N.A., Aitken, M.J., 1990. Optical dating of sediments: Initial quartz results from Oxford. Archaeometry 32, 19-31.

Street, M., 1998. The archaeology of the Pleistocene-Holocene transition in the northern Rhineland, Germany. Quaternary International 49/50, 45-67.

Stuiver, M., Polach, H.A., 1977. Reporting of ^{14}C data. Radiocarbon 19, 355-363.

Tavernier, R., 1946. L'évolution du Bas Escaut au Pleistocène supérieur. Bulletin de la Société belge de Géologie, Paléontologie et Hydrologie 55, 106-125.

Tavernier, R., De Moor, G., 1974. L'évolution du basin de l'Escaut. In: Macar, P. (ed.). L'évolution quaternaire des bassins fluviaux de la Mer du Nord méridionale. Colloque du Centenaire de la Société Géologique de Belgique, Liège, 159-233.

Terberger, Th., Barton, N., Street, M., 2009. The Late Glacial reconsidered - recent progress and interpretations. In: Street, M., Barton, N., Terberger, Th. (eds.). Humans, environment and chronology of the late glacial of the North European Plain. Proceedings of Workshop 14 of the 15th UISPP Congress, Lisbon, September 2006. RGZM Tagungen 6, 189-207.

Törnqvist, T.E., 1992. Accurate dating of organic deposits by AMS ^{14}C measurement of macrofossils. Radiocarbon 34, 566-577.

Van Campo, E., Duplessy, J.-C., Rossignol-Strick, M., 1982. Climatic conditions deduced from a 150-kyr oxygen isotope-pollen record from the Arabian Sea. Nature 296, 56-59.

Vandenberghe, D., 2004. Investigation of the optically stimulated luminescence dating method for application to young geological samples. Ph.D. thesis, Universiteit Gent.

Vandenberghe, D., 2005. Optical dating of sediments. Analysis Report GLL-001/04. Gent, Belgium.

Vandenberghe, D., Derese, C., Houbrechts, G., 2007. Residual doses in recent alluvial sediments from the Ardenne (S Belgium). Geochronometria 28, 1-8.

Vandenberghe, D., Hossain, S.M., De Corte, F., Van den haute, P., 2003. Investigations on the origin of the equivalent dose distribution in a Dutch coversand. Radiation Measurements 37, 433-439.

Vandenberghe, D., De Corte, F., Buylaert, J.-P., Kučera, J., Van den haute, P., 2008. On the internal radioactivity in quartz. Radiation Measurements 43, 771-775.

Vandenberghe, D., Kasse, C., Hossain, S.M., De Corte, F., Van den haute, P., Fuchs, M., Murray, A.S., 2004. Exploring the method of optical dating and comparison of optical and ^{14}C ages of Late Weichselian coversands in the southern Netherlands. Journal of Quaternary Science 19, 73-86.

Vandenberghe, D., Vanneste, K., Verbeeck, K., Paulissen, E., Buylaert, J.-P., De Corte, F., Van den haute, P., 2009. Late Weichselian and Holocene earthquake events along the Geleen fault in NE Belgium: OSL age constraints. Quaternary International 199, 56-74.

Vandenberghe, J., Van Huissteden, J., 1988. Fluvio-eolian interaction in a region of continuous permafrost. Proceedings, Vth International Conference on Permafrost, Trondheim, Norway, 2-5 August: 876-881.

Vandenberghe, J., Bohncke, S., Lammers, W., Zilverberg, L., 1987. Geomorphology and palaeoecology of the Mark Valley (southern Netherlands): geomorphological valley development during the Weichselian and Holocene. Boreas 16, 55-67.

Vandenberghe, J., Bohncke, S., Kozarski, S.,1994. Climate-related river activity at the Weichselian-Holocene transition: a comparative study of the Warta and Maas rivers. Terra-Nova 6, 476-485.

Van der Hammen, T., 1951. Late glacial flora and periglacial phenomena in the Netherlands. Leidse Geologische Mededelingen 17, 71-183.

Van der Hammen, T., Maarleveld, G.C., Vogel, J.C., Zagwijn, W.H., 1967. Stratigraphy, climatic succession and radiocarbon dating of the Last Glacial in The Netherlands. Geologie en Mijnbouw 46, 79-95;

Van der Hammen, T., Van Geel, B., 2008. Charcoal in soils of the Allerød-Younger Dryas transition were the result of natural fires and not necessarily the effect of an extra-terrestrial impact. Netherlands Journal of Geosciences 87, 359-361.

Van der Hammen, T., Wijmstra, T.A., 1971. The Upper Quaternary of the Dinkel valley (Twente, Eastern Overijssel, The Netherlands). Mededelingen Rijks Geologische Dienst 22, 55-212.

Van Geel, B., Coope, G.R., Van der Hammen, T., 1989. Palaeoecology and stratigraphy of the Lateglacial type section at Usselo (The Netherlands). Review of Palaeobotany and Palynology 60, 25-129.

Van Gils, M., De Bie, M., 2004. Federmessersites te Lommel-*Maatheide* (Limburg). Opgravingscampagne 2004. Notae Praehistoricae 24, 89-94.

Van Gils, M., De Bie, M., 2006. Steentijd in de Kempen. Prospectie, kartering en waardering van het laat-Paleolithisch en Mesolithisch erfgoed. In: Cousserier, K., Meylemans, E., In ‘t Ven, I (Eds.), Centrale Archeologische Inventaris (CAI) II. Thematisch inventarisatie- en evaluatieonderzoek, 7-16.

Van Gils, M., De Bie, M., Paulissen, E., Deforce, K., 2009. Kartering en waardering van een finaalpaleolithisch/mesolithisch sitecomplex te Arendonk-Korhaan (prov. Antwerpen). Boorcampagne 2003. Relicta 4, 9- 21.

Vanhoorne, R., Verbruggen, C., 1975. Problèmes de subdivision du Tardiglaciaire dans la région sablonneuse du nord de la Flandre en Belgique. Pollen et Spores 17, 525-543.

Van Huissteden, J., 1990. Tundra rivers of the last glacial: sedimentation and geomorphological processes during the Middle Pleniglacial in Twente, eastern Netherlands. Mededelingen Rijks Geologische Dienst 44, 3-138.

Van Huissteden, J., Schwan, J.C.G., Bateman, M.D., 2001. Environmental conditions and paleowind directions at the end of the Weichselian Late Pleniglacial recorded in aeolian sediments and geomorphology (Twente, Eastern Netherlands). Geologie en Mijnbouw / Netherlands Journal of geosciences 80, 1-18.

Van Huissteden, J. (Ko), Vandenberghe, J., Van der Hammen, T., Laan, W., 2000. Fluvial and aeolian interaction under permafrost conditions: Weichselian Late Pleniglacial, Twente, eastern Netherlands. Catena 40, 307-321.

Vanmontfort, B., Yperman, W., Lambrechts, B., Van Gils, M., Geerts, F., 2010a. Een finaalpaleolithisch en mesolithisch sitecomplex te Lommel, Molse Nete. Opgravingscampagne 2010. Notae Prehistoricae 30, 29-34.

Vanmontfort, B., Van Gils, M., Paulissen, E., Bastiaens, J., Meirsman, E., De Bie, M., 2010b. Landscape evolution and hunter-gatherer occupation in the Liereman landscape. Journal of Archaeology in the Low Countries 2-2, http://dpc.uba.uva.nl/jalc/02/nr02/a02.

van Mourik, J.M., Nierop, K.G.J., Vandenberghe, D.A.G., 2010. Radiocarbon and optically stimulated luminescence dating based chronology of a polycyclic driftsand sequence at Weerterbergen (SE Netherlands). Catena 80, 170-181.

Van Strydonck, M., 2005. Radiocarbon dating. In: Crombé (ed.). The last hunter-gatherer-fisherman in Sandy Flanders (NW Belgium). The Verrebroek and Doel excavation projects (Vol. 1). Archaeological Reports Ghent University (Gent), 127-130.

Verbruggen, C., 1971. Postglaciale landschapsgeschiedenis van zandig Vlaanderen. Botanische, ecologische en morfologische aspekten op basis van palynologisch onderzoek. Ph.D. thesis, Rijksuniversiteit Gent (Gent), 440 pp.

Verbruggen, C., 1979. Vegetational and palaeoecological history of the Lateglacial period in Sandy Flanders (Belgium). Acta Universitatis Ouluensis A.82; Geologica 3, 133-142.

Vermeersch, P.M., 2008. La transition Ahrensbourgien-Mésolithique ancien en Campine belge et dans le sud sableux des Pays-Bas. In: Fagnart, J.P., Thévenin, A., Ducrocq, T., Souffi, B., Coudret, P. (Eds.). Le début du Mésolithique en Europe du Nord-Ouest, Mémoire XLV de la Société préhistorique française, pp. 11-29.

Vermeersch, P.M., in press. The human occupation of the Benelux during the Younger Dryas. Quaternary International (2010), doi: 10.1016/j.quaint.2010.10.021.

Wallinga, J., Davids, F., Dijkmans, J.W.A., 2007. Luminescence dating of Netherlands' sediments. Netherlands Journal of Geosciences 86, 179-196.

Wintle, A.G., Murray, A.S., 2006. A review of quartz optically stimulated luminescence characteristics and their relevance in single-aliquot regeneration dating protocols. Radiation Measurements 41, 369-391.

Wouters, B.A., 1957. Een nieuwe vindplaats van de Ahrensburgcultuur onder de gemeente Geldrop. Brabants Heem 9, 2.

Wouters, L., Vandenberghe, N., 1994. Geologie van de Kempen. Een synthese. Niras, Brussel.

Yu, Z.C., Hoek, W.Z, Lowe, J.J. (Eds.), 2008. INTegration of Ice-core, Marine and Terrestrial records (INTIMATE): Refining the record of the Last Glacial-Interglacial Transition. Quaternary Science Reviews 27, 1-184.

Dankwoord

DANKWOORD

Eigenlijk is het afwerken van een doctoraat niet zo verschillend van het maken van een lange reis: eens het onderwerp van het project (de reisbestemming) en de vertrekdatum gekozen, kan je uitkijken naar het moment waarop je echt van start kan gaan, het avontuur tegemoet. Pas vertrokken weet je niet goed wat te verwachten, je weet niet waar je terecht zal komen. Je hebt het gevoel elke dag nieuwe ervaringen op te doen, nieuwe mensen en dingen te leren kennen. Naarmate de reis vordert, word je echter een ervaren reiziger, krijg je zicht wat je nog wil bereiken. Doorheen de reis slaat natuurlijk af en toe de vermoeidheid toe, verloopt niet alles zoals gepland, moet je pauzes inbouwen. Maar op die momenten kan je je optrekken aan alle activiteiten die nog op til staan, aan de steun van je vaste reisgezellen en aan deze van de mensen die je tijdens je reis ontmoet. En ook al is het fijn te reizen, op een bepaald ogenblik begin je naar thuis te verlangen, naar het einde van de reis, naar het moment waarop je de reiservaringen kan delen met je vrienden en familie, naar het volgende avontuur in je leven. Op dit punt ben ik nu gekomen… Ik zou echter niet aan dat volgende avontuur kunnen beginnen, zonder eerst de mogelijkheid te grijpen om mijn vaste en tijdelijke ‘reisgezellen’ te bedanken voor hun onvoorwaardelijke steun, vertrouwen, delen van kennis en ervaring.

Zowel mijn interesse voor luminescentiedatering als de kans om aan dit onderzoeksproject mee te werken heb ik te danken aan mijn promotor, Prof. Dr. Peter Van den haute. En hoewel hij, wegens een druk programma als lesgever, niet de tijd had om de dagdagelijkse begeleiding van het project op zich te nemen, stond hij steeds klaar met goede raad. Ik wil hem dan ook bedanken voor het vertrouwen dat hij mij schonk, voor de steun, en voor de interessante wetenschappelijke inzichten die hij met mij deelde.

Dr. Dimitri Vandenberghe heeft zich uitstekend gekweten van zijn taak als begeleider en co-promotor bij alle theoretische en praktische aspecten van dit onderzoek. Ik wil hem graag bedanken voor het schier eindeloze geduld bij het beantwoorden van mijn vragen en voor de constante aanmoediging. Verder wil ik hem ook bedanken voor zijn onvoorwaardelijke steun op moeilijke momenten, zowel professioneel als privé, voor het delen van zijn uitgebreide kennis en levenswijsheden, en voor de vele gezellige momenten op en naast het werk. Dimi, ik wens je alle succes toe bij het verder promoten van luminescentiedatering in Vlaanderen en daarbuiten, en hoop van harte dat je voor deze inspanningen beloond wordt.

Prof. Dr. Em. Etienne Paulissen (Katholieke Universiteit Leuven) wil ik graag bedanken voor de constructieve samenwerking te Opgrimbie, Arendonk en Lommel, voor het delen van inzichten in de Quartairgeologie van Noord-België, voor zijn kritische blik ten opzichte van luminescentiedatering, en voor de interessante wetenschappelijke discussies.

Dr. Kees Kasse (Vrije Universiteit Amsterdam) wil ik bedanken voor de bijzonder aangename en productieve samenwerking. Meer in het bijzonder dank ik hem voor de inwijding in de Quartairgeologische evolutie van Nederland en specifiek de Dinkelvallei, voor het fijne veldwerk te Lutterzand en Aalsterhut, voor de uitnodiging om korrelgrootteanalyses uit te voeren in het laboratorium aan de VU, en voor het hart-onder-de-riem-steken bij het afwerken van mijn doctoraatsthesis. Ik hoop dan ook dat hij terecht trots kan zijn op onze gezamenlijke artikels.

Ik wens de medewerkers aan het Vlaams Instituut voor Onroerend Erfgoed (VIOE), met name Rica Annaert, Nele Eggermont, Jan Bastiaens en Marijn Van Gils te bedanken voor de fijne samenwerking en voor het naar waarde schatten van de toepassing van luminescentiedatering bij archeologische studies. In datzelfde opzicht dank ik ook Els Meirsman, Bart Vanmontfort (beide Katholieke Universiteit Leuven), Philippe Crombé, Machteld Bats, Ann Zwertvaegher en de andere leden van het GOA team (allen Universiteit Gent). Ik hoop dat er in de toekomst nog meer samenwerking tussen archeologen en ons laboratorium kan plaatsvinden.

Ik ben Jan-Pieter Buylaert zeer erkentelijk voor zijn gastvrijheid tijdens mijn eerste bezoek aan Denemarken en voor het organiseren van een tweede. Great acknowledgement is made to Prof. Dr. Andrew Murray for giving me the opportunity to spend some time at the Nordic Laboratory for Luminescence Dating. It was greatly inspiring to work together with him, Kristina Thomsen and the rest of the Risø crew on their feldspar research. Furthermore, I would like to thank Esther and Reza for their warm companionship during the long hours in the office and the lab, and both them and the other guests at Risø guesthouse for the cosy evenings and the great times out in Copenhagen. Those three months in Denmark really gave me the energy to continue with the second half of my PhD research.

I would also like to thank the many luminescence and Quaternary researchers around the world that shared ideas, experiences and words of support with me. Thanks to them, I spent an unforgettable time at conferences in Belgium, The Netherlands, UK, Denmark, Poland, Sardinia and China.

Met plezier denk ik terug aan de (te) korte tijd die ik samen met Nicole Selen in ons laboratorium voor monstervoorbereiding heb mogen doorbrengen. Ik wil haar graag bedanken voor de geduldige uitleg bij alle stappen van de monstervoorbereiding, voor de gezellige, warme gesprekken tussenin en voor haar nooit aflatende interesse in mijn bezigheden. Nicole, ik wens je een spoedig en volledig herstel toe. Als er iemand dat verdient, ben jij het wel.
Gilles Velghe is een prima 'vervanger' van Nicole gebleken. Ik wil hem bedanken voor de hulp bij de monstervoorbereiding, de inwijding in het maken van wax pucks, de make-over van de OSL-labo's, en daarnaast voor het creëren van een geweldige sfeer op de MINPET-gang. Gilles, ik durf er om te wedden dat het InBio-labo op de Coupure momenteel één van de fijnste werkplekken aan de UGent is. Ik wens je veel geluk toe bij al je ondernemingen in de toekomst.

Graag bedank ik alle administratieve en technische personeelsleden op de vakgroep die hebben bijgedragen tot het voltooien van deze thesis, in het bijzonder Kurt Blom, die redder in nood speelde toen mijn laptop op een cruciaal moment crashte. Ook de collega-doctoraatsstudenten ben ik dankbaar voor het uitwisselen van ervaringen en fijne gesprekken in de wandelgangen.

Verder wens ik alle andere collega's op de MINPET te bedanken, in het bijzonder Florias, voor het tonen van zijn expertise in micromorfologie, Johan en Stijn, voor het organiseren van een aantal memorabele evenementen, en Ingrid, voor de vriendschap en voor het mij af en toe met mijn neus op de feiten drukken. Kathleen en Els, onze twee thesisstudenten, zorgden ervoor dat mijn bureau mooi gevuld raakte. Ik wil hen allebei bedanken voor hun aangename gezelschap, en Kathleen in het bijzonder ook voor haar vriendschap en het delen van levenswijsheden op cruciale momenten. Dragan, Alida and Stefan provided some foreign imput to our laboratory. I appreciated their company, both in the lab and on conferences, very much.

Zonder de steun van mijn vrienden was dit doctoraat nooit geworden wat het is. In het bijzonder dank ik Karen, voor het delen van mijn liefde voor Belgische bieren en voor muziek, en Katrien, voor het creëren van een warme thuis waar ik alle zorgen en frustraties voor even kon vergeten.

Ook mijn familie speelde een onmisbare rol in het afwerken van dit onderzoek. Zonder hun liefde, hun constante steun en aanmoediging, hun geduld en begrip had ik het de afgelopen vijf jaar nooit volgehouden.

Tot slot wil ik Janek bedanken. Janek, je kwam er ongeveer halverwege deze ‘reis’ bij en werd mijn grote steun en toeverlaat. Met jou ga ik met plezier de volgende avonturen tegemoet.

Dit onderzoek kwam tot stand met de financiële steun van het Fonds voor Wetenschappelijk Onderzoek en van het Bijzonder Onderzoeksfonds van de Universiteit Gent.